REFERENCE ONLY

UNIVERSITY OF LONDON THESIS

Degree	Year	Name of Author
PhD	2005	LO CELSO, C.

COPYRIGHT

This is a thesis accepted for a Higher Degree of the University of London. It is an unpublished typescript and the copyright is held by the author. All persons consulting the thesis must read and abide by the Copyright Declaration below.

COPYRIGHT DECLARATION

I recognise that the copyright of the above-described thesis rests with the author and that no quotation from it or information derived from it may be published without the prior written consent of the author.

LOANS

Theses may not be lent to individuals, but the Senate House Library may lend a copy to approved libraries within the United Kingdom, for consultation solely on the premises of those libraries. Application should be made to: Inter-Library Loans, Senate House Library, Senate House, Malet Street, London WC1E 7HU.

REPRODUCTION

University of London theses may not be reproduced without explicit written permission from the Senate House Library. Enquiries should be addressed to the Theses Section of the Library. Regulations concerning reproduction vary according to the date of acceptance of the thesis and are listed below as guidelines.

A. Before 1962. Permission granted only upon the prior written consent of the author. (The Senate House Library will provide addresses where possible).

B. 1962 - 1974. In many cases the author has agreed to permit copying upon completion of a Copyright Declaration.

C. 1975 - 1988. Most theses may be copied upon completion of a Copyright Declaration.

D. 1989 onwards. Most theses may be copied.

This thesis comes within category D.

☑ This copy has been deposited in the Library of UCL

☐ This copy has been deposited in the Senate House Library, Senate House, Malet Street, London WC1E 7HU.

Role of β-catenin signalling in adult epidermal cell fate specification

Cristina Lo Celso

A Thesis submitted for the degree of
Doctor of Philosophy
at University College London

September 2005

ProQuest LLC
789 East Eisenhower Parkway
P.O. Box 1346
Ann Arbor, MI 48106-1346

Abstract

The epidermis is maintained through self-renewal of stem cells and differentiation of their progeny into interfollicular epidermis, hair follicles and sebaceous glands. In order to investigate the role of β-catenin in cell fate selection in adult epidermis I used a drug-regulated system to activate β-catenin signalling at specific stages of the hair cycle and for different lengths of time in the epidermis of transgenic mice.

I found that following β-catenin activation resting hair follicles are recruited into the growth phase of the hair cycle, and new ectopic hair follicles form from existing hair follicles, interfollicular epidermis and sebaceous glands. The ectopic follicles grow in number and size to form trichofolliculomas. While a transient activation of β-catenin signalling is sufficient to trigger hair follicle morphogenesis, continuous activation is required to maintain hair follicle tumours, and titration of β-catenin signalling influences the quantity and timing of ectopic hair follicle formation. The new hair follicles form without major perturbation of the existing stem cell compartment, contain dermal papillae, undergo cycles of growth and regression, and express markers of the epidermal stem cell niche. Microarray analysis of the β-catenin induced genes suggested a role for the Hedgehog (Hh) and Notch pathways and vitamin D receptor downstream of β-catenin. I was able to investigate also the relationship between β-catenin and c-Myc in epidermal cell lineage choice. Finally, I developed an *in vitro* model for the analysis of lineage selection at the single cell level.

I demonstrate the advantage of temporal, spatial and dosage control of β-catenin signalling to analyse the effects of its activation in adult epidermis and to investigate epidermal stem cell self-renewal and differentiation, an approach that could be applied more broadly to look at the interaction between multiple pathways in adult skin homeostasis.

To all my family,
and especially Mum and Dad

Considerate la vostra semenza:
Fatti non foste a viver come bruti,
Ma per seguir virtute e canoscenza.

Dante, Inferno, XXVI 119-120

Table of Contents

List of Figures

List of Tables

Abbreviations

4OHT	4-hydroxytamoxifen
AM12	gag pol + envAM12 packaging cells
AP	ammonium persulphate
APC	adenomatous polyposis colon
BAMBI	BMP and activin membrane-bound inhibitor
BCA	bicinchoninic acid
BMP	bone morphogenetic protein
BMP	bone morphogenetic protein
bp	base pairs
BrdU	5' bromodeoxyuridine
BSA	bovine serum albumin
CD	cluster of differentiation antigen
cDNA	copy deoxyribonucleic acid
CDP	CCAAT displacement protein
cRNA	copy ribonucleic acid
CR-UK	Cancer Research UK
C-term	carboxy terminus
DAB	3,3-diaminobenzedene tetrahydrochlodride
DAPT	N-S-phenyl-glycine-t-butyl ester
DC	dermal condensate
DCS	donor calf serum
DED	dead, de-epidermised dermis
Dhh	Desert hedgehog
Dkk	Dickkopf
DMEM	Dulbecco's modification of Eagles' medium
DMSO	dimethyl sulfoxide
dNTP	deoxynucleotide triphosphate
DP	dermal papilla
DTT	dithiolthreitol
ECL	enhanced chemiluminescence
ECM	extracellular matrix
EDTA	ethyldiaminotetraacetic acid, disodium salt
EGF	epidermal growth factor
EMA	epithelial membrane antigen
EPU	epidermal proliferative unit
ER	oestrogen receptor
ERK	extracellular signal-regulated kinase
EST	expressed sequence tag
FAD	F12 + adenine + DMEM
FCS	fetal calf serum
GFP	green fluorescent protein
GMP	guanosy
GSK3-β	glycogen synthase kinase 3-β
H&E	haematoxylin and eosin staining

HBS	HEPES buffered saline
HEPES	N-[2-hydroxyethyl]piperazine-N'-[2-ethanesulphonic acid]
HES	Hairy and Enhancer of Split
HF	hair follocle
HGF	hepatocyte growth factor
HICE	hydrocortisone, insulin, cholera enterotoxin and EGF
HLH	helix loop helix
HMG	High Mobility Group
HRP	horseradish peroxidase
HSC	haematopoietic stem cell
IC	intracellular domain
IFE	interfollicular epidermis
Ig	immunoglobulin
IGF	insulin-like growth factor
Ihh	Indian hedgehog
IRS	(hair follicle) inner root sheath
JNK	Jun N-terminal kinase
K	keratin
K14	keratin 14
K14	keratin14
kb	kilo base pairs
kDa	kilo Dalton
KGF	keratinocyte growth factor
LB	Luria-Bertani broth
LDL	low density lipoprotein
Lef	lymphoid enhancer factor
LRC	label retaining cell
LRP	LDL-receptor related protein
MMTV	Molony murine tumour virus
Mo MuLV	Moloney murine leukemia virus
Mo MuLV	Moloney murine leukemia virus
mRNA	messenger ribonucleic acid
Myc	c-Myc
NFκB	nuclear factor κB
NICD	Notch intracellular domain
NR	nuclear receptor
N-term	amino terminus
O.D.	optical density
ORS	(hair follicle) outer root sheath
PAGE	polyacrylamide gel electrophoresis
PBS	phosphate-buffered saline
PBST	PBS/Tween
PCR	polymerase chain reaction
PEG	primitive epidermal germ
pen/strep	penicillin/streptomycin
PKC	protein kinase C
PKC	protein kinase C
PMSF	phenylmethanesulphonyl fluoride
PPAR	peroxisome proliferator-activated receptor
Ptc	Patched

PVDF	polyvinylidene fluoride
RAR	retinoic acid receptor
RBPJk	recombination signal sequence binding protein for Jk genes
RNase	ribonucleic acid endonuclease
rpm	revolutions per minute
SC	stem cell
SCC	squamous cell carcinoma
SDS	sodium dodecyl sulphate
se	standard error
SG	sebaceous gland
Shh	Sonic hedgehog
SMO	Smoothened
SSC	salt sodium citrate buffer
TA	transit amplifying cell
TAE	Tris-acetate-EDTA buffer
TBE	Tris-borate-EDTA buffer
TBS	Tris-buffered saline
TBST	TBS/Tween
TCF	T cell factor
TD	terminally differentiated cell
TE	Tris-EDTA buffer
TEMED	N,N,N',N'-tetramethylethylenediamine
TG/tg	transgenic
TGF	transforming growth factor
TGF	transforming growth factor
TGF	transforming growth factor
TM	transmembrane domain
VDR	vitamin D receptor
WIF	Wnt inhibitory factor
Wnt	mammalian homologue of Wingless
WT/wt	wild type

Acknowledgements

My first thank you to Fiona, for taking me in the lab and being a source of enthusiasm, optimism, encouragement and... pure energy!

Thank you to David and Violeta for sharing so many hours of work with me, and (in order of appearance in the thesis) to Soline, Carrie, Hector and Kristin for making me feel like I was dealing with the nicest mice in the world.

Thank you to my 'aunties' in the lab, Soline, Kristin, Laura and Ela – at least one of you was always there! And thank you to all present and past members of the Keratinocyte Lab for patience, advice, support, laugh, and plenty of London adventures (you are too many to mention, but you are all here!). In particular, thank you to Simon and Liz (and recently Paul) for keeping the lab running and having always a solution for all problems.

I am very grateful for all the support I have had from the Animal Unit (in particular Angela for taking care of all my mice and Claire for always finding time to help me with the paintbrush), from everybody in Histopath for dealing with (argh!) more than 1000 blocks, and also Rosemary, Richard and Bradley for in situ stuff and stainings and advice.

I'd like to thank all my friends in Torino and in London for making these two cities become one big extended home. I can't wait to have you all visiting me in Boston soon!

Thank you to my parents for being always there. The phone calls are becoming legendary, but they are really filling my life. And thank you to Peter for understanding me, and for nonstop enthusiastic support (and so many dinners!).

Chapter 1. Introduction

The epidermis has a complex and dynamic structure characterized by high cell turnover. It is maintained by a population of stem cells residing in the bulge area of the hair follicle (HF), but also scattered in the basal layer of interfollicular epidermis (IFE) and sebaceous glands (SG) (Fuchs et al., 2001; Watt, 2001). The molecular mechanisms regulating epidermal stem cell self-renewal and differentiation along the various epidermal lineages have been studied in transgenic mouse models and by culturing human epidermal cells (Honeycutt and Roop, 2004; Niemann et al., 2003; Watt, 2001).

1.1 Structure and development of the skin

The skin is at the interface between the body and the environment. Its main function is protection, therefore it is a strong and flexible mechanical barrier, and hosts many immune reactions. The most external part of the skin is the epidermis, lying on the dermis. A deeper component is the subcutaneous fat, lying on a muscular band known as the muscularis mucosa, which covers the whole body but is mainly evident in the face as it is responsible for facial expressions. Epidermis and dermis originate from ectoderm and mesoderm respectively and have very different structure and cellular components. The epidermis is the mechanical barrier and the dermis serves as support (Odland, 1991).

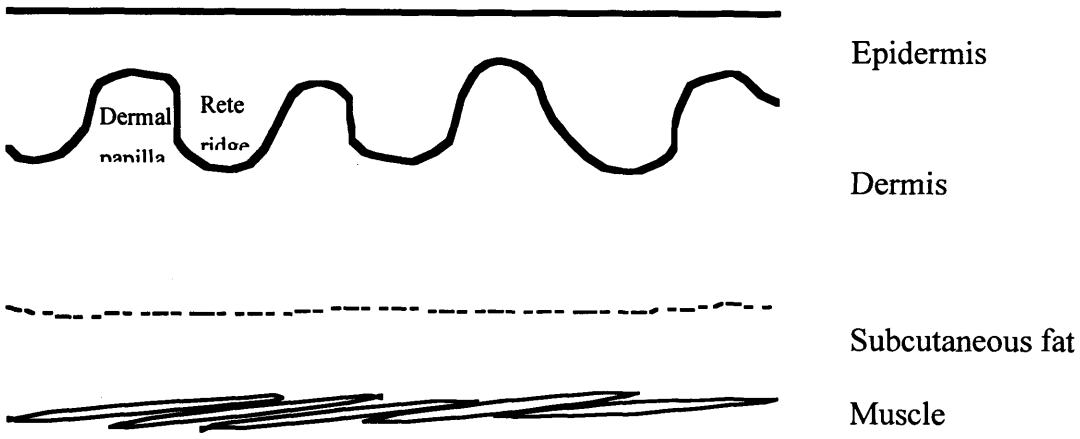

Figure 1. 1. Schematisation of the layers forming the skin.

1.1.1. The epidermis

The epidermis is a multilayered epithelium, with several appendages: hair follicles, sebaceous glands and sweat glands. While the interfollicular epidermis (IFE) is necessary in its integrity for a normal life, its appendages are not, but nevertheless have important roles in the maintenance of skin homeostasis. The keratinocytes are the most abundant cell type in the epidermis, tightly anchored to each other and organized in several layers in IFE and HF. The other cell types present in the epidermis are the sebocytes, the secretory and ductal cells of the sweat glands and cells of different origin like the melanocytes, Langherans cells and Merkel cells (Nasemann et al., 1983).

1.1.1.1. Interfollicular epidermis

In humans the interfollicular epidermis is formed by several layers of keratinocytes with different histological and molecular characteristics from the deepest to the most superficial (Fig.1.2). The basal keratinocytes are tightly anchored with integrins and hemidesmosomes to the basement membrane, formed by collagen, laminins and proteoglycans secreted by both IFE keratinocytes and dermal cells (Marinkovich et al., 1993). In human epidermis the basement membrane is not flat, and as a consequence the boundaries between IFE and dermis appear undulated in sections. The invaginations of

A

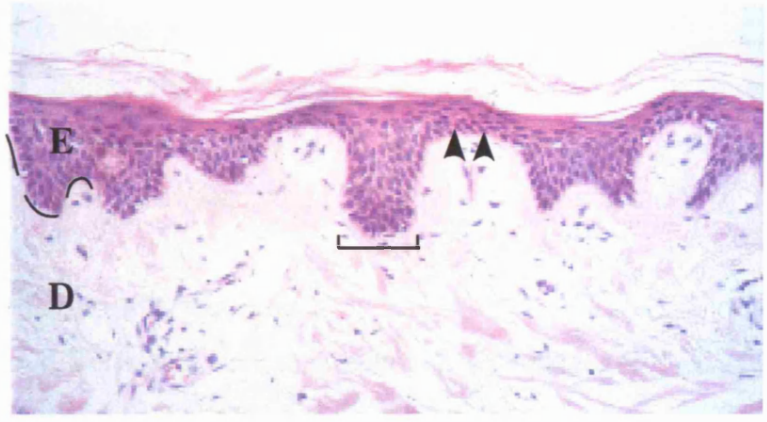

B

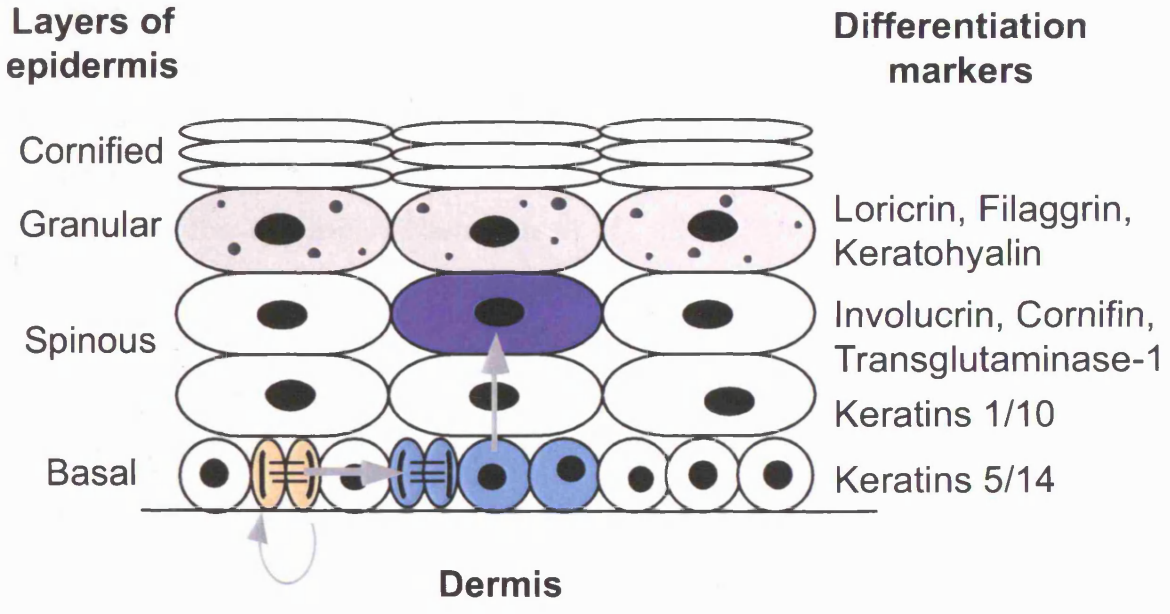

Figure 1.2. Organisazion of human interfollicular epidermis. (A) Hematoxylin and Eosin stained section of human skin showing the epidermis ("E") and the dermis ("D"). The basement membrane is indicated with a dotted line. The bracket marks the tip of a rete ridge and the arrowheadsa dermal papilla. Magnification 20X. (B) Diagram representing organisation of the interfollicular epidermis. Keratinocytes of the various layers of the epidermis are shown along with differentiation markers specific for those layers of cells. Within the basal, proliferative compartment of the epidermis, the putative stem cells are indicated in orange and transit amplifying daughters in light blue. A terminally differentiating cell that has left the basal layer and is migrating towards the surface of the skin is indicated in dark blue. Adapted from Robin Hobbs, PhD thesis, 2003.

human epidermis are named rete ridges, and the regions of dermis between them are referred to as dermal papillae (Odland, 1991). The keratinocytes of the basal layer have a columnar shape, with the long axis perpendicular to the basement membrane. Most proliferation takes place in the basal layer and the progeny of the basal cells moves upwards towards the surface while differentiating (Dover and Wright, 1991).

Above the basal layer, the spinous layer comprises 4-5 layers of polygonal cells that are starting to differentiate and are separated by spaces crossed by thick intercellular bridges (Lever and Schaumberg-Lever, 1993). The cells in the granular layer are diamond shaped, with their long axis parallel to the surface of the epidermis. They contain electrondense granules of keratohyalin and of precursors of the cornified envelope (e.g. loricrin), a highly insoluble cress-linked protein structure that assembles beneath the plasma membrane (Candi et al., 2005; Lever and Schaumberg-Lever, 1993). These cells are preparing to lose their nucleus and terminally differentiate. The thickness of the granular layer varies from 3-4 to 10 cells in regions with different thickness of the epidermis (Nasemann et al., 1983). The outermost layer of the epidermis is the cornified layer, which contains flat anuclear keratinocytes filled with aggregated keratin filaments and the crosslinked proteins and lipids of the cornified envelope (Nemes and Steinert, 1999). These cells are responsible for the barrier function of the skin, and are constantly shed and replaced by cells originating from the deeper layers (Candi et al., 2005).

Mouse IFE contains only 2 or 3 layers of viable suprabasal cells, but is organized in the same way as the human, with proliferating cells in the basal layer and differentiating cells in the upper layers. The other difference between human and mouse epidermis is that in mouse the dermal-epidermal interface is flat.

1.1.1.2. Epidermal appendages

Hair follicles, sebaceous glands and apocrine and eccrine sweat glands are connected to the interfollicular epidermis and all originate from primary epithelial germs (PEG) during embryonic development (Nasemann et al., 1983). The hair follicles are parallel to each other and elongate deeply in the dermis, at an angle of about 60 degrees with the surface. Human hair follicles have one or two sebaceous glands connected to their upper

part, and sometimes an apocrine sweat gland (Fig. 1.3). In some restricted skin regions eccrine glands and free sebaceous glands are directly connected to the IFE (Lever and Schaumberg-Lever, 1993).

Hair follicles

Hair follicles have a multilayered cylindrical structure that can be subdivided in three parts: the lower portion from the base of the follicle to the insertion of the arrector pili muscle, the middle portion (isthmus) from the arrector pili insertion to the sebaceous gland duct, the upper portion (infundibulum) from the connection to the sebaceous gland to the orifice in the interfollicular epidermis (Nasemann et al., 1983).

The lower part of the follicle is formed by several concentrical cell layers and terminates with a knoblike structure, the bulb, forming the base of the follicle (Fig. 1.4). This encircles the dermal papilla, an aggregate of dermal cells of various types, and some capillaries (Jahoda and Reynolds, 1996). The hair matrix cells in the bulb give rise to the hair and to the inner root sheath (IRS) of the hair follicle, so that their progeny moves upward while differentiating (Legue and Nicolas, 2005; Panteleyev et al., 2001).

The hair is composed of the hair medulla, only partially keratinized, the hair cortex, filled with hard keratins that contain high levels of disulfide bonds (Langbein and Schweizer, 2005) and the hair cuticle, formed by cells tightly attached to the inner root sheath cuticle. The IRS is formed, inward to outward, by the IRS cuticle, formed by flattened cells, the Huxley layer, consisting of two rows of cells, and the Henley layer, the first to keratinize during HF formation. The IRS does not contain hard keratins, but trichohyalin granules similar in morphology to the IFE keratohyalin, with the difference that trichohyalin stains eosinophilic while keratohyalin stains basophilic (Lever and Schaumberg-Lever, 1993). Differentiating IRS cells reach the isthmus, then disintegrate without contributing to the hair (Parakkal and Matoltsy, 1964). The companion layer is composed by flattened cells and it is located between IRS and ORS (Niemann and Watt, 2002).

The outer root sheath (ORS) represents a downward extension of the epidermis. It is thinnest at the level of the bulb, becomes multilayered and gradually thicker towards the

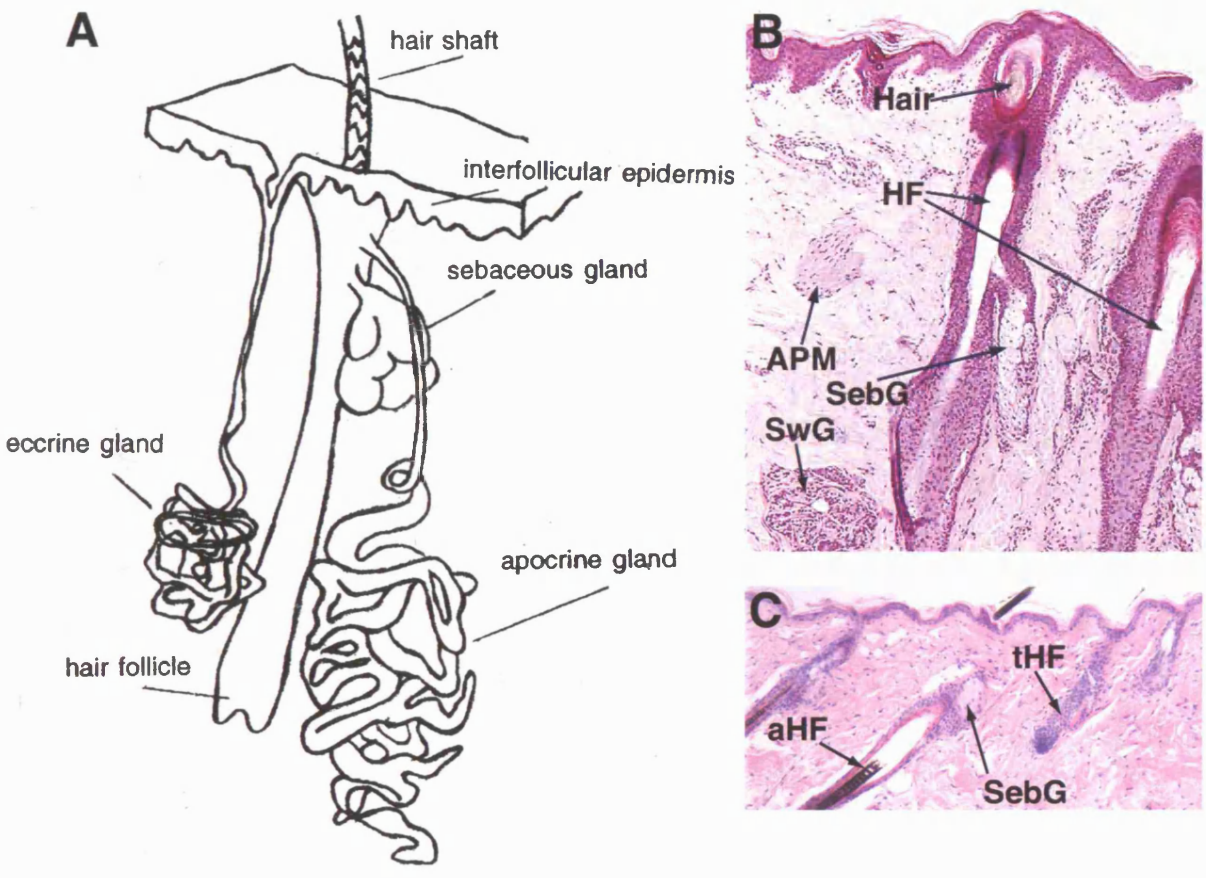

Figure 1.3. Epidermal appendages. (A) Schematic drawing representing the relationship between the hair follicles, interfollicular epidermis, sebaceous and sweat glands in human skin, all thought to derive from a common multipotent stem cell. Adapted from Odland, 1991 and Watt, 2001. (B) Histological section of human scalp ondicating the hair, hair follicles (HF), a sectioned arrector pili muscle (APM), sebaceous and sweat glands (SeG and SwG). (C) Histological section of mouse dorsal epidermis representing sebaceous glands (SebG) and hair follicles in anagen (aHF) and telogen (tHF) of the hair cycle. Note that in mouse epidermis the IFE is thinner, the dermal-epidermal interface is flat, and there are not sweat glands connected to the hair follicles. Magnification in B and C: 10X. For more details see main text.

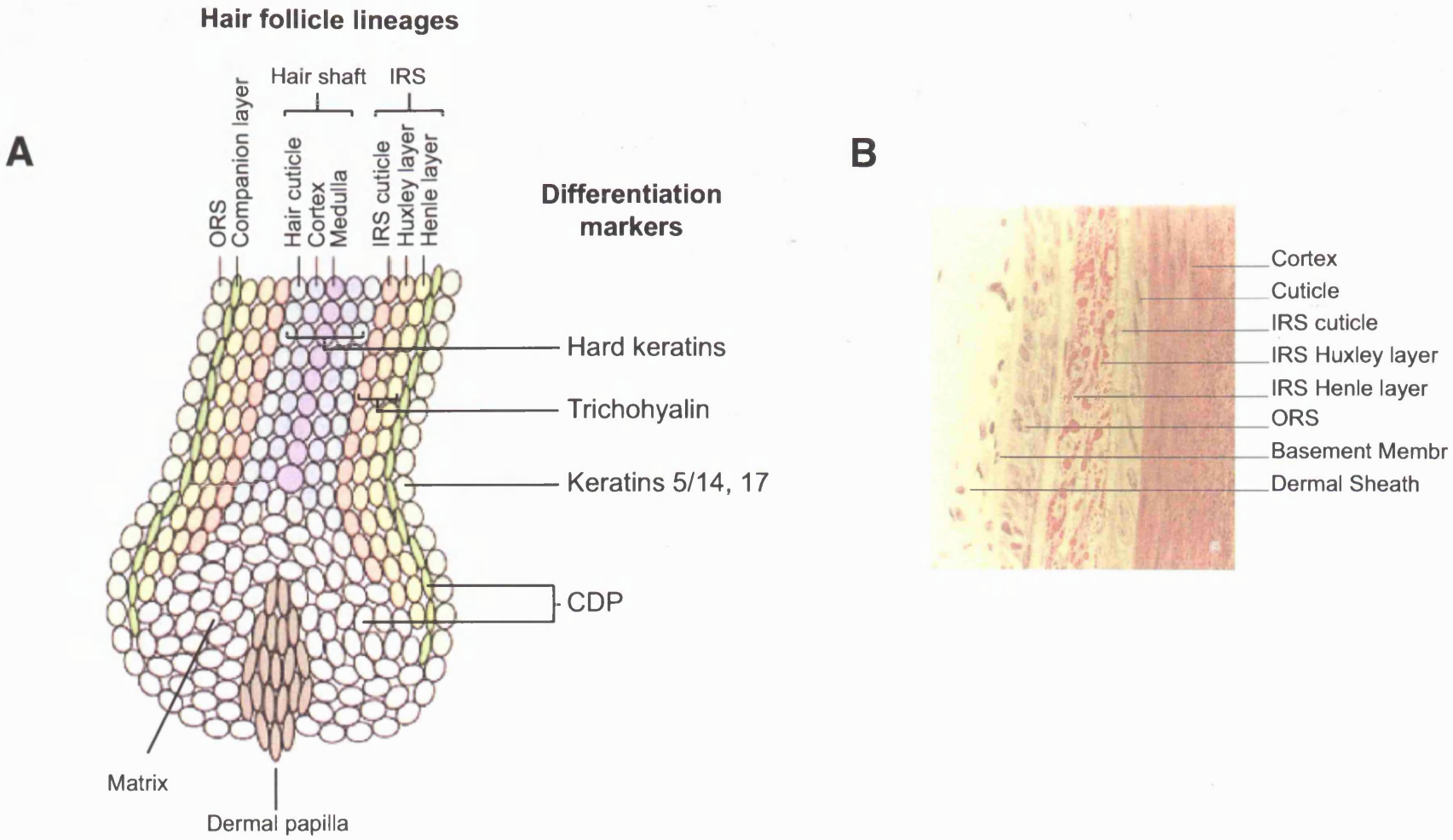

Figure 1.4. Hair follicle lineages. Schematic representation (A) and histological appearance (B) of the various cell layers in the lower portion of the hair follicle, with indication of the differentiation markers expressed in the various layers. MAtrix cells are undifferentiated and give rise to the cells forming the hair shaft and the IRS. Magnification 40X. For more details see main text. Adapted from Niemann and Watt, 2003 and McElwee, Hair biology course, http://www.thegentletouch.com/hairbiol/crs-frame.htm.

isthmus, and changes with the IFE in the infundibulum. A basement membrane similar to the one below the interfollicular epidermis, but thicker, wraps the ORS and is in turn surrounded by thick collagen bundles (Lever and Schaumberg-Lever, 1993).

Sebaceous glands

Most sebaceous glands (SG) are connected to hair follicles. Their size is influenced by androgens and correlates with the region of skin they lie in rather than the size of the follicle they are connected to. Quite big at birth because of the maternal hormones, they regress in size within few months and enlarge again at the onset of puberty (Strauss et al., 1991).

SG are formed by one or more lobules connected to a secretory duct composed by stratified epithelium similar to IFE (Knutson, 1974). The cells at the periphery of the lobules are undifferentiated and have cobblestone morphology; the ones located closer to the centre are full of lipid droplets and have a centrally located nucleus. The cells closest to the duct disintegrate in a process mediated by lysosomal enzymes (holocrine secretion) (Rowden, 1968), releasing the sebum in the HF canal. Sebum is a mixture of fat, fatty acid and cell remnants, different from the mixture of lipids produced by the IFE keratinocytes (Zouboulis et al., 1991). Its function is to lubricate the hair and the skin.

Apocrine and eccrine sweat glands

Apocrine sweat glands are long and twisted tubular glands located in the dermis and connected to the hair follicle. In humans they are present only in the axillae and in the anogenital region; their secretion contains fragments of cytoplasm of the secretory cells and is rich in odour. In mice, apocrine glands are confined to non hair-bearing regions (Nasemann et al., 1983).

Eccrine sweat glands are independent of the hair follicle, they are tubular glands located deeply in the dermis and subcutaneous fat and they have a long duct that connects them to the surface of the IFE. In mammals they are present only in the palms and soles, whereas in humans are distributed over the entire body surface (Lever and Schaumberg-

Lever, 1993). Their function is to regulate body temperature by secreting sweat that subsequently evaporates (Nasemann et al., 1983).

1.1.1.3. Embryonic development of the pilosebaceous unit

The development of the pilosebaceous unit is driven by a complex interaction between epidermal and dermal cells (Fig. 1.5). The first signal for HF formation originates from the dermis and induces a thickening of the basal cells of the embryonic epidermis, known as the placode. This instructs some dermal cells lying in close proximity to compact in the dermal condensate (DC), which will become the dermal papilla (DP). The DC induces the placode cells to proliferate and as soon as the hair bud forms a bulbous structure around the dermal papilla the follicle starts growing downward (Hardy, 1992). The cells in the hair peg that are not in contact with the DP differentiate to form the ORS, while the matrix cells maintain contact with the DP and give rise to the hair cone and the inner root sheath, a process that likely requires lateral communication between the layers of epithelial cells (Millar et al., 1999). The core cells of the hair peg and the overlying IFE keratinocytes die forming the hair canal (Hashimoto, 1970). The hair follicle grows at an angle and in the meantime produces a bump that will develop into the attachment for the arrector pili muscle, a higher bump that will develop into the sebaceous gland, and sometime a third bump that will develop into the apocrine gland (Lever and Schaumberg-Lever, 1993).

1.1.1.4. Other epidermal cells

Melanocytes migrate from the neural crest to colonize the epidermis during embryonic development. They produce melanin and via long dendritic processes they transfer it to the keratinocytes, which incorporate the melanin granules through phagocytosis (Nasemann et al., 1983).

Melanocytes are sparsely distributed along the human IFE basal layer and are quite abundant in the HF matrix all around the dermal papilla (Lever and Schaumberg-Lever, 1993). Quiescent melanocyte progenitors reside in the bulge region of the HF (Nishimura et al., 2002). They are activated after skin injury when they move upward in the regenerating ORS and IFE (Staricco and Miller-Milinska, 1962) and can also

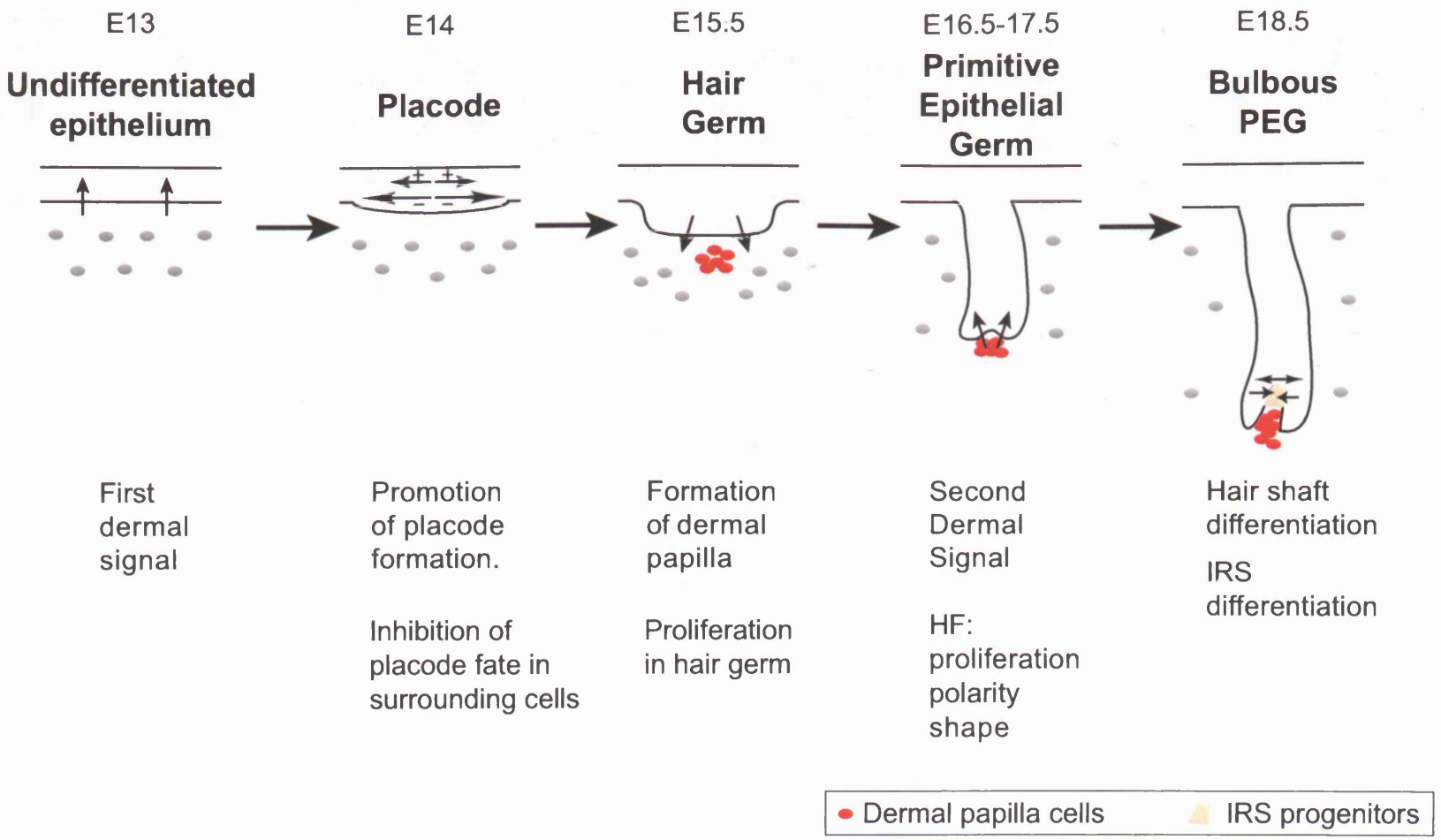

Figure 1.5. Embryonic development of the hair follicle. Diagram representing the first five stages of hair follicle development. At the top the embryonic days of mouse development are indicated, at the bottom the description of the stages. Arrows indicate intercellular signals. Adapted from Reddy et al., 2001, Millar, 2002 and Schmidt-Ullrich and Paus, 2005. For more details see main text.

migrate to adjacent hair follicles (Nishimura et al., 2002).

Langerhans cells are dendritic cells located usually in the suprabasal layers of the epidermis. They are resident macrophages that transfer the antigens that enter the epidermis to the immune system, rendering it a very important site for the initiation and regulation of immune responses (Romani et al., 2003).

Merkel cells are dispersed along the basal keratinocytes and are distinguishable only following appropriate histological and immunological staining. They are usually in close proximity of nerve endings and are believed to be epidermal nerve cells (Munger, 1991).

1.1.2. The dermis

The dermis constitutes the bulk of the skin. It is a connective tissue composed of collagenous and elastic fibres arranged in a matrix of glycosaminglycans. All these components are synthesized by the interspersed fibroblasts (Nasemann et al., 1983).

Specialized dermal fibroblasts and neural crest derived nestin positive cells are tightly packed in the HF dermal papilla, and multipotential progenitors for a variety of cell types can be isolated from the dermis (Fernandes et al., 2004; Sieber-Blum et al., 2004). Interspersed in the dermis are cells of the immune system, such as phagocytes and mast cells, responsible for the clearing of external particles via phagocytosis and triggering of the inflammatory response (Odland, 1991; Tharp, 1991). In addition the dermis contains nerves, blood vessels and the HF arrector pili muscles.

Each hair follicle is associated on one side, just below the sebaceous gland, to its arrector pili muscle. These are smooth or involuntary muscles that pull the hair follicles in vertical position to produce "gooseflesh" (Lever and Schaumberg-Lever, 1993).

The dermis is traversed by a complex network of nerves. The autonomous nerves reach the papillary dermis, the sebaceous and sweat glands, the arrector pili muscles and the vessels. They trigger the "gooseflesh" phenomenon, but probably have a much more complex role in the regulation of skin homeostasis. Sensory nerves are dispersed

throughout the dermis and terminate with both complex sensory bodies and free nerve ends (Nasemann et al., 1983).

The main network of cutaneous blood vessels is the subcutaneous plexus, at the junction between the dermis and the subcutaneous fat. Many arterioles, venules and capillaries are connected to this and form extremely ramified plexuses in the papillary dermis and around the hair follicles and sebaceous and sweat glands (Yen and Braverman, 1976)). There are also numerous lymphatic vessels draining the lower layers of the epidermis and the entire dermis (Odland, 1991).

1.2. Epidermal stem cells and their progeny

1.2.1. Epidermal turnover and hair follicle cycle

The upper layers of the IFE are constantly shed and replaced by cells deriving from the lower layers. All the squames of the outermost layer are shed from the human body in approximately 24 hours (Roberts et al., 1980)). One squame has a surface equivalent to about 25 basal cells; since about 4% of the basal cells are proliferating, as measured by pulse labelling of human subjects with tritiated thymidine (Dover, 1994) or by analysis of markers of proliferation (Pierard-Franchimont and Pierard, 1989), the basal layer regenerates itself competely approximately once a month (Jakic-Razumovic et al., 1992; Jensen et al., 1999).

The sebaceous glands are also characterized by rapid cell turnover. The sebocytes that disintegrate, liberating the sebum in the hair canal, are replaced by new differentiating cells originating from the periphery of the gland, where proliferation occurs. It has been calculated that in adult male mice most of the sebocytes transit through the gland in five days (Hamilton, 1974).

The hair follicles undergo continuous cycles of growth and regression (Fig. 1.6) (Paus and Cotsarelis, 1999; Stenn and Paus, 2001). Some time after HF formation, the matrix cells exhaust their proliferative capacity and keratinocytes in the HF lower portion

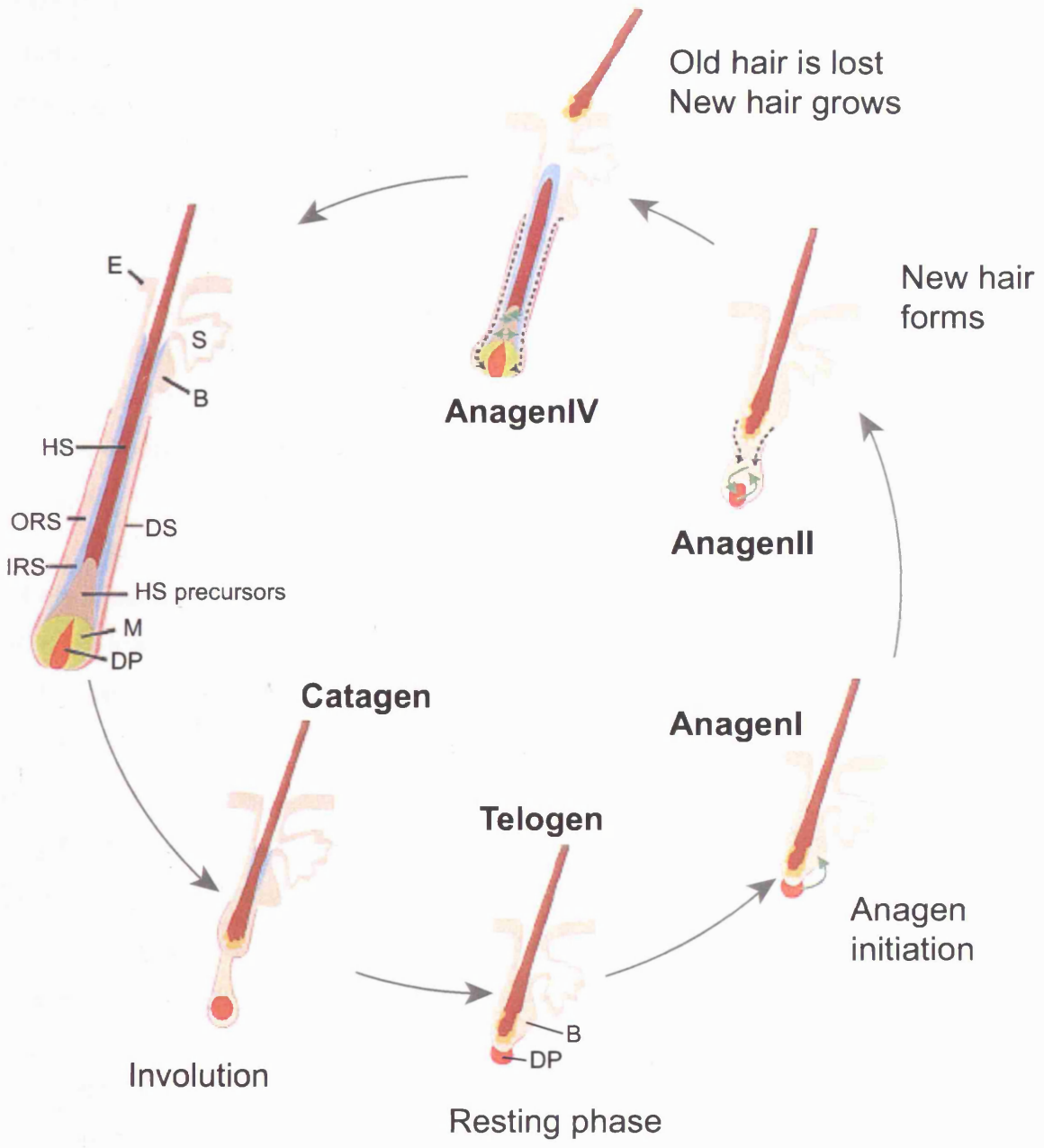

Figure 1.6. Schematic representation of the hair cycle. The various phases of the hair cycle are indicated (Catagen, Telogen, Anagen). The roman numerals indicate anagen substages. Abbreviations: E, epidermis; S, sebaceous gland; B, bulge; HS, hair shaft; ORS, outer root sheath;, IRS, inner root sheath; DS, dermal sheath; M, matrix; DP, dermal papilla. Adapted from Paus and Cotsarelis, 2001 and Reddy et al., 2001. For more detail see main text.

undergo apoptosis (Cotsarelis, 1997). During this phase, called catagen, the HF becomes shorter and the dermal papilla moves upward in the dermis, remaining in close proximity with the HF keratinocytes (Weedon and Strutton, 1981). At the end of this phase only the upper portion of the HF remains, with the dermal papilla extremely small and condensed in contact with the bulge. The HF remains in this quiescent state (called telogen) for a variable length of time, until the growing phase (anagen) starts again. During anagen the lower part of the HF thickens and grows deep in the dermis, pushing downward also the dermal papilla, which looks enlarged (Oliver and Jahoda, 1988). Matrix cells proliferate and their progeny differentiate moving upward and forming the IRS and a new hair shaft, which pushes away the old one (Oshima et al., 2001; Taylor et al., 2000).

The mechanisms regulating HF cycling are not completely understood (Stenn and Paus, 2001). It has been suggested that the proliferative capacity of the matrix cells works as a biological timer for the initiation of catagen (Paus and Cotsarelis, 1999). Different theories have been proposed about anagen initiation and the regeneration of the lower portion of the HF (Oshima et al., 2001; Panteleyev et al., 2001; Taylor et al., 2000), but they all acknowledge the crucial role of crosstalk between the dermal papilla and the HF keratinocytes (Niemann and Watt, 2002). Several microenvironmental cues delivered either by the vasculature or by the various cell types surrounding the HF are likely to play a role in the regulation of the hair cycle (Fuchs et al., 2001).

In rodents, the first two hair cycles in postnatal life are synchronized, and progressive asynchrony develops with subsequent cycles (Fuchs et al., 2001). There is some variation between different strains of mice, but generally, following hair formation, all follicles are in telogen at 3-4 weeks of age, in anagen at 5 weeks and again intelogen at 6-7 weeks. This second telogen phase has variable length and the HF are not synchronous in restarting anagen (Niemann et al., 2002).

1.2.2. Stem cells and transit amplifying cells

The high turnover of the epidermis, its ability to repair injuries and the inability of terminally differentiated cells to divide are indications for the presence of resident stem cells responsible for the maintenance of the tissue. The concept that stem cells give rise to all differentiated cells found in a tissue was proposed in 1901 (Adami, 1901), and this model was proposed to explain the characteristics of the epidermis in the early 1970s (Potten and Hendry, 1973) but the mechanisms that regulate stem cell self-renewal and differentiation are still subject of intense study and discussion (Mikkers and Frisen, 2005; Wagers et al., 2002; Watt and Hogan, 2000).

The balance between stem cell self-renewal and differentiation can be achieved by two distinct mechanisms: asymmetric divisions or populational asymmetry (Watt and Hogan, 2000). The outcome of stem cell division can be two stem cells, two differentiated daughters, one stem cell and one differentiated daughter (Watt, 2001). If this decision were cell autonomous the system would be too rigid to react to environmental alterations. Instead, it has been proposed that the specialized microenvironment regulates the proliferation of stem cells and the balance between self-renew and exit from the stem cell compartment (Schofield, 1978; Watt and Hogan, 2000). It is probably the combination of the intrinsic characteristics of the stem cells and their microenvironment that shapes their properties and defines their fate (Fuchs et al., 2004; Wagers and Weissman, 2004; Watt and Hogan, 2000). Asymmetric cell division has been observed in oesophageal epithelium (Seery and Watt, 2000) and recently also in the interfollicular epidermis (Lechler and Fuchs, 2005).

In the epidermis, stem cells divide infrequently even though they have a high capacity to self-renew (Lavker and Sun, 2000). Stem cells daughters can be either stem cells themselves or be destined to terminally differentiate. If this is the case, they are still able to sustain a certain number of cell divisions before their progeny terminally differentiate. The function of these rapidly dividing cells is to increase the number of differentiated cells derived from a single stem cell division and for this reason they are called transit amplifying (TA) cells. The main differences between stem and TA cells are the frequency of cell division (low vs. high) and the capacity to self-renew (indefinite vs. low) (Watt, 2001). An indication of the restricted number of cell

divisions of transit amplifying cells came from *in vivo* studies in mouse: when mouse epidermis is regenerated after skin irradiation, only about 10% of basal keratinocytes are able to form detectable foci of new epidermis (Potten, 1981; Potten and Hendry, 1973).

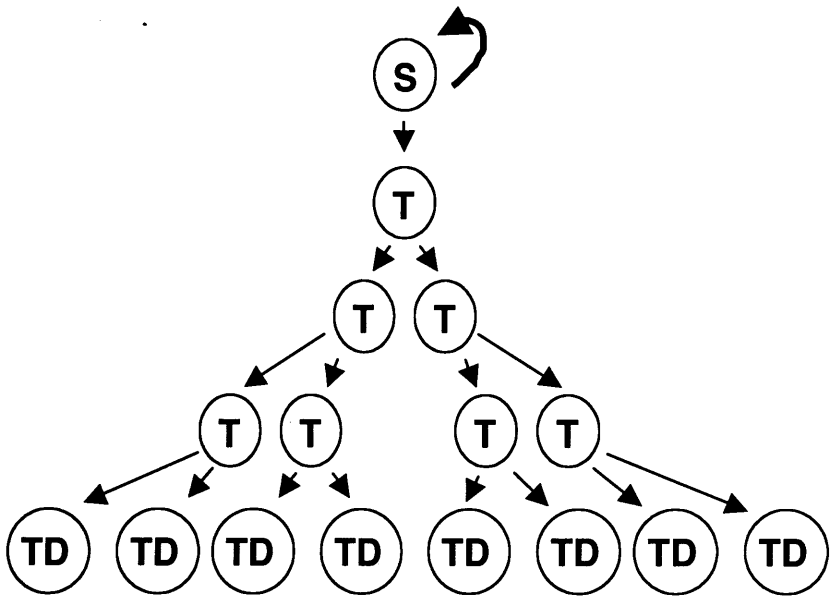

Figure 1. 7. Diagram illustrating the role of transit amplifying cells

A single stem cell (S) divides and gives rise to another stem cell and a transit amplifying cell (T). After three rounds of division, the progeny of the transit amplifying cell undergo terminal differentiation. Diagram reproduced from (Watt, 2001).

1.2.3 Identification of epidermal stem cells

Epidermal stem cells have initially been identified based on their proliferative characteristics. Culture of primary human keratinocytes at clonal density allowed the identification of stem cells based on their proliferative potential (Watt, 2001). While transit amplifying cells give rise to small clones of differentiated cells, stem cells give rise to big clones formed mainly by small cells that, once trypsinized and replated at clonal density, give rise to other big clones with similar characteristics (holoclones, see (Barrandon and Green, 1987). If these clones are transplanted onto nude mice they reconstitute all layers of human epidermis (Jones et al., 1995). The ability to undergo

clonal growth has been used to screen for cell surface markers of epidermal stem cells (Jones et al., 1995; Jones and Watt, 1993).

The traditional approach used to identify murine slow cycling epidermal cells consists in giving neonatal mice repeated injections of [^{3}H]-thymidine or Bromo-deoxy-uridine (BrdU) to virtually label all dividing cells and subsequently wait for a certain length of time until the rapidly dividing cells have diluted and lost the BrdU. The slow cycling stem cells are identified as label retaining cells (LRC) (Braun and Watt, 2004). In mouse epidermis there are scattered LRC in the basal layer of the IFE and SG, but most of the LRC are clustered in the bulge region of the hair follicle between the sebaceous gland and the connection to the arrector pili muscle (Bickenbach, 1981; Braun et al., 2003; Cotsarelis et al., 1990).

The two approaches have been reconciled in studies in rats showing that the clonogenic cells derive from the HF region containing LRC in mice (Oshima et al., 2001). The proliferative potential of LRC has been studied in vitro (Morris and Potten, 1994)) and, more recently, clonogenic keratinocytes have been isolated from mouse hair follicles (Morris et al., 2004).

1.2.4. Relationship between IFE, SG and bulge stem cells

Populated by quiescent cells and set aside in an anatomically protected region of the skin, the HF bulge is the perfect candidate to be the stem cell niche in mouse epidermis (Fuchs et al., 2001; Fuchs et al., 2004). Lineage marking analysis has shown that bulge cells give rise to the lower portion of the follicle at each anagen initiation, but they also reconstitute IFE and SG during injury repair (Morris et al., 2004; Oshima et al., 2001; Taylor et al., 2000).

The bulge stem cell hypothesis postulates therefore that epidermal stem cells reside in the bulge and their progeny migrate to maintain all the lineages found in the epidermis (Fuchs et al., 2004). Keratin 15 and CD34 expression in adult mouse skin is restricted to the bulge region (Liu et al., 2003; Tumbar et al., 2004), and by combining these markers with the slow cycling characteristics several groups have started to analyze the gene

expression profile of bulge cells looking for regulators of epidermal stem cells fate (Morris et al., 2004; Tani et al., 2000; Tumbar et al., 2004).

Even though the bulge region presents the ideal characteristics of the stem cell niche, and it has been shown that bulge cells can repopulate the entire epidermis (Oshima et al., 2001) and several molecular markers are expressed selectively in this region, long-term lineage marking studies have demonstrated that in undamaged epidermis there are distinct stem cell populations in the IFE and SG (Ghazizadeh and Taichman, 2001). When they receive the appropriate mesenchymal stimuli, IFE cells can be induced to differentiate into hair and sebocyte lineages (Ferraris et al., 1997; Reynolds and Jahoda, 1992). Even epidermal keratinocytes from foreskin, which is a non hair-bearing region, can form HF when grafted with mouse dermal papilla enriched cells (Ferraris et al., 1997; Kishimoto et al., 2000). Less is known about the potential of sweat gland cells, but they are thought to derive from multipotent epidermal progenitors, and in certain conditions are also able to repopulate stratified epithelium (Miller et al., 1998).

In normal intact skin bulge cells are necessary for hair follicle survival but not for epidermal homeostasis. When bulge cells are selectively killed in adult grafted epidermis, the skin loses the hair follicles, but the IFE is maintained normally. Moreover, in vivo lineage marking of bulge cells did not show a contribution of bulge cells to the IFE in homeostasis (Ghazizadeh and Taichman, 2001). Therefore, although the progenitors in each compartment of the epidermis can regenerate the entire epidermis and are true multipotent stem cells, at the steady state they only maintain the compartment they are lying in, and their fate choice is directed by the microenvironment. IFE, SG and bulge stem cells give rise to interfollicular keratinocytes, sebocytes and hair follicles respectively.

1.2.5. Lineage marking of the progeny of epidermal stem cells

In mouse dorsal epidermis the squames in the upper layers are arranged in ordered columns aligned with cells in the basal layer. These columns can be made clearly apparent by swelling the epidermis with an alkaline solution (Mackenzie, 1970). The basal cells that lie under the centre of each cornified cell are less likely to be in mitosis than the cells under the edge of the cornified cells (Mackenzie, 1970) and are more

likely to be LRC (Potten and Morris, 1988). These observations led to the Epidermal Proliferative Unit model, according to which the central basal cell is the stem cell that maintains all the differentiated cells in the column aligned above it (Potten, 1988 #74).

Analysis of chimeric follicles expressing different genotypic markers has shown that the ORS originates directly from the bulge cells, while the matrix contains progenitors of all 6 lineages found in the hair and IRS, and also more restricted progenitors for the 3 lineages of the hair and the 3 of the IRS (Kopan et al., 2002). It is still controversial whether the companion layer is generated by matrix precursors or directly from the bulge like the ORS (Legue and Nicolas, 2005; Niemann and Watt, 2002).

In the hematopoietic system there is a clear hierarchy between the stem cells and the differentiated cells. HSC are multipotent and give rise to progenitors whose potential becomes more and more restricted following cell division (Weissman, 2000). The study of the hematopoietic system has determined the model of multipotent stem cells giving rise to more restricted progenitors and finally committed progenitors for each lineage. It is not clear the degree of overlapping between the committed progenitor model and the stem/TA cell model in the epidermis. TA cells could be committed to differentiate along one or few lineages, like the hematopoietic progenitors. Alternatively, they could still be multipotent and differ from stem cells only by having restricted self-renewal ability. In this case, lineage choice would be determined by the environment (Watt, 2001). Instead of discrete populations of stem and transit amplifying cells, there may be a gradual loss of self-renewal capacity and multipotency and a gradually enhanced propension to undergo terminal differentiation along one lineage (Fig. 1.7) (Niemann and Watt, 2002).

1.2.6. Epidermal cancers

The epidermis is constantly subject to environmental assaults (UV irradiation, chemical carcinogens, viruses and other pathogens) that produce oncogenic mutations. Fortunately, relatively few skin cancers develop because the majority of epidermal cells are lost through differentiation (Owens and Watt, 2003). Only the stem cells, being permanent residents of the tissue, have the potential to accumulate the multiple genetic lesions that lead to neoplastic conversion and can give rise to tumours

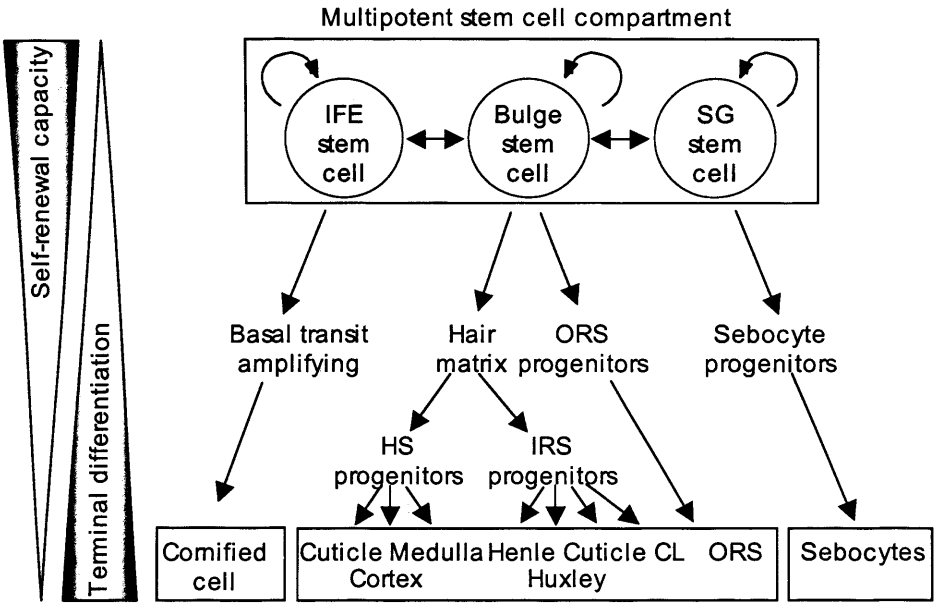

Figure 1.8. Model of lineage relationships within the epidermis. Multipotent progenitors reside in the interfollicular epidermis, hair follicle bulge and sebaceous gland and have unlimited self-renewal capacity. Even though they have the capacity to regenerate the entire epidermis (double arrows), at the steady state they only maintain the compartment they are lying in (arrows). Epidermal stem cell progeny gradually loses self-renewal potential and finally undergos terminal differentiation (triangles). Adapted from Niemann and Watt, 2002. For more details see main text.

(Morris et al., 2000). Moreover, the stem cells possess the highest potential for clonal expansion and so there is a higher probability that one of their progeny will acquire another mutation, and so on (Owens and Watt, 2003; Perez-Losada and Balmain, 2003).

TA cells and even differentiated keratinocytes can be induced to proliferate (Barrandon et al., 1989; Pelengaris et al., 1999) and in principle could give rise to tumours, but malignant epidermal tumours originating from TA calls have not yet been described (Owens and Watt, 2003). In addition, even though altered differentiated keratinocytes are going to be lost as a result of epidermal turnover, they could still influence tumour progression by regulating stem cell proliferation (Owens and Watt, 2003). For example, in mice treated with tumour inducing agents, suprabasal keratinocytes produce high levels of transforming growth factor-ß, which is an inhibitor of epidermal proliferation (Akhurst et al., 1988). Integrin expression by the suprabasal keratinocytes can exert a positive or negative effect on the underlying basal layer by affecting sensitivity to TGF-ß (Owens et al., 2003; Owens and Watt, 2001).

Tumours showing characteristics of each epidermal lineage have been described, ranging from benign adenoma to carcinoma. Usually histological analysis indicates their site of origin (Lever and Schaumberg-Lever, 1993). Squamous cell carcinomas (SCC, and in mice their benign precursors, papillomas) show signs of interfollicular differentiation and derive from the IFE. Basal cell carcinomas (BCC) look more undifferentiated and it has been proposed that they arise from the undifferentiated ORS cells (Bolognia and Braverman, 1999). Sebaceous adenomas are an example of tumours originating from the sebaceous glands and are formed by an outer layer of proliferating keratinocytes surrounding differentiated sebocytes. Trichofolliculomas and pilomatricomas arise from the hair follicles (Lever and Schaumberg-Lever, 1993). There are also mixed-lineage tumours. For examples, sebeomas show both sebaceous and squamous differentiation and sebaceous trichofolliculomas show sebaceous and hair differentiation (Owens and Watt, 2003).

It is possible that a tumour is more malignant if it arises from stem cells and more benign if it arises from committed progenitors, as described for leukaemias (Reya et al., 2001) and that tumours arising from stem cells are those showing multilineage

differentiation. However SCCs, the most malignant epidermal tumours, show only IFE differentiation (Sober et al., 1999).

1.3. Molecular regulation of epidermal lineage committment

All constituents of the microenvironment influence the lineage choice made by the stem cell progeny. They include extracellular matrix, diffusible factors (growth factors, cytokines, morphogens), direct contact with neighbouring cells, the availability of oxygen and nutrients, and even mechanical stimuli such as tension forces (Niemann and Watt, 2002; Spradling et al., 2001; Watt and Hogan, 2000). Epithelial-mesenchymal interactions between the keratinocytes and the dermis have a crucial role. The best characterized interaction of this type is between the dermal papilla cells and the hair follicles, which regulates both hair follicle development and cycle (Fuchs et al., 2001; Millar, 2002; Reynolds and Jahoda, 1992).

Several transcription factors and signalling pathways are involved in the regulation of epidermal homeostasis. Most signalling pathways involved in hair follicle development have a role also in the regulation of hair follicle cycling and in stem cell self-renewal and differentiation (Fuchs et al., 2001). These pathways (eg Wnt, Hh, Notch, BMP) are involved in embryonic development and adult homeostasis not only of the epidermis but also of many other tissues and are conserved through evolution (Millar, 2002).

1.3.1. Wnt/β-catenin pathway

β-catenin was first identified in vertebrates as a component of adherens junctions that was a homolog of Drosophila Armadillo (McCrea et al., 1991), known to affect embryonic patterning (Wieschaus and Riggleman, 1987). *Wnt* genes were first discovered for they oncogenic potential and subsequently known to be homologues of Drosophila Wingless (Rijsewijk et al., 1987). As Armadillo appeared to have a role not only in cell adhesion but also in signal transduction downstream of Wingless (Riggleman et al.,; 1990Peifer et al., 1993), β-catenin was soon identified as the key effector of the Wnt signalling pathway (Hinck et al., 1994) and in fact all components

of the pathway are highly conserved through evolution from hydra to humans (Miller, 2002; Wodarz and Nusse, 1998).

Wnt signalling regulates cell fate, proliferation, migration, polarity, and death (Miller, 2002). Wnt proteins act as morphogens in several developmental processes, such as neural crest induction (Steventon et al., 2005), somitogenesis (Aulehla et al., 2003), neurogenesis (Ciani and Salinas, 2005; Li and Pleasure, 2005), retinal development (Van Raay et al., 2005), lung and kidney branching (De Langhe et al., 2005; Lin et al., 2001).

Wnt signalling has also a key role in the homeostasis of a number of adult tissues, such as lung (He et al., 2005), cartilage (Yates et al., 2005), CNS (Sieber-Blum, 2003), intestine (Pinto and Clevers, 2005) and the hematopoietic system (Staal and Clevers, 2005). In particular, in adult tissues Wnt signalling regulates both lineage commitment and stem cell self-renewal (Niemann and Watt, 2002; Pinto and Clevers, 2005; Staal and Clevers, 2005).

Aberrant Wnt signalling is associated with a number of diseases and cancers (Nusse, 2005; Reya and Clevers, 2005). The most striking example is colon cancer, with 80% of the cases due to mutations in APC that abolish its interaction with β-catenin, and in most of the other cases activating mutations in β-catenin are found (Kolligs et al., 2002; Pinto and Clevers, 2005; Polakis, 1999). Activating mutations in β-catenin have been associated also with hepatocellular carcinoma, and with carcinoma of the ovarian and uterum endometrium (Polakis, 1999). Mutations in the regulatory regions of β-catenin promoters have been found in tumours of the brain (Zurawel et al., 1998) and prostate (Voeller et al., 1998; Yardy and Brewster, 2005) and in melanomas (Brantjes et al., 2002) and hair follicle tumours (Chan et al., 1999).

1.3.1.1. Canonical Wnt signalling cascade

Studies in Xenopus, in which activation of the Wnt pathway causes duplication of the body axis, gave the first information on the structure of the canonical Wnt pathway (Dominguez et al., 1995; Guger and Gumbiner, 1995; He et al., 1995; McMahon and Moon, 1989; Sokol et al., 1995).

β-catenin and Armadillo are both composed of an N-terminal domain of about 130 aa, a core formed by 13 armadillo repeats of 32 aa each, and a C-terminal tail of about 100aa (McCrea et al., 1991; Peifer et al., 1992). The two external domains are acidic, while the arm repeats form a single domain with a hydrophobic core and basic surface (Huber et al., 1997). The different domains are responsible for the interaction with several different proteins at the cell borders, in the cytoplasm and in the nucleus.

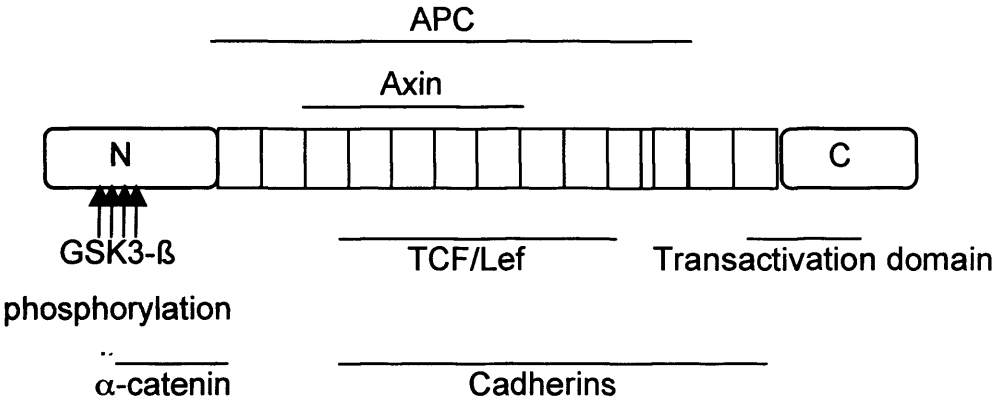

Figure 1. 9.

Diagram of β-catenin structure and interaction domains for adhesion and signalling. N, N-terminal domain; C, C-terminal domain. The rectangles represent the Armadillo repeats. Modified from Peifer and Polakis, 2000.

β-catenin is a structural component of the adherens junctions, where it binds E-cadherin through the Armadillo repeats (Aberle et al., 1994) in a complex containing α-catenin, vinculin and α-actinin (Knudsen et al., 1995; Weiss et al., 1998). β-catenin is therefore thought to have a role in connecting adherens junctions to the actin cytoskeleton (Barth et al., 1997).

The cytoskeletal component APC (Nathke, 2005) competes with E-cadherin for binding to β-catenin (Huelsken et al., 2001) and is part of a large multiprotein complex that

usually intercepts the cytoplasmic pool of β-catenin not complexed with cadherins (Peifer and Polakis, 2000). Axin/conductin is another component of the complex (Chia and Costantini, 2005; Polakis, 1999) and binds both APC and β-catenin (Hart et al., 1998; Sakanaka and Williams, 1999). The APC/Axin complex binds and activates the serine/theronine kinase GSK3-β (glycogen synthase kinase 3-β), putting it in close contact with β-catenin (Hart et al., 1998; Ikeda et al., 1998). GSK3-β phosphorylates β-catenin on selected residues of the N-terminal domain (in particular the Ser 33, 37, 41 and 45, see (Polakis, 1999). Phosphorylated β-catenin is ubiquitinated and subsequently degraded by the proteasome (Hart et al., 1999; Liu et al., 1999).

In the presence of Wnt signal GSK3-β is inhibited, so that β-catenin accumulates in the cytoplasm and eventually translocates to the nucleus (Henderson and Fagotto, 2002). There it regulates transcription of target genes by interacting with members of the TCF/Lef (T cell factor/ lymphoid enhancer factor) family of High Mobility Group (HMG) transcription factors, first identified as transcriptional regulators of T-lymphocyte differentiation (Brantjes et al., 2002; Huber et al., 1996; Molenaar et al., 1996; van de Wetering et al., 1992). The central armadillo repeats of β-catenin interact with these transcription factors, while the C-terminal domain functions as a transactivator (Molenaar et al., 1996; van de Wetering et al., 1997). The outcome of Wnt signalling in a cell is determined by the factors that β-catenin encounters in the nucleus: for example Lef1 is a transcriptional co-activator (Filali et al., 2002), while TCF3 is a repressor (Brantjes et al., 2002; Clevers and van de Wetering, 1997; Fuchs et al., 2001).

The Wnt signal that results in GSK3-β inhibition is quite complex. Wnt genes encode secreted proteins (Papkoff and Schryver, 1990; van Leeuwen et al., 1994) that interact with transmembrane receptors belonging to the Frizzled family (Wodarz and Nusse, 1998). The common effect is the activation of Dishevelled, which is necessary for the inactivation of GSK3-β (Klingensmith et al., 1994; Theisen et al., 1994). It is assumed that the gene multiplicity enables different cells to express and receive Wnt signals at different times, explaining how the Wnt pathway is involved in the development of many different organs (Cadigan and Nusse, 1997). LRP (LDL-receptor related protein) 5 and 6 are co-receptors of Wnts and are responsible for an additional level of

regulation of the pathway (Cong et al., 2004; Pinson et al., 2000; Tamai et al., 2000). There are also two classes of extracellular Wnt antagonists: the Frizzled-related protein WIF (Wnt inhibitory factor)-1 and Cerberus bind directly to Wnt proteins, while members of the Dickkopf (Dkk) family bind to the Wnt receptor complex (Kawano and Kypta, 2003).

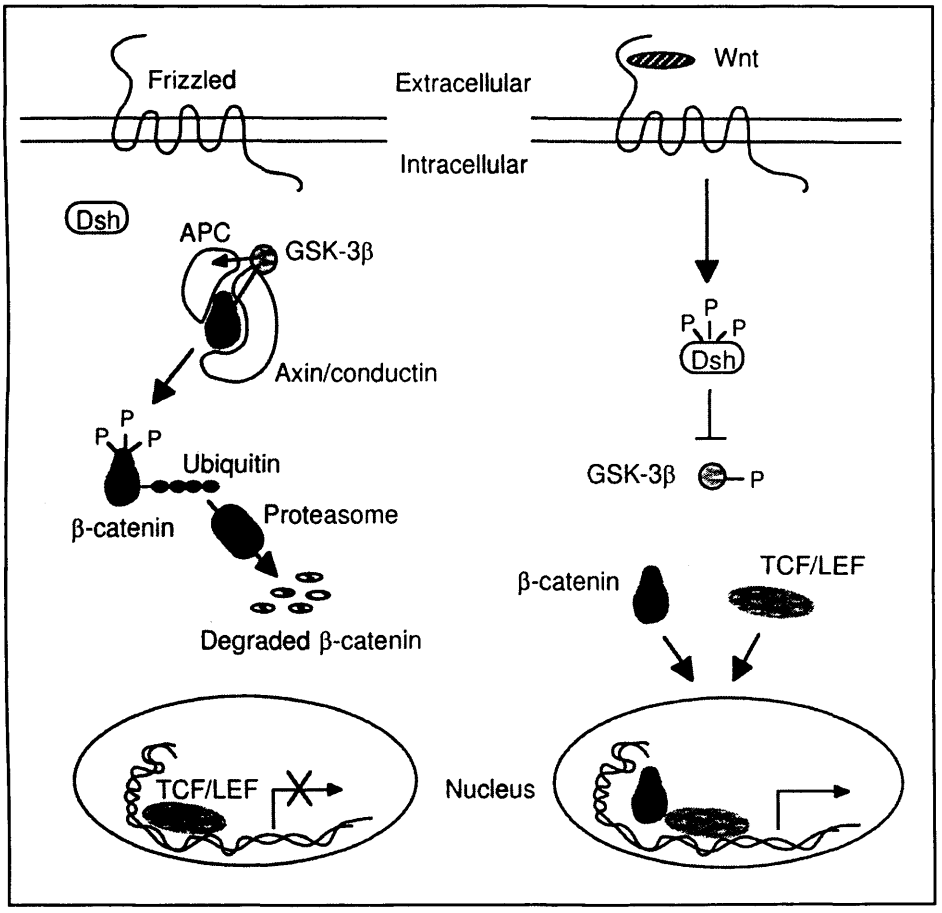

Figure 1. 10. Diagram representing the canonical Wnt signalling pathway.

In the absence of Wnt signal, cytoplasmic β-catenin is targeted for ubiquitination by a complex containing APC, Axin-Conductin and GSK3-β. Wnt binds the receptor Frizzled and signals via Dishevelled and the result is the inhibition of the APC/Axin/GSK3-β complex. Free β-catenin therefore translocates to the nucleus and regulates transcription by binding TCF/Lef transcription factors. Dickkopf is one of the inhibitors of Wnt signal. Figure reproduced from (Zhu, 1998). See main text for more details.

It is important to note that not all Wnt/Frizzled pairs signal via β-catenin stabilization, but some of them activate alternative (non-canonical) signalling pathways characterized by increase in intracellular calcium and activation of the kinases CamKII and PKC (Kuhl et al., 2000; Miller et al., 1999), or acting through cyclic GMP or JNK pathways (Veeman et al., 2003). The relationship between these different pathways is not clear, but it must be remembered that the effects of gain or loss of function of β-catenin do not completely reflect Wnt function. Moreover, Wnt signalling intersects and interacts with many other signalling pathways, and the factors regulating β-catenin stability are becoming more and more numerous (Fuchs et al., 2001). For example, Presenilin-1, known for its role in regulating Notch activity and the proteolysis of the β-amyloid precursor protein (Haass and Baumeister, 1999), is also interacting with β-catenin and facilitating β-catenin turnover independently of its other two activities (Murayama et al., 1998; Soriano et al., 2001).

1.3.1.2. Wnt/β-catenin signalling in skin

The first dermal signal inducing HF formation involves β-catenin activation. β-catenin appears in the nucleus of the dermal cells underlying the future placode (Noramly and Morgan, 1998), and Lef1 appears in the mesenchyme prior vibrissae formation (Kratochwil et al., 1996). There is evidence that the signal causing Lef1 induction could be a Wnt produced from the dorsal neural tube (Olivera-Martinez et al., 2001). Nuclear β-catenin and Lef1 subsequently appear in the placodes (Jamora et al., 2003), and b-catenin signalling plays a role during each stage of HF development (Fig.1.10) (Millar, 2002).

Several Wnt proteins and Wnt receptors are found in embryonic and adult adult mouse skin (Millar, 2002; Reddy et al., 2001; Reddy et al., 2004). Wnt10b and 10a are expressed in the placodes, and also Wnt3, 4, 6, 7b and 11 are detectable in embryonic epidermis, while Wnt3, 3a, 5a, 10a, 10b and 11 are expressed in different regions of anagen HF bulb (Reddy et al., 2001). During hair growth, Wnt signalling occurs in the

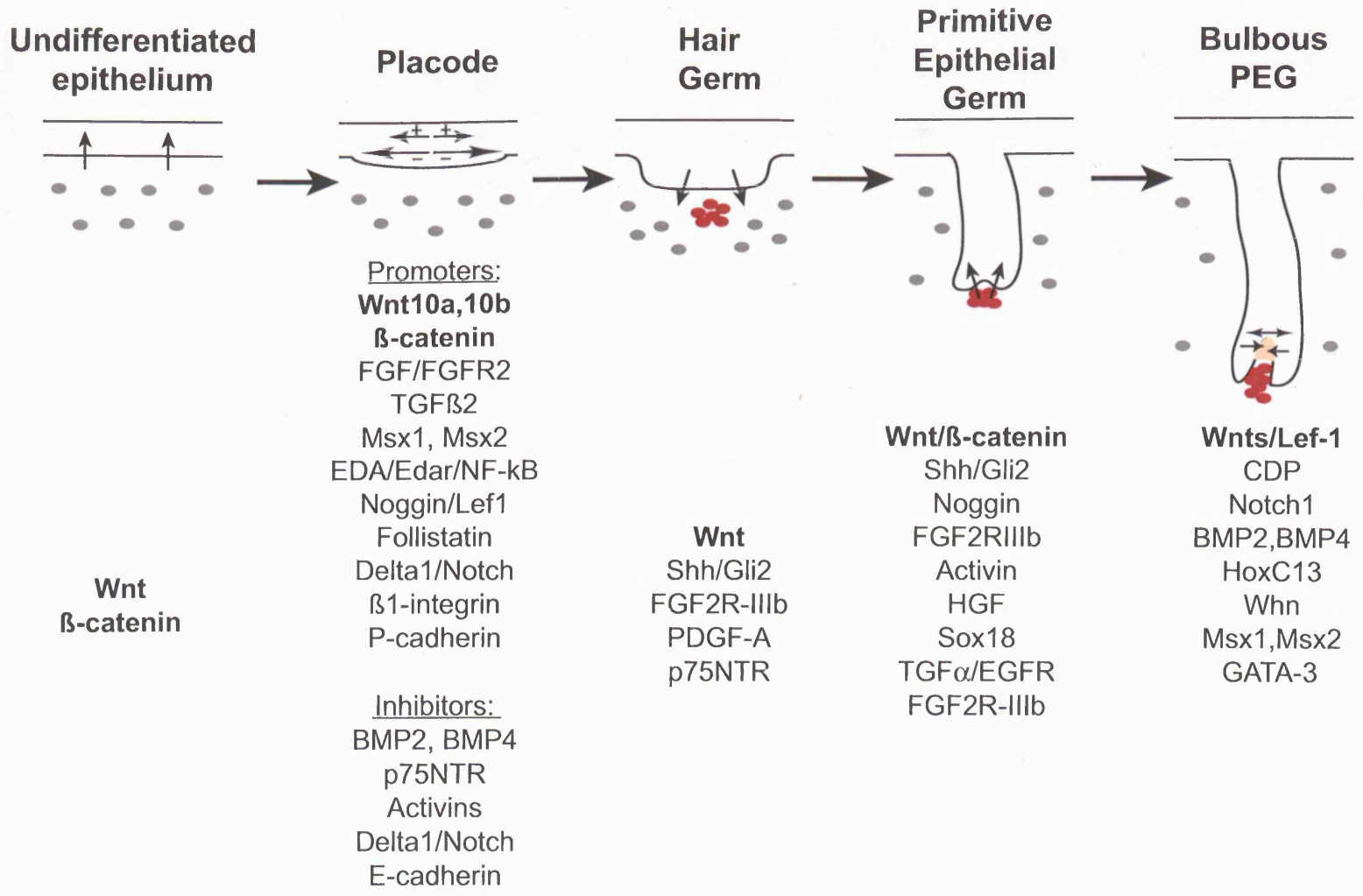

Figure 1.11. Intercellular signalling during hair follicle morphogenesis. Wnt signalling is involved in each stage of HF development (highlighted). Some of the signalling pathways indicated in the diagram are discussed in more detail in this thesis. Adapted from Reddy et al., 2001, Millar, 2002 and Schmidt-Ullrich and Paus, 2005. For more details see main text.

bulge, in the precortex cells of the matrix and in the dermal papilla, as indicated by accumulation of nuclear β-catenin or activation of a reporter gene (DasGupta and Fuchs, 1999; Merrill et al., 2001; Niemann et al., 2002). Hair shaft precursor cells express also Dishevelled2 and Wnt3 is expressed by adjacent cells (Millar et al., 1999). Wnt proteins maintain the hair inducing ability of dermal papilla cells in culture (Kishimoto et al., 2000). Lef1 is expressed in the matrix, where it binds specific consensus sequences in the regulatory elements of several hair keratin genes (DasGupta and Fuchs, 1999; Merrill et al., 2001). TCF3 is in the bulge (Merrill et al., 2001); in addition, a subpopulation of matrix cells is stained by an antibody against TCF3/4 (Kopan et al., 2002).

The keratin 14 (K14) promoter drives expression of any transgene in the basal layer of the interfollicular epidermis, the ORS and the sebaceous glands, therefore targeting all epidermal stem and progenitor cells (Byrne et al., 1994; Vassar et al., 1989; Wang et al., 1997). It has been used to interfer with the Wnt/β-catenin pathway in several transgenic mouse models. Mice overexpressing Wnt3 have fragile hair shafts (Millar et al., 1999). Mice expressing constitutively active β-catenin have hyperproduction of hair follicles and develop tumours similar to human pilomatricomas and trichofolliculomas (Gat et al., 1998). These benign tumours have a high degree of hair differentiation and in humans have been associated with activating mutations of β-catenin (Chan et al., 1999). In the opposite situation, if β-catenin is conditionally deleted in the skin during embryogenesis there is no hair formation, and if the deletion occurs after birth the hair is lost after the first hair cycle (Huelsken et al., 2001). Hair follicle development is completely abolished also when Dickkopf-1 is ectopically expressed (Andl et al., 2002). LEF1 gene targeting lead to mice lacking hair follicles and wiskers and with defects in all the structures that depend on epithelial-mesenchimal interaction for their development (van Genderen et al., 1994). Transgenic mice in which the Wnt pathway is blocked by a dominant negative form of Lef1 have progressive hair loss and develop epidermal cysts with interfollicular differentiation (Merrill et al., 2001; Niemann et al., 2002). Surprisingly, they also develop tumours, but this time with sebaceous differentiation (Niemann et al., 2002). All these transgenic models indicate the role of β-catenin in favouring differentiation along the hair lineages.

1.3.2. Signalling pathways and transcription factors interacting with β-catenin and regulating HF development and epidermal lineage commitment

It has recently been shown that in the epidermis the activity of β-catenin is regulated in a much more complex way than via Wnt alone. This is because the Wnt pathway interacts at many levels with other signaling pathways, such as BMP (Jamora et al., 2003), Notch (Nicolas et al., 2003) and Hedgehog (Millar, 2002). Growing interest is focussing also on the reciprocal regulation between β-catenin and nuclear receptors (Mulholland et al., 2005). Finally, a known β-catenin target gene, c-Myc (He et al., 1998), has opposite effects on epidermal lineage compared to β-catenin activation (Arnold and Watt, 2001; Braun et al., 2003).

Hair follicles and feathers develop in a very similar way (Millar, 2002) and therefore studies in both mouse and chick have contributed to our understanding of the molecular mechanisms regulating hair follicle induction and growth (Fig. 1.10). There is evidence that the same molecules are acting also in human HF development (Holbrook et al., 1993; Kaplan and Holbrook, 1994). For example, human families carrying mutations in genes involved in HF development show similar phenotypes to the correspondent mouse mutants (Millar, 2002).

1.3.2.1. BMP signalling.

Placode formation and HF induction are regulated by the interaction between β-catenin and bone morphogenetic proteins (BMP) signalling. Together with TGF-β isoforms and activins, BMPs are members of the TGF-β family of secreted cytokines. They bind to and activate serine/threonine kinase receptors transducing downstream signals through SMAD proteins (Waite and Eng, 2003). All TGF-β family members control a large number of biological functions including cell proliferation, differentiation, cell fate decision and apoptosis in many different tissues during embryonic development and postnatal life, but BMPs are the most studied in relation to hair follicle development and cycling (Botchkarev and Sharov, 2004).

During hair follicle formation BMP2 and 4 are expressed by epithelial and mesenchymal cells (Kratochwil et al., 1996; Kulessa et al., 2000), while only mesenchymal cells express the BMP inhibitor Noggin. Members of the BMP family are inhibitors of follicle formation (Noramly and Morgan, 1998) and several BMP inhibitors, and in particular Noggin, are expressed in developing follicles, blocking BMP action within the follicle but without diffusing into the interfollicular regions (Botchkarev et al., 1999). Inhibition of BMP signalling by the antagonist Noggin is required for HF induction (Botchkarev et al., 1999; Jamora et al., 2003). Dermal Noggin is necessary for the mainenance of Lef1 in the nucleus and its interaction with β-catenin, also in the nucleus because of the simultaneous Wnt signal (Jamora et al., 2003).

In adult epidermis several BMP family members produced in the hair shaft precursor cells and in the dermal papilla promote differentiation and contribute to lineage choices within the follicles. (Wilson et al., 1999). Noggin is required for normal anagen (Botchkarev et al., 2001) and inhibition of BMP signalling via overexpression of Noggin in the hair matrix impairs differentiation of the hair shaft: the precursors of hair shaft and hair cortex continue to proliferate and fail to differentiate (Kulessa et al., 2000). Overexpression of BMP4 in the ORS inhibits proliferation in the matrix and causes ectopic expression of hair keratin genes in the ORS (Blessing et al., 1993). Conversely, conditional ablation of BMP-receptor BMPR1A impairs IRS differentiation and excessive proliferation leads to the formation of cysts and matricomas (Andl et al., 2002; Kobielak et al., 2003).

BMP signalling is mediated by the homeobox transcription factors Msx1 and Msx2 (Kulessa et al., 2000), which are also expressed in the placode. Mice lacking Msx1 and Msx2 have reduced HF number (Satokata et al., 2000). Conversely, overexpression of Msx2 in the matrix reduces proliferation and induces premature differentiation (Jiang et al., 1999).

1.3.2.2. Hedgehog signalling

Hedgehog signalling has a key role in the regulation of patterning and differentiation during embryogenesis (Ingham and McMahon, 2001), and misregulation of Hedgehog

signalling is associated with several forms of cancer (Hooper and Scott, 2005; Taipale and Beachy, 2001).

The *hedgehog* (*hh*) gene was first identified in Drosophila (Nusslein-Volhard and Wieschaus, 1980) and has three homologues in verebrates: Sonic, Indian and Desert Hedgehog (Shh, Ihh and Dhh). Two multipass membrane proteins, Patched (Ptc) and Smoothened (Smo), transduce the Hh signal. In the absence of ligand, Ptc inhibits the activity of Smo, but Shh binding to Ptc represses Ptc activity, leading to derepression of Smo, modification and translocation of the Gli family of transcriptor factors and regulation of target genes (Hooper and Scott, 2005).

There are two vertebrates homologues of Drosofila Ptc, Ptc1 and Ptc2 (Bitgood et al., 1996). Shh, Ihh and Dhh are expressed in different patterns and regulate different developmental processes but they all bind to both Ptc1 and Ptc2, and regulate transcription via Gli1, Gli2 and Gli3 (Ingham and McMahon, 2001). Various factors regulate Hedgehog signalling: cleavage and lipid modification influence the range of action (short or long) of Hh proteins (Porter et al., 1996); Dispatched (Disp) is involved in the secretion of Hedgehog proteins (Burke et al., 1999); the membrane bound protein Hedgehog-interacting protein (Hip1) binds Hh proteins, attenuating the signal (Chuang and McMahon, 1999). Ptc itself is a target of Hedgehog signalling and its expression increases in response to Hh (Taipale et al., 2000).

In the epidermis, expression of Shh and Ptc are one of the earliest features of HF development and Shh signalling is required for the maturation of the hair germ (Mill et al., 2003; St-Jacques et al., 1998). Mice lacking Shh have placodes and dermal condensates but HF fail to develop further (Chiang et al., 1999; Karlsson et al., 1999; St-Jacques et al., 1998). When Shh signalling is blocked, some markers of follicular differentiation are still expressed, indicating that Shh is required primarily for proliferation and not differentiation (Callahan and Oro, 2001).

In adult epidermis Shh expression is restricted to a subpopulation of matrix cells, on the side of the anagen hair bulb closest to the IFE, while Ptc is expressed in all adjacent matrix cells (Gat et al., 1998; Oro and Higgins, 2003). Ptch and Gli1 are expressed in both HF and dermal papilla cells (Dahmane et al., 1997; Ghali et al., 1999). Shh induces

proliferation and is necessary for anagen induction. Mice treated with anti-Shh antibodies show impaired epithelial growth at sites of folliculogenesis (Wang et al., 2000) and adenovirus-mediated expression of Shh stimulates anagen initiation (Sato et al., 1999).

Aberrant regulation of Shh signalling is the primary cause of BCC, the most malignant and undifferentiated epidermal cancer (Callahan and Oro, 2001; Hutchin et al., 2005). Ptc is mutated in human nevoid basal-cell carcinoma syndrome (Hahn et al., 1996), mutations in Ptc and Smo have been found in human sporadic BCCs (Gailani et al., 1996; Xie et al., 1998) and Hh target genes are expressed in BCCs (Bonifas et al., 2001). Overexpression of Shh in mouse epidermis leads to alterations similar to BCC (Oro and Scott, 1997), and the same happens to mice overexpressing Gli transcription factors (Grachtchouk et al., 2000; Grachtchouk et al., 2003; Nilsson et al., 2000).

Hh signalling regulates not only hair growth but also sebocyte growth and differentiation. In adult epidermis Ihh is expressed in differentiated sebocytes and in sebaceous tumours Gli1 is activated in the underlying sebocyte progenitors (Niemann et al., 2003). Ihh stimulates the proliferation of sebaceous progenitor cells, and inhibition of Hh signalling with cyclopamine reduces proliferation and increases differentiation of cultured sebaceous cells (Niemann et al., 2003). Mice expressing a dominant negative mutant Gli2 fail to develop sebaceous glands and overactivation of Smoothened determines ectopic sebaceous differentiation (Allen et al., 2003).

There is evidence for crosstalk between the Hh and Wnt pathways both in normal development (Ingham and McMahon, 2001) and in tumours (Taipale and Beachy, 2001). Shh transcription is induced in mice overexpressing β-catenin (Gat et al., 1998) and inhibited by β-catenin deletion (Huelsken et al., 2001) or Dkk1 overexpression (Andl et al., 2002). Moreover, Wnt5a is upregulated in response to Shh in the dermal condensate of developing HF (Reddy et al., 2001) and there are other examples of positive regulation of Wnt expression by Gli proteins (Mullor et al., 2001). It has recently been shown that during embryonic hair follicle development Shh signalling induces proliferation by regulating the expression of N-Myc and CyclinD2 but also by inhibiting GSK-3β activity, resulting in a synergy between β-catenin and Hh signalling

(Mill et al., 2005). In Drosophila wing development there are examples of Wnt signalling repressing Hh response (Glise et al., 2002) and in epidermis Ihh and Ptch are upregulated in the sebaceous tumours of mice expressing dominant negative Lef1 (Niemann et al., 2003).

1.3.2.4. Notch signalling

The Notch gene encodes a single pass transmembrane receptor that becomes activated by transmembrane ligands Delta and Serrate/Jagged on neighbouring cells (Artavanis-Tsakonas et al., 1999). Upon activation, Notch undergoes proteolytic cleavage mediated by the γ-secretase complex (Pan et al., 2004), releasing an intracellular fragment called Notch Intracellular Domain (NICD) (Schroeder and Just, 2000). NICD moves to the nucleus, where it interacts with the DNA binding protein Suppressor of Hairless (SuH, RBPJk in vertebrates) and activates transcription of target genes (Bailey and Posakony, 1995; Lecourtois and Schweisguth, 1995; Tamura et al., 1995). The most common vertebrate targets are bHLH transcription factors of the Hairy and Enhancer of Split (HES) and HEY family (Fisher and Voorhees, 1996).

Four mammalian Notch receptors, three mammalian Delta homologues (Delta 1, 2 and 4) and two Serrate homologues (Jagged1 and 2) have been identified. All Delta and Jagged isoforms bind and activate all Notch receptors (Gu et al., 1995).

During embryonic development Notch mainly regulates differentiation decisions, in some cases inhibiting differentiation and maintaining stem cell populations, in others actively promoting differentiation along particular lineages (Morrison et al., 2000). In embryonic skin, Delta1 is expressed in the mesenchyme underlying the HF placodes (Crowe et al., 1998; Viallet et al., 1998) and it promotes expression of Notch1 in the epithelium, so that Notch positive cells form the placode while the neighbours are inhibited (Crowe et al., 1998; Viallet et al., 1998).

In adult mouse skin Notch1 and Jagged 1 and 2 are in the matrix (Kopan and Weintraub, 1993; Powell et al., 1998), whereas Notch3 is located in the precursors and differentiated cells of the hair cortex and cuticle (Lin et al., 2000). Notch1 is essential for hair follicle homeostasis (Vauclair et al., 2005). Expression of constitutively active

Notch in the hair cortex results in abnormal differentiation of the two neighbouring cell types, the medulla and the cuticle (Lin et al., 2000).

Notch is also expressed in differentiated IFE and keratinocyte specific Notch1 deletion results in IFE hyperproliferation (Rangarajan et al., 2001) and predisposes for the formation of tumours (Nicolas et al., 2003).

In human interfollicular epidermis the stem cells are clustered at the top of the dermal papillae and express higher levels of Delta1 than their neighbours. It has been demonstrated that Delta expressing cells are unresponsive to Notch signalling and are highly cohesive. At the edges of these clusters Notch signalling stimulates the entering in the transit amplifying compartment (Lowell et al., 2000). The Notch pathway is the first example studied of the effect of local intercellular interaction on epidermal proliferation and differentiation during development and adult life (Lowell and Watt, 2001).

There is evidence for crosstalk between the Wnt and Notch pathway during somitogenesis: Lef/TCF activates transcription of Delta in presomitic mesoderm (Hofmann et al., 2004) and Lef/TCF mutant mouse embryos have defective somitogenesesis and aberrant expression of Delta (Galceran et al., 2004). In the intestine, Notch activity correlates with Wnt signalling (Fre et al., 2005). Notch signalling is required for Wnt-mediated maintenance of undifferentiated hematopoietic stem cells in vitro (Duncan et al., 2005). In the epidermis, Notch1 suppresses Wnt signalling (Devgan et al., 2005), and a study in Drosophila indicates a ligand-indipendent ability of Notch1 to modulate β-catenin activity (Hayward et al., 2005).

1.3.2.5. Nuclear receptors

The family of nuclear receptors (NR) includes retinoic acid receptor (RAR), vitamin D receptor (VDR), estrogen receptor (ER) and peroxisome proliferator-activated receptors (PPAR). Stably localized in the nucleus, these receptors homo- or eterodimerize and act as transcription factors in the presence of their ligands (Alberts et al., 1989). Growing evidence indicates that also in the absence of their ligand they regulate transcription by binding different partners, and their interaction with β-catenin/Lef1 is the best

documented (Mulholland et al., 2005). On the one side β-catenin modulates the action of nuclear receptors, and on the other side NR bound to their ligands inhibit β-catenin signalling. Ablation of many of these receptors has effects on epidermal lineage commitment.

Vitamin D is crucial in the maintenance of calcium homeostasis in the organism (Holick, 2003) but plays a role also in the induction of differentiation in various epithelial cell types, including enterocytes (Palmer et al., 2001) and keratinocytes (Bikle, 2004).

Vitamin D inhibits tumour promotion in mouse skin (Chida et al., 1985) and vitamin D knock out epidermis is more sensitive to tumour induction (Zinser et al., 2002). Several non-hypercelcemic vitamin analogs have been generated as anti-cancer therapies (Guyton et al., 2001; Milliken et al., 2005; Peleg et al., 2005) and clinical trials have been started to assess the effect of vitamin D analogs on patients with various neoplasias (Guilford et al., 1998). These drugs have been observed to be effective in the treatment of prostate cancer (Krishnan et al., 2003).

VDR knock out mice develop rickets and osteomalacia, caused also by vitamin D deficient diet (Li et al., 1997). In addition, only VDR knock out mice develop progressive alopecia (Li et al., 1997). While calcium enriched diet normalizes ion homeostasis of these mice, only targeted expression of VDR in epidermal keratinocytes prevents alopecia (Chen et al., 2001; Li et al., 1998). It appears therefore that while the tumour suppressor activity of VDR depends on the presence of vitamin D, its role in HF maintenance is ligand independent. These observations agree with in vitro studies on colon carcinoma cells showing how β-catenin interacts with VDR to regulate transcription and the interaction is antagonized by vitamin D (Palmer et al., 2001).

Several retinoic acid receptors (RAR and RXR) are expressed in the epidermis (Billoni et al., 1997; Elder et al., 1991) and are involved in epidermal interfollicular differentiation (Fisher and Voorhees, 1996; Li et al., 2000). These receptors appear dispensable for epidermal embryonic development (Fisher and Voorhees, 1996), but are necessary for adult hair follicle maintenance (Li et al., 2000). Mice with inducible

epidermal deletion of the retinoid X receptor α (RXRα) have defective anagen initiation, show extensive hair loss and develop multilayered epidermal cysts in the dermis, constituting a possible example of transdifferentiation of hair follicle cells into interfollicular epidermis (Li et al., 2000; Li et al., 2001).

PPAR receptors regulate lipid metabolism, which plays an important role in the differentiation of both IFE keratinocytes and sebocytes (Rosenfield et al., 2000). In particular, PPARγ is selectively expressed in differentiating sebocytes and its activation induces the differentiation of rat preputial sebocytes but not keratinocytes in culture (Rosenfield et al., 1999). PPARγ KO/wt chimaeric mice develop normally, but their sebaceous glands are formed only by PPARγ wt cells (Rosen et al., 1999). β-catenin signalling reduces the levels of PPARγ and lipid production in preadipocyte cell lines (Ross et al., 2000), whereas PPARγ activation has been shown to reduce β-catenin expression levels (Moldes et al., 2003), enhance β-catenin degradation (Liu et al., 2004) and increase the expression of E-cadherin and, as a consequence, the proportion of membrane bound β-catenin (Ohta et al., 2002).

1.3.2.6. c-Myc

In human epidermis c-Myc (Myc) is expressed in the basal layer of the IFE, the bulge, the proliferating cells of the hair bulb and the differentiating matrix cells (Bull et al., 2001). Activation of Myc in cultured keratinocytes stimulates stem to TA cell transition and increases the number of terminally differentiated cells (Gandarillas and Watt, 1997). When inducible or constitutively active Myc is expressed in the basal layer of the epidermis, SG and ORS of transgenic mice the first effect produced is a dramatic increase in proliferation (Arnold and Watt, 2001; Waikel et al., 2001). IFE keratinocytes still execute a normal terminal differentiation and the thickening of the epidermis reflects an increase in the number of the differentiated layers. The hair follicles are abnormal, the sebaceous glands are hypertrophic and ectopic sebaceous differentiation occurs (Arnold and Watt, 2001; Waikel et al., 2001; Braun et al., 2003).

Myc acts in part by impairing epidermal cell adhesion to the ECM so that hair follicle keratinocytes, unable to migrate towards the bulb, differentiate along the sebaceous

lineage (Frye et al., 2003). Impaired adhesion to the niche is a known signal inducing exit from the stem cell compartment (Murphy et al., 2005). The number of LRC in the epidermis of mice overexpressing Myc is decreased (Waikel et al., 2001), in agreement with the report of Myc activation in hematopoietic stem cells leaving the niche (Murphy et al., 2005).

Myc has been shown to be a target of β-catenin in various cancer models (He et al., 1998). The relationship between Myc and β-catenin appear to be quite complex, as the two factors appear to have opposite effect on epidermal lineage specification (Niemann and Watt, 2002; Honeycutt and Roop, 2004).

1.3.3. In vitro models of lineage commitment of human epidermal cells

The study of the mechanisms regulating human epidermal cells proliferation and differentiation has been greatly facilitated by the ability to grow human keratinocytes in culture, supported by a feeder layer of mitotically inactive 3T3 fibroblasts (Rheinwald and Green, 1975). There is good evidence that keratinocyte cultures contain stem cells, since cultures generated from small areas of skin can generate normal epidermis for years after being grafted onto patients that have lost large areas of their epidermis (Gallico et al., 1984; Compton et al., 1989; Compton et al., 1998). Cultivation on feeder layer of 3T3 cells supports growth of keratinocytes at clonal density (Barrandon and Green, 1987; Rheinwald and Green, 1975). In these conditions primary keratinocytes display a variable proliferative capacity different types of clones can be attributed to stem or TA founder cells (Barrandon and Green, 1987; Jones and Watt, 1993).

The optimization of retroviral transduction protocols has allowed to genetically manipulate human primary keratinocytes and therefore to study the molecular mechanisms that regulate proliferation and differentiation in human epidermis (Levy et al., 1998). When monolayers of keratinocytes cultures reach confluence, the differentiated cells stratify on top of the proliferating ones and epidermal sheets are reconstituted (Zhu and Watt, 1996; Zhu and Watt, 1999).

Clonal analysis is traditionally the best method to assess the multipotency of stem and progenitor cells and for example it has lead to the identification of the three of lineage

specification from the hematopoietic stem cells to all the differentiated cells in the blood (Weissman, 2000). Even though so far only interfollicular differentiation has been observed in keratinocyte cultures, the combination of Myc or β-catenin retroviral transduction and clonal analysis could be an effective strategy to analyse and regulate lineage choice *in vitro*.

1.4. Summary and aims

The epidermis is maintained thanks to a population of resident stem cells able to self-renew and differentiate in all the lineages found in the interfollicular epidermis, hair follicles and sebaceous glands (Watt, 2001). Several transgenic mouse models indicate a role for β-catenin signalling in the regulation of epidermal lineage choice, but in none of them it is possible to regulate timing, duration and strength of β-catenin signalling.

1. I generated the ΔNβ-cateninER transgenic mice, in which I could control the activation of β-catenin signalling by applying the drug 4-hydroxytamoxifen (4OHT) on the skin, to investigate whether it was possible to alter lineage choice of adult stem and progenitor cells without prior embryonic priming.

2. I took advantage of the 4OHT-dependent activation of β-catenin in the ΔNβ-cateninER transgenic mice to assess whether a transient activation was sufficient to trigger hair growth and maintain hair follicle tumours. I titrated β-catenin activation in vivo in order to analyze the relationship between the levels of β-catenin signalling and the induction of ectopic hair follicle formation. This detailed analysis allowed me to examine the effect of β-catenin activation on the epidermal stem cell compartment.

3. Embryonic hair follicle morphogenesis is the result of a complex crosstalk between epithelial and mesenchymal cells (Millar, 2002; Schmidt-Ullrich and Paus, 2005). I analyzed β-catenin target genes in order to better understand the mechanisms regulating hair follicle induction and to find candidate genes interacting with β-catenin during this process.

4. As β-catenin and c-Myc activation have opposite influence on epidermal lineage commitment in vivo (Arnold and Watt, 2001; Gat et al., 1998), I developed a model of lineage selection in cultured epidermal cells to investigate the effect of the activation of the two genes at the single cell level.

Chapter 2. Materials and methods

2.1. Molecular biology

2.1.1. General solutions

The solutions marked with * were supplied by Cancer Research UK Central Services.

L-broth (LB) * (normal)

L-broth (LB) for bacterial culture comprised 1.5% Bacto-Tryptone (Difco), 0.5% yeast extract (Difco) and 170mM NaCl and was sterilized by autoclaving.

L-agar *

L-agar comprised 1.5% bacto-agar (Difco, w/v) in LB. The agar was dissolved by heating in a microwave oven and allowed to cool to 50°C before adding the selection antibiotic. The solution was then poured into 100mm bacteriological Petri dishes and left to set on a level platform. Agar dishes were stored at 4°C, agar side up, for up to two weeks.

Ampicillin stock solution

Ampicillin (Sigma, stock 100 mg/ml in dH_2O) was used as a selection antibiotic and was added to LB or L-agar to a final concentration of 100μg/ml.

TRIS/EDTA buffer (TE)

TE was used as a general DNA storage buffer and comprised 10mM Tris-HCl and 1mM EDTA, pH8.0 in dH_2O

Tris-acetate-EDTA buffer (TAE)

A 50x stock solution was prepared by dissolving 242g Tris base and 57.1 ml glacial acetic acid (BDH) in dH_2O. 100 ml 0.5M EDTA pH8.0 (*) were added and the final volume was made up to 1l.

Agarose/TAE gel

0.8-2% (w/v) ultra pure agarose (Gibco BRL) was melted in a microwave oven in 1x TAE buffer. Ethidium bromide was added at 0.05 μg/ml to agarose solution before casting. Typically, DNA was electrophoresed at constant voltage of 80-100V in 1x TAE buffer.

DNA loading buffer

6x DNA gel loading buffer comprised 0.25% bromophenol blue (Sigma), 0.25% xylene cyanol (Sigma) and 30% glycerol in dH_2O. The loading buffer was stored at 4°C.

2.1.2. DNA techniques

Enzymatic manipulation of DNA fragments

Restriction enzymes, Klenow polymerase and T4 DNA ligase were purchased from NEB and used for restriction digestions and DNA ligations, respectively. Calf intestinal alkaline phosphatase (Boehringer Mannheim) was used to remove 5' phosphate groups from vector DNA fragments to prevent vector religation without incorporation of insert DNA (containing 5' phosphate groups) in ligation reactions. When necessary, Klenow DNA polymerase (NEB) was used to generate blunt ends following digestion with restriction enzymes.

Bacterial transformation

One Shot TOP10 competent E. coli (Invitrogen) were used for cloning of DNA. 0.1μg DNA from ligations or 1ng plasmid DNA was added to 25μl aliquot of competent cells. The transformation was performed by heat shock according to the Manufacturer's instructions.

Preparation of plasmid DNA

To screen colonies after ligation and transformation, single colonies were picked and inoculated in 5ml LB medium containing ampicillin, then grown overnight in a 37°C agitator. 2 ml of the overnight culture was used for small scale preparation of plasmid DNA whilst the remainder was stored at 4°C. This initial plasmid purification was performed by the Equipment Park (CR-UK).

For maxi preparations, 0.5ml of the overnight culture was added to 200 ml LB plus ampicillin and incubated overnight at 37° in an agitator. Bacteria were pelleted by centrifugation at 4000 rpm for 15 min in a Beckman J2-21 centrifuge. The plasmid DNA was then purified using a Qiagen maxi kit according to the Manufacturer's instructions.

Quantitation of nucleic acids

Nucleic acids were diluted in 10mM Tris-HCl pH 8.5 and placed in disposable plastic UVettes (Eppendorf). Absorbance at 260nm and 280nm was read in an Eppendorf BioPhotometer with the correct DNA or RNA program set-up.

Purification of restriction enzyme digestion products

Reactions were run out on agarose gels. DNA fragments were visualized by ethidium bromide under low power UV light. Bands were excised using clean scalpels. Agarose gel fragments were melted and the DNA isolated using the Qiagen gel extraction kit according to the Manufacturer's instructions.

10μg of the transgene construct were further purified with an elutip column according to the manufacturer's instructions (Schleicher and Schuell), and then resuspended at a concentration of 5mg/ml in sterile injection buffer (10 mM Tris-HCl, 0.1 mM EDTA, pH 7.4) for pronuclear injection.

DNA Sequencing

ΔNß-cateninER squence was checked following mutagenesis and prior purification for pronuclear injection. Sequancing reactions were set up using BigDyeTerminator mix as made by the Equipment Park (CR-UK). Sequencing reactions were set up according to the Manufacturer's instructions and purified using DyeEx spin columns (Qiagen). Samples were run on capillary sequencing gels (Prism 3730) by the Equipment Park (CR-UK).

2.1.3. Vectors and cloning strategy

Vectors

pSP73 (Promega) contained the keratin 14 cassette and was obtained from Dr Kristin Braun in the laboratory and originally provided by E. Fuchs, Howard Hughes Medical Institute, Rockefeller University, New York (Vasioukhin et al., 1999). The K14 expression cassette contains a 2100 bp AvaI fragment of the keratin 14 promoter/enhancer, a rabbit β-globin 5' untranslated region (UTR), together with an intronic sequence upstream of a BamHI site, and the K14 3' UTR, followed by a polyadenylation site 3' downstream of the BamHI site.

pBabepuro (Morgenstern and Land, 1990) contained ΔNß-cateninER and was obtained from Dr David Prowse in the laboratory.

Cloning strategy

To generate the transgene construct the QuickChange Site-Directed Mutagenesis Kit (Stratagene) was used following the Manufacturer's instructions to eliminate a HindIII

restriction site present within ΔNß-catenin sequence. The following primers were used to mutagenize the HindIII site present in the ΔNß-cateninER sequence:

5bcat1344M ggtggaatgcaagcgttaggactccatctc
3bcat1373M gagatggagtcctaacgcttgcattccacc

DNβ-cateninER was excised from pBabepuro as an EcoRI/HindIII fragment, blunt-ended with Klenow DNA polymerase and cloned into the blunt-ended BamHI site of pSP73 containing the K14 expression cassette. DNb-cateninER sequence was checked following mutagenesis and after cloning into the K14 cassette. The transgene construct was excised from pSP73 with EcoRI and HindIII.

2.1.4. Affymetrix microarrays

RNA preparation

The isolation of total RNA from mouse skin was base upon methods developed by Dr Isabel Arnold and Dr David Owens and is as follows. Mice were killed and the portion of dorsal skin that had been clipped was removed and cut into 4 pieces of approximately $1cm^2$ of size. 3 pieces were quickly flash frozen in separate cryo-vials in liquid Nitrogen (the last piece was used to prepare frozen and paraffin embedded blocks) and stored in liquid Nitrogen for up to one month before processing.

Processing of the skin to obtain RNA was performed with care using standard RNA techniques (Sambrook et al., 1989). One square of skin from each mouse (approximately 50mg of tissue) was placed into 12ml of TRI reagent (Helena Biosciences) in a 50ml polypropylene tube (Nalgene) and homogenised at room temperature for 1 min using a Polytron homogenizer set to a high speed. The tube was kept at room temperature for 5 min and then kept on ice until all samples had bee homogenised. 1.2ml 1-bromo-3-chloropropane (BDP, Helena Biosciences) was then added, mixed vigorously by shaking for 15 sec and incubated at room temperature for 15 min. The samples were centrifuged at 12000g (11400rpm) in a Beckman J-20 centrifuge for 30min at 4°C. The upper, aqueous phase containing the RNA was

carefully removed into new polypropylene tubes (Nalgene). 12ml isopropanol were added and the samples were mixed by vortexing. Samples were placed at -20°C for one hour to precipitate the RNA, which was then pelleted by spinning at 12000g (11400rpm) in a Beckman J-20 for 30min at 4°C. The isopropanol was discarded and the pellet was dried and resuspended in RNase-free dH_2O. The extracted RNA was further purified using Qiagen RNeasy Mini Columns according to the Manufacturer's instructions and resuspent in 100µl of RNase-free dH_2O. The RNA was quantified as described before and the quality controlled by running samples on formaldehyde/agarose/ethidium bromide gels according to (Sambrook et al., 1989).

cDNA and cRNA preparation

Double-stranded cDNA was generated from 10 µg total RNA using Superscript Double Strand cDNA Synthesis Kit (Invitrogen) according to the Manufacturer's instructions, with a T7-polyT primer (Affymetrix). The cDNA was purified using the GeneChip Sample Cleanup Module (Affymetrix) and used to generate biotinylated cRNA by in vitro transcription using the Enzo BioArray High Yield Transcript Labeling Kit (Affymetrix). cRNA was purified using the GeneChip Sample Cleanup Module (Affymetrix) following the Manufacturer's instructions and quantified as described before. 25 µg of cRNA were fragmented in Fragmentation buffer provided with the GeneChip Sample Cleanup Module by incubating it at 94°C for 35 min exactly in a heating block.

The quality of cDNA, cRNA and fragmented cRNA was checked by running an aliquot of each on formaldehyde/agarose/ethidium bromide gels according to (Sambrook et al., 1989). The molecular weight markers used were 0.24-9.5 Kb RNA Ladder (Invitrogen) for cDNA and cRNA, and RNA Century Size Markers (Ambion) for the cRNA.

Microarrays hybridization and scanning

10 µg of fragmented cRNA were hybridized to the GeneChip Mouse Expression Set 430 (A and B chip) oligonucleotide arrays (Affymetrix), comprising 45037 probe sets. Complete annotations and spotting patterns can be found online at http://www.affymetrix.com. The hybridization was performed following the

Manufacturer's instructions using an Affymetrix GeneChip Instrument System. The arrays were washed and stained with streptavidin-phycoerythrin before being scanned on an Affymetrix GeneChip scanner. The hybridization and scanning of the arrays were performed by the Cancer Research UK Affymetrix Facility located in the Paterson Institute for Cancer Research, Manchester (UK).

Normalization and Filtering of the Array Data

Unscaled raw data were loaded from a text file on Genespring (Version 6.1, Silicon Genetics). Measurements less than 0.001 were set to 0.001. The normalization was set as follow: per chip normalization to the 50th percentile, per gene normalization to the median.

Spearman correlation was used to generate a condition tree and cluster all the chips as a quality control. As a result, one replicate for the conditions wt7 and wt0 (B chip) here removed.

All the data that passed the quality control were filtered using the Genespring advanced filtering tool. I identified probes with present or marginal flags in at least one out of 6 conditions, t test p value less than 0.05 in at least one condition, standard deviation less than 1.45 in at least 2 out of 6 conditions, and a change in relative expression levels of at least 2-fold in the 4OHT-treated transgenic samples compared to untreated transgenic and all the wild-type samples.

2.2. Transgenic mice

2.2.1. Generation of transgenic mice

Injection of the K14ΔNß-cateninER construct into the male pronucleus of fertilised F1 hybrid (CBA x C57BL/6) mouse embryos and subsequent implantation into pseudopregnant foster mothers was performed by Clare Hall Transgenic Services Unit.

Phenol/chloroform DNA extraction

To genotype mice, an approximately 5mm long tail snip was taken from each animal, frozen on dry ice and stored at -20° prior to DNA extraction. All tail snipping was performed by Clare Hall Animal Unit. Each tail snip was incubated in 0.7ml tail buffer containing 50mM Tris-HCl pH 8.0, 100mM EDTA, 100mM NaCl, 1% SDS and supplemented with 20µl of a 25mg/ml proteinase K (Sigma) solution at 55°C overnight. 0.7ml of 1:1 phenol/chloroform (Amresco) were added and samples mixed end-over-end for 20 min at room temperature before spinning in a bench top centrifuge at 14000rpm for 10 min. The upper phase (containing the DNA was carefully removed to prevent disturbance of the interface and placed in a new Eppendorf tube. 0.7ml of isopropanol were added and the solution mixed vigorously to precipitated the DNA. Samples were centrifuged again as before. The DNA pellet was then washed with 70% cold ethanol (4°C) and dried in a DNA Speed Vac (Savant) before resuspension in 100µl dH_2O. The DNA was allowed to dissolve in the dH_2O at room temperature overnight before being used for genotyping. When necessary, DNA was stored at 4°C.

Southern blot

Southern blot was performed to identify the founder lines and determine the number of copies of transgene integrated in their genome, but also as an alternative method to PCR for the genotyping of transgenic mice. 10µl of mouse tail snip DNA sample was digested with the appropriate restriction enzyme overnight to ensure complete digestion. Samples were run on a 0.8% agarose TAE gel. The gel was denatured in 400 mM NaOH for 30 min at room temperature with occasional agitation and the DNA transferred overnight onto Hybond N-Plus membrabe (Amersham Biosciences) by a standard Southern blotting technique (Sambrook et al., 1989). Themembrane as pre-hybridized in Church buffer (20 ml per blot, 0.5M Na phosphate pH 7.2, 7% SDS, 1mM EDTA, 0.5% Marvel, Premier Brands, dried milk powder) for 1-4 hours in a hybridization oven (supplied by Jencons) at 65°C in roller bottles. An Amersham Rediprime kit along with [a-^{32}P]-dCTP (ICN) were used to generate labelled probes. The labelling reaction was performed according to the Manufacturer's instructions for 1 hour at room temperature. Unincorporated nucleotide was removed from the reaction with Nick columns (Pharmacia) and the probe eluted in TE buffer. The purified, labelled probe was then denatured at 100°C for 5 min before adding to the pre-

hybridization Church buffer. The membrane was incubated with the probe overnight at 65°C in roller bottles before discarding the hybridization buffer, washing briefly in 2xSSC/0.1% SDS then for 15 min each first in 2xSSC/0.1% SDS then in 0.1xSSC/0.1% SDS. All washes were performed in roller bottles at 65°C.Themembrne was then placed in Sarin wrap in an autoradiography cassette with reflective screens at -70°C with X-ray film. Typically, overnight to one week exposure were necessary to produce a signal on the film.

In particular, for genotyping the genomic DNA was digested with EcoRV and the template for the generation of the radiolabelled probe was a 1.8kb fragment from the ΔNß-cateninER fusion protein, gel-purified from a RcoRV digestion fragment of pSP73 K14ΔNß-cateninER plasmid. For copy number determination, genomic DNA was digested with EcorRI and and the template for the generation of the radiolabelled probe was a 1.7kb fragment of the IL1a receptor. For determination of copy number the signals from the ΔNß-cateninER and IL1a receptor probes were collected on a Phosphorimager plates, scanned, normalized according to the size of the fragment labelled and relative intensities were compared as follows:

$$\text{Copy n°} = [(AVG_{\Delta N\beta\text{-cateninER}} - AVG_{background})/2]/[(AVG_{IL1a\ receptor} - AVG_{background})/5]$$

2.2.2. Transgenic mice breeding

All animal care and breeding was carried out by the Clare Hall Animal Unit. K14ΔNß-cateninER mice were maintained as heterozygotes and kept in C57BL/6 background. D2 line was also bred to homozygote to facilitate crossing with different transgenic lines. Embryos from all founder lines described were frozen and are kept in the Clare Hall Cryopreservation Unit.

K14ΔNß-cateninER mice (line D2) were crossed with K14N$^{ICD\Delta OP}$ER mice (from Dr Carrie ambler in the laboratory) and (line D4) K14MycER mice (Arnold and Watt, 2001), all in CBA X C57BL/6 background. Mice negative for all transgenes, positive for one (single transgenic) or two (double transgenic) were all obtained from such crosses.

To generate K14ΔNß-cateninER K14CreER Jagged1$^{flx/flx}$ mice, Jagged1$^{flx/flx}$ mice were crossed with K14ΔNß-cateninER (line D2) K14CreER (Vasioukhin et al., 1999) transgenic mice and the F1 backcrossed to regenerate the Jagged1$^{flx/flx}$ genotype.

2.2.3. Genotyping

DNA extraction for genotyping PCR

To routinely genotype mice, a small earsnip was taken from each animal by the Clare Hall Animal Unit and handled in the same way as the tailsnips. Each earsnip was incubated in 50µl of ear buffer containing 50mM Tris-Hcl pH 8.0, 20mM NaCl, 0.1% SDS supplemented with 2.5 µl of 25mg/ml proteinase K (Sigma) solution at 55°C for one hour, vortexed, and incubated at 55°C for other two hours. 150µl of dH_2O were added and the tubes were incubated for 10 min at 95°C and subsequently briefly centrifuged to collect condensate from the lid.

PCR reaction

The following primers (suppied by CR-UK oligo synthesis service and recently by DNA Technology AIS) were used for genotyping PCR of K14ΔNß-cateninER mice:

5xBcat2420 ATGCTGCTGGCTATGGTCAG
3mER1543 GCACACAAACTCTTCACC

In a 50 µl reaction, 1µl of each primer (25µm) was added to 25µl of 2xPCR master mix (Promega), 1µl of DNA preparation and 22µl of dH_2O. The following PCR conditions were used:

1 cycle	94°C,	1min
32 cycles	94°C,	30sec
	50°C,	30sec

72°C, 1min

1 cycle 72°C, 7min

10µl of the PCR product were run on a 2% agarose TAE gel as described above. Samples positive for ΔNß-cateninER produce a 0.6kb fragment. Transgene negative samples produce no PCR product.

Genotyping of K14CreER Jagged1$^{flx/flx}$ mice, K14N$^{ICD\Delta OP}$ER mice and K14MycER mice was performed in the laboratory by Dr Soline Estrach, Dr Carrie Ambler and Dr Kristin Braun respectively.

2.2.4. Experimental manipulation of mice

At the start of every experiment all the mice were 6-8 weeks old, and therefore in the resting phase of the hair cycle. All experimental treatments were performed in the Lincoln's Inn Field Animal Unit. Mice were shipped by van from Clare Hall (day -2), when necessary part of their dorsal skin was clipped on the following day (day -1) and treatment started the day after (day 0).

4OHT treatment

4-hydroxytamoxifen (4OHT) was purchased from Sigma, either 99% pure Z-isomer (biologically active) or minimum 70% pure Z-isomer and diluted in acetone at variable concentrations. The doses indicated always refer to the amount of Z-isomer, and were always prepared in of 200µl volume, as allowed by the laboratory's animal licence.

The DNβ-cateninER transgene was activated by topical application of 4-hydroxytamoxifen (4OHT; Sigma) to a clipped area of dorsal skin with a Gilson micropipette or to the tail skin with a paintbrush. Wild type littermates were used as

controls. No sex-specific effects of 4OHT were observed, but for the microarray experiment only females were used. No effects of 4OHT treatment were observed on wild type mice.

Mice usually received 1mg 4OHT every day. In the titration experiments (Fig. 4.6 and 4.7) mice received 0.5, 1.5 or 3mg 4OHT every second day. LRC mice received 1.5 mg every second day. K14ΔNß-cateninER x K14CreER x Jagged1$^{flx/flx}$ mice received 3mg 4OHT every second day to ensure the activation of CreER. K14ΔNß-cateninER x K14N$^{ICD\Delta OP}$ER received 1 or 1.5mg 4OHT every second day. K14ΔNß-cateninER x K14MycER mice received 1.5mg 4OHT every second day.

Double treatments

In order to study the interaction between β-catenin and Shh pathways, mice received daily topical applications of cyclopamine (Biomol, 50 μM in ethanol), and 1mg 4OHT once per week (D2 line) or every second day (D4 line). 4OHT was applied 30 minutes after cyclopamine.

To analyze β-catenin/Notch interaction D2 mice were treated every second day with DAPT (Sigma) 1mg/0.2ml acetone) and 30 minutes later with 4OHT (1mg).

In order to analyze the interaction between β-catenin and vitamin D receptor (VDR), D4 mice were treated every day with the vitamin D analog EB1089 (Leo Pharma A/S, 1μg/ml in acetone) and on the second day received a 1mg 4OHT dose 30 minutes after the EB1089.

BrdU injections

To be able to detect cells that were going through S-phase of the cell cycle (i.e. were actively cycling), 300μl of a 10mg/ml BrdU (Sigma) stock was injected intraperitoneal before harvesting of skin. The BrdU stock was made by dissolving BrdU powder in PBS which was then sterile filtered, aliquoted and stored at -20°C.

To generate label retaining cells (LRC), 10 days old mice received four intraperitoneal injections of BrdU (0.1 mg/g body weight) every 12 hours.

2.2.5. Grafting experiment

D4 mice were born in a sterile environment and back skin was collected from newborn puppies and grafted onto the back of nude mice by the Clare Hall Animal Unit. The skin was allowed to engraft and develop for 8 weeks, and subsequently treated with topical application of 4OHT every second day. As the grafts had a smaller area than the region of dorsal skin usually clipped in adult mice (see section 2.2.4), the dose of 4OHT was 30µl of 5mg/ml solution in acetone, so that the ratio mg 4OHT/cm^2 of skin was roughly maintained in comparison with the other experiments.

2.3. Cell culture

2.3.1. General solutions

The CR-UK Central Research Services provided sterile deionised water (dH_2O) and the solutions indicated by (*). All reagents used were of tissue culture grade and kept sterile.

Phosphate buffered saline (PBS, *)

8g NaCl, 0.25g Na_2HPO_4 and 0.25g KH_2PO_4 were dissolved in 1l dH_2O, the pH was adjusted to 7.2 and the solution was autoclaved. PBS was supplemented with 1mM CaCl2 (B) and 1mM MgCl2 (C) to make PBS-ABC.

EDTA solution (versene, *)

8g NaCl, 0.2g KCl, 1.15g Na_2HPO_4, 0.2g KH_2PO_4 and 0.2g ethyldiaminotetracetic acid (EDTA) and 1.5ml of 1% (w/v) phenol red solution were dissolved in 1l dH_2O, the pH was adjusted to 7.2 and the solution was autoclaved.

Trypsin solution (*)

8g NaCl, 0.1g Na_2HPO_4, 1g D-glucose, 3g Trizma Base, 2ml 19% (w/v) KCl solution and 1.5ml of 1% (w/v) phenol red solution were dissolved in 200ml dH_2O, the pH was adjusted to 7.7 and 0.06g penicillin and 0.1g streptomycin (Gibco BRL) were added. 2.5g of pig trypsin (Difco, 1:250) were dissolved in 200ml dH_2O; air was bubbled through the solution until the trypsin dissolved. The trypsin solution was added to Tris-buffered saline, made up to 1l with dH_2O, sterilised by filtration through a 0.22μm filter (Millipore) and stored at -20°C.

Mitomycin C stock solution

Mitomycin C is an inhibitor of DNA synthesis and nuclear division (Tomasz et al., 1987). It is used to metabolically inactivate J2-3T3 cells for the keratinocyte cultures and AM12 virus packaging cells before co-culturing them with SZ95 cells to infect. 4mg mitomycin C powder (Sigma) was dissolved in 10ml PBS. The stock solution (0.4 mg/ml) was sterilised by filtration through a 0.22μm filter (Millipore), aliquoted and stored at -20°C. Mitomycin C was added to the culture medium at a final concentration of 4 μg/ml in the treatment of J2-3T3 cells and of 8μg/ml in the treatment of AM12 cells.

2x HBS

To make a 2x stock of HBS to be used for calcium phosphate transfection, 8.0g NaCl and 6.5g HEPES sodium salt were dissolved in dH_2O to which was added 10 ml of a Na_2HPO_4 stock solution (5.25g Na_2HPO_4 in 500 ml dH_2O). The pH of the solution was brought to exactly 7.0 with NaOH or HCl and made up to 500 ml. The stock was aliquoted and stored at -20^0C until use.

Polybrene stock solution

100mg polybrene powder (Sigma) was dissolved in 20 ml PBS to produce a concentration of 5 mg/ml. The stock solution was sterile filtered through a 0.22μm filter, aliquoted and stored at -20^0C.

2.3.2. Cultured cell types

Primary mouse keratinocytes were isolated from 3-4 days old mice as described below. Spontaneously immortalised mouse keratinocyte lines were originally derived from adult mice (Romero et al., 1999) as described below. Human epidermal keratinocytes were isolated from neonatal foreskin, grown and serially passaged as described below. J2-3T3 cells were used as feeder cells to support human and mouse keratinocyte growth.

SZ95 cells were kindly provided by Dr Christos Zoubouli (Zouboulis et al., 1999) and were cultured as described below. Phoenix and AM12 cells retroviral packaging cell lines were used to infect SZ95 cells with ΔNß-cateninER, ΔNß-catenin and MycER as described below.

All cells, except for mouse keratinocytes, were cultured on plastic dishes or flasks of tissue culture grade (Falcon) in a humidified incubator at 37°C with 5% CO_2. Mouse keratinocytes were cultured as above, only at 32°C. Biocoat Collagen I-coated dishes (BD Biosciences) were used for primary mouse keratinocytes and to establish mouse keratinocyte cell lines.

Media or any solution added to cells were first warmed to 37°C. All cells were confirmed by the CR-UK Cell Production Unit as being negative for mycoplasma infection. Any cells with mycoplasma contamination were discarded.

2.3.3. J2-3T3 feeder cells

Clone J2 of 3T3 Swiss mouse embryo fibroblasts is a clone selected for its ability to support keratinocyte growth (Rheinwald and Green, 1975, Watt 1998). J2-3T3 cells were cultured in Dulbecco's modification of Eagle's medium (DMEM, E4, provided by CR-UK Cell Production Unit) supplemented with 10% (v/v) donor calf serum (DCS, Gibco BRL). When J2 cells approached confluence they were harvested by rinsing with versene solution and incubating at 37°C in trypsin diluted 1:5 in versene for 5 min. The trypsin was subsequently inactivated by dilution in serum-containing culture medium and the cells replated at a dilution of 1:10. J2-3T3 cells were replaced every 6-9 weeks with a new batch of low passage cells to avoid overgrowth of transformed J2-3T3s.

Preparation of J2-3T3 cells as feeder cells

The culture of human keratinocytes is supported by co-cultivation with mitotically inactivated J2-3T3 cells, which are referred to as feeder cells (Rheinvald and Green, 1975). Feeder cells were incubated with 4μg/ml mitomycin C for 2-3 hours at 37°C in order to inhibit mitosis. Cells were harvested and plated so that a 75cm^2 flask of treated J2-3T3s was divided equally between 9x 25cm^2 flasks or 6cm diameter plate. Keratinocytes or SZ95 cells were added within 24 hours of preparing the feeder layer.

Freezing and thawing of J2-3T3 cells

Cells were harvested as described above and pelleted. Cells obtained were resuspended in serum-containing 10% (v/v) sterile dimethyl sulphoxide (Gibco BRL). Cell suspensions from a confluent 75cm^2 flask were aloquoted into 4-6 cryovials (Nunc). Cryovials were stored in an insulated box at -70°C overnight and subsequently transferred to liquid Nitrogen for long term storage. Cells were thawed by transferring the cryotube from liquid Nitrogen directly into a water bath at 37°C. As soon as the cell suspension was thawedthe cell suspension was thawed, it was added to 10 ml medium and centrifuged at 1000rpm for 3min. The recovered cells were resuspended in medium and plated onto a collagen-coated plate.

2.3.4. Primary human keratinocytes

Keratinocyte culture medium (FAD + FCS + HICE)

FAD powder (F12 + adenine + DMEM: Imperial Labs) was supplemented with 3.07 g/l $NaHCO_3$, 100 IU/l penicillin and 100µg/l streptomycin. FAD medium (CR-UK) was bubbled with CO_2 until the pH dropped below 7.0, then sterilised by filtration through a 0.22µm filter (Millipore). Medium was prepared by the CR-UK Cell Production Unit and stored at 4°C until used.

Stock solution of additives were kindly prepared by Simon Broad in the laboratory. 10^{-5} cholera enterotoxin (ICN) was stored at 4°C. Hydrocortisone (Calbiochem) was dissolved in 95% ethanol at 5mg/ml and stored at -20°C. 100mg/ml recombinant human epidermal growth factor (EGF, Peprotech) was prepared by first dissolving in 1/100 volume 0.1M acetic acid (BDH) before adding to FAD medium containing 10% (v/v) batch-tested foetal calf serum (FCS, Imperial Labs) and stored at -20°C. The additives were combined into a 1000x stock solution (HCE): 1ml hydrocortisone, 100µl cholera enterotoxin and 1ml EGF stock solutions were added to 7.9 FAD medium with 10% FCS and stored at -20°C. The final concentrations in the medium were 10^{-10} cholera enterotoxin, 0.5µg/ml hydrocortisone and 10ng/ml EGF. 1000x insulin stock solution (5mg/ml in 5 mM HCl, Sigma) was stored at -20°C. The final concentration in the medium was 5µg/ml insulin. Complete keratinocyte medium (FAD + FCS + HICE) was prepared by adding 10% (v/v) FCS, 1000x HCE stock and insulin solutions to the FAD medium prior to use (Watt, 1998).

Isolation of primary human keratinocytes

Primary human keratinocytes were kindly prepared by Simon Broad in the laboratory. Neonatal foreskins were provided with the informed consent of the parents. Isolation of primary keratinocytes was carried out as soon a spossible after circumcision (Watt, 1998). Under sterile conditions, using a pair of forceps and curved scissors, a piece of foreskin was trimmed of dermal and fatty tissues. The foreskin was cut into pieces of

about 5mm^2 and transferred into a Wheaton Cellstir (Jencons) containing 5ml trypsin and 5 ml versene and stirred over a magnetic stirrer at 37°C. Dissociated cells were collected every 30 min and added to 5 ml keratinocyte culture medium. The number of cells obtained was counted using a haemocytometer. Dissociation of cells from the tissue was continued with addition of fresh versene and trypsin solution. This procedure was repeated 2 to 3 times before the number of cells obtained started to decrease. The yield from a neonatal foreskin was usually between 1-5x 10^7 cells. Feeder cells had been plated onto a 25cm^2 flask in readiness. Isolated cells were pooled, pelleted and plated at a density of 10^5 cells per 25cm^2 flask. Cells were cultured until just confluent. One flask of cells was tested for mycoplasma infection by the CR-UK Cell Production Unit, while the remaining cells were harvested and frozen at 10^6 cells per ml as described for J2-3T3.

Serial culture of human keratinocytes

Frozen keratiocytes (passage 2-5) were thawed as described for J2-3T3. Cells were typically seeded at a density of 1-2x 10^5 cells per 25cm^2 flask; keratinocytes that were freshly thawed were plated at a density of 4-8x 10^5 cells per 25cm^2 flask to allow for loss of viability resulting from freezing ad thawing.

Fresh medium was given to keratinocytes every 2 days. A day prior to any experimental manipulation, keratinocytes were fed with fresh medium. Keratinocytes were passaged just before they reached confluence. The cultures were rinsed once with versene and then incubated with versene for 5-10 min at 37°C. This treatment caused any remaining feeder cells to detach. Keratinocytes would round up but would not detach from the flask. The versene solution was discarded and the remaining keratincytes were incubated in 5 ml trypsin/versene solution (1 part trypsin and 4 parts versene) at 37°C for about 10 min, until all keratinocytes had detached from the flask. 5ml medium was added to the suspension and the number of cells was counted using a haemocytometer. The cells were pelleted and resuspended in medium as described and plated onto flasks with feeder cells. Keratinocytes could be cultured for up to 6-8 passages before they had to be discarded due to poor growth and excessive accumulation of terminally differentiated cells. Keratinocytes used for transfections were of early passage, 2-5.

To analyze by immunofluorescence the expression of markers of hair follicle and sebaceous differentiation primary keratinocytes were plated on J2-3T3 feeder cells on coverslips prepared in 24-well plates. Typically, 3x 10^4 keratinocytes were plated per coverslip, and cultured as on plastic until they reached the desired density. They were incubated with versene for 5-10 min at 37°C to eliminated the feeder cells, incubated in culture medium again for 30 min to allow spreading and subsequently fixed and immunostained.

Transfection of human primary keratinocytes

In order to check that the ΔNß-cateninER construct was expressed by basa epidermal cells and was responsive to 4OHT, primary keratinocytes were transfected on glass coverslips for immunofluorescence analysis. Glass coverslips were placed in well of 6-well plates (4 coverslips per well). Primary keratinocytes were harvested and plated at a density of 5-6.5x 10^5 per well of a 6-well plate in FAD+FCS+HICE. Cells were allowed to adhere for 1-2 hours before being rinsed twice in PS to remove any cells not adhered. Cells were subsequently culture overnight in keratinocyte serum free medium (KSFM, Gibco BRL) supplemented with bovine pituitary extract and insulin (Invitrogen) as per the Manufacturer's instructions. Keratinocytes were transfected with Fugene-6 (Roche). Fugene-6, 6µl, was added to 94µl of DMEM (Invitrogen) and left for 5 min at room temperature. Subsequently the DMEM-Fugene mixture was added to 2µg of DNA to be transfected and mixed well by pipetting. The DMEM-DNA-Fugene mix was left at room temperature for 15-20 min before addition of 700µl of KSFM with additives. The mixture was pipetted gently up and down twice before being added to the keratinocytes, which had been pre-washed in PBS. The transfection mixture was left on the cells at 37°C for 2 hours. Following transfection cells were rinsed twice with KSFM with additives to remove any remaining transfection mixture and cultured in KSFM with additives with or without 200nM 4OHT (Sigma, stock 2mM prepared in ethanol) for 1 hour to overnight.

2.3.5. Primary mouse keratinocytes

Primary mouse keratinocyte culture medium

A low calcium FAD medium was used which was prepared in the same way as normal FAD, except calcium salts were not included in the DMEM and F12 formulations. The FCS used as a supplement in low calcium FAD also had to have calcium salts removed. This was achieved by treatment with Chelex deionising resin as follows: 300g of Chelex 100 resin (Biorad; 100-200 mesh, sodium form) was added to 4l of dH_2O and stirred slowly at room temperature for at least an hour to generate a swollen resin form. The pH was adjusted to 7.0-7.5 with HCl and the swollen resin was then recovered by filtering through a stericup (Millipore). The recovered Chelex was added to 1L of FCS and stirred at room temperature for 1 h before being allowed to sit undisturbed for 30-60 min. The Chelex was removed and the FCS sterilised by filtering through a 0.22μm stericup (Millipore). The sterile chelated FCS was then aliquoted and stored at -20^0C. Complete low calcium FAD was prepared by adding 10 % chelated FCS to low calcium FAD supplemented with the HICE cocktail at the concentration used for standard complete FAD. Additionally, 1 % standard FAD was added to produce a final free calcium ion concentration of approximately 0.1 mM.

Isolation of primary mouse keratinocytes

Keratinocyte isolation from mouse neonates was performed according to (Roper et al., 2001). Newborn mice (2-4 days old) were killed and placed on ice for at least 1 hour. The mice were then washed sequentially with 10 % povidone and twice with 80 % ethanol. Under sterile conditions the tails, limbs and heads of the mice were amputated. For genotyping purposes the tail from each mouse was often frozen on dry ice and stored at -20^0C before DNA extraction (see Section 2.2.1). A longitudinal cut was then made along the back of the mice and the skin removed with forceps. Harvested skins were spread out epidermis side up in petri dishes and covered with trypsin solution overnight at 4^0C. The epidermis was then peeled off from the underlying dermis and minced into complete low calcium FAD using a pair of forceps. The released epidermal cells were pelleted by centrifugation at 1000 rpm for 3 min. The pellet was resuspended in complete low calcium FAD and filtered through a 70μm cell strainer (to remove

debris) onto Biocoat Collagen I-coated dishes (BD Biosciences). Typically, the cells isolated from 1 mouse were plated onto 1 well of a 6-well plate.

2.3.6. Establishment and culture of mouse keratinocyte lines

Keratinocyte lines were derived from adult wild type, D2 and D4 mice as described by (Carroll et al., 1995; Romero et al., 1999). The biggest possible region of dorsal skin of mice was clipped, the mice were killed and kept on ice for one hour. The mice were then washed sequentially with 10 % povidone, twice with 70 % ethanol and finally in sterile PBS. Under sterile conditions the dorsal skin was removed, placed epidermis side down in a Petri dish and, using a pair of forceps and a scalpel, was trimmed of dermal and fatty tissues. The skin was subsequently spread out epidermis side up in a new petri dish covered with trypsin solution and incubated overnight at 4^0C. The epidermis was then peeled off from the underlying dermis, minced into complete high calcium FAD medium (the same medium used for human keratinocytes) using a pair of forceps, transferred into a Falcon tube and agitated for 20 min at room temperature to allow keratinocyte dissociation. The mixture of dissociated cells and pieces of epidermis was separated using a cell strainer (Nunc) and the keratinocytes were pelleted, plated onto collagen I-coated plates already prepared with J2-3T3 feeder cells as described before and incubated at 32°C. Typically the keratinocytes collected from one mouse were plated in one 10cm diameter plate or 75cm^2 flask. The cells were kept in complete FAD medium all the time. The medium was changed every second day and for about one month the cells were replated 1:1 in a new plate of the same size every time they reached confluence (every 7-10 days), to eliminate the differentiated cells. These steps were repeated several times (5-9 passages total) and eventually the cultures started to show a higher proliferation rate. From this point cells were split 1:2-1:3 when passaged and soon the whole population showed increased growth rate, reaching confluence in 5-6 days. From this point the cells were cultured on normal plastic tissue culture plates, but always with J2-3T3 feeders. Passage 10-15 wild-type, D2 and D4 cells were harvested and frozen as described for the human keratinocytes and the J2-3T3 cells.

Luciferase assay

In order to perform luciferase assays, keratinocytes lines were transiently transfected with the following constructs: pRL (Renilla luciferase control, Promega), Topflash or Fopflash (firefly luciferase) (van de Wetering et al., 1997). Topflash and Fopflash constructs were provided by Dr David Prowse in the laboratory.

Typically, 4-6x 10^4 wild type, D2 and D4 keratinocytes were plated in quadruplicate in 24-well plates and allowed to adhere for 2 hours. The medium was then changed to KSFM with additives as described for human keratinocytes and the cells were incubated overnight at 32°C. The following day the transfection was performed using Genejuice reagent (Novagen) according to the Manufacturer's instructions. 0.2μg of DNA were trasfected per well (0.08 μg pRL and 0.12μg Topflash or Fopflash). The cells were incubated with the transfection mixture for 4 hours, then rinsed twice with KSFM and finally incubated with complete FAD supplemented with 4OHT for an additional 8-24 hours.

Cell lysis was performed using passive lysis buffer from the Dual-Luciferase Reporter Assay Kit (Promega). Cells were washed twice with PBS, 200μl of 1x buffer were added to each well and lysis was performed using a rubber cell scraper. Lysates were collected in eppendorf tubes, put on dry ice, subjected to two freeze/thaw cycles and finally centrifuged at 13000 rpm for 30 sec at 4°C. The clear lysates were transferred to fresh tubes and either stored at -70°C or used immediately for luciferase analysis.

Renilla and firefly luciferase activities were detected in enzymatic reactions prepared using the Dual-Luciferase Reporter Assay Kit (Promega) according to the Manufacturer's instructions. 25μl of each lysate were analyzed using a BioOrbit 1251 luminometer connected to an automated capillary system that automatically added the two luciferase substrates to the lysates. Renilla luciferase activity was used to normalize the data for transfection efficiency. Data from each experiment were normalized using the average activity detected from the wild type untreated samples.

2.3.7. SZ95 cells

SZ95 cells culture

SZ95 are derived from human facial skin sebocytes that have been immortalized by transfection of simian virus 40 large T antigen (Zouboulis et al 1999). Passage 30 SZ95 cells were kindly provided by Dr Christos Zouboulis (~~where?~~). The cells were cultured in Sebomed medium (Biochrom, Berlin) containing 10% FCS (Sera-Lab) and supplemented with 3 ng/ml keratinocyte growth factor (KGF, Peprotech), and 100 ng/ml epidermal growth factor (EGF, PeproTech). KGF 1000x stock solution was prepared by diluting 10μg powder in 3.34ml PBS. EGF was the same used for the keratinocyte medium.

SZ95 cells were typically seeded at a density of 2-4x 10^5 cells per $25cm^2$ flask or 6-8x 10^5 cells per $75cm^2$ flask and passaged (1:3-1:5) before they reached confluence, to avoid differentiation. The same versene/trypsin treatment as the one described for J2-3T3 cells was used. Medium was changed every two days and cells were kept at 37°C. Stock of SZ95 cells at passage 32-35 were frozen as described for J2-3T3 cells.

Induction of differentiation

SZ95 were induced to differentiate by culturing them at high density (Niemann et al., 2003) or by adding 10^{-6}M retinoic acid(Sigma)or 10^{-6}M prostagladinJ2 (Biomol) to the culture medium. Retinoic acid 1000x stock solution was prepared by desolving the powder in DMSO and subsequently diluting it in ethanol. ProstaglandinJ2 1000x stock solution was prepared by desolving the powder in ethanol (25mg/ml).

Clonogenicity assay

Equal numbers (100-1000) of viable keratinocytes and SZ95 cells were plated per 60mm dish in triplicates on top of mitomycin C-treated J2-3T3 feeder cells. All cells were kept in complete FAD medium, changed every second day. After 2 weeks the cultures were washed with PBS and the cells were fixed in 3.7% formaldehyde for 10 minutes at room temperature, washed in PBS and kept in PBS at 4°C until stained.

De-epidermalised Dermis (DED) Culture

Preparation of DED

The method for growing SZ95 cells on DED was based on the model set up for primary keratinocytes to achieve histological differentiation as close as possible to the epidermis *in vivo* (Prunieras et al., 1983). Human breast skin was provided with the informed consent of the patients. It was cut into $10cm^2$ pieces and the subcutaneous fat was scraped off. The skin was heated in PBS to 56°C for 20 minutes and the epidermis was peeled off. The remaining dermis was cut into $1cm^2$ pieces, placed into cryovials and snap frozen in liquid nitrogen. The vials were allowed to thaw at room temperature for 20 minutes and then frozen again in liquid nitrogen. This cycle of freezing and thawing was repeated 10 times in order to kill all of the cells in the dermis. After the last cycle the vials were stored at -70°C before sectioning.

SZ95 culture on DEDs

The vials were thawed and the pieces of DED were placed on sterile tissue culture inserts (Becton-Dickinson) in 6-well plates, with the denuded epithelial surface uppermost and exposed to the air. 10^5 SZ95 cells were harvested using the versene/trypsin treatment, washed twice in the culture medium and centrifuged at 1000rpm for 4 minutes. The cell pellet was resuspended in 20μl complete Sebomed culture medium and seeded onto the denuded epithelial surface of the DEDs. Cultures were fed by pipettin 1.5ml complete Sebomed medium ineach well every 2-3 days for 2-3 weeks.

DED cultures were kept intact, frozen on dry ice and stored at -70°C until use.

Retroviral producer cell culture

The Phoenix cell second-generation retrovirus packaging line (obtained from ATCC with kind permission of Dr G Nolan, Stanford University School of Medicine, Stanford, CA, USA) (Lorens et al., 2000) was used in conjunction with modified pBabepuro retroviral vectors (Markowitz et al., 1988a; Markowitz et al., 1988b) to generate retrovirus. The Phoenix line is based on the 293T embryonic kidney cell line

transformed with adenovirus E1a and containing a temperature sensitive T antigen. Gag-pol and envelope protein constructs were introduced separately into the 293T line and are driven by different, non-Moloney promoters to reduce recombination potential. Gag-pol was introduced with hygromycin as the co-selectable marker and the envelope protein constructs with diptheria resistance as the co-selectable marker. Both ecotropic and amphotropic Phoenix packaging lines are available but I only used the amphotropic. Cells were cultured in E4 medium supplemented with 10% FCS (Sigma) heat inactivated (FCS was incubated at 56°C for 30 min) and passaged, frozen and thawed as the J2-3T3 feeder cells were.

Retrovirus generation

To produce retrovirus using the Phoenix packaging line, cells were transfected with the retroviral vector construct using a calcium phosphate method. 18-24 h prior to transfection, Phoenix cells were plated at 8 x 10^6 cells per 10cm dish. 5 min before starting the transfection, chloroquine was added to the cells to 25 μM (from a 50mM stock). The chloroquine acts to inhibit lysosomal DNases and as DNA delivered via the calcium-phosphate method is thought to transit through lysosomes, chloroquine improves the efficiency of transfection. In a 15 ml tube, 10-20μg DNA was made up to 439 μl with dH_2O before addition of 61 μl of 2M $CaCl_2$. The solution was mixed thoroughly with finger tapping and then had 500 μl 2xHBS added. An automatic pipettor was used to vigorously bubble the combined solutions for 15s before adding dropwise onto the Phoenix cells' medium. The cells were inspected using a microscope for the presence of fine black particles and the medium rocked back and forth to ensure an even distribution. 24h post-transfection, the medium was replaced with fresh complete FAD (for subsequent infection of keratinocytes) and the cells transferred to 32^0C as the retrovirus is more stable at this temperature in comparison to 37^0C (Dr David Prowse, personal communication). Retrovirus-containing supernatant was collected at 24 and 48 hours after transfer to 32^0C and the Phoenix cells then disposed of.

Producer lines that are generated by retroviral infection have higher viral titres than those generated by transfection (Morgenstern and Land, 1990), hence virus released

into the culture medium by transfected Phoenix cells was used to infect the amphotropic packaging line AM12 (Markowitz et al., 1988a). AM12 cells were seeded on 100mm dishes at 1-2x 10^5 density the day before infection. 2.5ml infection medium (virus-containing medium freshely collected from the Phoenix cells and supplemented with 8 μg/ml polybrene; Sigma) was added to the AM12 cells. The second virus collection from Phoenix cells replaced the first infection medium and incubated overnight on the same AM12 cells. On the following day the infection medium was replaced with fresh culture medium (E4 + FCS). The selection medium containing 2.5 μg/ml puromycin was applied 48h later and changed every 2 days until cells reached confluence.

Amphotropic AM12 cells containing pBabePuroMycER, pBabePuroΔNß-catenin or pBabePuroInvolucrin-GFP reporter were prepared by Dr Isabel Arnold, Dr Laura Turner and Dr Masaru Honma respectively in the laboratory.

Infection of SZ95 cells

AM12 cells were treated with 8μg/ml mitomycin C for 3 hours, then washed twice with medium. SZ95 cells were plated at approximately 20% confluency and co-cultured in complete Sebomed with the AM12 cells for 2 days to one week. To improve the efficiency of the infection, polybrene was also added to a final concentration of 2.5 μg/ml (from a 5 mg/ml stock), but only for the first two days of co-culture. AM12 cells were subsequently removed with versene treatment and infected SZ95 cells were selected by adding puromicing to the medium. The concentration of puromicin used varied from 1mg/ml for the first day of selection to 0.6 mg/ml for an additional week. Expression of the various constructs was checked by western blot (described in section 2.4.2).

MycER, ΔNß-cateninER and empty vector SZ95 cells were incubated with 200nM 4OHT for 2 or 3 days to induce Myc or ß-catenin activation. When the cells were seeded on coverslips, 4OHT was added to the culture medium on the following day.

Time-lapse video microscopy

For time-lapse video microscopy, approximately 1-2x 10^5 infected SZ95 cells were plated on a 35 mm dish. On the following day fresh medium (containing 200nM 4OHT in the case of the MycER cells) was added and time-lapse video microscopy was set up. The cells were kept humidified at 37°C in 5% CO2 and videotaped for up to 48 hours. Frames were taken every 4 minutes using Olympus IMT1 or IMT2 inverted microscopes driven by Broadcast Animation Controllers (BAC 900) and fitted with monochrome CCD cameras and video recorders (Sony M370 CE and PVW-2800P, respectively). Recordings were digitised and the sequence of all frames was run on a PC. Motility was measured using a cell tracking extension (CR-UK) written for IPLab (Signal Analytics Inc.), and speed was calculated using a program written in Mathematica by Daniel Zicha (CR-UK).

2.4. Biochemical techniques

2.4.1. Protein extraction

Extraction of proteins with RIPA buffer

For analysis of ER levels in K14ΔNß-cateninER mice, primary keratinocytes and cells from keratinocyte lines were washed twice in PBS then lysed in RIPA buffer (50 mM Tris-HCl pH 7.4, 1% NP40, 0.25 % sodium deoxycholate, 150 mM NaCl, 1 mM EGTA), which was supplemented with protease and phosphatase inhibitor cocktails (Roche, one tablet per 10ml RIPA buffer).

Cells were incubated in RIPA buffer for 10-30 min at 4°C, and subsequently scraped. Cell debris was pelleted by centrifugation at 14000 rpm for 10 min at 4^0C in a bench top centrifuge. Cleared lysates were assayed for protein content and stored at -70^0C.

Extraction of proteins with Triton buffer

Triton extraction buffer contained 0.5% (v/v) Triton-X-100 (Sigma). 120 mM NaCl, 25mM KCl, 2mM $CaCl_2$, 15mM Tris-HCl pH 7.5. 2mM phenylmethanesulphonyl

fluoride (PMSF), 0.1 mM dithiothreitol (DTT) and 1μg/ml leupeptin (Sigma) were added to extraction buffer just before addition to the cells. The stock PMSF was a 0.1M solution in dH_2O and stored at -20°C. The Leupeptin stock solution was a 100μg/ml solution in dH_2O and stored at -20°C. Cells were washed twice in ice cold PBS, then extracted for 10 min at 4°C on a rocking platform. The cells were scraped from the culture plates and cell debris was pelleted by centrifugation at 14000 rpm for 10 min at 4^0C in a bench top centrifuge. The supernatant (Triton-soluble fraction) was assayed for protein content, aliquoted and stored at -70°C.

Hypotonic lysis and cell fractionation

To analyse the soluble pool of β-catenin, keratinocytes were lysed in hypotonic buffer at 4^0C (20 mM Tris-HCl pH 7.5, 1 mM $MgCl_2$, 1 mM sodium orthovanadate, 25 mM β-glycerophosphate with protease inhibitors) using a Dounce homogenizer and centrifuged at 600 g in a Beckman Optima TL Ultracentrifuge for 10 min to remove nuclei. The supernatant was centrifuged at 100,000 g for 1 hr at 4^0C; the particulate fraction was discarded and the soluble fraction was used for analysis.

BCA protein assay

The concentration of protein in samples was determined using a BCA protein assay kit (Pierce). The kit is based upon the Biuret reaction involving the reduction of Cu^{2+} ions to the Cu^{1+} (cuprous) ion by protein in alkaline medium. Chelation of the cuprous ion to bicinchoninic acid (BCA) molecules provides a sensitive colorimetric detection method with the reaction product exhibiting a strong absorbance at 562nm. The absorbance is linear over a 20-2000 μg/ml protein concentration range. A protein standard curve was produced from 0 to 2000 μg/ ml protein by making dilutions of a 2 mg/ ml BSA solution (Pierce) into PBS according to the Manufacturer's instructions. Protein samples to be assayed were diluted 1:4 to 1:5 in PBS to minimise interference of lysis buffer detergent and supplements with the reaction and also to place the protein concentration within the standard curve. The assay was set up on a 96-well plate (DYNEX Technologies) according to the Manufacturers instructions and all standards and samples were assayed in triplicate wells. The plate was incubated at 37^0C for 30 min and the absorbance at 562nm was then read on a Titertek Multiscan MCC/340 MKII

spectrophotometer. The protein concentration of each sample was determined against the standard curve.

2.4.2. SDS-PAGE and Western blotting

Laemmli sample buffer

2x Laemmli sample buffer (reducing) comprised 125mM Tris-HCl, pH6.8, 2% SDS, 20% glycerol, 0.02% bromophenol blue and 10% (v/v) β-mercaptoethanol (Sigma). The sample buffer was aliquoted and stored at -20^0C.

SDS-PAGE

Vertical mini-gel electrophoresis apparatus (Atto) was used. Gels were prepared between the glass plates using the method of Laemmli (Laemmli, 1970). Table 2.1 describes the gel compositions. Immediately after pouring the resolving gel solution, 0.5 ml of dH_2O was carefully applied to ensure a level interface as well as to eliminate an air-acrylamide interface. Gels were allowed to polymerise at room temperature for approximately 30 min. The dH_2O layer was discarded from the top of the resolving gel and the stacking gel solution was then poured. An 8 or 12 well comb was inserted to create wells and the gel was left to polymerise. After the gel had set, the comb was removed and the wells were flushed with SDS-PAGE running buffer which comprised 50mM Trizma base, 384mM glycine and 0.1% SDS.

Equal amounts of protein from each sample (typically 10-20μg total protein) were diluted into Laemmli sample buffer and placed in a 100^0C hot block for 5 min before being briefly spun down in a bench top centrifuge and applied to the wells using capillary pipette tips. 10μl pre-stained rainbow molecular weight markers (Amersham) were added to 10μl Laemmli sample buffer, boiled for 5 min and loaded into one of the wells. Samples were electrophoresed at 120V until the dye front had run off the bottom of the gel and the gel was then removed and prepared for Western blot.

Table 2. 1. Preparation of SDS-PAGE gels

Stock solutions

Solution A	40 % Acrylamide mix (37.5:1 acrylamide to bis-acrylamide ratio) (Amresco)
Solution B	3M Tris-HCl, pH 8.8 (BDH)
Solution C	10 % SDS in dH_2O
Solution D	2M Tris-HCl, pH 6.8 (BDH)
AP	10 % ammonium persulphate (Bio-Rad) in dH_2O, aliquots stored at -20^0C
TEMED	N,N,N',N'-tetramethylethylenediamine (Bio-Rad)

Resolving gels (15 ml)

stock solutions	**A**	**B**	**C**	**dH_2O**	**AP**	**TEMED**
8 %	3 ml	1.9 ml	0.15 ml	9.8 ml	0.15 ml	9 µl
10 %	3.75 ml	1.9 ml	0.15 ml	9.05 ml	0.15 ml	6 µl
12 %	4.5 ml	1.9 ml	0.15 ml	8.3 ml	0.15 ml	6 µl
15 %	5.625 ml	1.9 ml	0.15 ml	7.715 ml	0.15 ml	6 µl

Stacking gel (10 ml)

stock solutions	**A**	**C**	**D**	**dH_2O**	**AP**	**TEMED**
	1.275 ml	0.1 ml	0.625 ml	7.85 ml	0.1 ml	10 µl

Western blotting

After electrophoresis, proteins were transferred onto PVDF membrane (Millipore) which had been pre-wet in absolute methanol. Mini-Trans Blot Cells (Biorad) were used to transfer the protein and were set up according to the Manufacturer's instructions. Transfer took place at 4°C overnight at 30 Volts. The blot was then rinsed

briefly in TBS containing 0.1 % Tween-20 (TBST) before blocking with 5 % Marvel milk powder (99 % fat free, Premier Brands UK Ltd.) dissolved in TBST for at least 1 hour at room temperature.

Transfer buffer

The transfer buffer for Western blotting was made up freshly each time: 8.75g Trizma base and 43.5g Glycine were dissolved in 500 ml dH_2O to which was added 15 ml of a 10 % SDS solution. The buffer was made up to 1.2l before the addition of 300 ml of methanol and was then thoroughly mixed.

Probing blots with antibodies and ECL detection

Blocked membranes were incubated with primary antibody typically diluted in 5 % milk powder solution in TBST. Some antibodies (according to manufacturers instructions) were diluted in 5 % BSA in TBST. Incubation with primary antibody was at 4^0C overnight with gentle agitation. After 3 x 20-30 min washes with TBST, the blots were incubated for 1 hour at room temperature with HRP-coupled secondary antibody (Amersham) diluted 1:5000 in 5 % milk, TBST. Membranes were then washed 3 or 4 times with TBST again. To detect bound HRP, a chemiluminescence kit was used according to the Manufacturer's instructions (ECL, Amersham). X-ray films (Kodak) were exposed in autoradiography cassettes lined with reflective screens. Densitometry of bands produced on films was carried out using NIH Image v1.58.

If blots were to be re-probed, they were stripped in a 200mM Glycine pH 2.5 solution containing 0.4% SDS for 30 min at room temperature with agitation. Blots were then rinsed in 1M Tris-HCl pH 7.5 and washed 3 times for 5 min each with TBST before re-blocking and subsequent incubation with another primary antibody.

2.5. Histology and histochemistry

2.5.1. General solutions

Paraformaldehyde solution

A 10 % solution was prepared by adding paraformaldehyde powder (BDH) to PBS and heating at 60^0C until mostly dissolved. A few drops of 1M NaOH were added to completely clear the solution which was then allowed to cool to room temperature before adjusting the pH to 7.6 with HCl. The stock was aliquoted and stored at -20^0C. A 4 % paraformaldehyde solution was used to fix cells and tissue.

Neutral buffered saline (Prepared by CR-UK)

50g NaCl and 150g Na_2SO_4 were dissolved in 8l of dH_2O before addition of 1l of 40 % formaldehyde. The final solution was made up to 10l. The pH was adjusted to 7.0 and the solution was not autoclaved.

Gelvatol mounting solution

The Gelvatol mounting solution was prepared as described by Harlow and Lane(Harlow and Lane, 1988). 2.4g Gelvatol (Monsanto Chemicals) was mixed with 6g glycerol (Sigma) and vortexed. 6ml dH_2O was added, mixed and left to stand for 90 minutes at room temperature. 12.5ml of 200mM Tris-HCl, pH8.5 was added and the solution was vortexed, heated to 50°C and vortexed again. Heating and vortexing were repeated three times and the solution placed on an end over end mixer overnight at room temperature. DABCO (Sigma) was added as an antifade agent to 2.5 % and mixed to dissolve. The solution was then centrifuged at 2000rpm for 10 minutes at room temperature and stored in aliquots at -20^0C until use.

2.5.2. Preparation of paraffin and cryosections

Paraffin sections

To collect mouse skin for paraffin sections, the back of the mouse was shaved before removing the skin and stretching out onto a backing card (dermal/connective tissue side down). Small rectangles of skin (approximately 15mm x 5mm) were cut out and placed into neutral buffered saline overnight before transferring to a 70 % ethanol solution. The supported skin was then mounted in paraffin blocks by the CR-UK Histopathology Unit. 5mm sections were then cut from the blocks using a microtome and mounted onto glass slides. Prior to immunostaining, sections were dewaxed by washing twice in Xylol followed by four washes in isopropanol solutions of decreasing concentration (100 %, 96 %, 75 %, 50 %). Sections could be stained with haematoxylin/eosin (H&E) for observation of skin histology (performed by CR-UK Histopathology Unit).

For general immunostaining, dewaxed sections were placed in 500ml 10 mM citrate buffer (pH6) antigen retrieval solution and microwaved for 20 min at full power. The slides were then left to cool down in the retrieval solution for 20 min at room temperature before washing in PBS and then processing according to the standard immunostaining procedure.

Frozen sections

To produce frozen sections of mouse skin, small rectangles of skin sample were placed on nitrocellulose membrane for support and subsequently in a plastic mould containing O.C.T compound (BDH) and then frozen on dry ice. Frozen blocks were stored at -70^{0}C before cutting 6-10μm sections with a cryomicrotome (Reichart-Jung) and mounting onto slides (Superfrost Plus, BDH).

Frozen DED samples were cut in half in an orientation perpendicular to the surface of the tissue and sections were cut from the middle outward. The sections were mounted onto slides (Superfrost Plus, BDH) and stored at -70°C. DED sectioning was performed by the CR-UK Histopathology Unit, which provided also frozen scalp sections.

To examine the morphology of the tissues frozen sections were stained with haematoxylin and eosin (H&E). For immunofluorescence staining, frozen sections were thawed at room temperature for 30 minutes.

2.5.3. Alkaline phosphatase detection

Alkaline phosphatase activity was visualised in frozen sections with NBT-BCIP method (Filipe and Lake, 1990). The sections were pre-incubetd in freshly made NTMT buffer (100 mM Tris-HCl pH 9.5, 50 mM $MgCl_2$, 100 mM NaCl, 0.1% TritonX100) for 10 minutes, changing the buffer after the first 5 min. They were subsequently incubated in NTMT buffer containing 4.5 µl/ml Nitro blue tetrazoliun chloride (NBT, Roche) and 3.5 µl/ml 5-bromo-4-chloro-3-indolyl phosphate (BCIP, Roche) for about 5 minutes, or until the reaction had produced visible blue staining, as checked under the microscope. The reaction was stopped with 3 x 10 min washes with PBS containng 0.1% Triton-X-100. The sections were counterstained with Fast Red and mounted in Permount (Fischer Scientific) by the CR-UK Histopatology Unit.

2.5.4. Nile Red staining

Nile red (Sigma) was used to detect lipid droplets in scalp frozen sections and cultured cells alone or in combination with immunstainings. A 1000x stock solution was prepared by desolving the powder in methanol at a concentration of 10µg/ml and diluted in PBS for use. Unfixed scalp sections and paraformaldehyde fixed cells were incubated with Nile red for 15 min. They were subsequently washed 3 times with PBS and mounted in Gelvatol. When in combination with immunostaining, Nile Red incubation followed the incubation with secondary antibody. Staining was detected from cells permeabilized with 0.2% triton (see below) for 2 minutes but any stronger permeabilization procedure would disrupt the cytoplasmic lipid droplets.

2.5.5. Antibodies

All the antibodies used are listed in Tables 2.x to 2.y. (Key to antibody used: WB, Western blot; IF, Immunofluorescence/histochemistry; WM: whole mount immunostaining; O/N, overnight incubation for immunostaining; Rb, rabbit; Mo, mouse; Hu, human; Go, goat; Mc, monoclonal; Pc, polyclonal).

Table 2. 2. Primary antibodies

Antibody	Antigen Specificity	Species	Dilutions	Source/References
AC40	actin	Mo Mc	WB 1:1000	Sigma
clone 15B8	ß-catenin	Mo Mc	IF 1:100 WB 1:1000	Sigma
clone 14	ß-catenin	Mo Mc	IF 1:100	Transduction laboratories
OBT0030	BrdU	Rat Mc	IF 1:100 WM 1:100	Oxford Biotechnology
RAM34	CD34 Mo	Rb Pc	IF 1:25	BD Pharmingen
N/A	CDP Mo Hu	Rb Pc	IF 1:500	(Ellis et al., 2001)
sc-6327	CDP Mo Hu	Go Pc	WM 1:100	Santa Cruz
SQ37C	cornifin alpha Hu	Rb Pc	IF 1:500	(Fujimoto et al .,1997)
D1-72-13G	cyclin D1	Mo Mc	IF 1:100	Zymed
E29	EMA Hu	Mo Mc	IF 1:100 WB 1:1000	Dako
sc-1647	Erk2	Mo Mc	WB 1:2000	Santa Cruz
18341	fatty acid synthase Mo	Rb Pc	IF 1:50 O/N	IBL
c-15	Ihh Mo Hu	Go Pc	IF 1:50 O/N	Santa Cruz
SY5	involucrin Hu	Mo Mc	IF 1:100 WB 1:2000	(Hudson et al., 1992)
c-20	Jagged1 Mo	Go Pc	WM 1:100	Santa Cruz
MK-1	keratin 1 Mo	Rb Pc	IF 1:100	Covance
MK-10	keratin 10 Mo	Rb Pc	IF 1:100	Covance
MK14	keratin 14 Mo	Rb Pc	WM 1:1000	Covance
N/A	keratin 17 Mo Hu	Rb Pc	IF 1:1000	(McGowan and Coulombe, 1998)
LP1K	keratin 7 Mo Hu	Mo Mc	IF 1:100 WB 1:1000	(Markey et al., 1992)
2D12	Lef1 Mo	Mo Mc	IF 1:100	Upstate
N-262	Myc Hu	Rb Pc	IF 1:100 WB 1:500	Santa Cruz
MC-20	oestrogen receptor Mo	Rb Pc	IF 1:50 WB 1:500	Santa Cruz
HL7	oestrogen receptor Mo	Rb Pc	IF 1:100	(Arnold and Watt 2001)
ERP2	oestrogen receptor Mo	Rb Pc	IF 1:100	(Lo Celso et al. 2004)
N/A	Patch C-terminus Hu	Rb Pc	WB 1:200	Research Genetics
SAP4G5	tubulin alpha Hu	Mo Mc	WB 1:10 000	Sigma

Table 2. 3. Secondary antibodies

Antigen specificity	Conjugate	Species	Source
mouse IgG, whole molecule	Alexa 488	Goat, Donkey	Molecular Probes
goat IgG, whole molecule	Alexa 488	Rabbit, Donkey	Molecular Probes
rabbit IgG, whole molecule	Alexa 488	Goat, Donkey	Molecular Probes
rat IgG, whole molecule	Alexa 488	Goat	Molecular Probes
mouse IgG, whole molecule	Alexa 594	Goat, Donkey	Molecular Probes
rabbit IgG, whole molecule	Alexa 594	Goat, Donkey	Molecular Probes
mouse IgG, whole molecule	HRP	Sheep	BD Biosciences
rabbit IgG, whole molecule	HRP	Donkey	BD Biosciences
goat IgG, whole molecule	HRP	Rabbit	Sigma
mouse IgG, whole molecule	Biotin	Rabbit	DAKO
rabbit IgG, whole molecule	Biotin	Donkey	DAKO
goat IgG, whole molecule	Biotin	Rabbit	DAKO

2.5.6. Immunohistochemistry and immunofluorescence

Preparation of cells for immunofluorescence

Cells were cultured on tissue culture plastic microscope slides (Nunc) or on glass coverslips (Chance Propper Ltd.) prepared by the CR-UK Washing Room. Coverslips were first boiled in 7x detergent (ICN) for 30 minutes to remove silicone coating. They were rinsed thoroughly first in tap water and then in dH_2O. Washed coverslips were rinsed briefly in absolute ethanol and spread out on filter paper to dry completely before autoclaving.

Culture medium was discarded from cells and they were rinsed in PBS before fixing in 4% paraformaldehyde solution for 10 minutes at room temperature and stored in PBS at 4°C for up to two weeks.

Immunoihistochemistry and immunofluorescence general protocols

Paraffin and frozen sections were prepared as described in section 2.5.2.
Cells and frozen sections were fixed in 4% paraformaldehyde for 10 min at room temperature and permeabilized with 0.2% Triton-X-100 for 5 min at room temperature. Fixed sections were washed with 3 changes of PBS before immunostaining.

Frozen and paraffin sections that were to be stained by immunohistochemistry rather than immunofluorescence were incubated prior to immunostaining in 3% H_2O_2 in dH_2O for 5 min to quench peroxidase activity present in the tissue.

Aspecific staining was blocked with 10 % goat serum (Sigma) or 0.2% fish skin gelatin (Sigma) in PBS for 1-2 hours at room temperature. The samples were then incubated with primary antibody diluted to an optimal concentration in PBS 1% BSA (ICN). Typically, samples were incubated with the primary antibody for 1h at room temperature or at 4^0C overnight as indicated in the antibody table. Sections were then washed in PBS or TBS 3 times.

For immunofluorescence, secondary antibody coupled to a fluorophore (either Alexa 488 or Alexa 594) was used at a dilution of 1:1000 in PBS 1% BSA (ICN) for 30 min at room temperature before washing as before. Sections were finally rinsed 3 times in dH_2O for 5 min each to remove PBS and mounted in gelvatol solution. In some experiments, sections were double stained using two primary antibodies of distinct species in succession and then probed at the same time with species-specific secondary antibodies coupled to different fluorophores. Also, DAPI (Molecular Probes) or propidium iodide (Sigma) could be used to produce a nuclear counterstain. Stained sections were viewed using either a Zeiss Axiophot microscope (Carl Zeiss) or a Zeiss LSM 510 confocal laser scanning microscope (Carl Zeiss) with an argon laser at 488nm and 568nm and a helium-neon laser at 633nm.

To detect ER expression, immunostaning was performed on frozen sections as described before, with the difference that the sections were incubated for 90 minutes in 10% goat serum (Sigma) in PBS, then for 40 minutes with the ER primary antibodies.

The anti-CD34 antibody was biotinylated and Alexa488-conjugated streptavidin (Molecular Probes) was used instead of secondary antibody. Biotin block was performed using the Vectro Laboratories kit according to the Manufacturer's instructions before incubation with 10% serum.

For immunohistochemistry, a secondary antibody coupled to biotin was used (biotinylated rabbit anti-mouse from DAKO was used at a dilution of 1:750). Sections were washed twice in PBS before incubation for 30 min at room temperature with streptABComplex/HRP (prepared according to the Manufacturer's instructions, DAKO). Slides were washed twice again in PBS and then developed in di-amino-benzydine (DAB, Sigma) substrate solution for 3-5 min at room temperature in the dark (DAB solution was repared by adding one tablet of DAD to one tablet of hydroxyurea to 10ml dH_2O). After 3 washes in dH_2O sections were counterstained with haematoxylin and mounted by the CR-UK Histopatology Unit.

The Mouse on Mouse kit (Vector Laboratories) was used following the Manufacturer's instructions when a monoclonal antibody was used on mose sections for either immunofluorescence or immunohistochemistry.

BrdU immunostaining protocol

BrdU that had been incorporated into the DNA of those cells going through S-phase of the cell cycle could be detected by immunofluorescence as follows. Paraffin skin sections were dewaxed as above and placed in Automation Buffer (Biomeda Corporation) for 5 min. Slides were then incubated in prewarmed 2N HCl at 37^0C for 30 min followed by borate buffer pH 7.6 for 3 min at room temperature. The sections were digested in prewarmed 0.01 % trypsin in 0.05M Tris pH 7.5 for 3 min at 37^0C before a further incubation in Automation Buffer for 5 min at room temperature. The sections were blocked with 10 % goat serum in Automation Buffer for 30 min before incubation for 1 h at room temperature with anti-BrdU antibody (Becton Dickinson)

diluted 1:25 into 1 % BSA in Automation Buffer. After 3 washes of 20 min each with Automation Buffer slides were probed with Alexa 488 – conjugated secondary antibody for 20 min at room temperature. The secondary antibody was diluted in 1 % BSA in Automation buffer. Finally, after 3x PBS washes, nuclear counterstaining was obtained by incubating the sections with 1μg/ml propidium iodide in PBS in the dark. Washes in dH_2O and mounting of slides were performed as described in the previous section.

2.5.7. Tail epidermis whole mounts

Preparation of tail epidermis for whole mount analysis

The method to prepare wholemounts of mouse tail epidermis was developed by Dr Kristin Braun in the laboratory (Braun et al., 2003) and was a modification of the method to prepare human epidermal wholemounts (Jensen et al., 1999). A scalpel was used to slit the tail lengthways. Skin was peeled from the tail, cut into pieces (0.5x0.5 cm^2) and incubated in 5 mM EDTA in PBS at 37°C for four hours. Forceps were used to gently peel the intact sheet of epidermis away from the dermis and the epidermal tissue was fixed in 4% formal saline (CR-UK) for 2 hours at room temperature. Fixed epidermal sheets were stored in PBS containing 0.2% sodium azide at 4°C for up to 8 weeks prior to labelling.

Immunostaining of whole mount preparations

Epidermal whole mounts were blocked and permeabilised by incubation in PB buffer for 30 minutes (Jensen et al., 1999). PB buffer consists of 0.5% milk powder, 0.25% fish skin gelatin (Sigma) and 0.5% Triton X-100 in TBS (0.9% NaCl, 20 mM HEPES, pH 7.2). Primary antibodies were diluted in PB buffer and tissue was incubated overnight at room temperature with gentle agitation. Epidermal wholemounts were then washed for at least 4 hours in PBS containing 0.2% Tween 20, changing the buffer several times. Incubation with secondary antibodies was performed in the same way as the primary antibodies. Samples were rinsed in distilled water and mounted in Gelvatol (described before). In some experiments, whole mounts were double stained using two

primary antibodies of distinct species in combination and then probed at the same time with species-specific secondary antibodies coupled to different fluorophores. To detect BrdU-labelled cells, after permeabilisation and prior to incubation with the anti-BrdU antibody, whole mounts were incubated for 20-30 minutes in 2M HCl at 37°C.

2.5.8. In situ hybridization

The templates for the Shh and Ptc riboprobes were provided by Dr B. Spencer-Dene (Revest et al., 2001) and prepared according to the CR-UK In Situ Hybridization Service's instructions by Dr David Prowse in the laboratory. In situ hybridisation was performed by the CR-UK In Situ Hybridization Service, using ^{35}S-labeled riboprobes. Hybridisation with a β-actin antisense probe served as positive control.

2.6. List of suppliers and distributors

Affymetrix Inc. Santa Clara, California, USA

Ambion Inc. Austin, Texas, USA

Amersham Biosciences, Amersham, Buckinghamshire, UK.

Amresco, Solon, Ohio, USA.

Atto, supplied by Biorad.

Beckman Instruments, Palo Alto, California, USA

BD Biosciences, Erembodegen, Belgium.

BD PharMingen, San Diego, California, United States.

BDH Laboratory Supplies Inc. Hemel Hempstead, Hertfordshire, UK.

Becton-Dickinson, Lincoln Park, New Jersey, USA.

Biochrom, Berlin, Germany.

Biomeda Corporation (automation buffer)

Biomol International, LP.Hamburg, Germany.

Biorad Laboratories Inc. Hemel Hempstead, Hertfordshire, UK.

Boehringer Mannheim UK Ltd. Lewes, East Sussex, UK.

Calbiochem – Novabiochem (UK) Ltd. Nottingham, UK.

Carl Zeiss Ltd. Welwyn Garden City, Hertfordshire, UK.

DAKO A/S, Glostrup. Denmark.

Difco aboratories, Manston, Wisconsin, USA.

DNA Technology AIS, Aharus, Denmark.

Eppendorf, Histon, Cambridge, UK.

Falcon, part of Nunc A/S, Roskilde, Denmark.

Fischer Scientific, Loughborough, Leicestershire, UK.

Gibco BRL/Life Technologies Ltd. Paisley, Renfrewshire, UK.

Helena biosciences, Sunderland, Tyne & Wear, UK.

IBL, Hamburg, Germany.

ICN Pharmaceuticals Ltd. Thame, Oxon, UK.

Imperial Laboratories (Europe) Ltd. Andover, Hampshire, UK.

Invitrogen, Paisley, UK.

Jencons, Leighton Buzzard, Beds, UK.

Leo Pharma A/S, Ballerup, Denmark.

Millipore, Harrow, Middelsex, UK.

Molecular Probes, Leiden, Netherlands.

Monsanto Chemicals, Springfield, Massachusetts, USA.

Nalgene Nunc International, Rochester, New York, USA.

Novagen, Madison, Wisconsin, USA.

New England Biolabs (NEB). New York, USA.

Nunc A/S, Roskilde, Denmark.

Oxford Biotechnology, Kidlington, Oxfordshire, UK.

Peprotech, Rocky Hill, New Jersey, USA.

Pharmacia Biotech, Uppsala, Sweden.

Pierce, Rockford, Illinois, USA.

Premier Brands UK Ltd. Knighton, Stafford, UK.

Promega UK Ltd. Southampton, UK.

Qiagen Ltd. Crawley, UK.

Roche, Lewes, East Sussex, UK.

Santa Cruz Biotech Inc. Santa Cruz, California, USA.

Savant supplied by Life Sciences International, Basingstoke, Hampshire, UK.

Schleicher and Schuell, London, UK.

Sera-Lab, Crawley Down, Sussex, UK.

Sigma Chemical Co. Poole, Dorset, UK.

Silicon Genetics, part of Agilent Technologies UK Ltd. South Queensferry, UK.

Stratagene, LA Jolla, California, USA.

Vector Laboratories, Burlingame, California, USA.

Zymed, San Francisco, California, USA.

Chapter 3. Effects of β-catenin activation in adult mouse epidermis

In this chapter I describe the generation and characterization of K14ΔNβ-cateninER transgenic mice. In these mice β-catenin activity is induced by 4-hydroxytamoxifen (4OHT) treatment, allowing me to investigate the ability of adult epidermal stem and progenitor cells to respond to β-catenin activation without any embryonic priming. The mice have allowed me to analyze in more detail the effect of β-catenin activation on epidermal proliferation and tumour formation.

3.1. Generation of K14ΔNβ-cateninER mice

3.1.1. ΔNβ-cateninER construct

I received the cDNA encoding ΔNβ-cateninER (Fig. 3.1A) from Dr. David Prowse in the laboratory. The cDNA was a fusion between a stabilized form of β-catenin and the ligand binding domain of a mutant mouse oestrogen receptor. β-catenin was lacking the N-terminal 147 amino acids, comprising the residues normally phosphorylated by GSK-3β (T2 mutant, Funayama et al., 1995; Zhu and Watt, 1999). The ligand binding domain of the oestrogen receptor (ER) was engineered to be insensitive to endogenous oestrogen but responsive to the drug 4-hydroxytamoxifen (4OHT, Littlewood et al., 1995). The ability of the fusion protein to respond to 4OHT by inducing transcription of β-catenin responsive genes had already been validated by Dr David Prowse in the laboratory (unpublished data and Lo Celso et al., 2004).

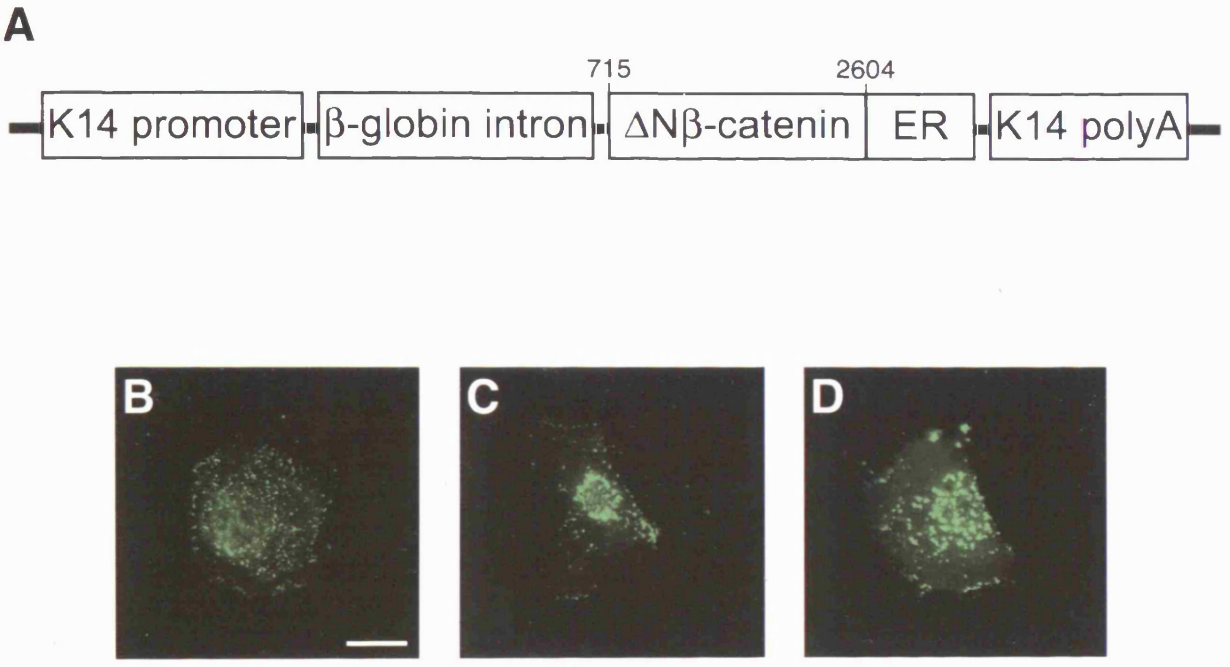

Figure 3.1. K14ΔNβ-cateninER construct. (A) ΔNβ-catenin is the sequence of Xenopus β-catenin, nucleotide 714 to 2604. It is fused to a mutated ligand binding domain of the oestrogen receptor and the fusion protein is cloned into the K14 cassette, which contains a portion of the keratin14 promoter, the β-globin intron and the keratin14 polyadenylation sequence. (B,C,D) Human primary keratinocytes were transfected with the K14ΔNβ-cateninER construct, fixed before (B) or after 4 hours of incubation with 4OHT (C,D) and stained with an antibody against the oestrogen receptor. Scale bar: 20 μm.

I subcloned the ΔNβ-cateninER cDNA into the K14 cassette (Fig. 3.1A), kindly provided by Elaine Fuchs (Arnold and Watt, 2001; Niemann et al., 2002; Vasioukhin et al., 1999), in which the keratin 14 promoter drives expression of the transgene in all the basal cells of the interfollicular epidermis and outer root sheath of mouse epidermis (Byrne et al., 1994; Vassar et al., 1989; Wang et al., 1997).

I verified the responsiveness of the K14ΔNβ-cateninER construct to 4OHT by transfecting it into human primary keratinocytes and immunostaining the transfected cells either untreated or following 1, 2 or 4 hours incubation with 4OHT 200nM using an antibody against the oestrogen receptor (HL7, gift from H. Land, (Arnold and Watt, 2001). In untreated cells the staining was punctate and diffuse in the cytoplasm and also present at the cell borders, but never in the nucleus (Fig. 3.1B). The cellular distribution of the fusion protein changed already after one hour of 4OHT incubation, with the greatest effect at 4 hours (Fig. 3.1C,D). The staining appeared always punctate but bigger aggregates concentrated predominantly in the nucleus or in the perinuclear region. This result was expected, since the ER is normally complexed with the heath shock proteins in the cytoplasm and only in the presence of 4OHT is free to translocate to the nucleus (Janes et al., 2004).

3.1.2. ΔNβ-cateninER transgenic founder lines

The purified K14ΔNβ-cateninER construct was injected into fertilized eggs by the CR-UK Transgenic Services. I screened by PCR and Southern blot all the mice generated, identifying 10 different founder lines. I subsequently selected five lines for further study according to the ability of the founders to transmit the transgene to their offspring and to the copy number of transgene integrated in their genomes (Fig. 3.2A). Line B1 and 3593 had a single copy of the transgene, line D2 had 12 copies, line C5 had 18 and line D4 had 21.

The amount of ΔNβ-cateninER protein expressed in the different lines varied according to the number of copies of transgene integrated in the genome, as shown by Western blot on primary cells isolated from the skin of transgenic mice from the highest and lowest copy number lines (Fig. 3.2B).

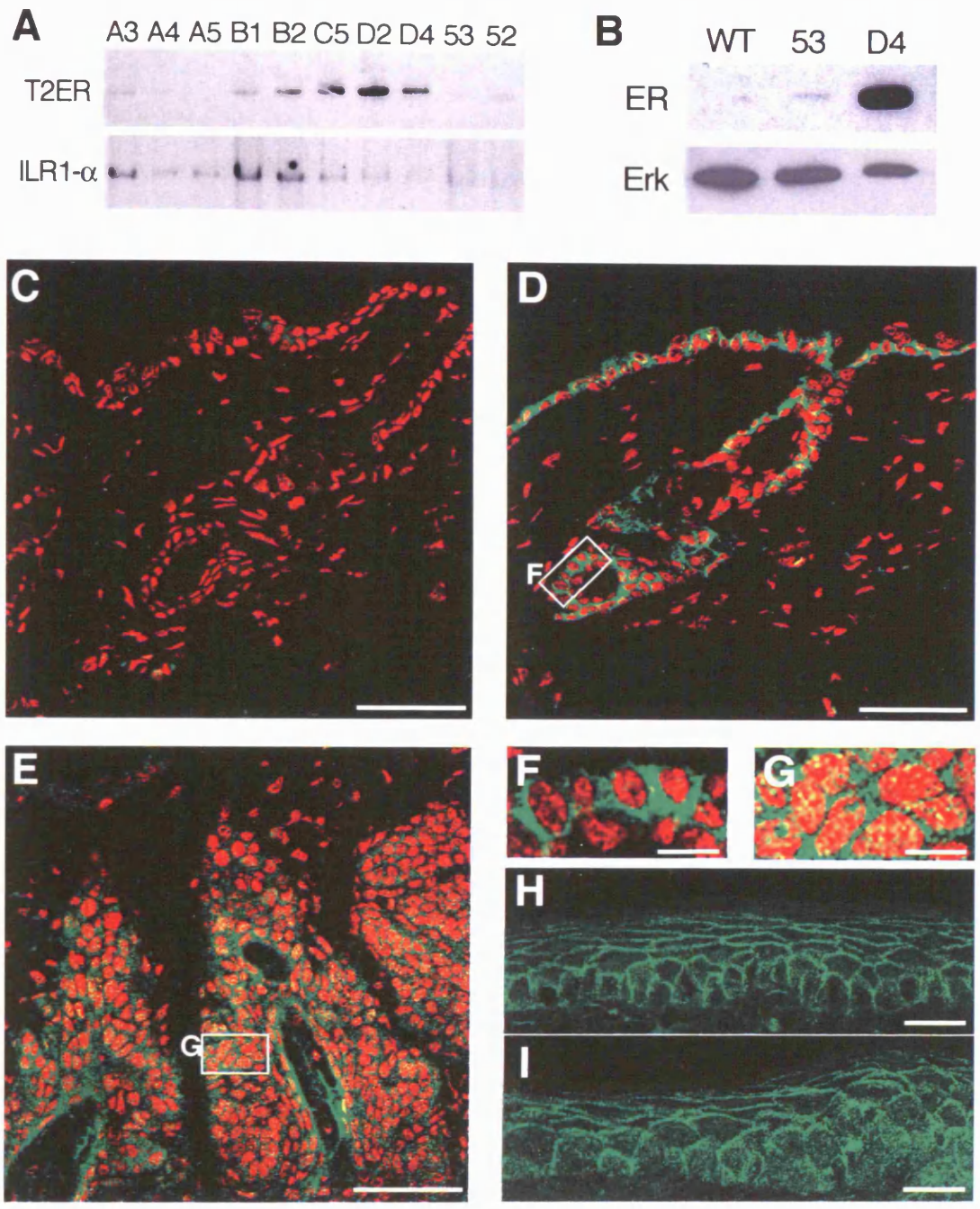

Figure 3.2. K14ΔNβ-cateninER transgenic mice. (A) Southern blot indicating the relative copy number of transgene integrated in the genome of the 10 founder lines generated compared to the interleukin1α receptor, present in only one copy in the genome. (B)Western blot of primary keratinocytes cultured from wild-type (WT) or transgenic (lines 3953 and D4) mice, probed with anti-ER (top panel) or, as a loading control, anti-Erk MAPK (bottom panel) antibodies. (C-G) Anti-ER immunofluorescence staining (green) of wild-type (C) or transgenic (D-G) K14ΔNß-cateninER (line D4) mouse back skin, untreated (C,D,F) or following 7 days treatment with 4OHT (E,G). Nuclei were stained with propidium iodide (red). F and G show higher magnification views of boxed areas in D and E. (H,I) Anti-ß-catenin immunofluorescence staining of transgenic K14Δ Nß-cateninER (line D4) mouse back skin untreated (H) or 24 hours following 4OHT application. Scale bars: 100μm (C-E), 25 μm (F-I).

I confirmed the expression of the ΔNβ-cateninER protein in the basal layer of the epidermis and outer root sheath of hair follicles of transgenic mice by means of immunofluorescence on back skin cryosections using antibodies against the oestrogen receptor. The epidermis of wild type animals did not express any protein detectable with the anti-ER antibodies (Fig. 3.2C). In transgenic untreated mouse skin ER staining was distributed along the basal layer of the interfollicular epidermis and outer root sheath of the hair follicles. The staining appeared in the cytoplasm and at the cell borders, with no obvious variation in intensity from cell to cell (Fig. 3.2D,F). In 4OHT treated transgenic epidermis punctuated nuclear staining similar to the one observed in the transfected keratinocytes was evident in all transgene-positive cells, although it was more intense in the hair follicles than in the interfollicular epidermis (Fig. 3.2E,G). Immunostaining for β-catenin was similar to the one observed for ER (Fig. 3.2H,I).

3.2. Consequences of ΔNβ-cateninER activation in the various transgenic lines

3.2.1. Macroscopic phenotype

In pilot experiments I clipped the back skin of transgenic mice from the different founder lines and wild type littermates and topically treated it with 4OHT every day to assess whether there was any macroscopic phenotype. All the mice were 6 weeks old and were thus in the resting (telogen) phase of the hair cycle with their clipped skin appearing pink and thin. Before the application of 4OHT all the transgenic mice were indistinguishable from the wild type because the transgene was inactive.

Wild type animals did not regrow hair for several weeks, whether treated with 4OHT (Fig. 3.3A) or with acetone vehicle. None of the transgenic mice treated with acetone displayed any phenotype. B1 mice did not appear to be affected by 4OHT treatment. 3953 mice were treated for 3 weeks and showed patchy hair regrowth. The skin of D2 mice became first uniformly black and showed complete hair regrowth within 14 days of treatment (Fig. 3.3B). When the mice were clipped a second time to allow further

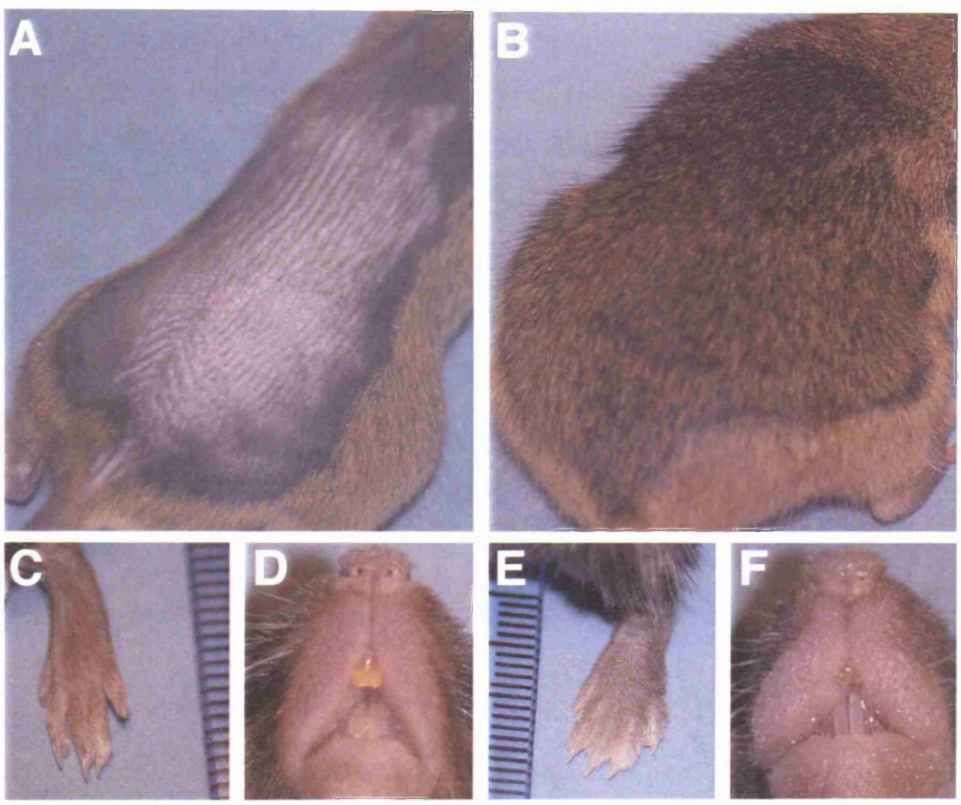

Figure 3.3. Macroscopic phenotype of K14ΔNß-cateninER mice. Wild type (A,C,D) and transgenic (B,E,F) animals were shaved, then received daily applications of 4OHT (1mg in 0.2 ml acetone) on their back skin. The effects observed were hair growth (A, wt and B, D.2 mice after two weeks of treatment) and swollen lips and feet (wt: C, D; D.4 mice: E,F. All after seven days of treatment).

4OHT treatment the hair grew back to normal length within 24 hours. After 9 days of 4OHT treatment, the skin of D4 transgenic mice was very dark, thick and wrinkled, and, although new hair growth was stimulated, the hairs failed to fully elongate. C5 mice showed the same gross phenotype as the D4, although the onset was slightly delayed. The feet and lips of both D4 and C5 mice became swollen (Fig. 3.3C-F) and the mice developed worsening feeding and respiratory difficulties, so that they could not be treated for more than 7-9 (D4) or 15 days (C5) and had to be sacrificed shortly after. These effects were unexpected but not completely surprising since 4OHT could be spread to other locations than back skin during grooming. The respiratory problems were probably caused by the swelling of the area around the nose and in the oral cavity, but since keratin14 is expressed also in the trachea (Liu et al., 1994). I could not exclude a localized effect of ΔNβ-cateninER activation. Table 3.1 summarizes the effects observed in the transgenic lines analyzed.

Table 3. 1. Transgene copy number and macroscopic phenotype

Line	Copy no	T2ER expression	Hair growth	Swollen feet and lips	Breathing difficulties
B1	1	Low	No	No	No
3953	1	Low	Patches	No	No
D2	12	Intermediate	Yes	No	No
C5	18	High	Yes	Yes	Yes
D4	21	High	H&E only	Yes	Yes

3.2.2. ΔNβ-cateninER activation induces the anagen phase of the hair cycle

The histological analysis of back skin samples collected from each line at the end of the treatment showed alterations that correlated with the observed macroscopic phenotypes. I never observed any effect of 4OHT treatment on wild type mice (Fig. 3.4A), as already described in Arnold and Watt (2001). 4OHT treatment did not induce any appreciable histological changes in B1 skin, where all the hair follicles remained in telogen like in wild type littermates (Fig. 3.4B). In line 3953 I could only observe induction of anagen in some regions (Fig. 3.4C), an effect that was clearly induced also in the D2 line. For these reasons I did not dedicate further analysis to the two lower

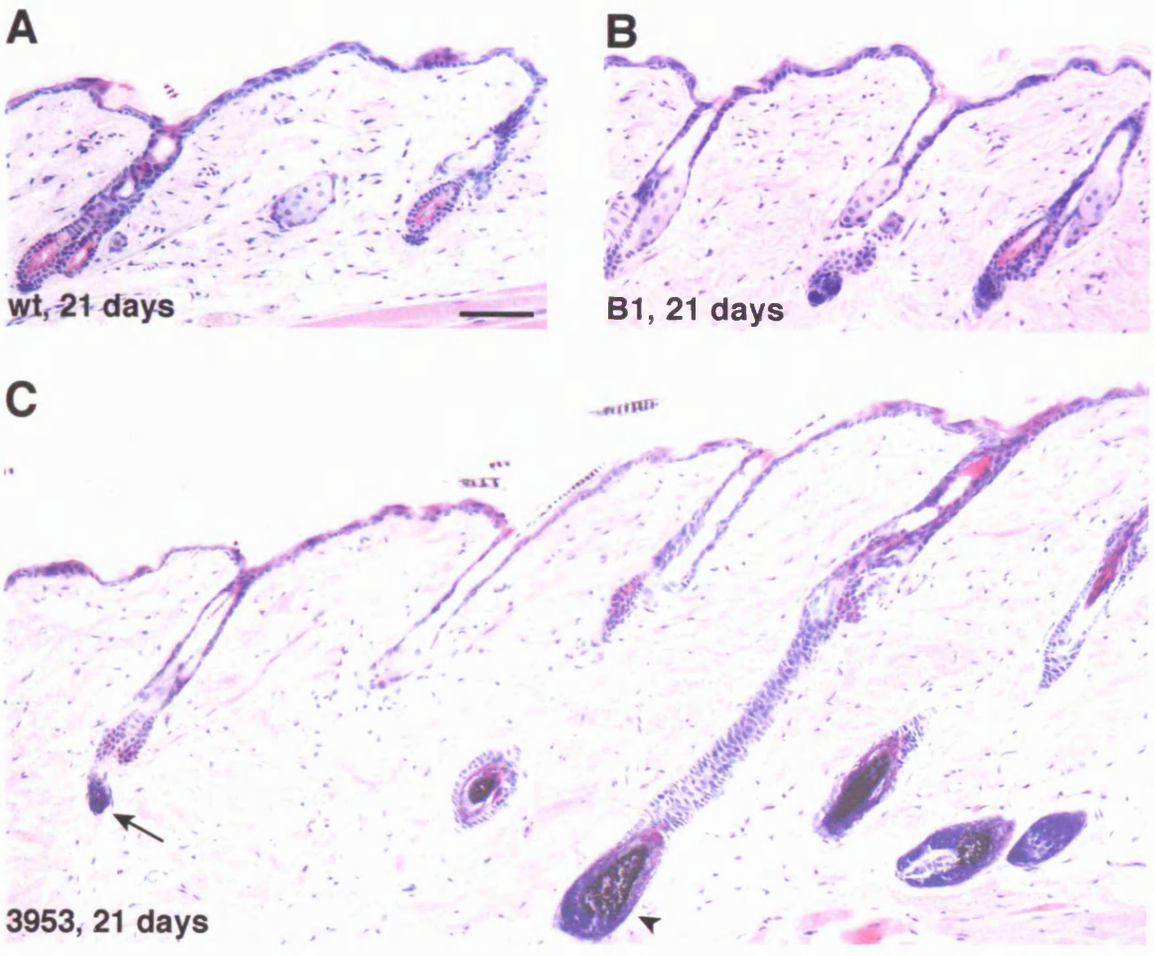

Figure 3.4. Effect of 4OHT treatment on wild type and low copy number lines. (A,B) Histological sections of wild type (A) and B1 (B) mice, where no effect of 21 days 4OHT treatment was observed. (C) Histological section from 3953 transgenic mouse treated with 4OHT for 21 days, showing the boudary between a region still in telogen and a region in which anagen phase of the hair cycle has been induced. Arrow indicates telogen follicle, arrowhead indicates anagen follicle. Scale bar: 100μm.

copy number lines B1 and 3953. Also the line C.5 was not further analysed because it presented 4OHT induced changes similar to the line D4, only later. I therefore focused my attention on the two lines that showed the most striking macroscopic/visible phenotype, D2 and D4.

3.2.3. β-catenin activation induces epithelial outgrowths originating from the permanent portion of hair follicles

I performed a time course experiment in which I treated transgenic mice and wild type littermates daily with 4OHT and collected back skin samples at intervals for up to 4 weeks for the D2 mice and 9 days for the D4 mice. Although the transgene was expressed throughout the basal layer of the interfollicular epidermis (Fig. 3.2D), in D2 mice this was surprisingly unaffected and histological sections showed no difference in the thickness and differentiation of interfollicular epidermis of transgenic and wild type littermates (Fig. 3.5) The effects of β-catenin activation were concentrated in the hair follicles.

In the D2 line the first changes were visible at day 3-5 and corresponded to an elongation and thickening of the hair follicles (Fig. 3.5C, D). By day 7 the anagen phase of the hair cycle had clearly started and by day 14 the hair follicles were in full anagen (Fig. 3.5E, F). The main difference between D2 follicles and normal anagen follicles was the appearance of additional epithelial outgrowths originating from the permanent portion of the outer root sheath and from the sebaceous glands (arrows, Fig. 3.5E,F). These outgrowths were first visible at day 7 and kept growing in size and number over time, eventually forming a variable number of cysts clearly visible by day 21 (arrowhead in Fig. 3.5G).

Further growth and fusion of the outgrowths made the histology of each D2 follicle from day 21 onwards resemble a trichofolliculoma, a type of hair follicle tumour that had previously been reported to be induced by constitutive overexpression of stabilised β-catenin (Gat et al., 1998), and also in humans has been associated with activating mutations in the β-catenin gene (Chan et al., 1999). At day 28 the follicles of D2

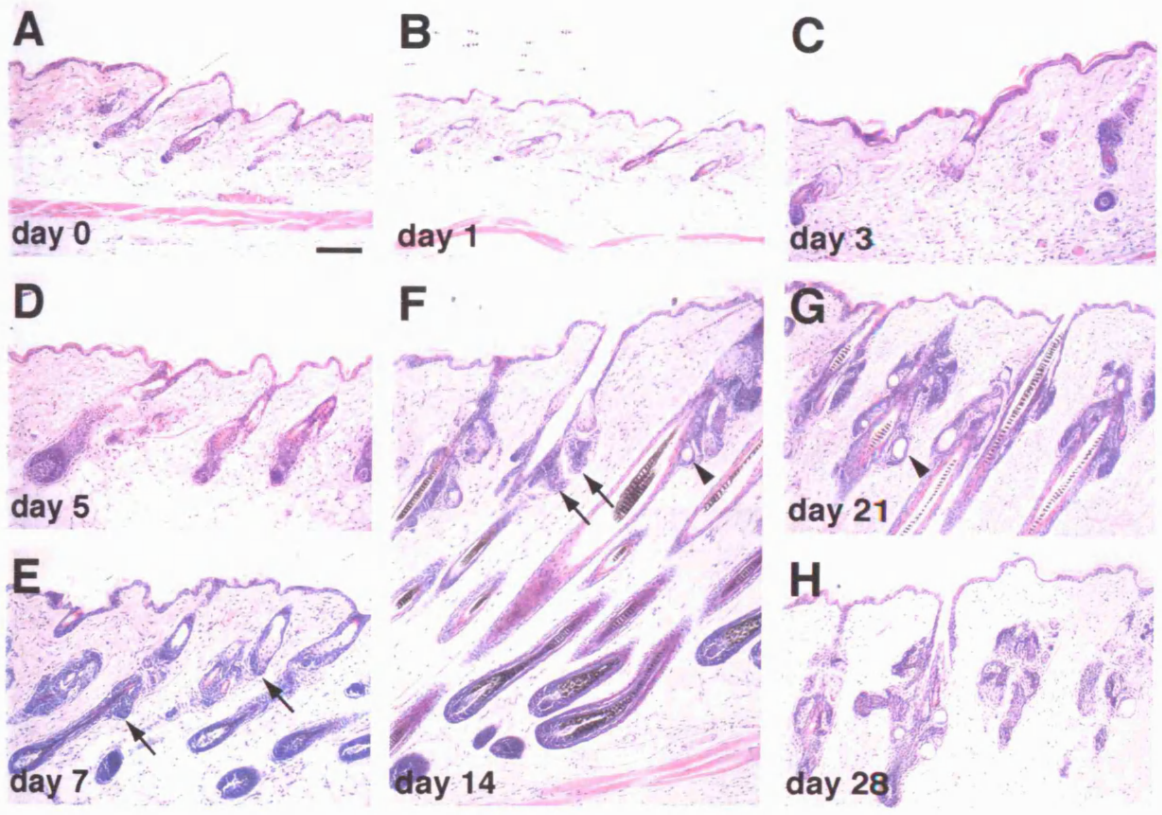

Figure 3.5. Effect of 4OHT treatment on D2 back skin. Histological analysis of the effects of sustained ß-catenin activation in back skin of D2 transgenic mice . Arrows indicate outgrowths from the permanent portion of hair follicles (days 7 and 14). Arrowheads indicate small empty cysts (days 14, 21). Scale bar: 100µm.

epidermis were entering catagen (regression phase) but the tumours were still enlarging and thus the epithelial outgrowths accounted for most of each follicle mass (Fig. 3.5H).

In D4 transgenic skin elongation of the hair follicles was already visible 1 day after the beginning of 4OHT treatment (Fig. 3.6B). By day 3 anagen had clearly started and epithelial outgrowths were already developing from the sebaceous glands (arrow in Fig. 3.6C) and from the permanent portion of the outer root sheath below the sebaceous glands. From day 5 the follicles became progressively thicker, and the outgrowths larger (Fig. 3.5D).

By day 7 the sebaceous glands were entirely surrounded by proliferating cells (arrows in Fig. 3.6E) and at later time points they were no longer visible. The hair follicles failed to fully elongate and instead appeared much thicker than normal, with several extra layers of keratinocytes. Occasionally, even some patches of interfollicular epidermis appeared hyperproliferative (bracket in Fig. 3.6F). In contrast to the hair follicles of D2 mice, the D4 follicles tended not to produce normal hair shafts and their infundibulum was full of cornified material. This probably accounted for the abnormal macroscopic appearance of the pelage.

In order to assess the progression of the D4 phenotype I arranged the grafting of skin from wild type and D4 newborn mice onto nude mice. In this system 4OHT does not cause the recipient mice to develop the respiratory problems that affect D4 transgenic mice and the grafts can be treated for a longer length of time. I allowed D4 skin to graft and develop for 8 weeks, then I topically applied 4OHT on the grafts (every second day, 30 ul of 5 mg/ml) for two or four weeks and subsequently analyzed their histological appearance (Fig. 3.7).

While the wild type epidermal grafts remained similar to untreated wild type epidermis (Fig. 3.7A), D4 grafts treated for two weeks resembled the samples collected from D4 mice at similar time points (Fig. 3.7C). The phenotype shown by D4 grafts treated for four weeks was greatly exacerbated (Fig. 3.7D), especially in comparison to D2 mice treated for the same length of time. The grafts had papillomatous appearance, some of the hair follicles had entered anagen and grown deep in the dermis and the subcutaneous fat, but they all displayed hyperproliferative infundibular regions, engulfed with

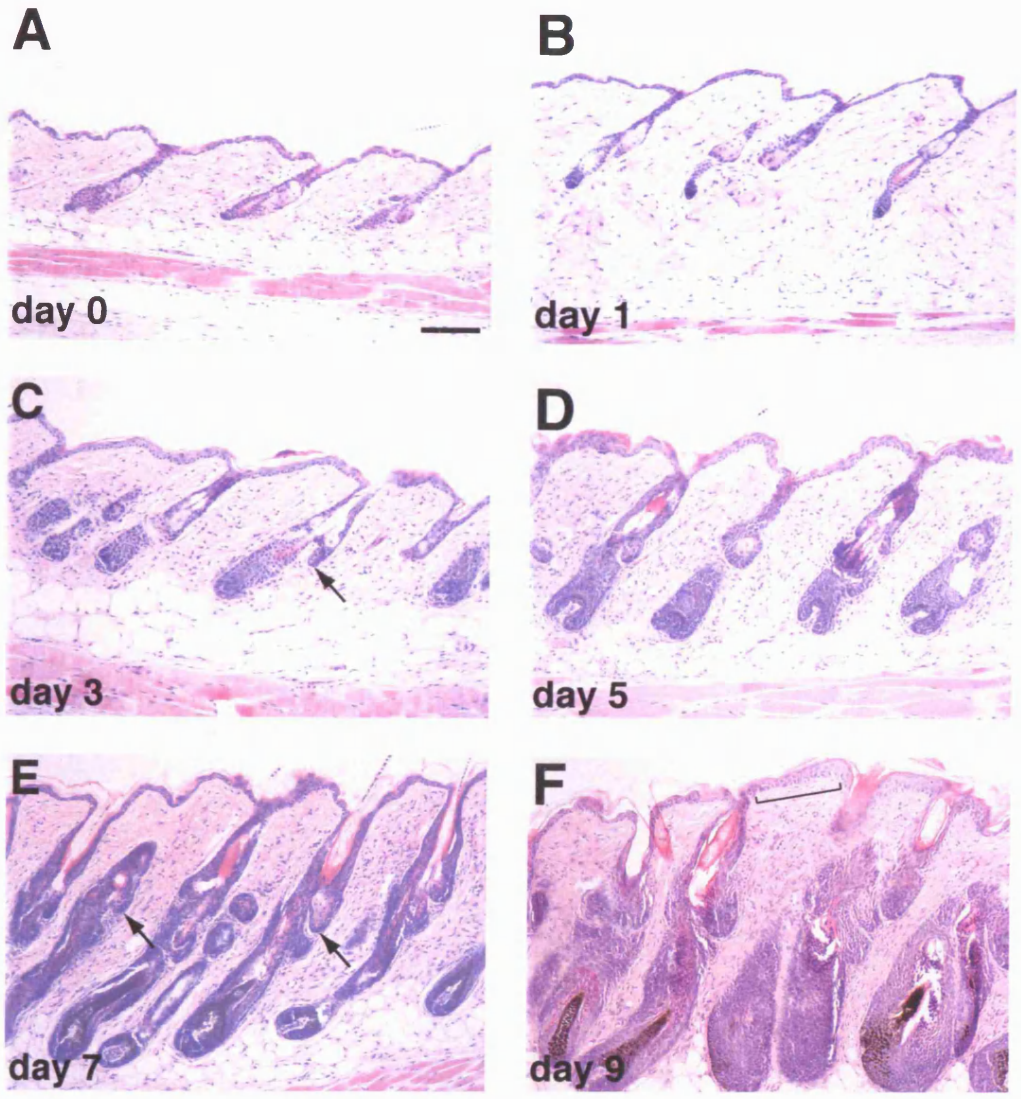

Figure 3.6. Effect of 4OHT treatment on D4 back skin. Histological analysis of the effects of sustained ß-catenin activation in back skin of D4 transgenic mice treated for the number of days indicated. Arrows indicate outgrowths from the permanent portion of hair follicles (day 3) and from sebaceous glands (day 7). Bracket indicates a region of hyper-proliferative IFE (day 9). Scale bar: 100 μm.

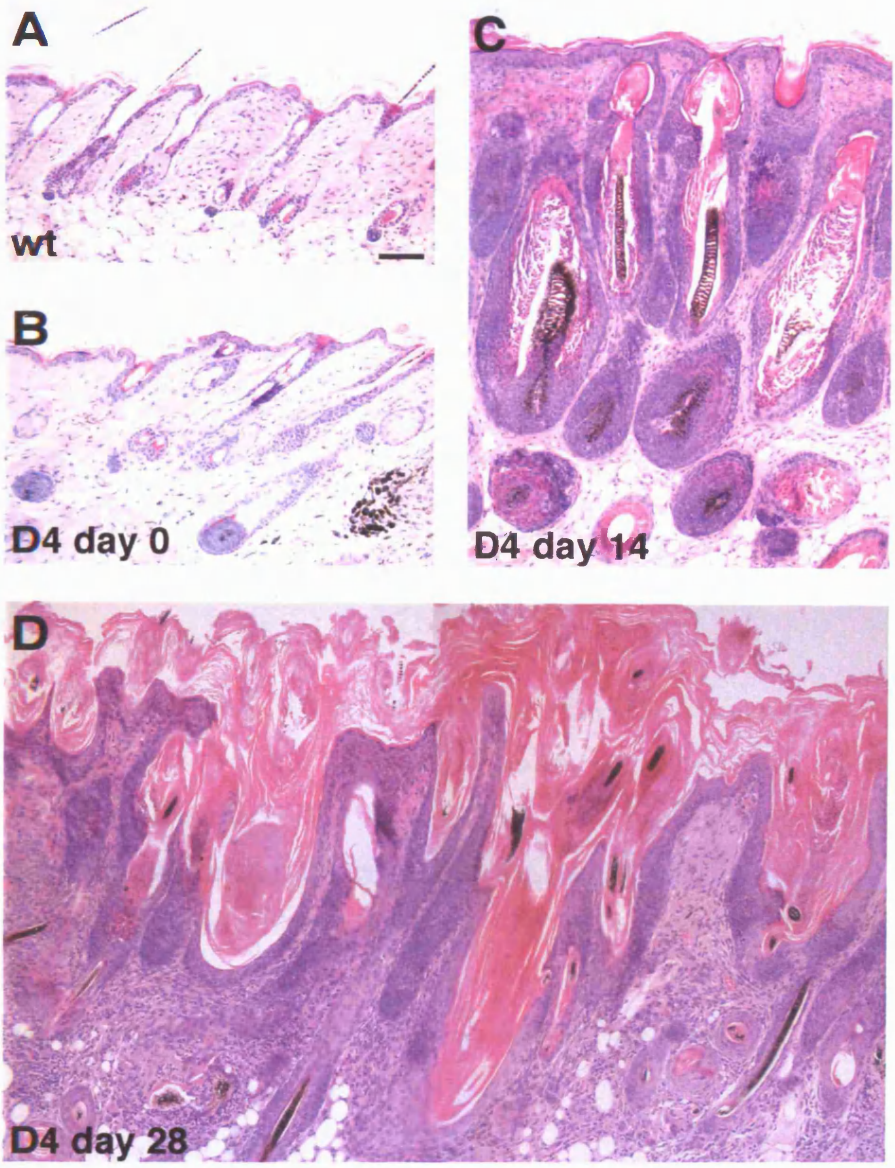

Figure 3.7. D4 back skin grafts. Histological appearance of back skin grafts from wild type (A) and D4 transgenic (B-D) newborn onto nude mice, 8 weeks after grafting (A,B) or after 2 (C) or 4 additional weeks (D) of 4OHT treatment. Scale bar: 100µm.

cornified material that made the whole graft look dry and scaly. The enlarged infundibular regions eventually touched each other excising regions of interfollicular epidermis. The IFE that still remained visible was hyperproliferative and there were no sebaceous glands left. The dermis was filled with cells probably involved in an inflammatory reaction. These grafts had histological appearance similar to the human dermatological conditions seborrheic keratosis and acanthosis nigricans, which are both benign hyperproliferative lesions (Lever and Schaumberg-Lever, 1993). These conditions have never been associated with mutations in the β-catenin gene in humans, but seborrheic keratosis is developed by mice expressing suboptimal levels of presenilin1, a protein involved in Notch signalling activation and β-catenin downregulation (Tournoy et al., 2004).

3.2.4. β-catenin induces de novo hair follicle formation in postnatal interfollicular epidermis

In addition to the changes in existing hair follicles (Fig. 3.5,6), I could observe de novo hair follicle formation in the interfollicular epidermis of both D2 and D4 transgenics (Fig. 3.8). This was particularly striking in D4 paw skin, which I started to analyze as soon as I noticed the swelling of the feet. On the dorsal surface of the paw the density of follicles was higher in transgenics treated with 4OHT for 7 days (Fig. 3.8B,F) than in littermate controls (Fig. 3.8A,E). In transgenic skin I could observe many downgrowths of interfollicular epidermis invaginating into the underlying dermis, closely resembling rudimentary hair follicles (arrows in Fig. 3.8F). On the dorsal region of the digits of D4 mice the interfollicular epidermis was hyperproliferative, with an excess of cornified material extending into the neck of preexisting hair follicles (Fig. 3.8F). Also in D2 paw skin new hair germs appeared after 21 days of 4OHT treatment, but the IFE never became hyperproliferative (Fig. 3.8G).

I observed multiple epithelial projections from the IFE into the dermis also in non hair-bearing regions, such as the ventral surface of the paw (the foot pad) and the internal surface of the ear. In these regions of wild type skin the dermal/epidermal boundary is flat (Fig. 3.8A,C,H). In the equivalent regions of treated transgenics the boundary was more complex, as a result of multiple invaginations with the appearance of rudimentary hair germs (Fig. 3.8B,D,I) (Byrne et al., 1994).

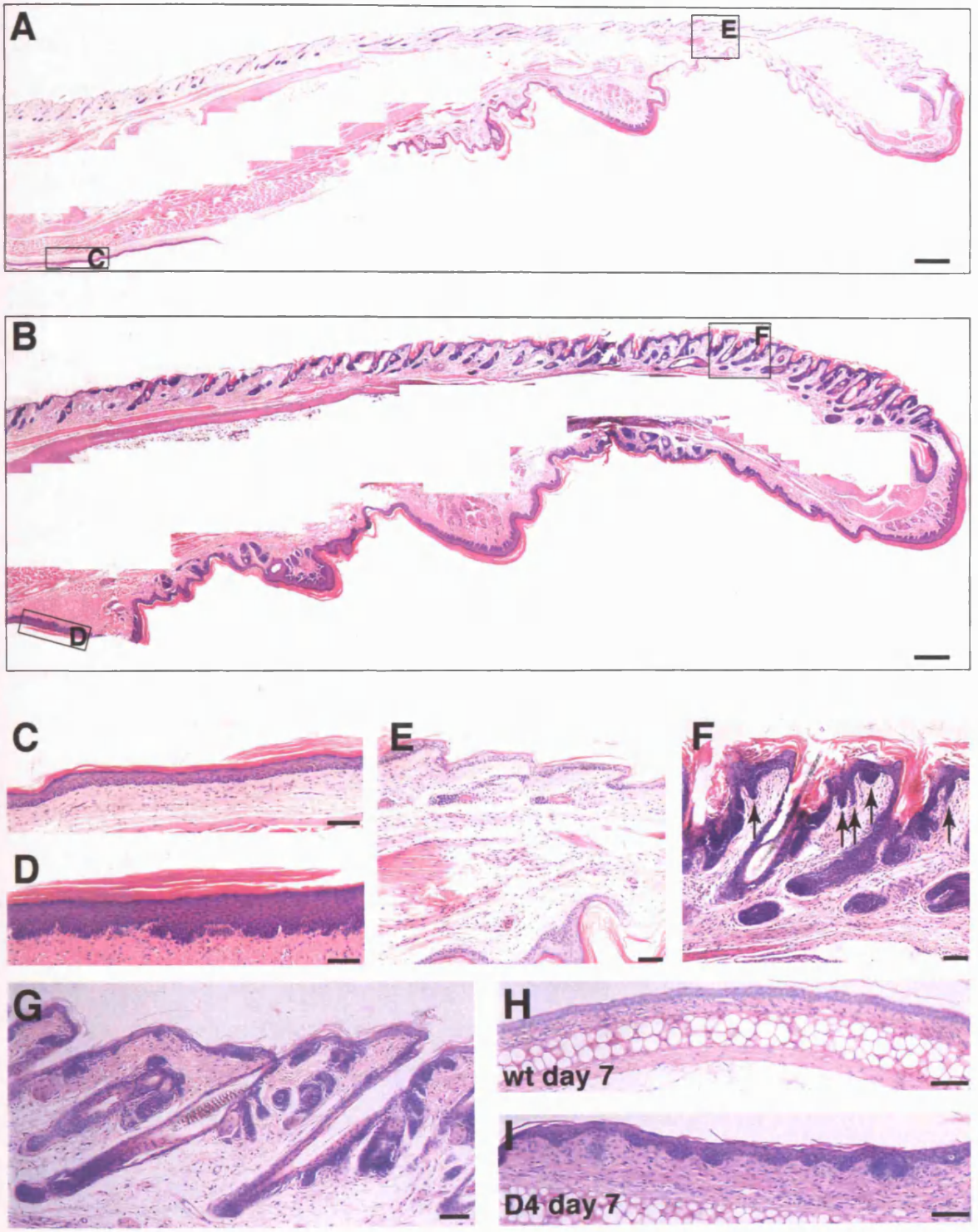

Figure 3.8 De novo hair follicle formation in interfollicular epidermis. (A-G) Histology of paw skin from (A,C,E) wild-type and (B,D,F,G) transgenic (B,D,F: line D4; G: line D2) mice treated daily with 4OHT for one week (A to F) or 21 days (G). A,B are montages reconstructed from images of sections covering the entire circumference of the paw. The boxed regions in A,B are shown at higher magnification in C,E and D,F respectively. Arrows in F indicate new follicles arising from interfollicular epidermis. (H,I) Histology of the internal side of the ear of wild-type (H) or transgenic (I, line D4) mice treated daily with 4OHT for one week. Scale bars: 500μm (A,B), 100μm (C-I).

When I performed a more extensive and accurate analysis of the back skin of D2 and D4 treated mice I could occasionally observe the induction of new rudimentary and mature hair follicles originating from IFE also in this region, in D4 skin (Fig. 3.9A) more frequently than D2 (Fig. 3.9B,C).

3.2.5. ΔNβ-cateninER induced hair follicles contain dermal papillae

One of the first stages of hair follicle development is the formation of the dermal papilla, a group of densely packed fibroblasts surrounded by the bulb keratinocytes. When I analyzed the epithelial outgrowths arising both from pre-existing hair follicles and IFE I could observe at their tip a structure reminiscent of a dermal papilla (Fig. 3.9C). Moreover, as the wild type dermal papilla cells express high levels of alkaline phosphatase (Handjiski et al., 1994; Van Mater et al., 2003), I could detect high alkaline phosphatase activity in the mesenchyme adjacent to all epithelial projections in both D2 and D4 transgenic lines (Fig. 3.10). It appeared thus that, even though during embryogenesis the dermis is believed to produce the first signal to direct hair follicle morphogenesis, β-catenin activation in adult epidermal keratinocytes is sufficient to induce dermal papilla formation.

3.2.6. Shh signalling is active in ΔNβ-cateninER induced hair follicles

Another feature of hair follicle development is the upregulation of Sonic Hedgehog (Shh) and its receptor Patched (Ptc) (Chiang et al., 1999; St-Jacques et al., 1998). In particular, Ptc induction is a sign of the activation of Shh signalling pathway, required for the growth of the hair germ downwards in the dermis (Wang et al., 2000).

I selected representative wild type and transgenic skin samples for in situ hybridization analysis of Shh and Ptc expression. In wild type anagen hair follicles Shh mRNA was confined to a group of matrix cells on one side of the bulb and Ptc was expressed in all the adjacent cells (Fig. 3.11A-D, arrows) (Oro and Higgins, 2003). Following ΔNß-cateninER activation Shh and Ptc were upregulated in all the epithelial outgrowths

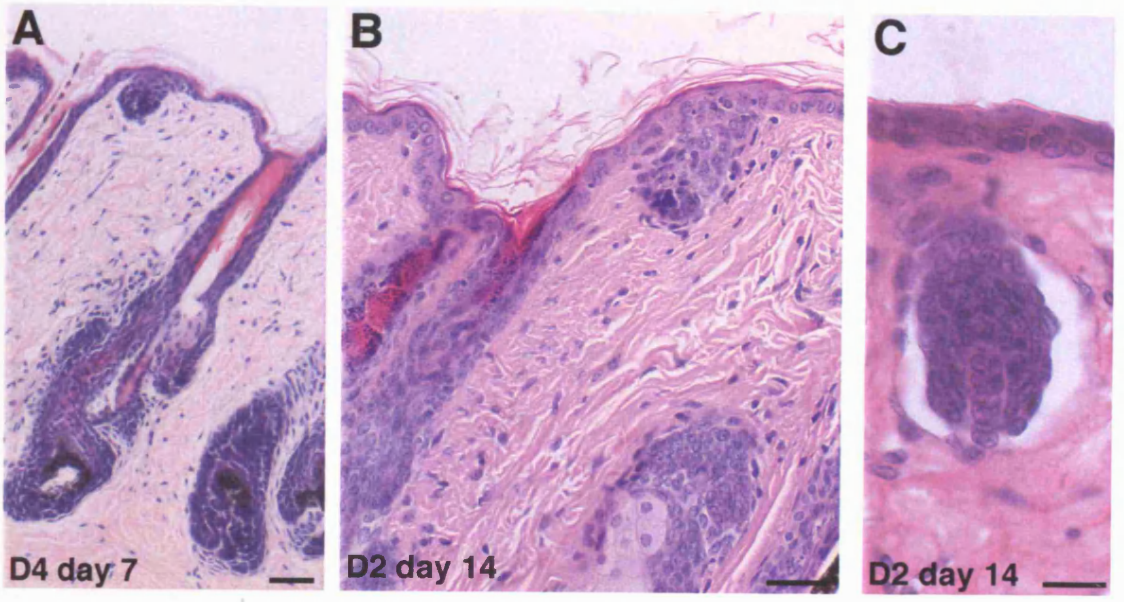

Figure 3.9. De novo hair follicle formation from interfollicular epidermis in back skin. Histology of back epidermis of D4 (A) or D2 (B,C) transgenic mice treated with 4OHT for the time indicated. Scale bars 100μm (A), 50 mm (B) and 25 μm (C).

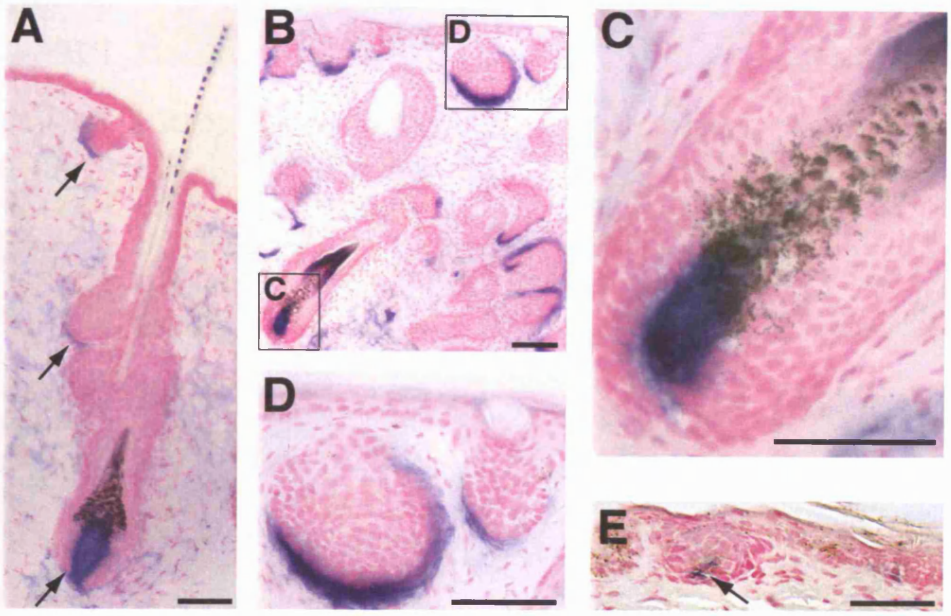

Figure 3.10. ß-catenin activation induces the formation of dermal papillae. Visualisation of alkaline phosphatase activity (blue) as a dermal papilla marker in back (A) and paw (B-E) skin of transgenic (line D4) mice 8 days after a single application of OHT. Arrows in A show alkaline phosphatase-positive cells associated with the original dermal papilla (lowest arrow) and with new follicles arising from interfollicular epidermis (top arrow) and outer root sheath (middle arrow). Arrow in E indicates alkaline phosphatase positive staining in a new follicle arising from IFE. The boxed regions in B are shown at higher magnification in C,D. C is close up of original dermal papilla. D is close up of two new rudimentary follicles. Scale bars: 100 μm.

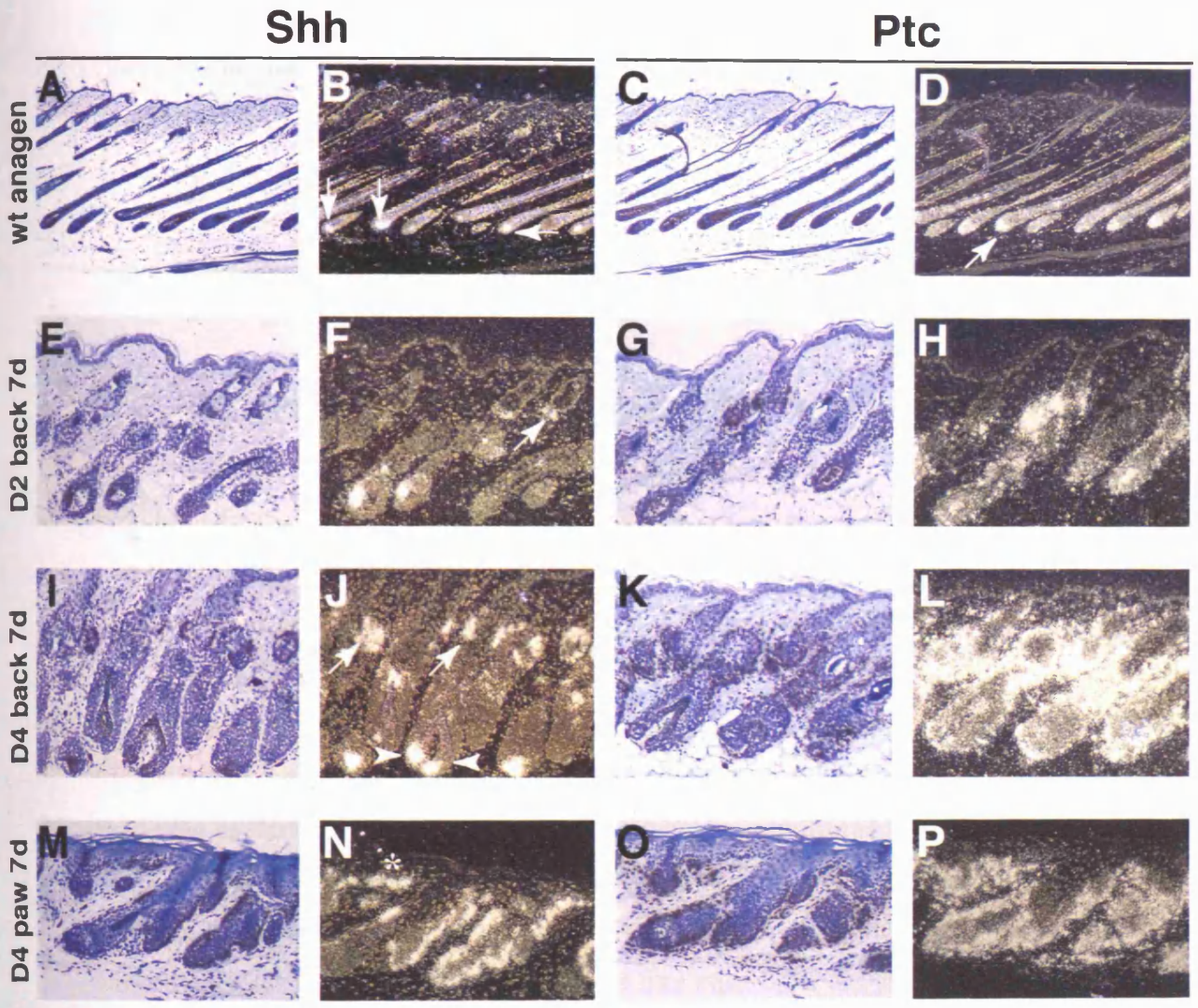

Figure 3.11. Shh and Ptc expression. In situ hybridisation was performed on the dorsal skin of (A-D) untreated wild-type mouse with anagen follicles, (E-H) D2 or (I-L) D4 transgenic mice treated with 4OHT for 7 days, and (M-P) on the dorsal paw skin of D4 transgenic mice treated with 4OHT for 7 days. (B,F,J,N) Dark field views of Shh in situ hybridisations in (A,E,I,M) respectively. (D,H,L,P) Dark field views of Ptc in situ hybridisations in (C,G,K,O) respectively. Arrows in B indicate asymmetric Shh expression in the bulb of the hair follicle, while the arrow in D indicates more uniform Ptc expression in the bulb. Arrows in F,J show Shh expression in the outgrowths arising from the permanent portion of the follicles. Arrowheads in J show abnormal symmetrical expression of Shh in the bulb of the hair follicle and the asterisk in N indicates Shh expression in epithelial downgrowths in the interfollicular epidermis. Scale bar: 100 μm.

originating from existing back skin hair follicles (Fig. 3.11E-I). Moreover, in D4 back skin follicles Shh expression was no longer asymmetric but rather was observed on both sides of the hair bulb (Fig. 3.11J,L). Shh and Ptc were also expressed in the downgrowths from the interfollicular epidermis on the dorsal surface of the paws (Fig. 3.11M-P) and the internal surface of the ears of D4 mice. The induction of Shh and Ptc in all the observed epithelial outgrowths supported the conclusion that they were rudimentary hair follicles.

3.2.7. ΔNβ-cateninER activation induces localized proliferation

Hair follicle development is characterized by the proliferation of the keratinocytes in the growing hair germ, and Shh is known to be a proliferative signal for epidermal cells. I investigated the effect of ΔNβ-cateninER activation on the proliferative status of the epidermis by analyzing BrdU incorporation and Cyclin D1 expression.

BrdU injected in the mice one hour before sacrifice is incorporated in the DNA of all the cells in S phase and can be visualized by immunostaining (Braun et al., 2003). In wild type epidermis only few sparse keratinocytes are proliferating at the same time, as I could confirm (Braun et al., 2003). 4OHT treatment did not change the level of proliferation in wild type epidermis (Fig. 3.12A), and as usual untreated transgenic skin was indistinguishable from that of wild type littermate controls. Following as short as 5 days of 4OHT treatment there was an evident increase in the proliferation of transgenic epidermis (Fig. 3.12B-D). In D2 mice BrdU positive cells were visible along the ORS and in the bulb of the follicles (Fig. 3.12C) as described for normal anagen follicles (Morris and Potten, 1994), and in the new outgrowths. In D4 mice the number of positive cells was even higher, and in particular along the ORS more than one cell layer contained cells in S phase (Fig. 3.12B), reflecting the thickening of the hair follicles observed on histological sections. Interestingly, the IFE of transgenic mice did not appear affected, apart from the regions in which new hair follicle formation occurred (Fig. 3.12D).

Cyclin D1 has a role in cell cycle progression and is a known target of β-catenin signalling (Tetsu and McCormick, 1999). The expression of this gene mirrored the

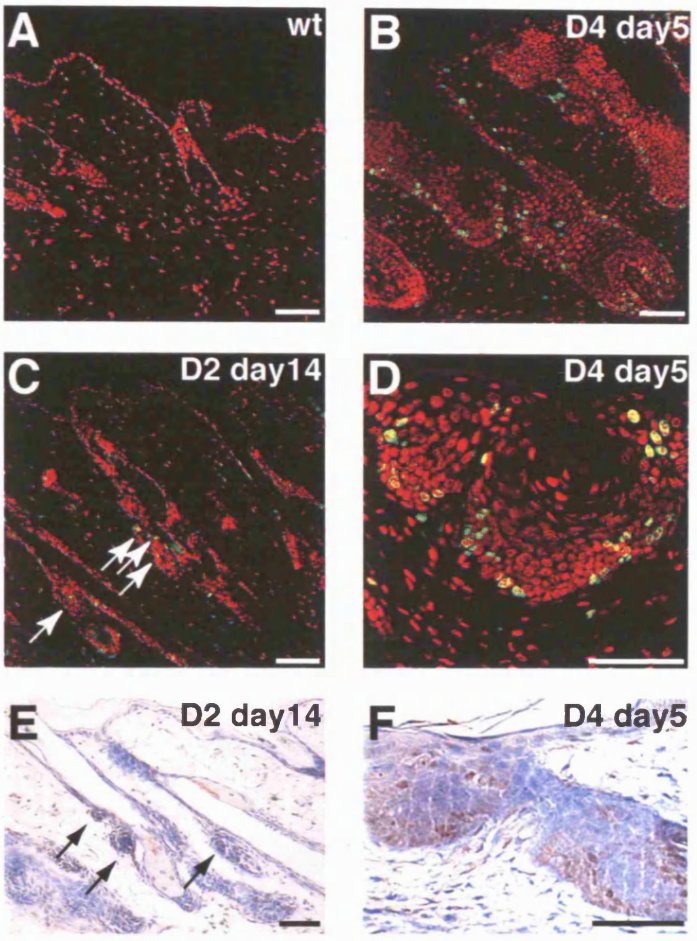

Figure 3.12. Proliferation induced by 4OHT treatment. Analysis of proliferation in back skin of (A) wild type or (C,E) D2 transgenic mice and in (B,D,F) paw skin of D4 transgenic mice. (A-D) BrdU labelling (green) with propidium iodide nuclear staining (red). Green fluorescence of hair shafts is non specific. (E,F) Cyclin D1 immunohistochemistry (brown) with haematoxylin counterstain (blue). Mice were treated with 4OHT for the periods indicated. Arrows in C and E indicate outgrowths arising from the hair follicles that are positive for BrdU and Cyclin D1, respectively. Scale bars: 100 μm.

pattern of BrdU incorporation and appeared increased in all the epithelial outgrowths and in the ORS and bulb of all the pre-existing follicles (Fig. 3.12E-F).

3.3 Effects of ΔNβ-cateninER on lineage commitment

The histological appearance, the presence of derma papillae, the induction of Shh and Ptc and the pattern of proliferation suggested that ΔNβ-cateninER was inducing new hair follicle formation. I obtained a further confirmation of this hypothesis by analyzing the expression of markers of the different epidermal lineages in skin sections from 4OHT treated transgenic and wild type anagen control mice.

3.3.1. Hair lineages

Keratin 17 is normally expressed along the ORS (McGowan and Coulombe, 1998) and as expected was strongly expressed in all the epithelial outgrowths developing from the IFE, hair follicles and sebaceous glands in D2 and D4 mice (Fig. 3.13A,D,E,H). Interestingly, all the cysts observed in the D2 mice stained positive for keratin 17 (Fig. 3.13E), suggesting that they could represent an attempt to form a hair canal.

The transcriptional repressor CCAAT Displacement Protein (CDP) is expressed in the bulb and inner root sheath precursor cells (Ellis et al., 2001) and Lef1 is localized in the matrix (DasGupta and Fuchs, 1999). I confirmed the expression of these two markers in the bulb of wild type anagen follicles (Fig. 3.13B,C) and also in all induced hair follicles in D2 and D4 back and paw epidermis (Fig. 3.13F,G,I,J). CDP positive staining appeared in all the bulb cells of β-catenin induced ectopic follicles, while Lef1 was clearly localized in a few keratinocytes at the border between the epithelium and the mesenchyme.

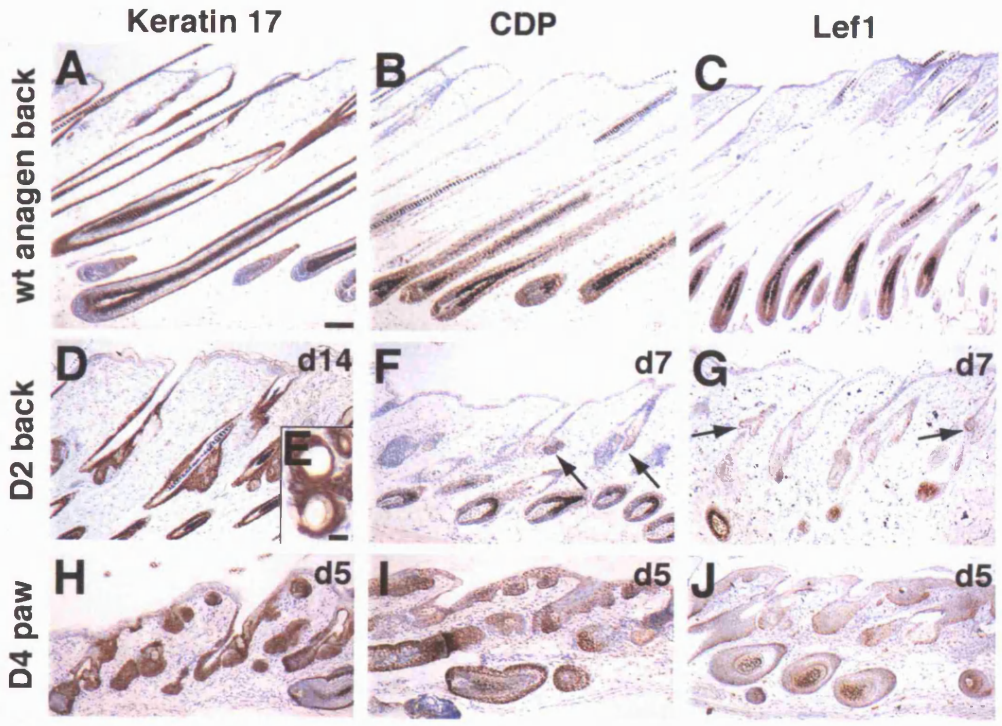

Figure 3.13. Expression of hair follicle differentiation markers. (A-C) Untreated wild type anagen follicles. (D-G) Dorsal back skin of D2 transgenic mice treated with 4OHT for the periods indicated (21 days in E). (H-J) Dorsal paw skin of D4 transgenic mice treated with 4OHT for 5 days. Paraffin sections were immunostained with (A,D,E,H) anti-keratin 17, (B,F,I) anti-CDP, or (C,G,J) anti-Lef1 antibodies and counterstained with haematoxylin. Arrows in F and G show positive staining in the epithelial outgrowths from preexisting follicles. Scale bars: 100 μm (20μm in E).

3.3.2. Sebaceous differentiation

I chose fatty acid synthase and Indian Hedgehog (Ihh) as markers of sebaceous differentiation. Fatty acid synthase is an enzyme involved in the production of the long-chain fatty acids contained in the sebum and its expression is restricted to the sebaceous glands (Fig. 3.14A-B) (Kusakabe et al., 2000). Also Ihh is expressed in the sebaceous glands (Fig. 3.14F), and recently it has been associated with the control of sebocyte growth and differentiation (Niemann et al., 2003).

The analysis of both markers gave very consistent results. While in the lines D2 and C5 I could observe duplication of the sebaceous glands during the first 15 days of 4OHT treatment (Fig. 3.14C), the sebaceous glands were lost at later time points and only a few sebocytes were found localized in small clusters scattered within the trichofolliculomas (Fig. 3.14D,G). In D4 transgenic epidermis the sebocytes were soon surrounded by fatty acid synthase and Ihh negative proliferating cells, and within 9 days of treatment any sign of sebaceous differentiation was lost (Fig. 3.14E,H).

3.3.3. Interfollicular differentiation

Apart from the development of new hair germs, the interfollicular epidermis of D2 and D4 mice appeared largely unaffected by β-catenin activation. I never observed alterations in the expression of keratin 14 in the basal layer or involucrin in the cornified layers and hair follicle infundibulum. Dr David Prowse in the laboratory performed immunostaining for keratin 1 and 10 in the suprabasal layers and also did not report any abnormality.

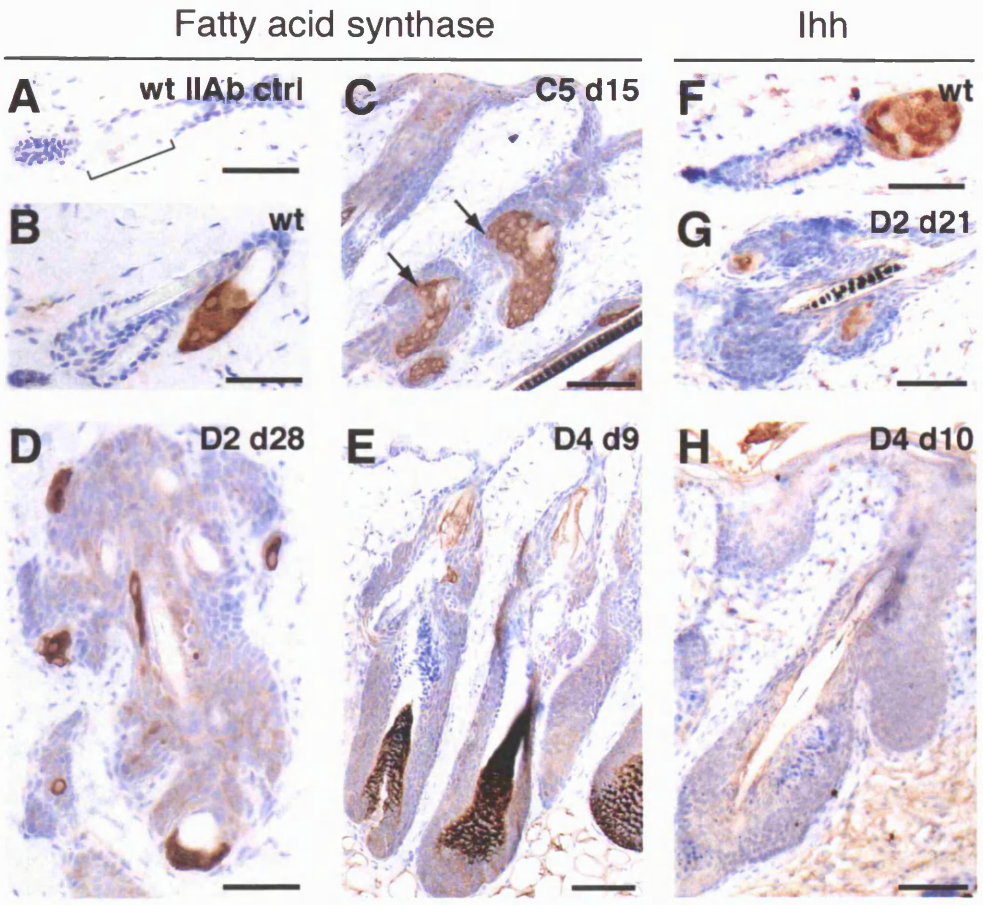

Figure 3.14. Effect of ß-catenin activation on sebocyte differentiation. Immunolocalisation of fatty acid synthase (B-E) and Indian Hedgehog (F-H) in dorsal back skin of (B,F) untreated wild-type mouse skin, (C) C5 transgenic treated with 4OHT for 15 days (arrows highlight duplication of sebaceous gland), (D,G) D2 transgenic and (E,H) D4 transgenic treated with 4OHT for the time indicated. A is wild-type follicle stained with secondary antibody only (bracket indicates the sebaceous gland). Scale bars, 100 µm.

3.4 Discussion

ΔNβ-cateninER is a fusion protein containing a constitutively active form of β-catenin fused to a mutated ligand binding domain of the oestrogen receptor. The protein is insensitive to endogenous oestrogen but responds to 4-hydroxytamoxifen (4OHT) treatment by translocating to the nucleus and regulating transcription, reproducing endogenous β-catenin activity. The keratin 14 promoter is active from day 9.5 of embryonic development (Byrne et al., 1994) and has been used to target the expression of several transgenes to the basal layer of the interfollicular epidermis, hair follicle outer root sheath and sebaceous glands. By generating the ΔNβ-cateninER transgenic mice I could alter β-catenin signalling in adult epidermal stem and progenitor cells and investigate whether they are still able to respond to β-catenin activation even though they have not received any embryonic priming.

I analyzed the effects of β-catenin activation in adult epidermis in different founder lines, observing a correlation between the phenotype produced and the number of copies of transgene integrated in the genome. I selected the two most interesting founder lines (D2 with lower and D4 with higher number of transgene copies) for further analysis and showed that adult epidermal stem and progenitor cells in the different epidermal compartments can undergo lineage conversion to form hair follicles. This indicates that adult epidermal stem and progenitor cells retain a remarkable plasticity and that β-catenin activation is sufficient to trigger hair differentiation at the expenses of sebaceous differentiation. Moreover, these observations are in agreement with a similar study (Van Mater et al., 2003) in which the keratin 5 promoter is used to drive expression of a stabilized form of β-catenin in the basal layer of IFE, ORS and SG. induction of anagen and ectopic hair formation is observed also in this case.

β-catenin activation induced all existing hair follicles to enter the growing phase of the hair cycle (anagen). While β-catenin activity has already been reported in growing anagen follicles (DasGupta and Fuchs, 1999), in the D4 transgenic line high levels of β-catenin signalling induced excessive proliferation and abnormal anagen, which did not

result in new hair growth. Intermediate levels of β-catenin signalling are therefore necessary to induce normal anagen. Moreover, in the D2 transgenic line anagen stopped before the end of 4OHT treatment, in agreement with the suggestion that additional factors are required for anagen maintenance (Fuchs et al., 2001) and that the lifespan of matrix cells could be a biological clock for the end of anagen (Paus and Cotsarelis, 1999).

Interestingly, while it is believed that a dermal signal to the epidermis is responsible for the induction of hair follicle morphogenesis, in the case of the K14ΔNβ-cateninER transgenic mice β-catenin activation in the keratinocytes is sufficient to start the formation of new hair follicles and dermal papillae. The dermal signal is likely to be Wnt mediated and results in the re-localization of β-catenin to the nucleus of epidermal cells (Hardy, 1992; Kishimoto et al., 2000; Millar, 2002). In the ΔNβ-cateninER transgenic mice the process could therefore be starting one step ahead. It has recently been suggested that the Wnt signal has to be accompanied by inhibition of BMP signal in order to obtain a stable nuclear co-localization of β-catenin and its co-factor Lef1 (Jamora et al., 2003). This is not the case in the K14ΔNβ-cateninER transgenic mice, where β-catenin activation is the only event occurring in the keratinocytes. One possible explanation is that in adult epidermis β-catenin activation is sufficient to upregulate Lef1, or alternatively some cells already have a sufficient amount of Lef1 in the nucleus and therefore are able to respond to β-catenin stimulation. More accurate and sensitive methods for the detection of Lef1 in adult epidermis could contribute to solve this question. Also the fact that even though β-catenin was activated throughout the epidermis only localized proliferation was observed at the sites of HF formation suggests that there may be differences between cells in the IFE and ORS. Interestingly, fewer hair follicles developed from the interfollicular epidermis in back skin compared to paw skin, demonstrating that the epidermis presents regional differences in the responsiveness to β-catenin activation.

The number of ectopic follicles developing from the interfollicular epidermis correlated with the transgene copy number, higher in D4 mice than in D2. This suggests that probably β-catenin signalling has to reach a certain threshold in order to trigger hair follicle morphogenesis in the IFE. The report of the presence of the repressor TCF3 in

the hair follicle bulge (Fuchs et al., 2001) could explain why I never observed new hair follicles originating from this region.

The finding that β-catenin activation causes the epidermis to induce a new dermal papilla opens up an unexpected way in which the epidermis could influence the homing, localisation and properties of a range of different cell types. Dermal papilla cells are different from the other dermal fibroblasts. They have multi-lineage potential, contain neural precursors (Fernandes et al., 2004; Joannides et al., 2004; Toma et al., 2001) and can even produce cells of erythroid and myeloid lineages (Lako et al., 2002). Not only can epidermal β-catenin signalling control selection of the epidermal lineages, it may also stimulate the differentiation of other cell types by recreating some of the inductive interactions that occur during normal epidermal development.

Both anagen induction and de novo hair follicle formation are likely to be mediated by β-catenin dependent induction of Shh, which has already been reported as a target of β-catenin signalling in the epidermis (Gat et al., 1998; Huelsken et al., 2001). Shh is expressed in the bulb of growing hair follicles and is required for both anagen initiation and hair follicle development (Callahan and Oro, 2001; Chiang et al., 1999; Oro and Scott, 1997; Sato et al., 1999; St-Jacques et al., 1998; Stenn and Paus, 2001; Wang et al., 1997). The level of Shh induction correlated with the level of β-catenin expression in the D2 and D4 transgenic lines, and the abnormal distribution of Shh mRNA in the D4 mice could be responsible for the abnormal anagen of their follicles. Ptc is a target of Shh signalling (Freeman, 2000), and the increase in Ptc expression observed in the transgenic mice is an indication of the induction of Shh signalling.

The morphological appearance of the outgrowths, the expression of hair follicle differentiation markers and the induction of Shh signalling suggest that β-catenin activation in adult epidermis is triggering hair follicle morphogenesis following the same steps and mechanisms of embryonic hair follicle specification and development. While the cysts observed in the D2 mice were probably empty hair canals, it is difficult to decide whether the few sebocytes observed in the D2 mice treated for more than 3 weeks were remnants of the original sebaceous glands of if they were newly formed, as

an attempt of the new hair follicles to generate their own sebaceous glands. Very detailed lineage marking analysis would be required to address this point.

The initial duplication and subsequent loss of sebaceous glands is quite puzzling. It could be helpful to consider that c-Myc is induced by β-catenin (He et al., 1998) and direct activation of c-Myc in adult epidermis stimulates sebocyte differentiation in both hair follicles and interfollicular epidermis (Arnold and Watt, 2001; Braun et al., 2003). However, when β-catenin signalling is blocked with a ΔNLef1 transgene there is ectopic sebocyte differentiation and sebocyte tumours appear (Braun et al., 2003; Niemann et al., 2002). One interpretation of these results is that sebocyte differentiation is promoted by intermediate levels and duration of β-catenin signalling and blocked by higher levels and duration.

Just as β-catenin levels regulate lineage choice in the epidermis, they also influence the types of tumour that develop when signalling is deregulated (Owens et al., 2003). Long-term β-catenin activation results in hair follicle tumours (Chan et al., 1999; Gat et al., 1998) whereas inhibition of β-catenin signalling with ΔNLef1 leads to the formation of sebaceous tumours (Niemann et al., 2002; Niemann et al., 2003). The tumours induced by sustained activation of ΔNβ-cateninER were highly differentiated and resembled human trichofolliculomas, consistent with the earlier observations of (Chan et al., 1999; Gat et al., 1998). Interestingly, even though aberrant β-catenin signalling is associated with a number of malignant tumours, in the K14ΔNβ-cateninER transgenic mice I could only observe benign hair follicle tumours in the D2 line and dramatic but confined proliferation in the D4 line. One explanation could be that β-catenin is inducing p53 (Damalas et al., 2001), wich serves to limit growth.

Chapter 4. Control of β-catenin signal timing and strength

In the previous chapter I described how repeated 4OHT applications on the skin of K14ΔNβ-cateninER transgenic mice induced β-catenin signalling activation in epidermal stem and progenitor cells. ΔNβ-cateninER activation is 4OHT dependent, so that β-catenin signalling goes back to physiological levels when 4OHT treatment is suspended. In this chapter I took advantage of this characteristic to analyze in more detail the role of β-catenin signalling in anagen initiation, ectopic hair follicle induction and hair follicle tumour formation. The observation that the severity of the phenotype displayed by the different transgenic lines analyzed correlated with the number of copies of the transgene inserted in the genome (Chapter 3) suggested that not only the timing but also the strength of β-catenin signalling may be critical. I therefore investigated in more detail the differences in β-catenin signalling in the D2 and D4 lines (intermediate and high copy number), and whether different doses of 4OHT could modulate the effects of β-catenin activation within each line. Whole mount analysis of tail epidermis appeared to be the best method to evaluate the effects of β-catenin signalling titration, and allowed me also to investigate the effects of β-catenin activation on the epidermal stem cell compartment, as β-catenin signalling has been linked in many tissues to stem cell fate regulation (Liu et al., 2004; Megason and McMahon, 2002; Reya et al., 2003; Staal and Clevers, 2005).

4.1. Transient activation of β-catenin signalling

I treated ΔNβ-cateninER mice with 4OHT for different lengths of time and analyzed their skin some time after the end of the treatment to investigate whether transient activation of β-catenin was sufficient to induce anagen in existing follicles, de novo follicle formation and hair follicle tumours. In the figures 4.1-3 and 4.10 each kinetic experiment is summarized in a diagram in which continuous lines represent 4OHT treatment and continuous ΔNβ-cateninER activation while dotted lines represent periods when no 4OHT was applied on the skin. Black spots, when present, represent the administration of 4OHT, which was sometimes daily and sometimes every second day. Red spots represent examined time points.

4.1.1. Transient activation of β-catenin is sufficient to induce anagen and de novo hair follicle formation

When I applied a single dose of 4OHT on the skin of D2 and D4 mice and collected it one week later, the histological appearance I observed was indistinguishable from that of skin treated with seven daily doses (Fig. 4.1, compare to Fig. 3.5,6). The single dose of 4OHT was sufficient in D2 mice to induce anagen in the existing follicles, where also the first signs of epithelial outgrowths arising from the sebaceous glands were visible (Fig. 4.1B). In D4 mice I observed not only anagen induction but also the thickening of the follicles in back skin (Fig. 4.1C) and de novo hair follicle formation from the outer root sheath and interfollicular epidermis in paw skin (Fig. 4.1D).

Similarly, mice treated for five days with 4OHT and then examined after 5 or 10 days were phenotypically indistinguishable from mice treated continuously for 10 or 15 days (Fig. 4.1E,F, compare to Fig. 3.5,6).

Interestingly, even when I treated D2 mice only once a week their back skin appeared after two weeks very similar to skin from mice treated with 14 daily doses (Fig. 4.1G, compare to Fig. 3.5F). In these mice all the follicles were in advanced anagen and

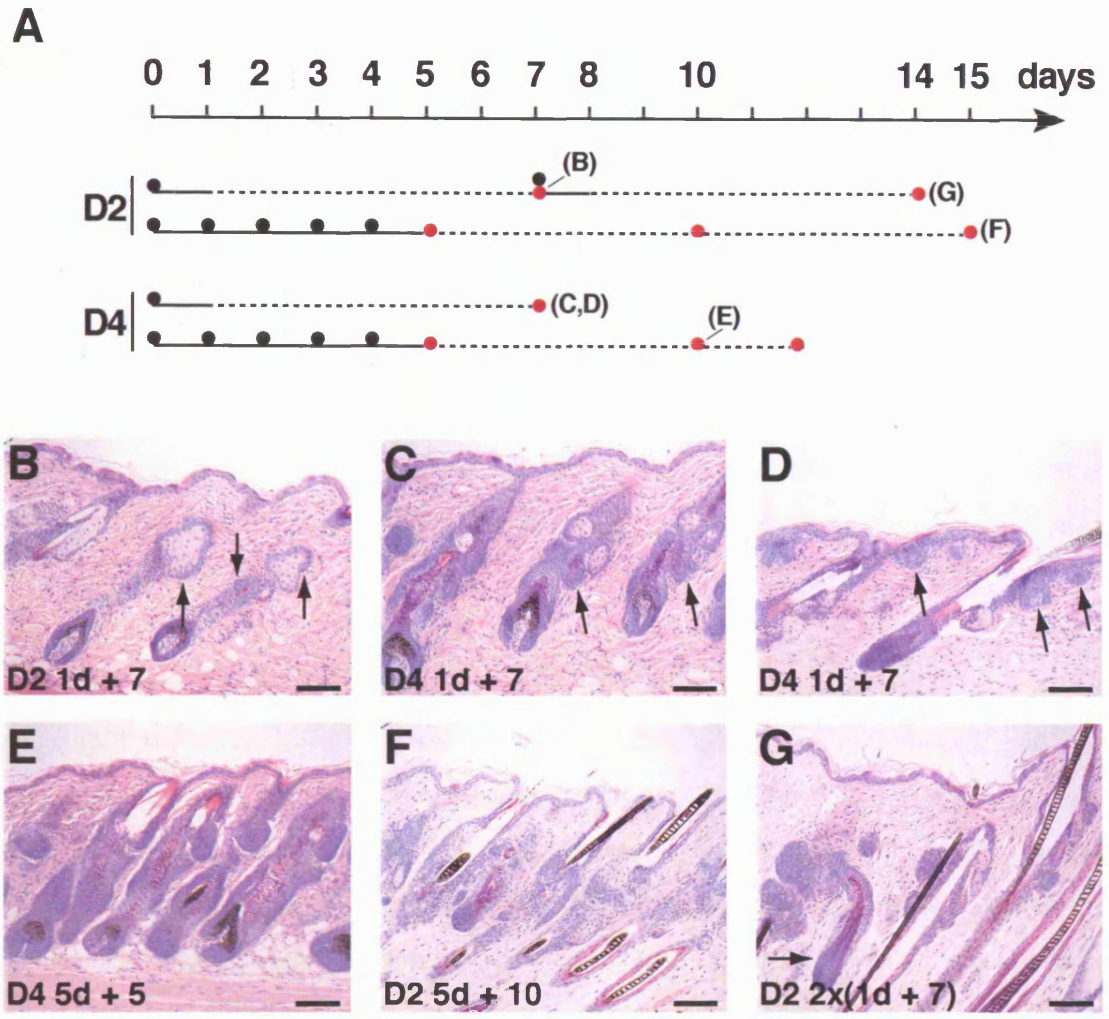

Figure 4.1. Effects of transient ß-catenin activation in K14ΔNß-cateninER transgenic mice. (A) Schematic representation of experiments performed with the D2 and D4 transgenic lines. The arrow represents time in days. Black dots show 4OHT application. Red dots are time points analysed. Continuous lines represent periods of daily 4OHT treatment and dashed lines indicate no 4OHT treatment. (B-G) Transgenic mice (D2 or D4 line as written) received the number of doses of 4OHT indicated (d) and were kept without 4OHT for number of days shown (+). (G) The treatment was the same as B and C but repeated twice. (B,C,E-G) back skin, (D) paw skin. Arrows in B and C show epithelial outgrowths from the permanent portion of the hair follicles and from sebaceous glands. Arrows in D indicate new hair buds arising from interfollicular epidermis. Arrow in G points at an ectopic hair follicle in advanced progression state. Scale bars: 100μm.

presented outgrowths arising from ORS and sebaceous glands, sometimes already similar to hair follicles at an advanced developmental stage (arrow in Fig. 4.1G).

Transient activation of β-catenin signalling was thus sufficient to induce anagen and trigger hair follicle morphogenesis.

4.1.2. ΔNβ-cateninER nuclear exclusion kinetics

The long-lasting effects of 4OHT treatment were fascinating, but since ΔNβ-cateninER is resistant to ubiquitination I checked that a single 4OHT treatment corresponded to transient β-catenin signalling. I therefore analyzed the localization of ΔNβ-cateninER in skin sections collected every 24 hours for one week following a single administration of 4OHT (Fig. 4.2).

I used an antibody recognizing the oestrogen receptor, which gives almost no background signal on wild type sections (Fig. 4.2B), and clear cytoplasmic and cell border staining in transgenic untreated sections (Fig. 4.2C, see also Fig. 3.2D,F). Even though it was very difficult to see intense nuclear signal at any time point, 24 hours after 4OHT treatment the staining appeared dramatically changed, concentrated in big aggregates and often in close proximity of the nucleus (Fig. 4.2C). As this was the same kind of staining I observed when I analyzed sections from mice that had been treated for longer time and had developed a clear phenotype (cfr Fig. 3.2E,G), I assumed that the aggregates were an indication of active β-catenin signalling. The punctate staining appeared unchanged two days after 4OHT administration (Fig. 4.2D). By day 3 the appearance of the staining started to revert (Fig. 4.2E) and from day 4 no aggregates were visible in the nuclei (Fig. 4.2F-I), thus indicating that, following a single dose of 4OHT, ΔNβ-cateninER is detectable in the nucleus for about two days. Continuous β-catenin signalling is therefore achieved not only with daily 4OHT applications but also by treating the mice every second day, allowing the design of less labour-intense and more cost-effective 4OHT treatment protocols.

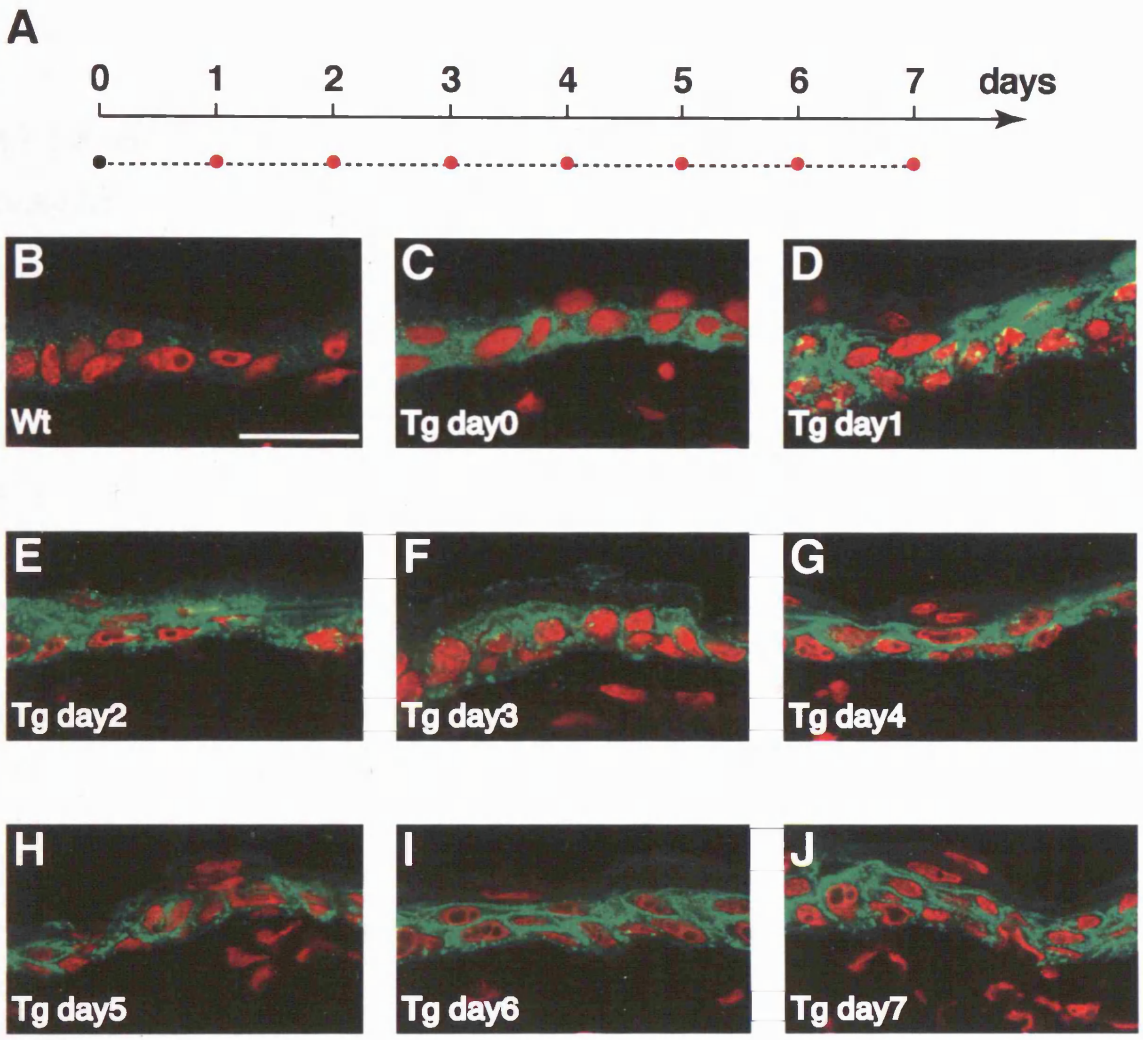

Figure 4.2. Re-localization of ΔNβ-cateninER following a single 4OHT dose. (A) Schematic representation of the experiment performed. The arrow represents time in days. Black dot shows 4OHT application. Red dots are time points analysed. (B-J) Immunolabelling of back skin frozen sections from mice collected at the indicated number of days following a single 4OHT application. A: wild type littermate control, C-J: D4 transgenic mice. Green signal is ER staining, in red is propidium iodide nuclear staining. Scale bar: 30μm.

4.1.3. Continuous β-catenin activation is necessary to maintain hair follicle tumours

Since as little as a single 4OHT treatment was sufficient to trigger anagen phase and de novo hair follicle morphogenesis, I investigated whether a transient activation of β-catenin was sufficient also for tumour maintenance. I examined D.2 skin several weeks after an initial 28 days 4OHT treatment, sufficient to induce trichofolliculomas (Fig. 4.3).

Interestingly, in the few days following the end of 4OHT treatment the mice manifested very dark and necrotic ears, but they spontaneously healed within two weeks, suggesting that in ear (and probably also in back) skin the tumours continued to expand for a while in the absence of 4OHT before regression began.

28 and 106 days after the end of 4OHT treatment the trichofolliculomas had largely regressed. The original hair follicles were back in telogen, but they did not return completely to normal. They retained small epithelial outgrowths and cysts, that were the biggest structures associated to the follicles (Fig. 4.3C-D). This experiment showed that continuous activation of β-catenin is necessary to sustain the growth of trichofolliculomas.

While the tumours induced by continuous β-catenin activation were positive for cyclin D1 (Fig. 4.3E), Lef1 (Fig. 4.3F) and keratin 17 (Fig. 4.3G), after regression cyclin D1 expression was lost and Lef1 appeared confined to the hair follicle dermal papilla (Fig. 4.3I). The residual tumour masses remained positive for keratin 17 (Fig. 4.3J) and negative for the interfollicular epidermal marker keratin 1 (Fig. 4.3H). As expected, while the tumours showed nuclear β-catenin staining (Fig. 4.3K,L) this was lost when the tumours regressed (Fig. 4.3M,N).

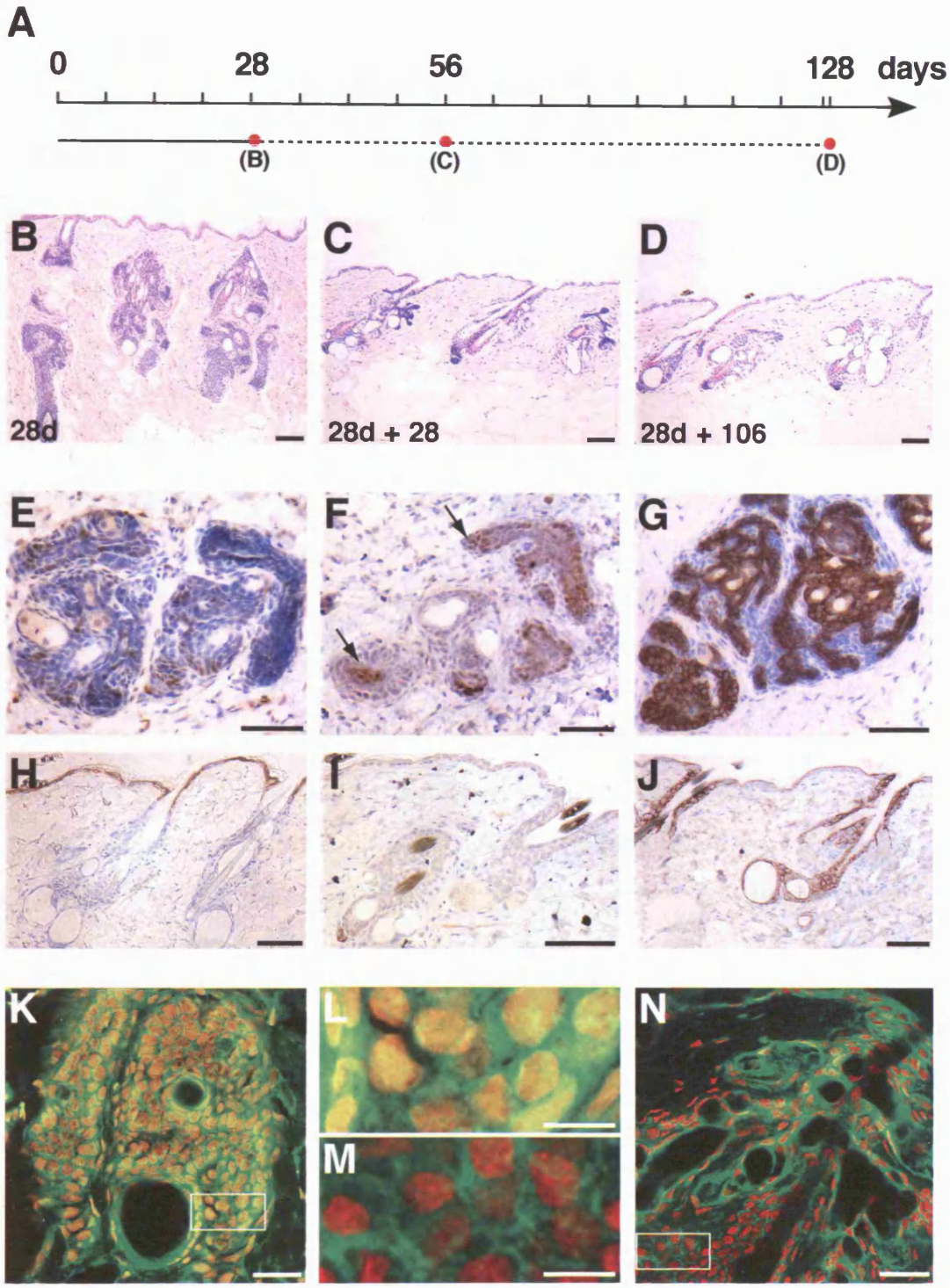

Figure 4.3. Continuous activation of ß-catenin is necessary to maintain hair follicle tumours. (A) Schematic representation of the experiment performed with D2 transgenic mice. The arrow represents time in days. Continuous line represents daily 4OHT treatment and dashed line indicates no 4OHT treatment. Red dots are time points analysed. (B-D) Histology of back skin from mice that received the number of doses of 4OHT indicated (d) and were kept without 4OHT for the number of days shown (+). (E-N) expression of cyclin D1 (E), Lef1 (F,I), keratin 17 (G,J), keratin 1 (H) and ß-catenin (green, K-N) in D2 tumours, after 28 days of 4OHT treatment (E-G,K,L) or 28 days of treatment followed by 28 (M,N) or 106 (H-J) days without 4OHT. Arrows in F highlight Lef1 expression. L,M are high magnification views of boxed regions in K, N respectively. (K-N) red fluorescence is propidium iodide counterstain. Scale bars: 100 µm (B-J), 50µm (K,N), 25µm (L,M).

4.2. Titration of β-catenin signal strength

4.2.1. Relative levels of ΔNβ-cateninER and endogenous β-catenin

In order to investigate in more detail the levels of ΔNβ-cateninER compared to endogenous β-catenin, I generated spontaneously immortalised keratinocyte lines derived from wild type, D2 and D4 transgenic mice. I confirmed by immunofluorecence that they retained the expression of ΔNβ-cateninER in the cytoplasm and partially at the cell-cell border and that 4OHT stimulation altered the subcellular localization of the transgene in a way similar to intact skin (Fig. 4.4A, compare with Fig. 3.1 and 3.2).

ΔNβ-cateninER protein in D4 keratinocytes total lysates was about two fold more abundant than in D2 (Fig. 4.4B). ΔNβ-cateninER ran as a band of approximately 110 kD, slightly higher than endogenous β-catenin, allowing me to use an antibody against the C-terminal region of β-catenin to compare the amount of the endogenous and fusion proteins within the same cell line (D4). Surprisingly, in lysates of total Triton soluble proteins, ΔNβ-cateninER was considerably less abundant than endogenous β-catenin (Figure 4.4C).

Most endogenous β-catenin is stably complexed with E-cadherin at the cell-cell borders (Zhu and Watt, 1999). To examine the amount of ΔNβ-cateninER available for signalling, I preformed hypotonic lysis followed by subcellular fractionation, therefore depleting the extracts of the nuclear and cell membrane-bound pools of β-catenin. ΔNβ-cateninER and endogenous β-catenin in the remaining soluble cytoplasmic fraction were similar in abundance (Figure 4.4D), indicating that in transgenic epidermis the amount of β-catenin available for signalling is approximately two fold that in wild type epidermis.

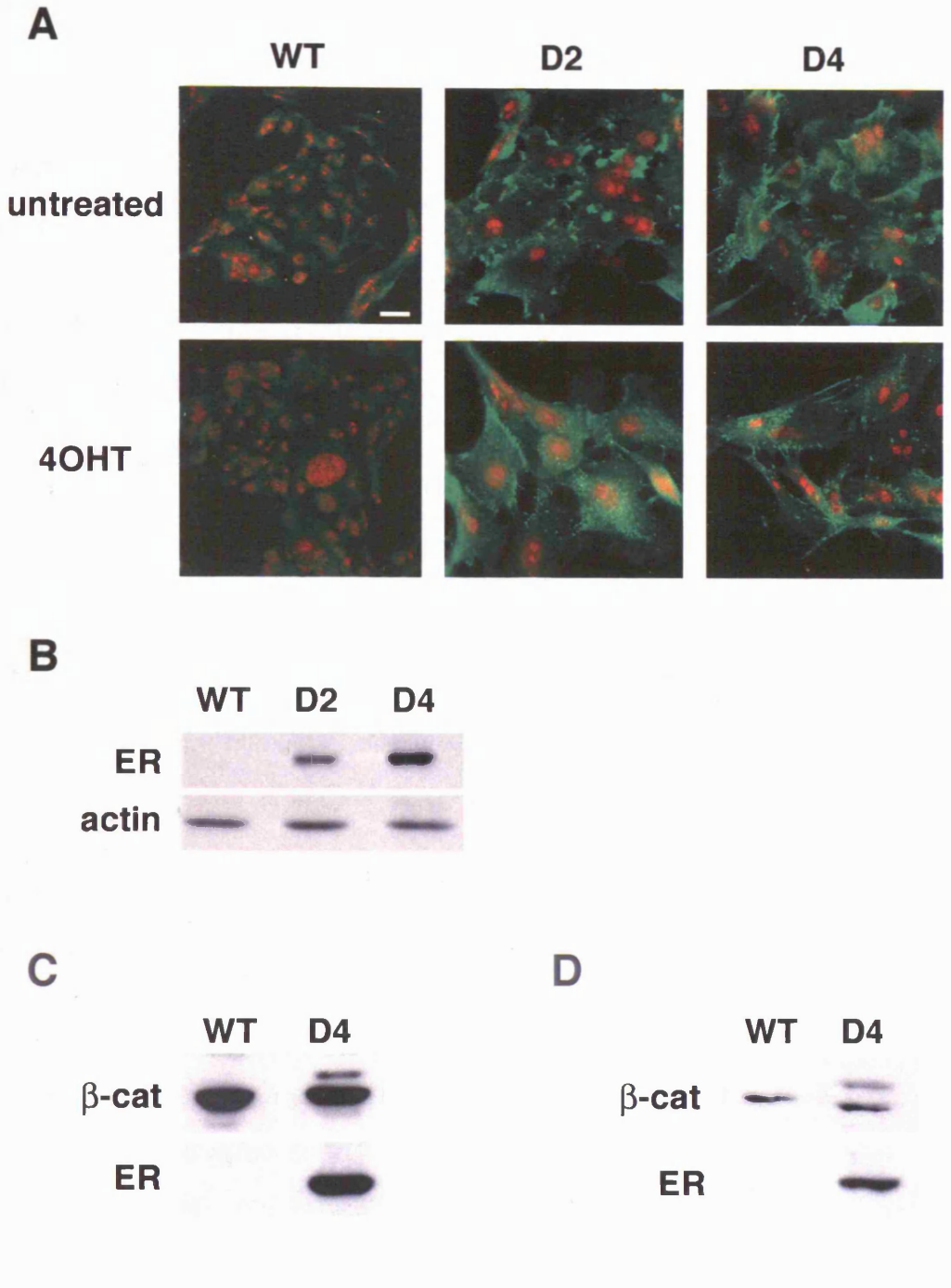

Figure 4.4. ΔNß-cateninER and endogenous ß-catenin in D2 and D4 keratinocyte lines. (A) Immunostaining showing ΔNß-cateninER localization before (top row) and after (bottom row) incubation with 4OHT. No staining was detected in wild type cells (left hand side). Red staining is propidium iodide nuclear counterstain. Scale bar: 20μm. (B) Western blot of primary keratinocytes derived from wild-type (WT) or transgenic (lines D2 and D4) mice, probed with anti-ER (top panel) or, as a loading control, anti-actin (bottom panel) antibodies. (C,D) Western blot of total triton extracts (C) or soluble cytoplasmic fractions (D) from wild-type (WT) or transgenic (D4) cell lines, probed with anti-ß-catenin (top panels) or anti-ER (bottom panels) antibodies. The upper band detected with anti-ß-catenin antibody was ΔNß-cateninER as it was also detected with anti-ER antibody.

4.2.2. D4 cells are more sensitive than D2 to 4OHT stimulation

I analyzed whether the difference in the amount of ΔNβ-cateninER in D2 and D4 cells led to a different response to 4OHT treatment at the level of transcriptional activation. I transfected wild type, D2 and D4 keratinocytes with a luciferase construct containing an enhancer with multiple Lef1/Tcf binding sites (TOPFLASH) or, as a negative control, one with mutated Lef1/Tcf binding sites (FOPFLASH) (van de Wetering et al., 1997). In preliminary experiments 4OHT treatment of cells expressing ΔNβ-cateninER transfected with FOPFLASH did not result in induction of luciferase. As this result agreed with previous work already shown by Dr. David Prowse in the laboratory (Lo Celso et al., 2004), I did not pursue it further. TOPFLASH activation occurred within 8h of addition of 4OHT to the medium and was greater at 24h (Fig. 4.5A), therefore in all the subsequent experiments I analyzed luciferase activity of transfected wild-type, D2 and D4 keratinocytes after incubation with 4OHT for 24 hours.

I compared TOPFLASH activation using a range of concentrations of 4OHT (Figure 4.5B). 4OHT did not induce transcriptional activation at any concentration in wild-type cells. I detected luciferase activity only at the highest 4OHT concentration in D2 cells, while in D4 cells there was significant activation at concentrations of 2×10^{-8}M and higher. Interestingly, even though D4 cells expressed more ΔNβ-cateninER protein, the maximum activation achieved in D2 and D4 cells was the same, the main difference between the two lines being therefore their sensitivity to low 4OHT concentrations.

4.2.3. Titration of β-catenin activation in vivo

I next examined whether I could titrate β-catenin signalling strength within each transgenic line in vivo by treating the mice with different doses of 4OHT: 0.5 mg (low) dose, 1.5 mg (medium, similar to what I used in the experiments described in Chapter 3) and 3 mg (high).

Since the investigation of the effects of β-catenin titration would require a detailed morphological analysis and tail whole mounts preparations are the best method to visualize even subtle alterations in mouse epidermis, I started to focus my attention on

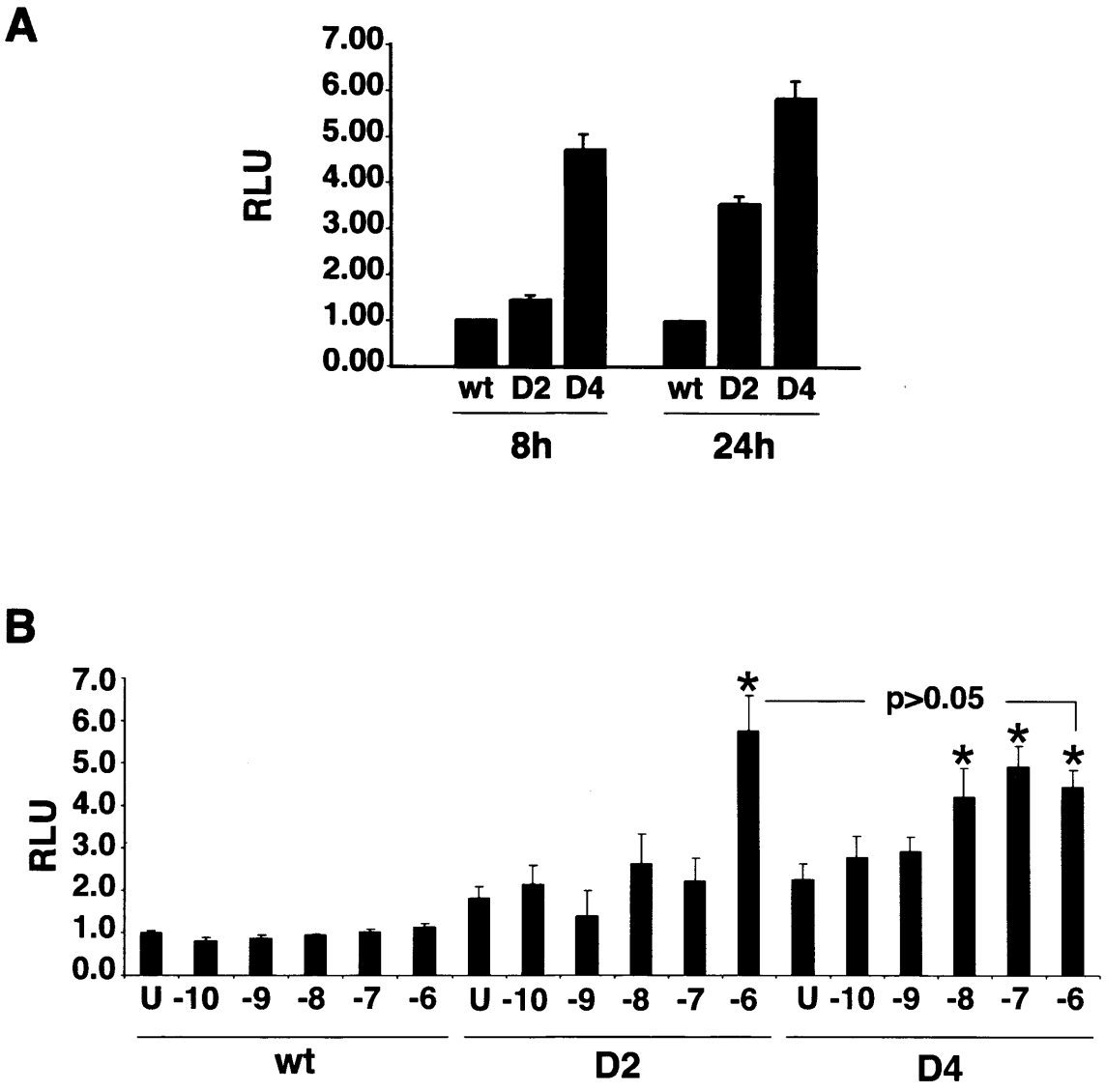

Figure 4.5. Trascriptional activation of ß-catenin responsive promoter in wild-type and transgenic cell lines. Wild-type, D2 and D4 cells were transfected with TOPFLASH reporter construct and incubated (A) with 200nM 4OHT for 8 or 24 hours or (B) with none (U) or increasing 4OHT concentrations, from $2x10^{-10}$ M(-10) to $2x10^{-6}$ M (-6), for 24 hours before being analysed. Relative light units (RLU) are shown. Each bar represents the mean of at least 3 replicates in up to 4 experiments, with standard error. Asterisks indicate significant increase of RLU relative to untreated.

tail epidermis. I analyzed ΔNβ-cateninER localization in sections of tail skin from mice that had been treated 24 hours earlier with the three different doses of 4OHT (Fig. 4.6). I observed a dose dependent redistribution of ΔNβ-cateninER in IFE, SG and HF in both D2 and D4 mice, even though in D2 sections the overall staining was less intense.

In untreated epidermis ER immunoreactivity was most abundant at cell-cell borders. After treatment with 3mg 4OHT, cell border staining was reduced and there was punctate staining in the nucleus and cytoplasm (cfr also Fig. 3.2). In epidermis treated with 1.5mg the staining was still primarily nuclear and cytoplasmic, while with 0.5mg 4OHT cell-cell border staining was predominant.

4.2.4. Control of hair follicle number and location by transgene copy number and 4OHT dose

When I topically applied 4OHT on the tail of K14ΔNβ-cateninER transgenic mice, the epidermis of this region appeared to respond to 4OHT treatment in a similar way to dorsal paw in both transgenic lines. For example, in sections of D2 tail skin treated for 21 days ectopic hair follicles had developed from IFE, SG and ORS (Fig. 4.7A,B, cfr Fig. 3.9A). The best advantage of analyzing tail skin was that not only all β-catenin induced alterations were present at the same time, but they could be visualized extremely clearly in three dimensions in whole mount preparations, in which the epidermis with all the connected appendages is observed from the dermal side (Fig. 4.7C,D). In acetone vehicle treated tail epidermis the hair follicles had prominent sebaceous glands and were organized in triplets separated by regions of flat interfollicular epidermis, a picture indistinguishable from wild type (Braun et al., 2003). In 4OHT treated epidermis the hair follicles appeared elongated as they were in anagen and ectopic follicles of various sizes protruded from the sebaceous glands, the interfolicular epidermis and occasionally also from the ORS (white, grey and black arrows respectively in Fig. 4.7D). All the ectopic follicles could be easily visualized as they expressed the bulb marker CDP (Fig. 4.7E). Also the presence of dermal papillae could be assessed, because of the surrounding keratinocytes arranged in the characteristic cup-like structure (asterisks in Fig. 4.7D,E).

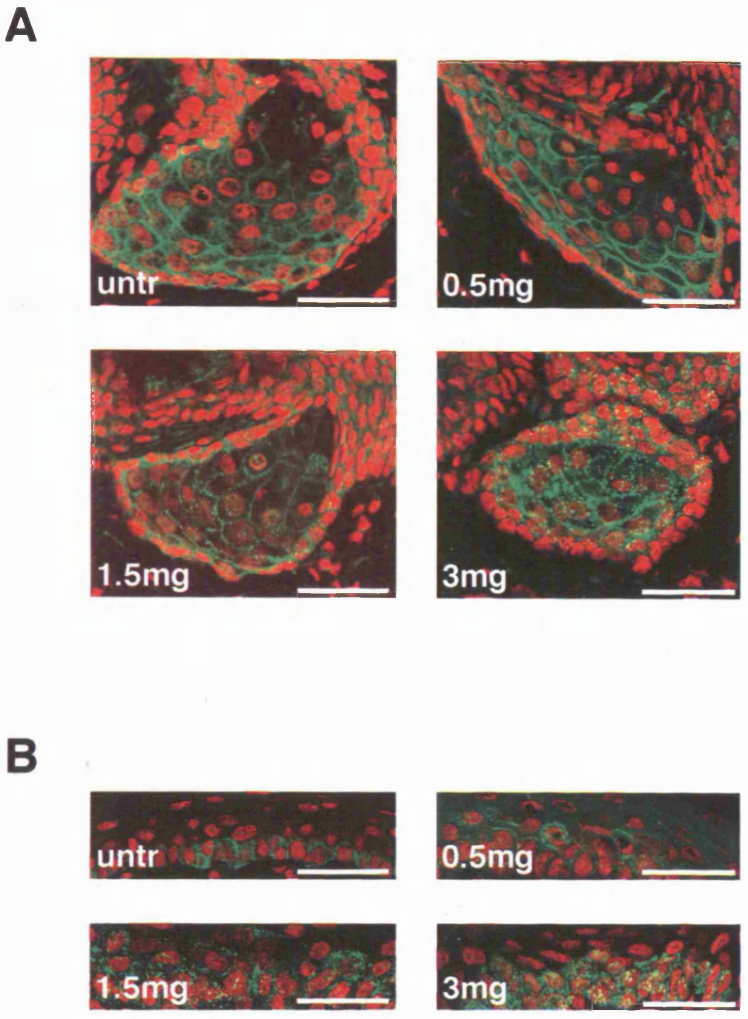

Figure 4.6. In vivo titration of ß-catenin signalling. Sections of D4 transgenic tail skin were immunostained with anti-ER antibody. A: sebaceous glands, B: interfollicular epidermis of skin either untreated (top left panels) or treated for 24 h with the 4OHT doses shown. Red fluorescence is propidium iodide nuclear counterstain. Scale bars: 50 µm.

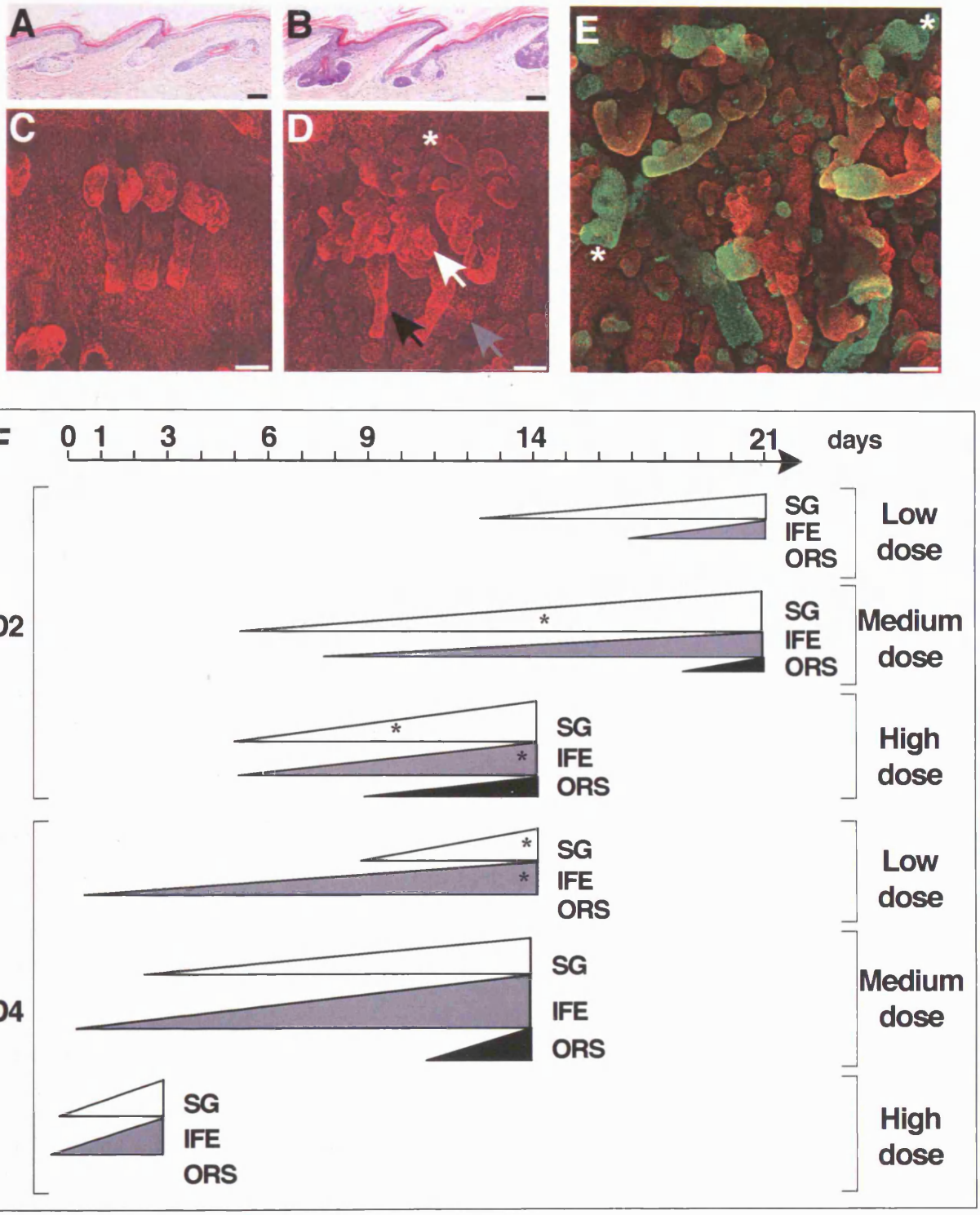

Figure 4.7. Whole mount analysis of the effects of ß-catenin titration. (A-D) Histologial sections (A,B) and keratin 14 whole mount immunostaining (C,D) of D2 transgenic tail skin either untreated (A,C) or after 21 days of 4OHT treatment. Arrows in D indicate ectopic hair follicles arising from IFE (greyarrow), SG (white) and ORS (black). (E) Tail epidermis of D2 transgenic treated with 4OHT immunostained with anti-keratin 14 (red) and anti-CDP (green) antibodies. (F) Diagram showing ectopic hair morphogenesis progression in D2 (upper part) and D4 (lower part) transgenic mice treated with 0.5 (low), 1.5 (medium) or 3mg (high dose) 4OHT every second day. Triangle tips represent the appearance and heigth the number and size of CDP positive patches in SG (white), IFE (grey) and ORS (black). Asterisks indicate appearance of dermal papillae. The diagram is a schematization of Violeta Silva-Varga's whole mount immunostainings. Scale bars: 100µm.

I titrated β-catenin activation in vivo by applying different doses of 4OHT on the tail of D2 and D4 transgenic mice and wild type littermate controls for different lengths of time. Violeta Silva-Vargas, another PhD student in the laboratory with experience in whole mount immunostaining techniques, evaluated ectopic hair follicle differentiation in all the treated tails using the anti-CDP antibody (Braun et al., 2003; Ellis et al., 2001) and quantified the number of hair germs and more developed hair follicles in all epidermal compartments over time.

In D2 mice 4OHT dose affected the number of patches of ectopic CDP expression and the time of their appearance. The higher the dose of 4OHT, the earlier and more numerous the CDP positive patches, and the earlier they developed into more mature hair follicles with dermal papillae. At all doses the number of positive outgrowths per unit increased over time. The number of ectopic hair follicles generated with the medium dose was higher than at low dose. Interestingly, at high dose the number of CDP positive areas was lower than at the medium dose, but high dose patches were larger.

As expected, D4 epidermis responded more rapidly than D2 to 4OHT, and by day 1 ectopic hair follicles were detectable. The number of CDP-positive patches was higher than in D2 mice treated with the same dose at early time points, but it did not increase over time because patch size tended to be greater and individual patches merged with one another. For the same reason distinct projections of CDP-positive epithelium and dermal papillae were hardly ever observed.

In D2 mice CDP was most readily induced in the sebaceous glands, while the ORS appeared to be the most refractory region, so that by the time that hair germs appeared as little bumps protruding from the ORS the follicles originating from the sebaceous glands were elongated and had already embraced a dermal papilla. In D4 mice the IFE was most sensitive and even though the HF remained most refractory, over time CDP expression was observed along most of the D4 ORS. The diagram in Fig. 4.7F is a schematization of the effects observed.

In conclusion, not only transgene copy number but also 4OHT dose influenced the strength of β-catenin signalling and different regions of the epidermis had different sensitivity to 4OHT treatment. It is therefore possible to titrate β-catenin activation in vivo to finely control the number and location of ectopic hair follicles.

4.2.5. Regional variation in the expression of ΔNβ-cateninER in tail skin

In order to explain the different sensitivity to 4OHT stimulation observed in IFE, ORS and sebaceous glands I examined whether there was regional variation in transgene expression in tail epidermis (Fig. 4.8). All basal cells of the IFE, ORS and periphery of the SG expressed ΔNβ-cateninER, but, unlike in the back, in tail skin I observed heterogeneity in expression levels, with higher levels being detected in the sebaceous gland than the IFE or ORS. IFE expression was heterogeneous, with patches of cells at the junction between the ORS and the IFE expressing higher levels than cells in other regions (brackets in Fig. 4.8B). The same expression pattern was observed in both transgenic lines and also in K14MycER mice (Arnold and Watt, 2001) and Aznar-Benitah and Watt personal communication). Interestingly, the areas of IFE showing the highest expression of the transgene did not correlate with the ones where ectopic follicles were induced (cfr Fig. 4.7B). The higher levels of ΔNβ-cateninER expression in the sebaceous glands could explain though why D2 sebaceous glands were most sensitive to hair follicle induction.

4.3. β-catenin induced hair follicles develop independently of bulge stem cells but express epidermal stem cell markers

As whole mount immunolabelling of tail epidermis is the best method to visualize label retaining cells and the bulge region of the hair follicle (Braun et al., 2003), I collaborated with Violeta Silva-Vargas also to analyze the effects of β-catenin activation on the epidermal stem cell compartment using BrdU label retention as a marker (Braun et al., 2003).

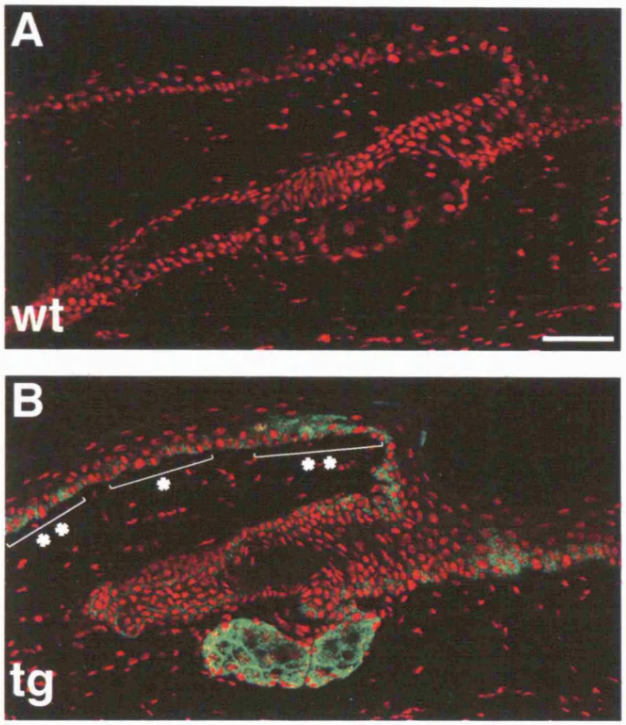

Figure 4.8. ΔNβ-cateninER expression in tail epidermis. Sections of wild-type (A) and D4 transgenic (B) tail skin stained with anti-ER antibody (green fluorescence). Brackets in B indicate patches of higher (**) or lower (*) transgene expression in IFE. Red fluorescence is propidium iodide nuclear counterstain. Scale bar: 100 μm

In wild-type mice and untreated transgenic mice LRC were concentrated in the bulge, and there were scattered LRC in the sebaceous glands and IFE (Figure 4.9A; (Braun et al., 2003). At times when ectopic hair follicle formation was well advanced in IFE and SG there was no evidence of LRC depletion in the bulge (Fig. 4.9B). The number of LRC in the bulge eventually declined significantly by day 28 in D2 mice (Fig. 4.9C), when the trichofolliculomas represented the biggest component of the epidermis. Also in D4 mice ectopic hair germs developed without apparent involvement of bulge LRC, but BrdU staining was lost when the follicles became thicker and hyperproliferative. Interestingly, Violeta Silva-Vargas showed that the expression of other bulge markers such as keratin 15 and CD34 (Liu et al., 2003; Tumbar et al., 2004) was never reduced, and that LRC were lost because they divided (Silva-Vargas et al., 2005). Lineage tracing experiments performed by Dr Braun and Dr Giangreco in the laboratory indicated that that the majority of new follicles in the IFE were derived from IFE rather than from neighbouring hair follicles (Silva-Vargas et al., 2005), strengthening the conclusion that ectopic hair follicle induction occurred independently of bulge stem cells.

In D2 mice treated with 4OHT for at least three weeks, keratin 15 and CD34 expression was detectable in the ectopic hair follicles in whole mount preparations (Silva-Vargas et al., 2005). When I analyzed CD34 expression in more detail in sections of back and tail epidermis I observed positive immunostaining not only in the bulge region of wild type and transgenic follicles (Fig. 4.9D, arrow in E) but also in all sites of new HF formation (Fig. 4.9E,F). CD34 staining in ectopic follicles was slightly weaker than in the pre-existing bulge and mostly extended along the length of the new follicles, an expression pattern that I observed also in E18.5 hair germs (Fig. 4.9G). FACS sorting and clonal analysis of the CD34/α6 integrin double positive cells from wild type and D2 treated mice performed by Dr Giangreco in the laboratory indicated that the transgenic keratinocytes have an enhanced colony forming efficiency in vitro, another characteristic of epidermal stem cells.

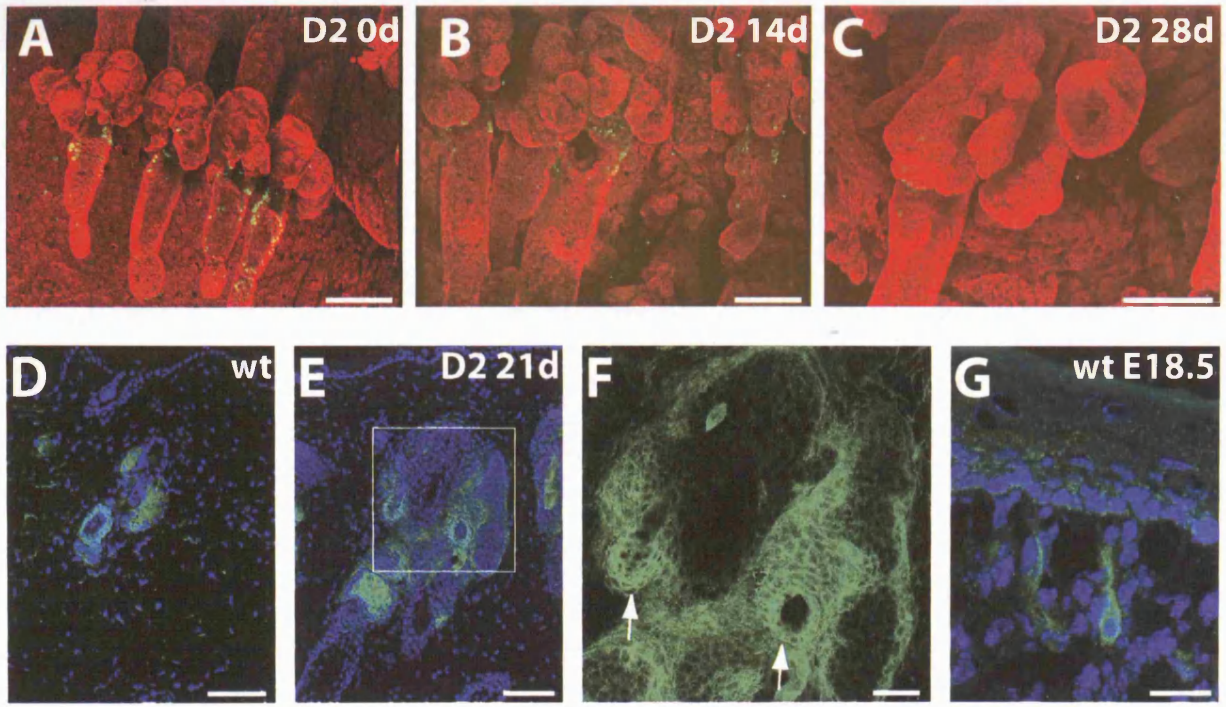

Figure 4.9. Effect of ß-catenin activation on the stem cell compartment. (A-C) Whole mount immunostaining of D2 transgenic tail epidermis treated for the number of days indicated (d). Red fluorescence: keratin 14. Green fluorscence: BrdU (LRC). The panels are a gift of Violeta Silva-Vargas. (D-G) CD34 expression (green fluorescence) in wild-type littermate control (D,), D2 (E,F) or embryonic day E18.5 (G) back skin. Adult mice (D-F) were treated with 4OHT for 21 days. F shows at higher magnification CD34 staining in the area boxed in E. Arrows in F point at bulge regions of pre-existing follicles. Scale bars: 100µm (A-E), 50µm (F,G).

4.4. β-catenin induced hair follicles cycle reflecting 4OHT treatment

Since the β-catenin induced hair follicles contained keratinocytes with epidermal stem cell properties, and I had already shown that upon 4OHT withdrawal they regressed to a state similar to telogen, I investigated whether a second treatment with 4OHT would push the new follicles into anagen or trigger the formation of even more numerous hair germs.

I treated D2 mice for three weeks to induce new follicles, left the skin untreated for the following three weeks, and finally applied 4OHT again for one or two weeks (Fig. 4.10). As expected, at the end of the three weeks of treatment ectopic hair follicles had developed (Fig. 4.10B), and after 4OHT withdrawal the pre-existing follicles were back in telogen and the ectopic follicles had regressed (Fig. 4.4C). The second treatment induced the original follicles to re-enter anagen with the same kinetics as the first treatment (cfr Fig. 3.5): they had clearly started the growth phase within a week of stimulation, and were fully elongated by the end of the second week (Fig. 4.4D,E). Also the ectopic follicles re-grew, this time looking wider than before and displaying an anagen-like bulb surrounding a dermal papilla within one week of 4OHT treatment (Fig. 4.4D, arrow). The number of ectopic follicles did not appear changed compared to the first treatment, an observation confirmed by Dr. Adam Giangreco when he counted the sites of ectopic CDP expression. The second 4OHT treatment thus induced the ectopic follicles to re-grow without stimulating extra ones to form.

I could observe the same effects of 4OHT intermittent treatment in whole mount preparations of tail skin (Fig. 4.10F-H), where in addition I could monitor the retention of BrdU label. Bulge LRC appeared unaffected not only after the first three weeks of treatment, but also by the end of the first week of the new 4OHT application, indicating that the new hair follicles not only form but also cycle independently of bulge LRC (Fig. 4.10F,H).

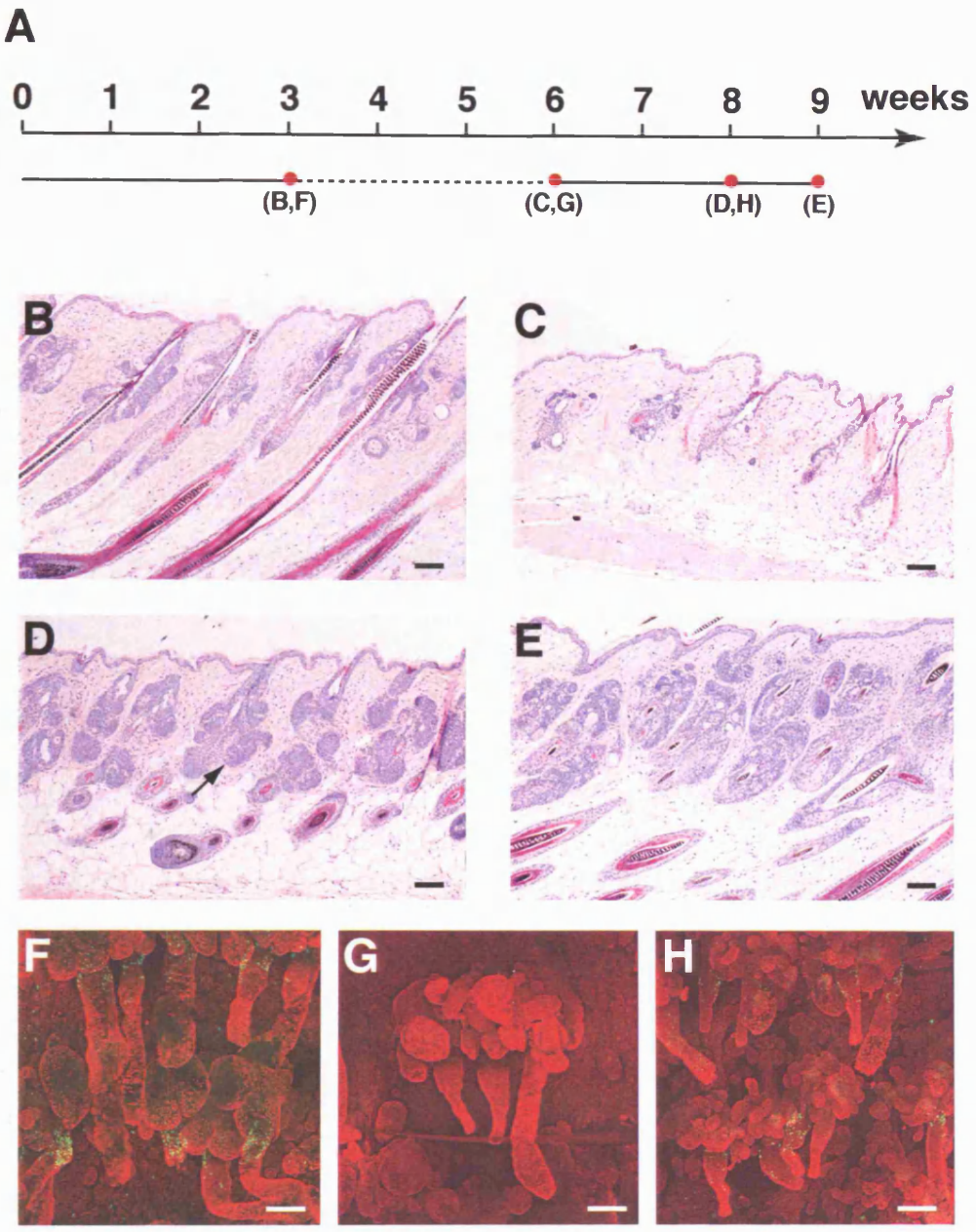

Figure 4.10. ß-catenin induced hair follicles cycle reflecting 4OHT treatment. (A) Schematic representation of the experiment. The arrow indicates time in weeks. Continuous lines represent 4OHT treatment and dashed lines indicate no 4OHT treatment. Red dots are time points analysed. Arrow in D points at an ectopic follicle with dermal papilla. (B-E) Histological sections of D2 back skin after 3 weeks of 4OHT treatment (B), 3 additional weeks without treatment (C) and one (D) or two (E) weeks of second 4OHT treatment. (F-H) Whole mount preparations of D2 tail epidermis treated as in B (F), C (G) and D (H) and immunostained with anti-keratin 14 antibody. Green fluorescence in F,H represent LRC (anti-BrdU immunostaining). Scale bars: 100µm.

4.5. Discussion

By adjusting the 4OHT treatment protocols on the ΔNβ-cateninER transgenic mice it was possible to finely regulate the timing of β-catenin activation in adult epidermis *in vivo*. A single 4OHT treatment was as efficient as seven daily applications to induce anagen initiation and ectopic hair follicle formation, even though ΔNβ-cateninER had cleared from the nucleus within three days. The effects of transient β-catenin activation were not confined to the transgene-positive cells but extended to neighbouring cells, as proved by the induction of dermal papillae in the surrounding mesenchyme. The cascade of events activated by β-catenin is likely to be characterized by its own regulatory mechanisms and it is not so surprising that its final effects are detectable days after the original β-catenin signal has ceased.

Following the same mechanism, the hair follicle tumours kept growing for a while after 4OHT withdrawal, as indicated by the worsening conditions of the ears. Interestingly, the ears healed and the hair follicle tumours regressed and three months later what remained were remnants of the tumour mass that mainly comprised empty hair canals. Thus, while the hair development program only needed to be triggered by β-catenin and could progress independently, continued β-catenin activation was needed to maintain the tumours, which could not grow autonomously. Additional oncogenic changes, such as mutation of p53 or Ras, would probably be necessary to convert the trichofolliculomas into malignant tumours capable of autonomous growth (Hahn and Weinberg, 2002; Owens and Watt, 2003; Perez-Losada and Balmain, 2003).

The observations that the tumours originated from growing ectopic follicles (cfr Chapter 3), that β-catenin signalling is detected in matrix cells during anagen (DasGupta and Fuchs, 1999), and that the tumour remnants were reminiscent of telogen hair follicles indicate that the termination of β-catenin signalling in the lower portion of the follicles could be a physiological mechanism of catagen induction. Not surprisingly, the re-initiation of 4OHT treatment induced the ectopic follicles to grow again.

The strength of β-catenin signalling was controlled in vivo by applying different doses of 4OHT on transgenic mice from different copy number lines. The increased sensitivity to 4OHT treatment observed in vitro in the D4 keratinocyte line compared to D2 corresponded to the faster and more dramatic induction of the phenotype in the D4 mice. The fact that, once the sensitivity threshold was reached, the levels of transcriptional activation after incubation with different 4OHT concentrations were the same in D4 and D2 cell lines may represent a limitation of the in vitro assay. This is because in vivo differences were detectable at earlier time points and there was a clear correlation between the dose of 4OHT and the extent of ΔNβ-cateninER re-localization. The concept that cells exhibit a graded response to a gradient of β-catenin regulatory activity was previously established in studies of a panel of ES cell lines with different APC mutations (Kielman et al., 2002), and the experiments described here are an example of parallel β-catenin titration *in vitro* and *in vivo*.

The levels of ΔNβ-cateninER expression in different regions of tail epidermis did not completely explain the different sensitivity of ORS, IFE and SG to ectopic hair follicle induction. Moreover, transgene expression was uniform in back skin but in that region I also observed differences in the responsiveness to β-catenin activation. In the tail of both transgenic lines the ORS of existing HF was most refractory, and interestingly even though I observed a high number of ectopic follicles originating from the ORS of back hair follicles they tended not to arise from the bulge region. This is consistent with growing evidence that bulge cells are quiescent and surrounded by an environment that makes them refractory to a range of signalling pathways (Blanpain et al., 2004; Tumbar et al., 2004). Factors that are upregulated in the bulge include the secreted Wnt antagonist Dickkopf-3 (Morris et al., 2004; Tumbar et al., 2004),and Tcf3, which can act as a repressor of Wnt signalling (Merrill et al., 2001).

The observation that ectopic HF formation occurred without any evident perturbation of bulge LRC agrees with those studies indicating that not all multipotent epidermal progenitors reside in the HF bulge region (Ferraris et al., 1997; Ghazizadeh and Taichman, 2001). It has long been proposed that mouse IFE is organised into 'epidermal proliferative units': at the base of each one lies a single stem cell surrounded by committed progenitors (transit amplifying cells) (Potten and Morris, 1988). If the

ectopic follicles originate from epidermal stem cells this model would explain why only a certain number of them could be generated, but it is not possible to exclude that also TA cells could give rise to ectopic follicles and lineage marking experiments are suggesting that the new follicles are not clonal in origin (Silva-Vargas et al., 2005).

The ectopic follicles could undergo 4OHT dependent cycles of growth and regression. The re-growth phenotype observed could not be interpreted as a true hair growth cycle (Millar, 2002), since it was entirely 4OHT dependent, but it would not be feasible to look for a spontaneous re-starting of anagen phase of the ectopic follicles. A very important observation was that in response to reapplication of 4OHT there was no further increase in the number of HF, but rather the ectopic follicles enlarged. This implies that there is some mechanism to limit the number of new follicles; it is tempting to speculate that it may involve the same type of intercellular signalling events that control the spacing of new follicles during embryonic development (Millar, 2002).

Remarkably, not only was new follicle formation initiated without any detectable involvement of existing bulge cells, but new follicles contained cells that expressed CD34, indicating that cells with bulge stem cell characteristics can be formed from non-bulge epidermal cells. β-catenin induced hair follicle morphogenesis recapitulates the steps of embryonic hair follicle development (see Chapter 3). CD34 expression during embryonic development has not been reported elsewhere, but bulge-like cells in the β-catenin induced follicles present other characteristics of epidermal stem cells. CD34 expression observed in the embryos could indicate that during development CD34 positive epidermal stem cells are first distributed along the hair germs and only subsequently confined in the bulge region.

If given the appropriate signal, any proliferation-competent cell can form a new HF expressing both ORS and bulge markers, than β-catenin activation is a way to increase epidermal stem cell number. It has previously been reported that β-catenin activation in cultured human epidermal cells increases the number of stem cells (Zhu and Watt, 1999); whether this occurs through expansion of the pre-existing stem cell pool or through generation of new stem cells from committed progenitors remains to be explored (Pearton et al., 2004). Whichever is the case, a role for Wnt signalling in

increasing stem cell number has been recently reported in a wide range of tissues, including the blood, mammary gland and nervous system(Liu et al., 2004; Megason and McMahon, 2002; Reya et al., 2003; Zhang et al., 2003).

Chapter 5. Crosstalk between β-catenin and other signalling pathways during HF morphogenesis

Several signalling pathways are known to play a role in HF morphogenesis, but still little I known about how they interact to regulate this process (Millar, 2002). Activation of β-catenin in adult epidermis triggers *de novo* HF formation in IFE, SG and ORS. The first signs of this process are visible in ΔNβ-cateninER mice (D2 line) after seven days of 4OHT treatment. Microarray analysis of the changes occurring in the gene expression profile during this phase gave insights on the β-catenin target genes but also on the molecular mechanisms of HF induction. I used the response to 4OHT treatment in ΔNβ-cateninER transgenic mice as a simple biological assay to validate the role of some of the induced genes in the regulation of hair follicle morphogenesis and cycling.

5.1. Microarray analysis of β-catenin target genes

I closely collaborated with Violeta Silva-Vargas to isolate RNA from whole dorsal skin of wild type and D2 female mice either untreated, or after one or seven days of b-catenin activation. All mice were six weeks old and in telogen phase at the beginning of the experiment and the treatment used to induce b-catenin activation was 1mg 4OHT applied every day. Three mice per group were analyzed and, once checked that they presented the expected histological appearance, 18 independent samples were generated and analyzed separately. In summary, wild type and transgenic at day 0,1 and 7 were the six conditions analyzed in triplicate (Fig. 5.1A).

The Affymetrix chip technology was used to analyze the transcription of more than 45000 probe sets, representing over 34000 Unigene clusters (Fig. 5.1B). Genespring

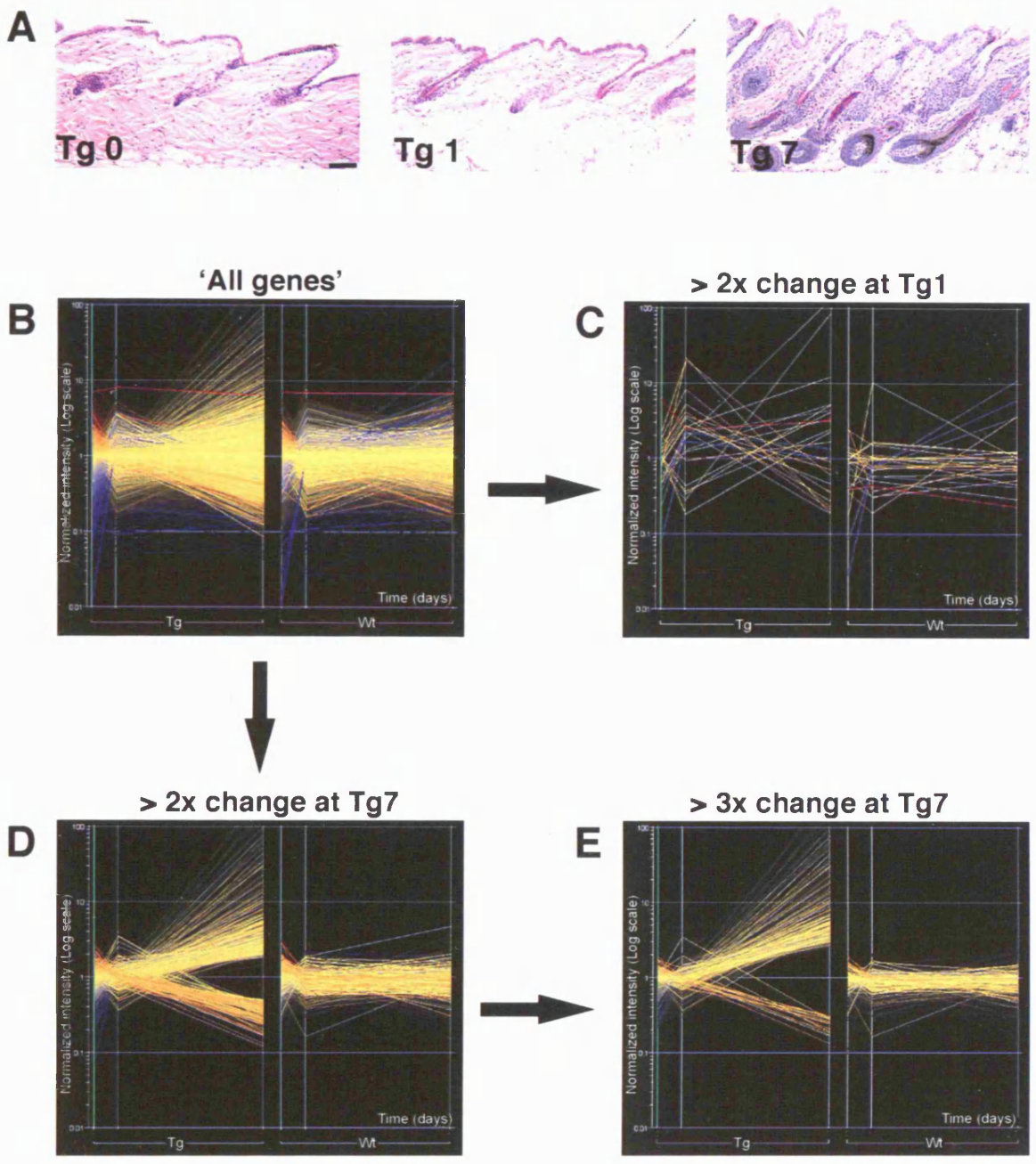

Figure 5.1. Microarray analysis of ß-catenin induced genes. (A) Histological sections of skin from D2 transgenic mice untreated (left) or treated with 4OHT for 1 (middle) or 7 (right) days, corresponding to the analyzed conditions 'Tg0', 'Tg1', and 'Tg7'. Scale bar 100µm. (B-E) Diagrams produced using Genespring software representing the expression data collected for all (B) or selected probes (C: expression changed at least 2 fold at transgenic day1, D: expression changed at least 2 fold at transgenic day7, E: expression changed at least 3 fold at transgenic day7). On the horizontal axes the conditions analyzed are ordered by by genotype (transgenic or wild type) and days of treatment (0,1,7). On the vertical axes normalized expression values are in logarithmic scale. Each line represents one probe set and its color indicates the expression level at Tg0 (blue: low levels, red: high levels, yellow: intermediate levels).

microarray analysis software was used for quality control and normalization of the raw chip data and to identify genes with a significant change in expression in at least one condition out of six. I selected the probes showing a change in relative expression levels of at least 2 fold when the conditions 'transgenic day 1' and 'transgenic day 7' were compared with untreated transgenic or all wild-type littermates. Only 25 probe sets showed significantly altered expression after the first 4OHT dose (Fig. 5.1C), but 862 did after 7 days of treatment (Fig. 5.1D). The number of probe sets to consider for further analysis was made more manageable by choosing a threshold of three fold induction/suppression (Fig. 5.1E). 390 probe sets were identified as >3 fold up regulated and 49 probe sets >3 fold down regulated after 7 days of 4OHT treatment.

RNA was hybridized onto both the A and B chips from the MOE430 set. The B chip represents mainly unknown ESTs and RIKEN clones, and many probes that changed at least three fold corresponded to unknown genes that I did not analyze further. Many of the known genes were represented by more than one probe set, and the expression data generated by the different probe sets were usually very similar. Once the unknown sequences and the repetitions had been eliminated, I generated a list of 171 establishes genes upregulated and 28 downregulated, which I subdivided according to functional categories (Tables 5.1 to 4).

Some of the upregulated genes corresponded to known targets of β-catenin or to markers of hair follicle differentiation that I had already validated in previous analysis (see Chapter 3 and also (Gat et al., 1998; Lo Celso et al., 2004; Van Mater et al., 2003). Keratin 17 expression increased almost two fold, correlating with its expression in the new follicles (Fig. 3.13), and several hair keratins were increased more than 20 fold. CDP was upregulated 5 fold and Lef1, 6 fold (Fig. 3.13). Shh and Ptch (Fig. 3.11) were upregulated 57 and 14 fold, respectively. Cyclin D1 was upregulated 5 fold and the induction of several cell cycle regulators was consistent with the local increase in proliferation that occurs in response to β-catenin (Fig. 3.12).

The β-catenin target genes I identified were very diverse, but the category with the biggest number of induced genes was the one containing transcription factors and

TABLE 5.1

Functional classification of genes induced more than 3 fold at Tg day 7

Signalling/Transcription factors	45
Metabolism	25
Keratins	17
Cell cycle regulation	16
DNA remodeling and repair	9
Cytoskeleton	9
Extracellular matrix	7
Cell junction	6
Ion channels	5
Melanin synthesis	5
Kinases	5
Proteolysis/Ubiquitination	4
Kinesin related	3
Transmembrane proteins	2
Vescicle transport	2
Other	11
TOTAL	171

TABLE 5.2
Genes induced more than 3 fold at Tg day7 (Signalling and transcription factors excluded)

Affy Probe ID	Fold Change		Gene name	Genebank
Metabolism				
1425376_at	3.1	Alox15b	arachidonate 15-lipoxygenase, second type	Alox15b
1418847_at	4.2	Arg2	arginase type II	NM_009705
1419373_at	12.1	Atp6v1b1	ATPase, H+ transporting, V1 subunit B, isoform 1	NM_134157
1426959_at	4.6	Bdh	3-hydroxybutyrate dehydrogenase	BC027063
1416563_at	4.2	Ctps	cytidine 5'-triphosphate synthase	NM_016748
1419270_a_at	3.1	Dutp	deoxyuridine triphosphatase	AF091101
1425295_at	3.3	Ear11	eosinophil-associated ribonuclease 11	BC020070
1419031_at	3.2	Fads2	fatty acid desaturase 2	BB430611
1448470_at	18.9	Fbp1	fructose bisphosphatase 1	NM_019395
1448485_at	5.3	Ggt1	gamma-glutamyltransferase 1	NM_008116
1417422_at	140.5	Gnmt	glycine N-methyltransferase	NM_010321
1420589_at	8.6	Has3	hyaluronan synthase 3	NM_008217
1416761_at	8.6	Hsd11b2	hydroxysteroid 11-beta dehydrogenase 2	BC014753
1439634_at	3.1	Hsd17b4	hydroxysteroid (17-beta) dehydrogenase 4	AW490446
1450860_at	4.6	Lap3	leucine aminopeptidase 3	AK010384
1444487_at	5.9	Lrat	lecithin-retinol acyltransferase	Lrat
1419017_at	5.4	Lrp4	low density lipoprotein receptor-related protein 4	NM_016869
1447683_x_at	3.8	Mettl1	tRNA methylase	AV118676
1456748_a_at	3.2	Nipsnap1	4-nitrophenylphosphatase SNAP25-like protein 1	AV306253
1419323_at	8.3	Padi1	peptidyl arginine deiminase, type I	NM_011059
1419767_at	29.0	Padi3	peptidyl arginine deiminase, type III	NM_011060
1426259_at	6.3	Pank3	pantothenate kinase 3	BC027089
1421856_at	45.0	S100a3	S100 calcium binding protein A3	AF087470
1425179_at	3.7	Shmt1	serine hydroxymethyl transferase 1 (soluble)	AF237702
1448562_at	13.2	Upp	uridine phosphorylase	NM_009477
Keratins				
1436557_at	92.5	Kb36	keratin complex 2, gene 6g	BM936589
1421589_at	32.5	Krt1-1	keratin complex 1, acidic, gene 1	NM_010659
1427179_at	57.8	Krt1-3	keratin complex 1, acidic, gene 3	X75650
1418742_at	205.9	Krt1-4	keratin complex 1, acidic, gene 4	NM_027563
1427751_a_at	7.3	Krt1-5	keratin complex 1, acidic, gene 5	X65506
1449378_at	142.3	Krt1-c29	keratin complex-1, acidic, gene C29	NM_010666
1460185_at	74.3	Krt2-18	keratin complex 2, basic, gene 18	NM_016879
1423952_a_at	3.2	Krt2-7	keratin complex 2, basic, gene 7	BC010337
1450536_s_at	6.1	Krtap12-1	keratin associated protein 12-1	NM_010670
1450539_at	5.2	Krtap5-1	putative; keratin-associated protein 5-1	NM_015808
1427211_at	60.3	Krtap8-1	keratin associated protein 8-1	AA727386
1422209_s_at	9.4	Krtap9-1	keratin-associated protein 9-1	NM_015741
Hair keratins				
1420409_at	60.5	Krt1-24	keratin complex 1, acidic, gene 24	NM_016880

1427365_at	32.7	Krt2-10	keratin complex 2, basic, gene 10	X99143
1427290_at	5.2	Krt2-19	keratin complex 2, basic, gene 19	AF312018
1448457_at	89.9	Krt2-6g	keratin complex 2, basic, gene 6g	NM_019956
1427719_s_at	28.1	Krt2-ps1	kertain complex 2, basic, pseudogene 1	AF312019
Cell Cycle				
1424046_at	3.9	Bub1	budding uninhibited by benzimidazoles 1 homolog	AF002823
1447363_s_at	4.9	Bub1b	budding uninhibited by benzimidazoles 1 homolog,beta	AU045529
1416076_at	4.4	Ccnb1	cyclin B1	X58708
1450920_at	3.2	Ccnb2	cyclin B2	AK013312
1417419_at	4.8	Ccnd1	cyclin D1	M64403
1416124_at	5.9	Ccnd2	cyclin D2	BB840359
1448314_at	4.4	Cdc2a	cell division cycle 2 homolog A (S. pombe)	NM_007659
1429499_at	3.8	Fbxo5	F-box only protein 5	AK011820
1426817_at	3.4	Mki67	antigen identified by monoclonal antibody Ki 67	X82786
1419402_at	3.7	Mns1	meiosis-specific nuclear structural protein 1	NM_008613
1417299_at	3.0	Nek2	NIMA (never in mitosis a)related expressed kinase 2	NM_010892
1448191_at	3.7	Plk	polo-like kinase homolog (Drosophila)	NM_011121
1448595_a_at	3.2	Rex3	reduced expression 3	NM_009052
1418969_at	3.7	Skp2	S-phase kinase-associated protein 2 (p45)	NM_013787
1448113_at	3.1	Stmn1	stathmin 1	BC010581
DNA remodeling and repair				
1416746_at	3.3	H2afx	H2A histone family, member X	NM_010436
1429171_a_at	5.1	Hcapg	chromosome condensation protein G	AV277326
1438009_at	7.7	Hist1h2ae	histone H2A homolog	W91024
1423260_at	3.0	Idb4	inhibitor of DNA binding 4	BE981185
1436808_x_at	3.7	Mcmd5	mini chromosome maintenance deficient 5	AI324988
1417939_at	10.4	Rad51ap1	RAD51 associated protein 1	NM_009013
1427275_at	3.5	Smc4l1	structural maintenance of chromosomes 4-like 1	BI665051
1454694_a_at	3.8	Top2a	topoisomerase (DNA) II alpha	BM211413
1429835_at	18.3	Xrcc1	X-ray repair complementing defective repair CHO cells1	AK009778
Cytoskeleton				
1441628_at	3.3	Diap3	Diaphanous homolog 3	BB201495
1419513_a_at	3.5	Ect2	ect2 oncogene	NM_007900
1452280_at	3.6	Farp1	FERMRhoGEF (Arhgef) pleckstrin domain protein 1	BB097480
1435551_at	3.3	FHOS2	Diaphanous protein homolog 3	BG066491
1453748_a_at	3.2	Kif23	Mitotic kinesin-like protein-1	BG082989
1447364_x_at	3.0	Myo1b	myosin IB	AA406997
1421546_a_at	3.4	Racgap1	Rac GTPase-activating protein 1	NM_012025
1435154_at	3.2	Tuba6	tubulin, alpha 6	AV099404
1415978_at	7.1	Tubb3	tubulin, beta 3	NM_023279
Extracellular matrix				
1456901_at	43.9	Adamts20	GON-1 C. elegans ortholog	AI450842
1449827_at	3.6	Agc1	aggrecan 1	NM_007424

1449154_at	12.7	Col11a1	procollagen, type XI, alpha 1	NM_007729
1422831_at	3.5	Fbn2	fibrillin 2	NM_010181
1440765_at	3.2	Fras1	Fraser syndrome 1 homolog	AI604810
1450156_a_at	3.1	Hmmr	hyaluronan mediated motility receptor (RHAMM)	NM_013552
1416342_at	3.4	Tnc	tenascin C	NM_011607
Cell junction				
1426300_at	4.0	Alcam	activated leukocyte cell adhesion molecule	U95030
1426673_at	4.6	Cdh3	cadherin 3	X06340
1415801_at	3.8	Gja1	gap junction membrane channel protein alpha 1	M63801
1423271_at	19.8	Gjb2	gap junction membrane channel protein beta 2	AV239646
1448397_at	10.7	Gjb6	gap junction membrane channel protein beta 6	BC016507
1426864_a_at	3.7	Ncam1	neural cell adhesion molecule 1	X15052
Ion channels				
1437540_at	3.5	Mcoln3	mucolipin 3	AV313762
1448502_at	3.5	Slc16a7	solute carrier family 16, member 7	NM_011391
1438160_x_at	6.1	Slc21a12	solute carrier family 21, member 12	AV348121
1434502_x_at	5.6	Slc4a1	solute carrier family 4, member 1	BB448377
1418935_at	14.1	Trpm1	transient receptor potential cat. channel M1	NM_018752
Melanin biosynthesis				
1418028_at	7.6	Dct	dopachrome tautomerase	NM_010024
1418211_at	4.9	p	pink-eyed dilution	NM_021879
1422523_at	8.7	Si	silver	NM_021882
1417717_a_at	8.1	Tyr	tyrosinase	M20234
1415862_at	12.9	Tyrp1	tyrosinase-related protein 1	BB762957
Kinases				
1447940_a_at	3.6	Braf	B-type RAF kinase	BB327307
1418260_at	3.3	Hunk	hormonally upregulated Neu-associated kinase	NM_015755
1416558_at	3.7	Melk	maternal embryonic leucine zipper kinase	NM_010790
1426580_at	3.0	Stk18	serine/threonine kinase 18	AK006459
1448627_s_at	4.2	Topk-pendir	T-LAK cell-originated protein kinase	NM_023209
Proteolysis/ubiquitination				
1418989_at	12.5	Ctse	cathepsin E	NM_007799
1425916_at	4.8	Capn8	calpain 8	AB050203
1415811_at	8.2	Np95	nuclear protein 95	NM_010931
1452954_at	3.7	Ube2c	ubiquitin-conjugating enzyme E2C	AV162459
Kinesin related proteins				
1435306_a_at	3.4	Kif11	kinesin family member 11	Kif11
1451128_s_at	3.5	Kif22-ps	kinesin family member 22, pseudogene	Kif22-ps
1437611_x_at	4.0	Kif2c	kinesin family member 2C	Kif2c

Transmembrane proteins				
1448303_at	3.6	Gpnmb	glycoprotein (transmembrane) nmb	NM_053110
1429178_at	3.3	Odz3	odd Oz/ten-m homolog 3 (Drosophila)	BB472509
Vescicle transport				
1415845_at	5.6	Syt4	synaptotagmin 4	AV336547
1438841_s_at	6.8	Vti1b	vesicle transport through interaction with t-SNAREs 1B	AV002218
Other induced genes				
1420686_at	41.1	Cryba4	crystallin, beta A4	NM_021351
1416776_at	23.9	Crym	crystallin, mu	NM_016669
1435373_at	8.1	Csnk1e	casein kinase 1, epsilon	BM213197
1436723_at	4.3	Fshprh1	FSH primary response 1	BB258991
1423520_at	3.4	Lmnb1	lamin B1	BG064054
1450774_at	31.2	Ly6g6d	lymphocyte antigen 6 complex, locus G6D	NM_033478
1420467_at	5.3	Pcg	MHC psoriasis candidate gene	NM_020576
1425559_a_at	4.0	Sah	SA rat hypertension-associated homolog	AB022340
1433892_at	3.6	Spag5	sperm associated antigen 5	BM208112
1420707_a_at	4.1	Traip	TRAF-interacting protein	NM_011634
1446278_at	4.0	Utx	Untranslated X chromosome gene	BB077029

TABLE 5.3
Signalling related genes induced more than 2 fold at Tg day7

Affy Probe ID	Fold Change		Gene name	Genebank
Wnt				
1418532_at	2.7	Fzd2	frizzled homolog 2 (Drosophila)	NM_020510
1455604_at	4.1	Fzd5	frizzled homolog 5 (Drosophila)	BB795235
1460187_at	2.4	Sfrp1	secreted frizzled-related sequence protein 1	BI658627
1425425_a_at	5.5	Wif1	Wnt inhibitory factor 1	BC004048
1448594_at	4.1	Wisp1	WNT1 inducible signaling pathway protein 1	NM_018865
1450772_at	2.6	Wnt11	wingless-related MMTV integration site 11	NM_009519
1448818_at	3.2	Wnt5a	wingless-related MMTV integration site 5A	BC018425
1419708_at	2.4	Wnt6	wingless-related MMTV integration site 6	NM_009526
1454734_at	6.3	Lef1	lymphoid enhancer binding factor 1	BB033554
Hedgehog				
1437933_at	47.1	Hhip	Hedgehog-interacting protein	BB040396
1439663_at	14.5	Ptch	patched homolog	BB040049
1422655_at	6.7	Ptch2	patched homolog 2	NM_008958
1436869_at	57.4	Shh	sonic hedgehog	AV304616
1449058_at	6.8	Gli	GLI-Kruppel family member GLI	NM_010296
1446086_s_at	6.0	Gli2	GLI-Kruppel family member GLI2	AW546128
BMP				
1423753_at	7.7	Bambi	BMP and activin membrane-bound inhibitor	AF153440
1448601_s_at	3.7	Msx1	homeo box, msh-like 1	BC016426
1449559_at	8.0	Msx2	homeo box, msh-like 2	NM_013601
Notch				
1418106_at	3.4	Hey2	hairy/enhancer-of-split related with YRPW motif 2	NM_013904
1438886_at	2.2	Heyl	hairy/enhancer-of-split related with YRPW motif-like	BB310549
Other receptors				
1448710_at	3.6	Cxcr4	chemokine (C-X-C motif) receptor 4	D87747
1419429_at	5.6	Cntfr	ciliary neurotrophic factor receptor	NM_016673
1444503_at	2.0	Gbas	EGF-like receptor	AW764297
1421118_a_at	2.3	Gpr56	G protein-coupled receptor 56	NM_018882
1420538_at	43.9	Gprc5d	G protein-coupled receptor C5D	NM_053118
1450157_a_at	2.1	Hmmr	hyaluronan mediated motility receptor (RHAMM)	NM_013552
1435393_at	4.3	Mc1r	melanocortin 1 receptor	BB765942
1418175_at	2.9	Vdr	vitamin D receptor	BC006716
Other signalling pathway members and regulators				
1437800_at	2.3	Edaradd	EDAR associated death domain	BB160562
1439200_x_at	62.4	edr	erythroid differentiation regulator	BE686792

1451591_a_at	2.3	Efnb1	ephrin B1	BC006797
1432399_a_at	2.2	EphA1	Eph receptor A1	AK017662
1421929_at	3.2	Epha4	Eph receptor A4	BB706548
1455188_at	3.4	Ephb1	Eph receptor B1	BQ176283
1441375_at	3.1	Lrig1	Leucine-rich repeats and immunoglobulin-like domains 1	AU043080
1452287_at	3.4	Msi1h	RNA binding protein	BB414973
1417455_at	3.8	Tgfb3	transforming growth factor, beta 3	BC014690
1460642_at	2.3	Traf4	Tnf receptor associated factor 4	NM_009423
1429295_s_at	3.7	Trip13	thyroid hormone receptor interactor 13	AK010336

Other transcription factors

1437667_a_at	3.4	Bach2	BTB and CNC homology 2	AW553304
1428572_at	3.2	Basp1	brain abundant, membrane attached signal protein 1	AK011545
1457072_at	6.2	Bcl11a	B-cell CLL/lymphoma 11A	BF731393
1427819_at	2.5	Bcl2	B-cell CLL/lymphoma 2	BC027249
1424890_at	3.1	Bnc	basonuclin	U88064
1451417_at	5.9	Brca1	breast cancer 1	U31625
1436983_at	2.4	Crebbp	CREB-binding protein	BG069466
1437431_at	4.8	Cutl1	CCAAT displacement protein	BB032125
1448877_at	6.2	Dlx2	distal-less homeobox 2	NM_010054
1450475_at	7.5	Dlx3	distal-less homeobox 3	U79738
1443591_at	3.0	Dlx4	distal-less homeobox 4	BB827848
1436434_at	2.6	E2f2	Transcription factor E2F2	BG967674
1438887_a_at	3.2	Gcl	germ cell-less homolog (Drosophila)	BM239632
1451899_a_at	2.1	Gtf2ird1	general transcription factor II I repeat domain 1	AF343349
1452534_a_at	2.8	Hmgb2	high mobility group box 2	X67668
1416155_at	2.8	Hmgb3	high mobility group box 3	NM_008253
1425874_at	7.2	Hoxc13	homeo box C13	AF193796
1426298_at	3.5	Irx2	Iroquois related homeobox 2 (Drosophila)	AF295369
1419539_at	2.9	Irx4	Iroquois related homeobox 4 (Drosophila)	NM_018885
1422734_a_at	5.8	Myb	myeloblastosis oncogene	BC011513
1417656_at	2.5	Mybl2	myeloblastosis oncogene-like 2	NM_008652
1417155_at	8.1	Nmyc1	neuroblastoma myc-related oncogene 1	BC005453
1441030_at	2.4	Rai14	Retinoic Acid Induced 14	BB308974
1437486_at	3.7	Rai3	Retinoic Acid Induced 3	BG064659
1425565_at	2.1	Rest	RE1-silencing transcription factor	AW557564
1422864_at	3.2	Runx1	runt related transcription factor 1	NM_009821
1450191_a_at	2.4	Sox13	SRY-box containing gene 13	NM_011439
1419157_at	12.3	Sox4	SRY-box containing gene 4	BE952590
1423500_a_at	4.4	Sox5	SRY-box containing gene 5	AI528773
1427787_at	3.4	Sp6	trans-acting transcription factor 6	AA438081
1425779_a_at	2.4	Tbx1	T-box 1	AF326960
1427764_a_at	3.4	Tcfe2a	transcription factor E2a	D29919
1429488_at	2.6	Zdhhc21	zinc finger, DHHC domain containing 21	AK017682

TABLE 5.4

Genes suppressed more than 3 fold at Tg day 7

Affy ID	Fold Change	Gene name	Genebank
1422940_x_at	0.066 Serpinb4	serine/cysteine protease inhibitor, cladeB, member4	BB699605
1419537_at	0.127 Tcfec	transcription factor EC	NM_031198
1418672_at	0.189 Akr1c13	aldo-keto reductase family 1, member C13	NM_013778
1420942_s_at	0.198 Rgs5	regulator of G-protein signaling 5	BF585144
1450488_at	0.211 Ccl24	chemokine (C-C motif) ligand 24	AF281075
1452013_at	0.236 Atp10a	ATPase, class V, type 10A	AF156549
1421762_at	0.249 Kcnj5	K+ inwardly-rectifying channel, subfamilyJ, member5	NM_010605
1418939_at	0.250 Hlx	H2.0-like homeo box gene	NM_008250
1453588_at	0.250 Car3	carbonic anhydrase 3	BB213876
1415994_at	0.253 Cyp2e1	cytochrome P450, family 2e, polypeptide 1	NM_021282
1449547_at	0.259 Asb14	ankyrin repeat and SOCS box-containing protein 14	NM_080856
1421425_a_at	0.261 Dscr1l1	Down syndrome critical region gene 1-like 1	AB061524
1448775_at	0.271 Ifi203	interferon activated gene 203	NM_008328
1421551_s_at	0.276 Ifi202b	interferon activated gene 202B	NM_011940
1419473_a_at	0.277 Cck	cholecystokinin	NM_031161
1417275_at	0.284 Mal	myelin and lymphocyte differentiation protein	NM_010762
1435751_at	0.286 Abcc9	ATP-binding cassette, sub-family C, member 9	BG791642
1423439_at	0.293 Pck1	phosphoenolpyruvate carboxykinase 1, cytosolic	AW106963
1459737_s_at	0.298 Ttr	transthyretin	AA408768
1424649_a_at	0.298 Tm4sf3	transmembrane 4 superfamily member 3	BC025461
1448602_at	0.298 Pygm	muscle glycogen phosphorylase	NM_011224
1416007_at	0.303 Satb1	special AT-rich sequence binding protein 1	BG092481
1436201_x_at	0.304 Mbp	myelin basic protein	AV328388
1422582_at	0.310 Lep	leptin	U18812
1423253_at	0.313 Mpz	myelin protein zero	AI385618
1427306_at	0.324 Ryr1	ryanodine receptor 1, skeletal muscle	X83932
1438855_x_at	0.329 Tnfaip2	tumor necrosis factor, alpha-induced protein 2	BB233088
1450723_at	0.330 Isl1	ISL1 transcription factor, LIM/homeodomain (islet 1)	BQ176915

members of various known signalling pathways. I therefore analysed this category in more detail, and to generate a more accurate picture of the signalling pathways responding to β-catenin activation I considered all signalling-related genes and transcription factors induced more than 2 fold, listed in Table 5.3. As expected, several members of the Wnt pathway were induced, reflecting the activation of the pathway.

Other signalling pathways with a known role in hair follicle development and maintenance were represented. The Hedgehog pathway was the most upregulated, but the BMP inhibitor Bambi (Sekiya et al., 2004) and the BMP effectors Msx1 and 2 (Kulessa et al., 2000) were also induced, and so were members of the Notch pathway (Crowe et al., 1998; Viallet et al., 1998), the vitamin D receptor (Li et al., 1997), the homeobox gene HoxC13 (Godwin and Capecchi, 1998), and Edaradd, the effector of the TNF family member ectodysplasin, also involved in the early steps of hair follicle development (Headon and Overbeek, 1999; Srivastava et al., 1997).

5.2. Sonic Hedgehog signalling is necessary downstream of β-catenin to induce ectopic hair follicles

Members of the Hedgehog signalling cascade were among the most highly induced genes. In addition to Shh and Ptch, Ptch2 (6.6 fold), Gli1 (6.7 fold) and Gli2 (6 fold) were upregulated. In addition, N-Myc, a target of Shh (Mill et al., 2005; Oliver et al., 2003) was upregulated 8 fold at 7 days. I had previously observed increased expression of Shh and Ptc following β-catenin activation in the epidermis (Gat et al., 1998; Lo Celso et al., 2004). Since Shh drives proliferation during normal hair germ development and hair follicle anagen (Callahan and Oro, 2001) and β-catenin activation resulted in local increases in proliferation (Lo Celso et al., 2004), I investigated whether Hedgehog signalling was required for ectopic HF formation.

I treated K14ΔNβ-cateninER transgenic mice with a single 1mg dose of 4OHT, sufficient to trigger hair morphogenesis, and daily applications of the Hedgehog antagonist cyclopamine, which inhibits Hedgehog signalling by binding to Smoothened

(van den Brink et al., 2004) for one week (Fig. 5.2). Neither cyclopamine alone nor in combination with 4OHT induced any visible alteration in wild type mice. Examination of skin by conventional histology showed that cyclopamine blocked the induction of anagen and ectopic HF formation in D2 mice, (Fig. 5.2B,C). In D2 mice treated with 4OHT only all follicles were in anagen and showed the first sings of ectopic hair follicle formation. Only few follicles in some double treated transgenic mice entered anagen, and even though I observed some degree of variation from mouse to mouse in the number of anagen follicles (Fig. 5.2C), I could never observe ectopic hair germs.

In D4 double treated mice the β-catenin phenotype was not completely abolished, but instead reduced, as illustrated very clearly in whole mount preparations from tail epidermis (Silva-Vargas et al., 2005). The thickening of the existing follicles and the size of the ectopic ones appeared reduced (Fig. 5.2D,E), so that overall both classes of follicles presented a better morphology. The picture observed was thus very similar to 4OHT treated D2 mice, indicating that impairment of Hedgehog signalling was another way to titrate the effects of β-catenin activation. By looking at the incorporation of BrdU I could confirm that cyclopamine reduced the number of proliferating cells in D4 epidermis (Fig. 5.2E). I therefore concluded that Hh signalling acts downstream of β-catenin and is responsible for the proliferative component of hair morphogenesis.

5.3. Notch signalling activation is a critical step in β-catenin induced HF morphogenesis

Only the transcription factors Hey2 and HeyL represented the Notch pathway in the list of signalling related genes that I first generated, but when I specifically looked for other members of the cascade present on the arrays I found 9 Notch related probe sets showing an induction at Tg day 7 compared to Tg day 0 of at least 1.5 fold with a p value smaller than 0.05 (Table 5.5).

I checked the expression of Jagged1, the main Notch ligand expressed in adult mouse epidermis (Powell et al., 1998), in whole mount preparations of ΔNβ-cateninER

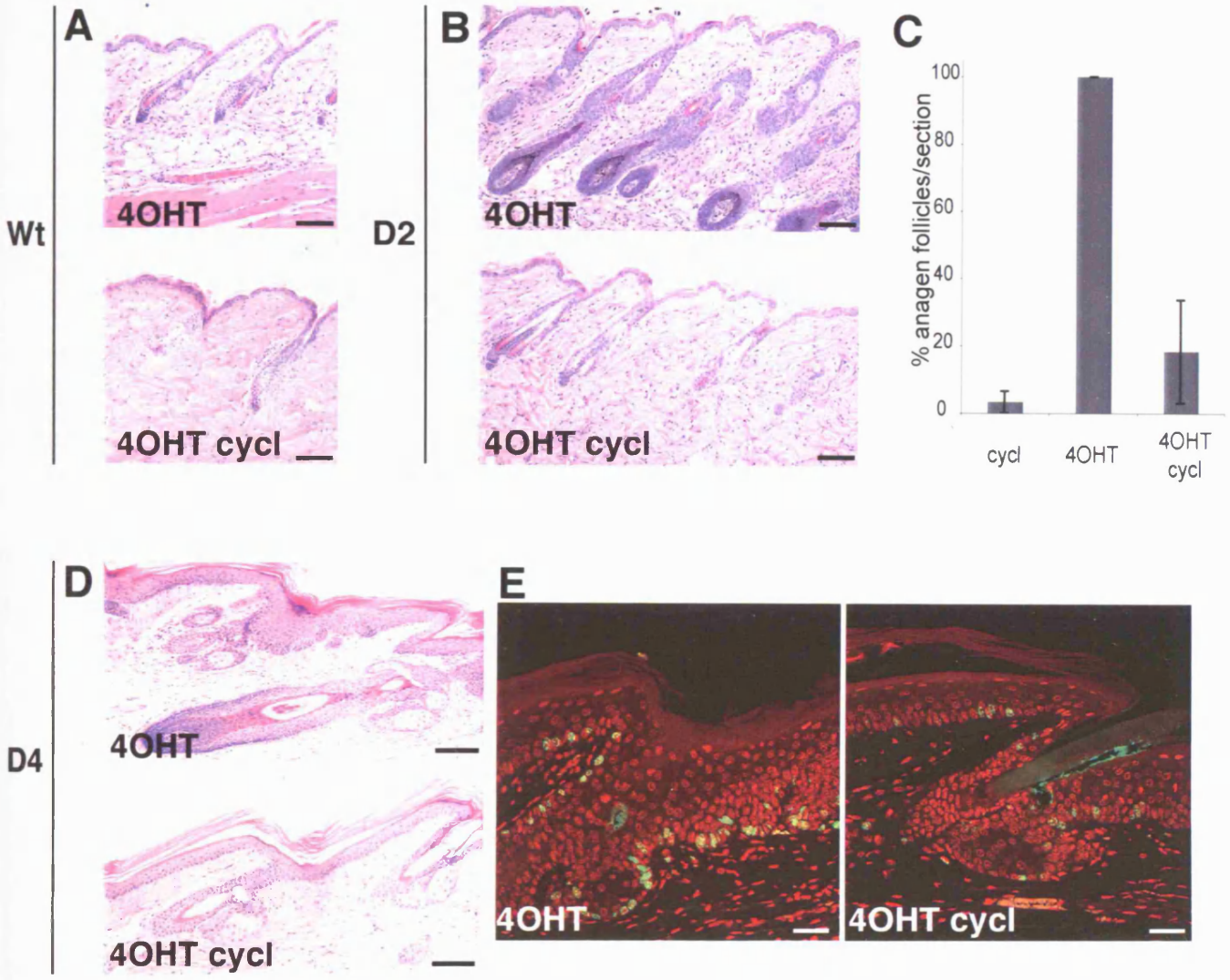

Figure 5.2. Hedgehog signalling is required for β-catenin induced hair follicle formation. Wild type (A), D2 (B,C) and D4 mice (D,E) were treated as indicated, either with 4OHT alone (4OHT) or with 4OHT and cyclopamine (4OHT cycl) for one week. (A,B) Sections of dorsal epidermis stained with hematoxylin and eosin. (C) 4OHT treatment reduced of about 80% the number of anagen follicles in D2 mice. (D,E) Sections of tail epidermis stained with hematoxylin and eosin (D) or anti-BrdU antibody (E, green fluorescence) to visualize proliferating cells. Red fluorescence is propidium iodide nuclear counterstaining. Scale bars: 100μm (A,B,D) and 50μm (E).

TABLE 5.5
Notch signalling induced probes at Tg day7 compared to Tg day0, with p value <0.05

Affy Probe ID	Fold Change		Gene name	Genebank
1456010_x_at	8.614	Hes5	hairy and enhancer of split 5 (Drosophila)	BB561515
1438886_at	3.3	HeyL	hairy/enhancer-of-split related with YRPW motif-like	BB310549
1423029_at	2.823	Hes2	hairy and enhancer of split 2 (Drosophila)	NM_008236
1418106_at	2.54	Hey2	hairy/enhancer-of-split related with YRPW motif 2	NM_013904
1419303_at	2.497	HeyL	hairy/enhancer-of-split related with YRPW motif-like	BG695100
1419302_at	2.415	HeyL	hairy/enhancer-of-split related with YRPW motif-like	BG695100
1421105_at	2.163	Jag1	jagged 1	AA880220
1421106_at	2.023	Jag1	jagged 1	AA880220
1418102_at	1.595	Hes1	hairy and enhancer of split 1 (Drosophila)	BC018375

transgenic tail skin treated with 4OHT for various length of time. In wild type epidermis Jagged1 is expressed in the hair follicle bulb, and from there a line of positive cells forms a characteristic streak on one side of the hair follicle reaching approximately the bulge region (Fig. 5.3A, courtesy of Dr. Soline Estrach). In ΔNβ-cateninER transgenic mice I observed positive staining for Jagged1 in the bulb of pre-existing anagen follicles and in all the ectopic ones depending on β-catenin activation (Fig.5.3B). Jagged1 was highly expressed in D2 tail epidermis following 3 weeks of 4OHT treatment (Fig. 5.3B, top left panel), but was almost completely lost 3 weeks after the end of the treatment, when the pre-existing follicles were in telogen and the ectopic ones had regressed (Fig. 5.3B, top right panel). The expression increased again with a second 4OHT treatment, reaching in two weeks levels similar to those observed after the first 3 weeks of treatment (Fig. 5.3B, bottom panels).

In order to better understand the role of Jagged1 in β-catenin induced hair follicle morphogenesis I analyzed triple transgenic mice, Jagged1$^{flx/flx}$ x K14CreER x K14ΔNβ-cateninER, generated by Dr. Soline Estrach in the laboratory (K14CreER: (Vasioukhin et al., 1999). The mice reached six weeks of age without experiencing any perturbation in either Notch or β-catenin signalling and at that point I applied 4OHT on their skin to activate ΔNβ-cateninER and CreER at the same time. I could therefore analyze the effect of β-catenin activation in the absence of Jagged1 induction. While ΔNβ-cateninER positive, CreER negative control mice displayed darkening of the skin and hair regrowth, at the end of three weeks of treatment the skin of the triple transgenic mice remained thin and pink like that of wild type ΔNβ-cateninER negative CreER negative control littermates.

Histological analysis of back skin from the three groups of mice confirmed my first observations. While in ΔNβ-cateninER positive CreER negative back skin the follicles were in anagen and presented several epithelial outgrowths, triple transgenic skin was indistinguishable from wild type: the follicles remained in telogen and there was no sign of ectopic hair follicle formation (Fig. 5.4A,C,E). In tail epidermis whole

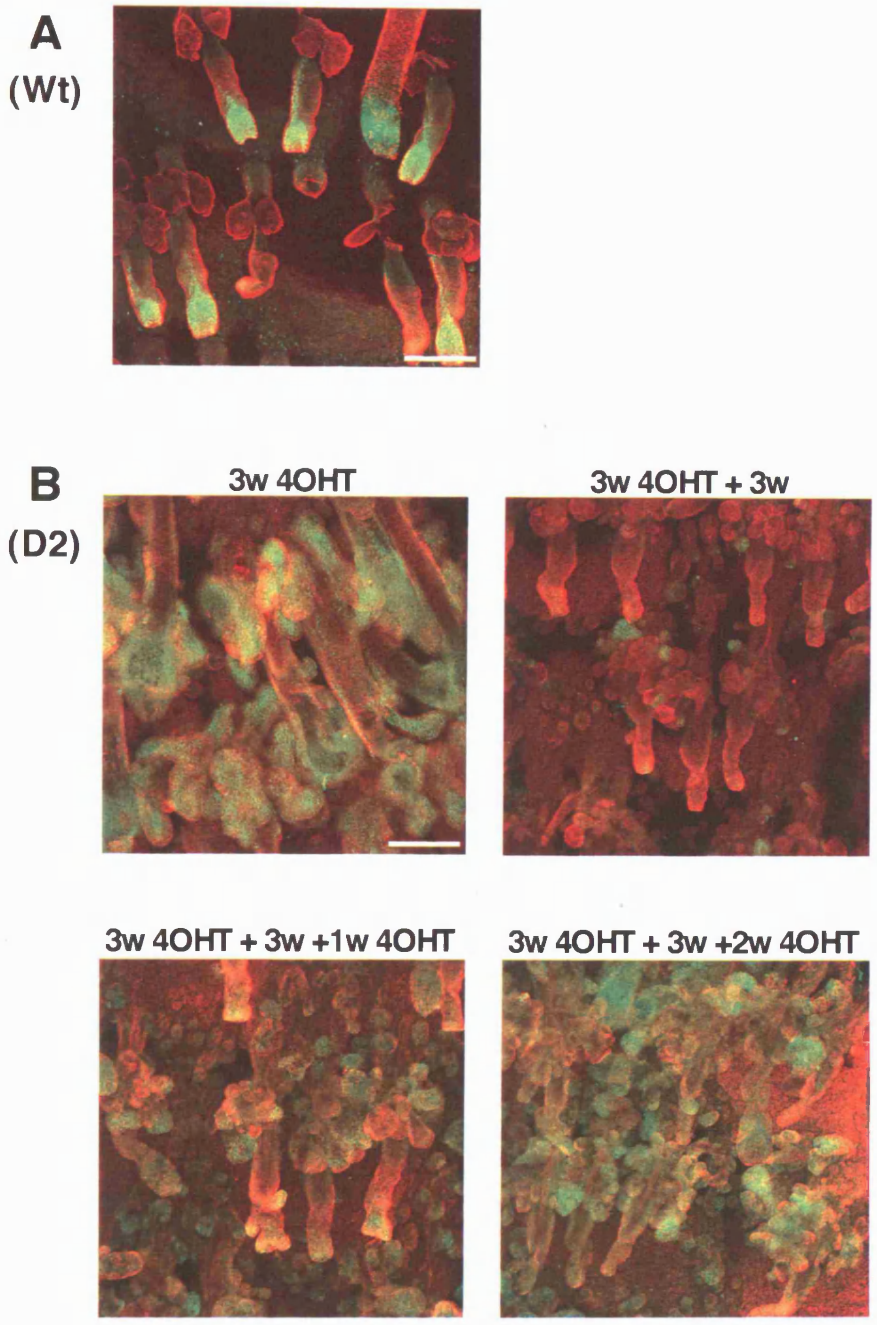

Figure 5.3. Jagged1 expression is indicative of active β-catenin signalling. Tail epidermis whole mount preparations immunostained with anti-Jagged1 (green fluorescence) and anti-keratin 14 (red fluorescence) antibodies. (A) Wild type epidermis. (B) D2 transgenic epidermis treated with 4OHT for 3 weeks (3w 4OHT), left untreated for the following three weeks (3w 4OHT + 3w), and treated again for one (3w 4OHT + 3w + 1w 4OHT) or two weeks (3w 4OHT + 3w + 1w 4OHT). Panel A is a gift of Dr. Soline Estrach. Scale bars: 100μm.

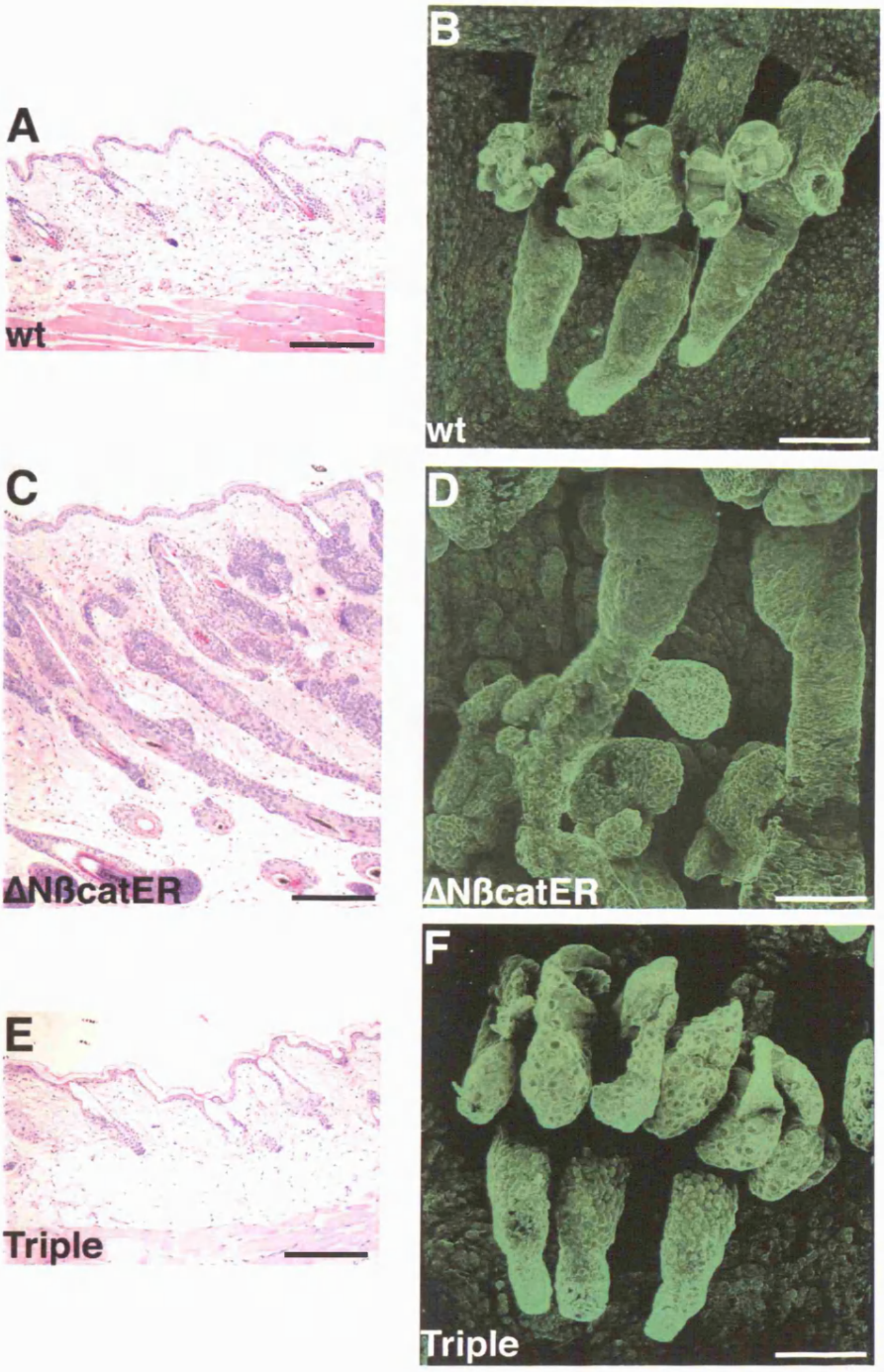

Figure 5.4. Jagged1 deletion blocks β-catenin induced ectopic hair follicle formation. Back skin histological sections (A,C,E) and whole mount tail preparations immunostained with anti-keratin 14 antibody (B,D,F). Samples were collected from wild type (A,B), ΔNβ-cateninER single transgenic (C,D) and ΔNβ-cateninER CreER Jagged1$^{fl/fl}$ triple transgenic mice (E,F) following three weeks of 4OHT treatment. Scale bars: 100μm.

mount preparations Jagged1 deletion abolished β-catenin driven hair follicle formation in the interfollicular epidermis (Fig. 5.4B,D,F).

In parallel experiments I could analyze the effects of β-catenin activation when Notch signalling was inhibited. I treated back skin of ΔNβ-cateninER transgenic mice with both 4OHT and DAPT to activate β-catenin and inhibit γ-secretase, the enzyme responsible for Notch cleavage and activation (Cheng et al., 2003). Similarly to the conditional deletion of Jagged1, DAPT treatment reduced the effects of β-catenin activation (Fig. 5.4A,B). The follicles of mice that received both treatments for two weeks entered anagen, but were not as elongated as the ones from mice treated with 4OHT only and ectopic HF induction was inhibited.

A model of Notch activation in the epidermis was also available in the laboratory. Dr Carrie Ambler had generated K14N$^{ICD\Delta OP}$ER transgenic mice, carrying a truncated form of the intracellular domain of Notch fused to the ligand binding domain of the oestrogen receptor. 4OHT treatment leads to N$^{ICD\Delta OP}$ER activation and Notch signalling in the basal cells of IFE, SG and ORS. When I applied 4OHT on the skin of double transgenic ΔNβ-cateninER x N$^{ICD\Delta OP}$ER mice that Dr. Ambler had generated I observed a more dramatic effect than in single ΔNβ-cateninER transgenic mice. After two weeks of treatment the hair follicles of double transgenic back skin were in full anagen, like those of ΔNβ-cateninER, but the process of de novo hair follicle morphogenesis appeared more advanced, with many ectopic follicles already presenting a dermal papilla, inner root sheath and hair shaft (arrow in Fig. 5.5C). Activation of Notch signalling appeared therefore to potentiate the effects of β-catenin activation by promoting ectopic HF differentiation. The combined results obtained with Notch gain and loss of function suggested that Notch signalling is a critical step in β-catenin induced HF morphogenesis.

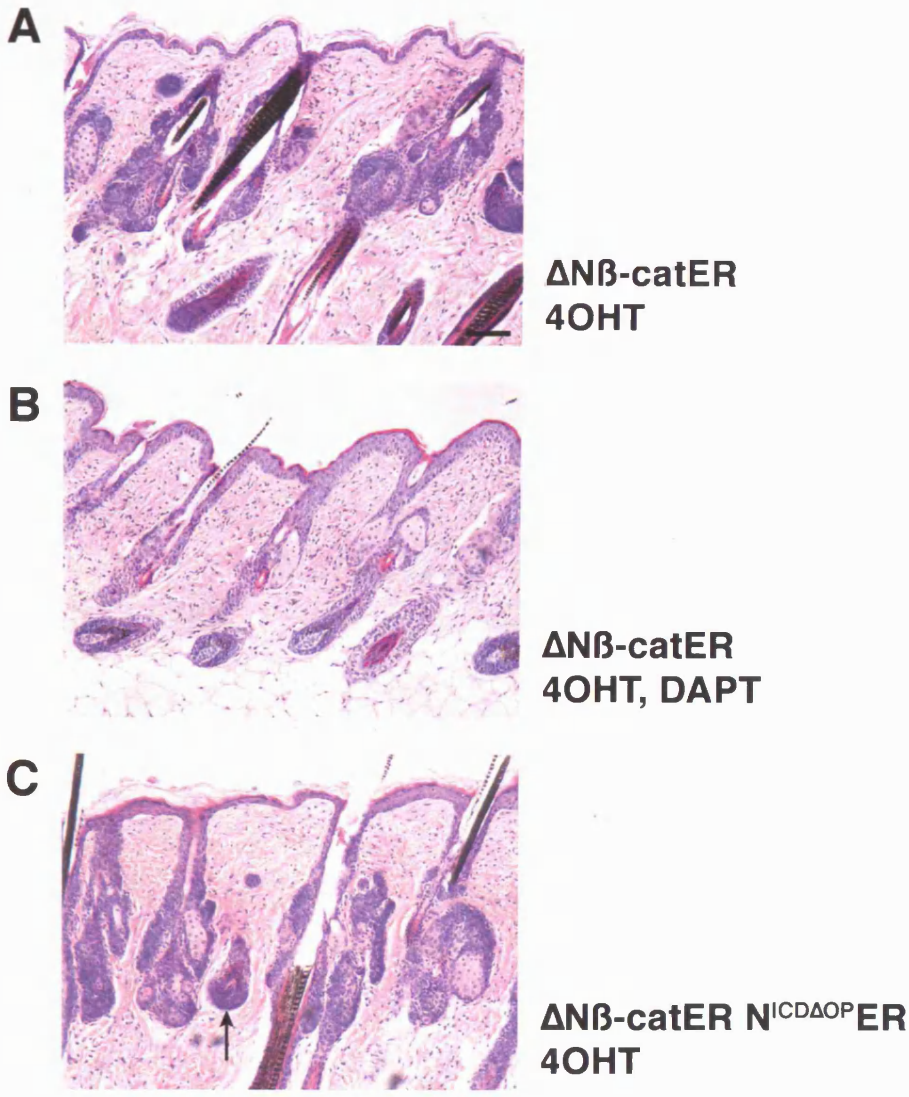

Figure 5.5. Notch inhibition impairs and Notch activation enhances β-catenin induced ectopic hair follicle formation. Histological sections of back skin from ΔNß-cateninER transgenic (A,B) or ΔNß-cateninER $N^{ICD\Delta OP}$ER double transgenic mice (C) treated for two weeks with 4OHT alone (A,C) or 4OHT and γ-secretase inhibitor DAPT (B). Arrow in C indicates ectopic hair follicle with dermal papilla, inner root sheath and hair shaft. Scale bar: 100μm.

5.4. Vitamin D receptor contributes to β-catenin induced HF formation in the absence of vitamin D

Another β-catenin target gene with a known role in hair follicle maintenance was the vitamin D receptor (VDR), induced 2.9 fold. VDR knock out mice develop alopecia that is not rescued by calcium enriched (Li et al., 1998; Li et al., 1997) diet and *in vitro* studies have shown a reciprocally inhibitory interaction between β-catenin and VDR (Palmer et al 01). Vitamin D has been reported to inhibit not only transcriptional activity but also nuclear localization of β-catenin (Palmer et al., 2001).

To test whether vitamin D could antagonize β-catenin activation in the epidermis, I applied both 4OHT and the vitamin D analog EB1089 (Milliken et al., 2005) on the tail of D4 transgenic mice. The dose of vitamin D analog was toxic for the animals and the experiment had to be terminated after only five days of treatment. However, even at this early time point the effect of EB1089 on K14ΔNβ-cateninER epidermis was evident (Fig. 5.6). I could not observe any major alteration in tail skin from wild type and transgenic mice treated with the analog alone. As expected, 4OHT treated D4 skin had thickened follicles with sebaceous glands surrounded by proliferating cells and many ectopic hair germs originating from the interfollicular epidermis. Strikingly, all these effects were abolished by the vitamin D analog: the IFE-dermal boundary remained flat and the sebaceous glands appeared normal, indicating that β-catenin probably needs to interact with ligand-free VDR in order to drive HF morphogenesis.

5.5. Myc activation blocks the effects of β-catenin signalling in mouse epidermis

c-Myc is a known target of β-catenin (He et al., 1998) but the microarray analysis did not show any change in its expression in ΔNβ-cateninER mice in the first seven days of 4OHT treatment. In the K14ΔNβ-cateninER transgenic mice ectopic hair differentiation

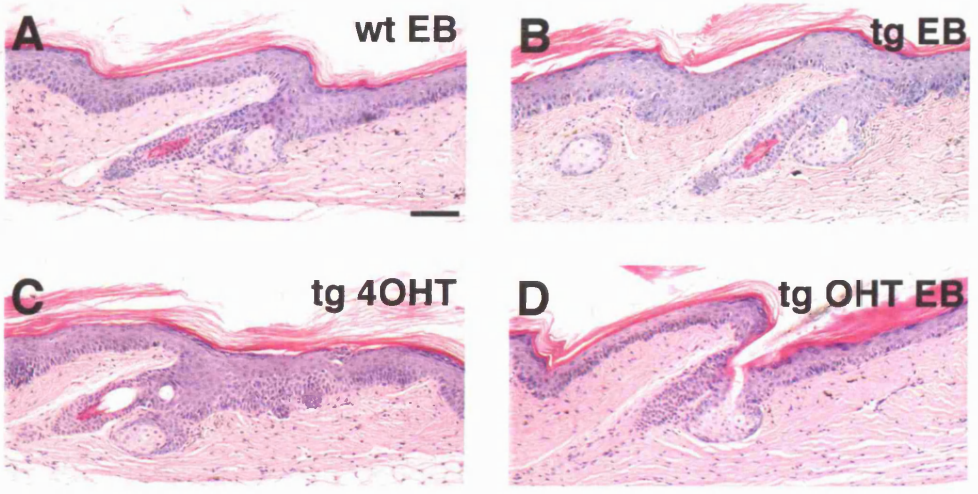

Figure 5.6. The vitamin D analog EB1089 antagonizes β-catenin effects. Histological sections of tail skin from wild type (A) and ΔNβ-cateninER (line D4) transgenic mice (B-D) treated with vitamin D analog EB1089 (A,B) or 4OHT (C) or both (D). Scale bar: 100μm.

is induced at the expenses of interfollicular and sebaceous differentiation. Moreover, in K14MycER mice activation of c-Myc by 4OHT treatment leads to hyperproliferative interfollicular epidermis and sebaceous glands, reduced HF differentiation and ectopic sebocyte differentiation in the interfollicular epidermis (Arnold and Watt, 2001; Braun et al., 2003). In order to better understand the relationship between β-catenin and c-Myc signalling in the epidermis I analyzed the consequences of their simultaneous activation in K14ΔNβ-cateninER K14MycER double transgenic mice that Dr. Kristin Braun had generated in the laboratory.

Histological analysis of tail skin from double and single Myc or β-catenin (line D4) transgenic mice treated with 4OHT for 5 days confirmed the contrasting role of the two genes. In ΔNβ-cateninER skin several ectopic hair germs protruded from the interfollicular epidermis and the number of sebocytes appeared already reduced, with several layers of proliferating cells surrounding the sebaceous glands (Fig. 5.7B). In contrast, in MycER skin the epidermal-dermal boundary was flat and the sebaceous glands appeared enlarged due to an increase in the size of all sebocytes, even at the periphery of the glands (Fig. 5.7C). Double transgenic skin presented a mixture of the alterations observed in the single transgenics, all clearly attenuated. The interfollicular epidermis remained flat and I could find only one or two ectopic follicles per section examined. The sebaceous glands in double transgenics presented an intermediate phenotype compared to the two single transgenics, usually presenting regions with enlarged sebocytes and regions with several layers of proliferating cells (Fig. 5.7D).

I confirmed the attenuation of the β-catenin phenotype by examining the expression of markers of hair and sebaceous differentiation. Keratin 17 expression, present not only in the pre-existing follicles but also in all the ectopic ones in ΔNβ-cateninER mice (Fig. 5.8A), was confined to the ORS in both MycER and double transgenic skin, where no positive cells appeared in the interfollicular epidermis (Fig. 5.8B,C). On the contrary, immunostaining for fatty acid synthase, which was lost at the periphery of ΔNβ-cateninER sebaceous glands (arrow in Fig. 5.8D), was present in the entire sebaceous glands of MycER and double transgenic mice (Fig. 5.8E,F).

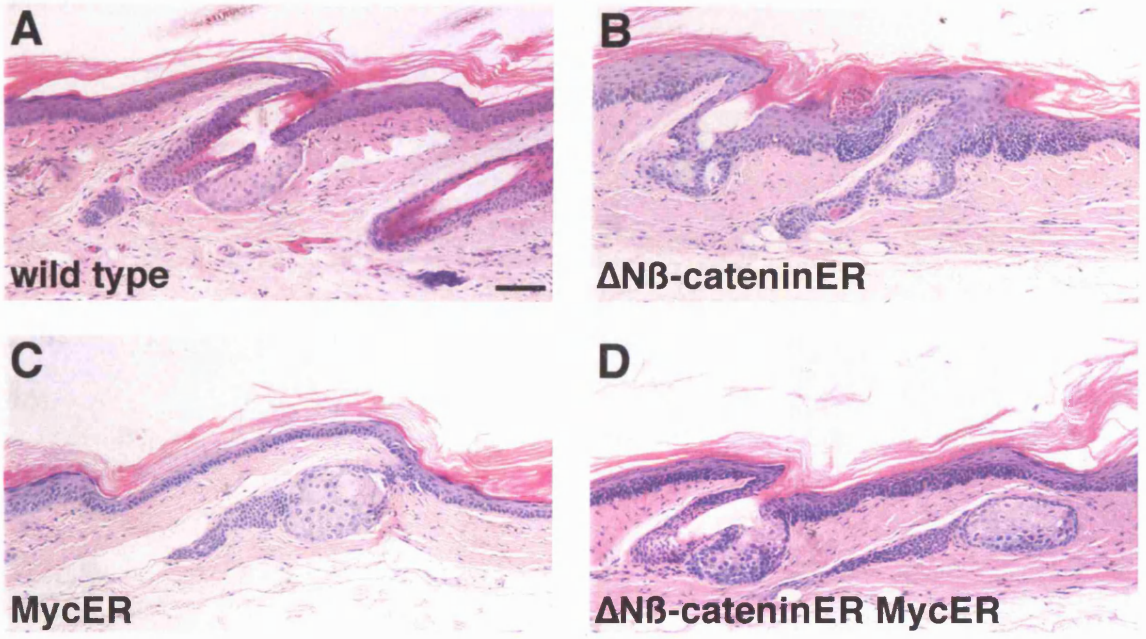

Figure 5.7. Myc activation blocks the effects of β-catenin signalling. Histological sections of tail skin from wild type (A), ΔNβ-cateninER (B), MycER (C) or ΔNβ–cateninER MycER double transgenic mice (D) treated with 4OHT for 5 days. Scale bar: 100μm.

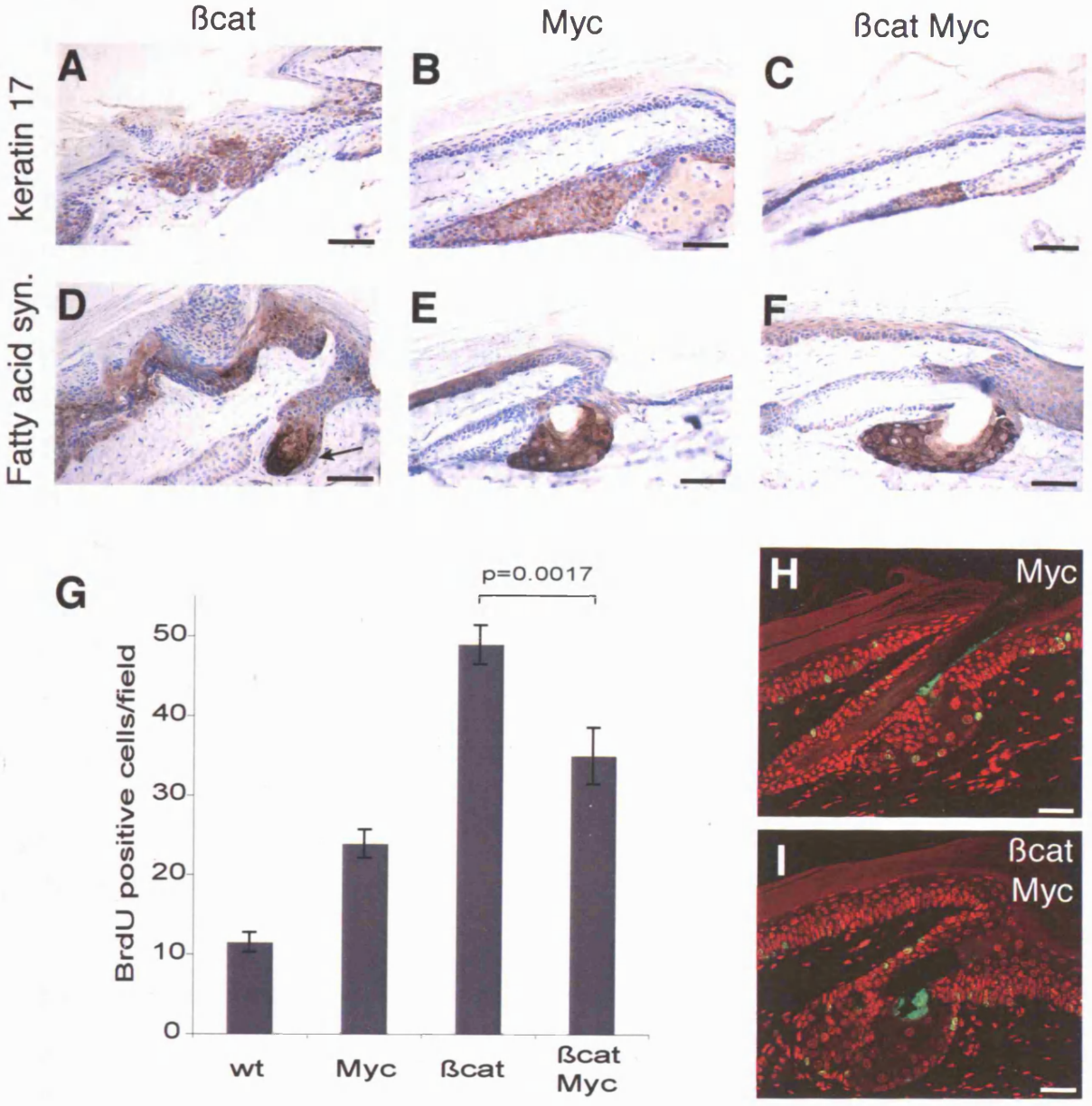

Figure 5.8. Effects of ß-catenin and Myc activation on lineage commitment and differentiation. (A-F) Sections of tail skin from ΔNß-cateninER (A,D), MycER (B,E) or ΔNß-cateninER MycER double transgenic mice (C,F) treated with 4OHT for 5 days and immunostained with anti-keratin 17 (A-C) or anti-fatty acid synthase (D-F) antibodies. Arrow in D indicates fatty acid synthase negative cells at the periphery of ΔNß-cateninER sebaceous glands. Blue is hematoxylin counterstaining. (G-I) Wild type (wt), MycER (Myc), ΔNß-cateninER (ßcat) and double transgenic (ßcat Myc) mice were injected with BrdU one hour before skin collection, tail skin sections were immunostained with anti-BrdU antibody (green fluorescence) and the number of positive cells per microscopic field (25x) was counted. Red fluorescence in H,I is propidium iodide nuclear counterstaining. Scale bars: 100μm (A-F), 50 μm (H,I).

As both β-catenin and c-Myc stimulate proliferation (Chapter 3 and (Arnold and Watt, 2001), but Myc appeared to suppress β-catenin mediated ectopic hair follicle formation, I assessed the levels of proliferation in single and double transgenic epidermis by counting the number of cells that had been labelled with a single BrdU injection one hour before skin collection (Fig. 5.8G). I observed the highest number of positive cells per microscopic field in sections from ΔNβ-cateninER transgenic mice, concentrated at each site of *de novo* hair follicle formation and in the bulb of anagen follicles (Fig. 5.8G and for staining appearance cfr Fig. 5.12 and Fig. 5.2F). Also in MycER skin the number of proliferating cells was higher than in wild type, but in this case BrdU labelled cells were more evenly distributed along the whole epidermis and sometimes found even in the central region of sebaceous glands, where usually only terminally differentiated sebocytes would be found (Fig. 5.8H). Double c-Myc and β-catenin activation resulted in a partial but significant ($p = 0.0017$) reduction in proliferation compared to β-catenin activation alone (Fig. 5.8G). As ectopic hair germs were not developing anymore, BrdU positive cells were not clustered, but instead evenly distributed along IFE, ORS and SG periphery (Fig. 5.8I).

5.6. Discussion

β-catenin activation in adult mouse epidermis triggers a complex morphogenetic process that leads to the formation of ectopic hair follicles from IFE, ORS and SG. Analysis of β-catenin induced genes in the early steps of this process allowed me to investigate the mechanisms that result in the reprogramming of epidermal progenitor cells to undergo differentiation along hair lineages. There was no dramatic change in the gene expression profile of ΔNβ-cateninER transgenic skin in the first day following 4OHT application. However, a high number of transcription factors and members of signalling cascades were induced after 7 days of treatment, even though there were only a few early signs of the β-catenin phenotype at this stage. The results of the β-catenin array experiment reflect the complexity of both anagen and ectopic hair follicle induction and suggest that a cascade of signalling events may be responsible for *de novo* hair follicle morphogenesis.

The fact that several induced signalling pathways (e.g. Shh, Notch) are known to regulate HF morphogenesis (Millar, 2002) confirms that *de novo* hair follicle morphogenesis in the ΔNβ-cateninER transgenic mice recapitulates the same processes that take place during embryonic development. Gene expression profiling of the different phases of the hair cycle has highlighted many genes that also appeared in my arrays (Lin et al., 2004), suggesting that probably the same pathways and transcription factors regulate HF induction, anagen initiation and lineage conversion.

The upregulation of two classes of Wnt inhibitors, Wif1 and Sfrp1 extracellular (Kawano and Kypta, 2003) and Gas2 and calpain8 intracellular (Benetti et al., 2005) probably reflected an attempt of the cells to downregulate β-catenin signalling. Induction of the Hedgehog inhibitor Hip could explain why, despite the activation of Hedgehog signalling, the ΔNβ-cateninER transgenic mice never developed the tumours that result from activating mutations in the Hedgehog pathway (Chapter 3 and Callahan and Oro, 2001; Oro and Scott, 1997). Wnt and Hedgehog inhibitors probably have a role in shaping the response to β-catenin activation, similarly to the combination of HF inducers and inhibitors regulates hair germ formation during embryonic development (Millar, 2002).

β-catenin activation increased the expression of many cell cycle, metabolism and DNA related genes, reflecting the increase in proliferation that I observed in the epidermis (Chapter 3). The DNA-related genes were either histones or factors involved in the repair of DNA damage, a cellular function recently associated with maintenance of stem cell integrity (Park and Gerson, 2005). β-catenin has been associated with stem cell self-renewal in many tissues (Chapter 4 and (Staal and Clevers, 2005) and some of the genes I have identified could therefore represent early steps of a common stem cell response to β-catenin activation. In agreement with this, some known stem cell niche components, such as tenascin C or S100 (Tumbar et al., 2004) were induced in the microarray.

During embryonic development there is a complex interplay between Hedgehog and Wnt signalling (Taipale and Beachy, 2001) and inappropriate activation of either

pathway is associated with a range of epidermal cancers in humans and mice (Gat et al., 1998; Chan et al., 1999; Callahan and Oro, 2001; Niemann et al., 2002; Lo Celso et al., 2004) Shh signalling was upregulated in response to β-catenin activation in ΔNβ-cateninER epidermis, and inhibition of Shh with cyclopamine reduced β-catenin induced HF formation in D2 and D4 transgenic lines. In the absence of cyclopamine, 4OHT induced HF morphogenesis progressed further in D2 mice than in D4 mice. Moderate levels of β-catenin signalling in D2 epidermis influence lineage choice but still lead to a very precise morphogenetic program, while the higher levels in D4 epidermis result in more generalized proliferation. Ectopic hair formation in D4 epidermis, even though readily initiated, does not proceed much further than the hair germ step (Cfr Chapter 3 and 4). The ability of cyclopamine to convert the D4 to the D2 phenotype suggests that the D4 phenotype results from Hedgehog induced proliferation being too extensive to allow proper morphogenesis. Hedgehog antagonists would therefore be useful in the treatment of epidermal tumours in which either Wnt or Hedgehog signalling is activated (Reya et al., 2001; Taipale and Beachy, 2001 Niemann, 2002 #17).

The Notch pathway is another signalling cascade involved in many embryonic developmental processes and also in hair follicle maintenance (Morrison et al., 2000; Vauclair et al., 2005). Jagged1 and Hes and Hey genes were induced by β-catenin activation and impairment of Notch signalling inhibited ectopic hair follicle formation. Simultaneous activation of β-catenin and Notch accelerated ectopic hair follicle development, indicating that Notch signalling contributes to a more prompt response to β-catenin activation. The number of HF arising from IFE did not increase, indicating that some other mechanisms must regulate the number and spacing of β-catenin induced follicles. While Shh appears to be responsible for the proliferative component of ectopic hair follicle formation, Notch signalling is probably activated in parallel to mediate the differentiation of the growing follicles.

The interplay between β-catenin and vitamin D signalling in ectopic hair follicle induction is harder to pinpoint. VDR deletion does not impair embryonic hair follicle development but determines progressive alopecia in the adult mice (Li et al., 1997). The induction of VDR in the β-catenin arrays probably reflects the ability of β-catenin to

interact with VDR and other nuclear receptors to regulate transcription in the absence of their ligands (Mulholland et al., 2005). Vitamin D sequesters VDR from β-catenin and antagonizes the nuclear localization of β-catenin in colon carcinoma cells (Palmer et al., 2001). The reduction in the ΔNβ-cateninER phenotype in mice treated with 4OHT and the vitamin D analog EB1098 suggests that this could be the case also in epidermis.

Vitamin D analogs inhibit the progression of colon (Huerta et al., 2002) and mammary tumours (Milliken et al 2005) and the proliferation of prostate cancer cells (Peleg et al., 2005). It will be interesting to compare the effect of EB1098 and cyclopamine treatment in whole mount preparations the see whether in both cases the D4 phenotype reverts to D2. If so, both VDR and Shh may mediate the proliferative effect of β-catenin.

An even more complex relationship is between the two oncogenes β-catenin and c-Myc. Reported as a β-catenin target (He et al., 1998), Myc was not induced in the β-catenin array experiment. N-Myc was up-regulated, but this could be a consequence of Shh signalling activation (Mill et al., 2005). The gene expression profile of mouse epidermis following β-catenin activation was extremely different from that following Myc activation, analyzed in a different study in the laboratory (Frye et al., 2003), and reflected some of the phenotypic differences between K14MycER and K14ΔNβ-cateninER mice. The consequences of Myc activation are irreversible (Arnold and Watt, 2001). On the contrary, β-catenin effects eventually regress on withdrawal of 4OHT (Chapter 4). Myc is associated with exit from the stem cell compartment (Gandarillas and Watt, 1997; Murphy et al., 2005), while β-catenin is associated with stem cell self-renewal (Zhu and Watt, 1999) and the induction of complex developmental processes (Staal and Clevers, 2005). The reduction of β-catenin effects in ΔNβ-cateninER MycER double transgenic mice suggests that Myc could be prematurely blocking the morphogenetic program induced by β-catenin. For example, Myc impairs cell migration (Frye et al., 2003), which is an important component in both hair germ growth and anagen initiation (Millar, 2002; Oshima et al., 2001).

The response to 4OHT treatment in ΔNβ-cateninER transgenic mice was extremely reproducible (see Chapter 3 and Chapter 4). The experiments that I performed are an example of how β-catenin dependent ectopic hair follicle formation can be used as a

simple biological assay to analyze the crosstalk between β-catenin and other signalling pathways and its role in the regulation of hair follicle morphogenesis and cycling.

Chapter 6. Lineage analysis on human cultured epidermal cells

In the previous chapters I described how in the K14ΔNβ-cateninER transgenic mice activation of β-catenin leads to lineage conversion of epidermal progenitor cells to form ectopic hair follicles at the expense of sebaceous and interfollicular epidermal differentiation. Conversely, c-Myc (Myc) overexpression in the basal layer of the epidermis promotes ectopic sebaceous differentiation in IFE and HF (Arnold and Watt, 2001; Braun et al., 2003). In this chapter I have explored whether it is possible to develop a model of lineage selection in cultured keratinocytes, which would facilitate investigation of lineage selection mechanisms at the single cell level.

6.1 Markers of hair follicle differentiation

I examined whether two markers of HF progenitors, keratin 17 and CDP (Chapter 3, Ellis et al., 2001; McGowan and Coulombe, 1998) were expressed in cultured IFE keratinocytes. The anti-keratin 17 and anti-CDP antibodies that I previously used as markers of hair differentiation on mouse sections crossreacted with the human antigens. On scalp sections I observed keratin 17 expression along the entire ORS, although I also obtained positive keratin 17 staining in the sebaceous glands (Fig. 6.1A). I detected keratin 17 expression also in cultured keratinocytes: small colonies of proliferating cells stained positive (Fig. 6.1B), confluent sheets, negative (Fig. 6.1C). Keratin 17 expression is therefore indicative of the proliferative status rather than the differentiation of cultured keratinocytes. This is not surprising, because expression of keratin 17 has been described in hyperproliferative epidermis (Mazzalupo et al., 2003).

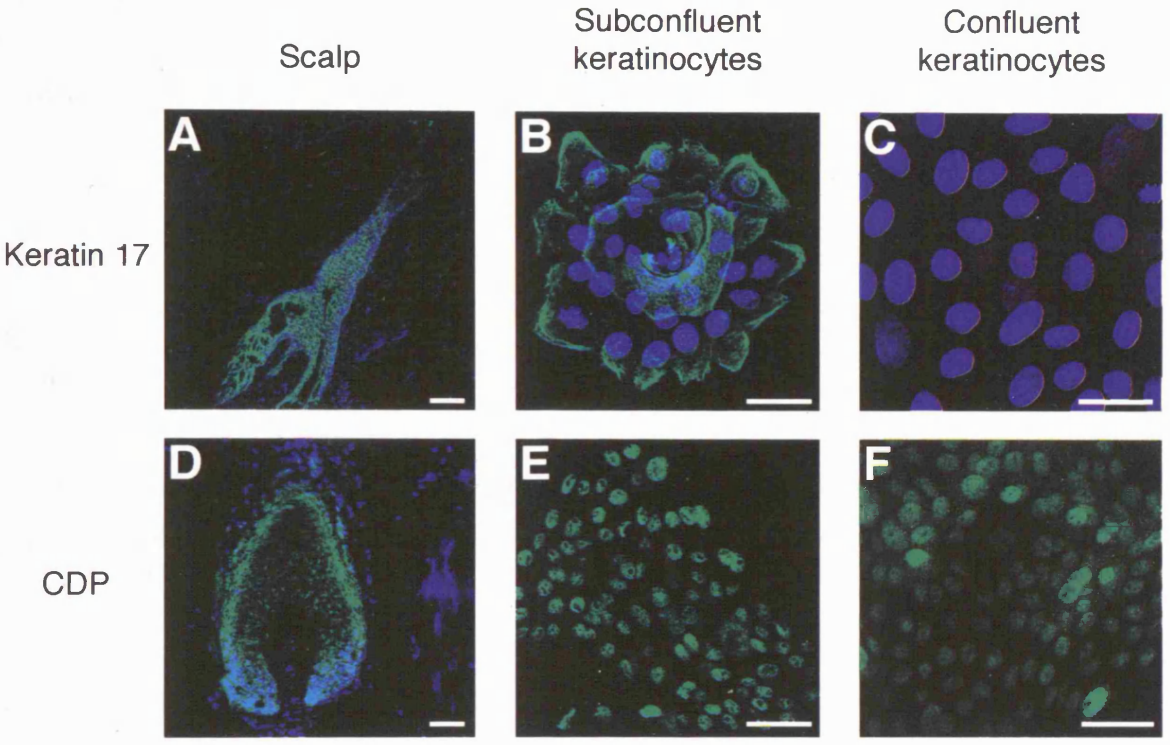

Figure 6.1. Markers of hair follicle differentiation. Human scalp sections (A,D) and primary subconfluent (B,E) and confluent (C,F) keratinocytes cultures were immunostained with anti-keratin 17 (A-C) and anti-CDP (D-F) antibodies. Blue fluorescence is DAPI nuclear counterstain. Scale bars: 100μm(A), 50μm (B-F)

CDP staining on scalp sections was restricted to the hair follicle bulb and companion layer (Fig. 6.1D, (Ellis et al., 2001). Also cultured keratinocytes stained positive, with higher levels of CDP expression in subconfluent cells and slightly lower levels in confluent cultures (Fig. 6.1E,F). This result ruled out CDP as HF lineage marker in culture. Again, this was not unexpected, because of recent studies indicating a role for CDP downstream of ras in proliferating cells (Michl et al., 2005).

6.2 Markers of sebocyte differentiation

The difficulties in the identification of hair lineage markers suitable for *in vitro* experiments, coupled to the intrinsic weakness of two-dimensional cultures for the analysis of hair follicle differentiation, prompted me to focus my attention on sebaceous differentiation.

The main product of the sebaceous glands is sebum, which is a mixture of lipids and cellular debris (Rowden, 1968). As a consequence, a very simple way to highlight sebocytes in skin sections is to use lipophylic dies such as Oil Red O or Nile Red (Fig. 6.2A, (Catalano and Lillie, 1975; Mullor et al., 2001). While useful and reliable on sections, these dyes would not allow the distinction between interfollicular keratinocytes and sebocytes *in vitro*, as also the keratinocytes produce high amounts of lipid droplets that are incorporated in the cornified envelope (Candi et al., 2005).

The enzyme fatty acid synthase, involved in the synthesis of long chain fatty acids, is selectively expressed in the sebaceous glands (Kusakabe et al., 2000), and with the same antibody that I previously used on mouse skin sections I could visualize sebaceous glands also in human scalp sections (Fig. 6.2B). The staining was restricted to the glands and did not overlap with involucrin, a marker of interfollicular differentiation that, together with cornifin, is expressed also in the hair follicle infundibulum and sebaceous gland duct (Fig. 6.2E,F). However, the same antibody positively stained cultured keratinocytes. I did not establish whether this reflected cross-reactivity with

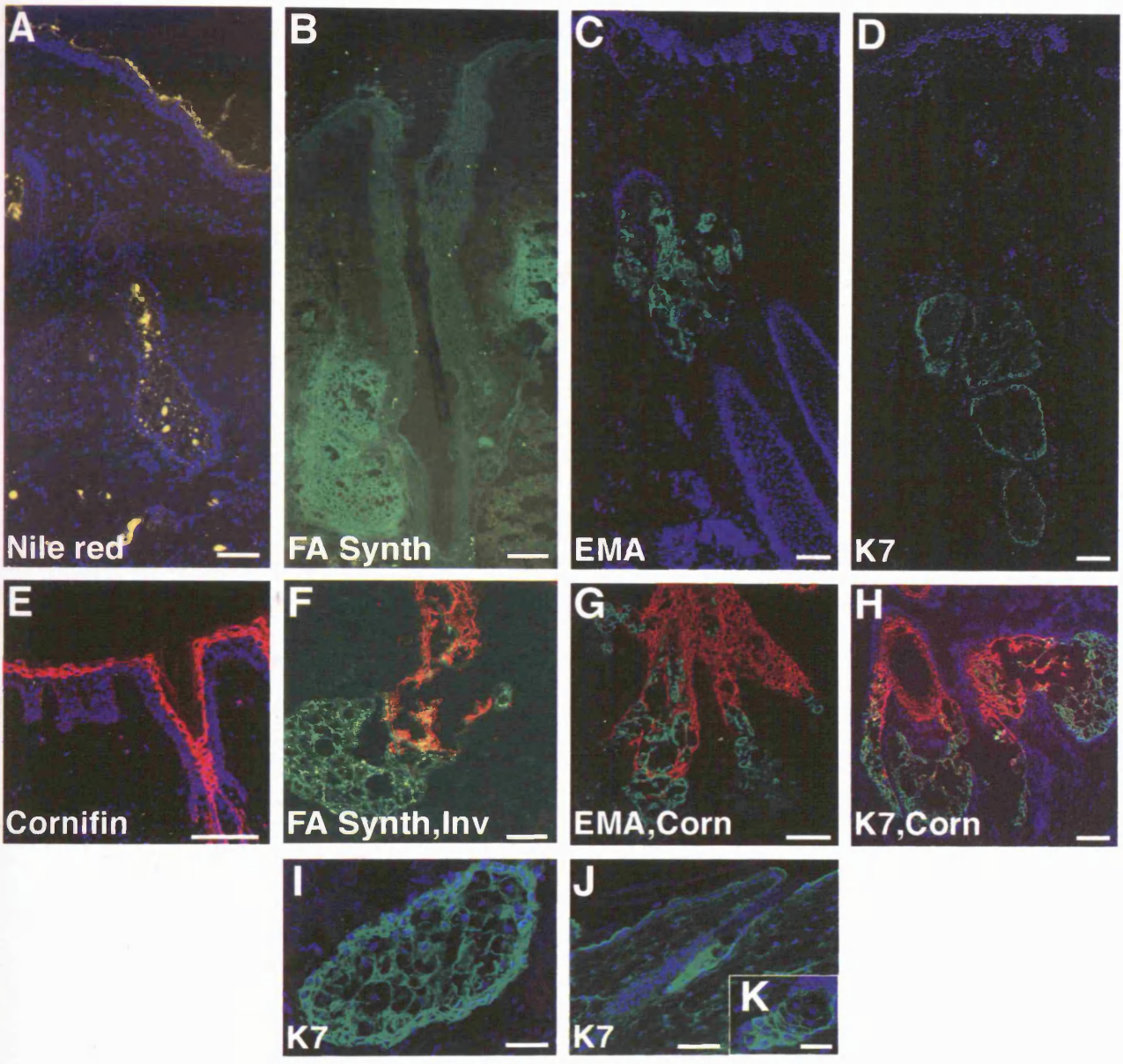

Figure 6.2. Markers of sebaceous differentiation. (A-E) Scalp sections were stained using nile red (A) or antibodies against fatty acid synthase (B), EMA (C), keratin 7 (D) or cornifin (E). (F-H) Scalp sections were double labelled with anti-fatty acid synthase (F), anti-EMA (G) or anti keratin 7 (H) antibodies (green fluorescence) and anti-involucrin (F) or anti-cornifin (G,H) antibodies (red fluorescence). (I-K) Anti-keratin 7 antibody labelled the sebaceous glands in both human scalp (I) and mouse skin (J,K). Blue fluorescence in A,C,D,E,H-K is DAPI nuclear counterstain. Scale bars: 100μm (A-H), 50μm(I,J), 25μm(K).

another antigen or whether fatty acid synthase is produced in culture as a result of high lipid metabolism necessary for membrane synthesis in proliferating cells.

Epithelial membrane antigen (EMA) is a highly glycosylated protein expressed in sebaceous glands but also secreted in the milk (Latham et al., 1989). Several antibodies are available against the milk isoform and are routinely used for the histopathological classification of mammary tumours (Peat et al., 1992). I obtained the best sebaceous gland staining with the E29 antibody (Fig. 6.2C). The staining was restricted to the glands and only marginally overlapped with cornifin (Fig. 6.2E,G). Only few basal cultured keratinocytes stained positive with this antibody, however none of the anti-EMA antibodies tested cross-reacted with mouse sebaceous glands.

Sebocytes share with all other basal keratinocytes the expression of keratin 14 (Byrne et al., 1994), but they selectively express keratin 7. I used the LH1K antibody, raised against the human isoform of keratin 7, to visualize sebaceous glands in human scalp (Fig. 6.2D,I) and confirm the net separation between keratin 7 and cornifin positive cells in the sebaceous gland ductel region (Fig. 6.3H). Even though in mouse epidermis expression of keratin 7 visualized using a mouse specific antibody is described in the hair follicle inner root sheath, the LH1K antibody selectively labelled mouse sebaceous glands (Fig. 6.2J,K).

6.3 SZ95 cells are a model of human sebaceous differentiation

As human primary sebocytes are difficult to isolate and keep in culture, I used the SZ95 cell line as a model. Derived by immortalization of human facial sebocytes with simian virus 40 large T antigen, they retain several typical characteristics of primary sebocytes (Niemann et al., 2003; Zouboulis et al., 1999). I confirmed that they are equivalent to sebocytes at early stages of differentiation by treating them with different inducers of terminal differentiation and monitoring the amount of cytoplasmic lipid droplets (Fig. 6.3A). While only few untreated control cells contained lipid droplets, stained by Nile Red, after 7 days of incubation with retinoic acid (RA) all cells had several lipid

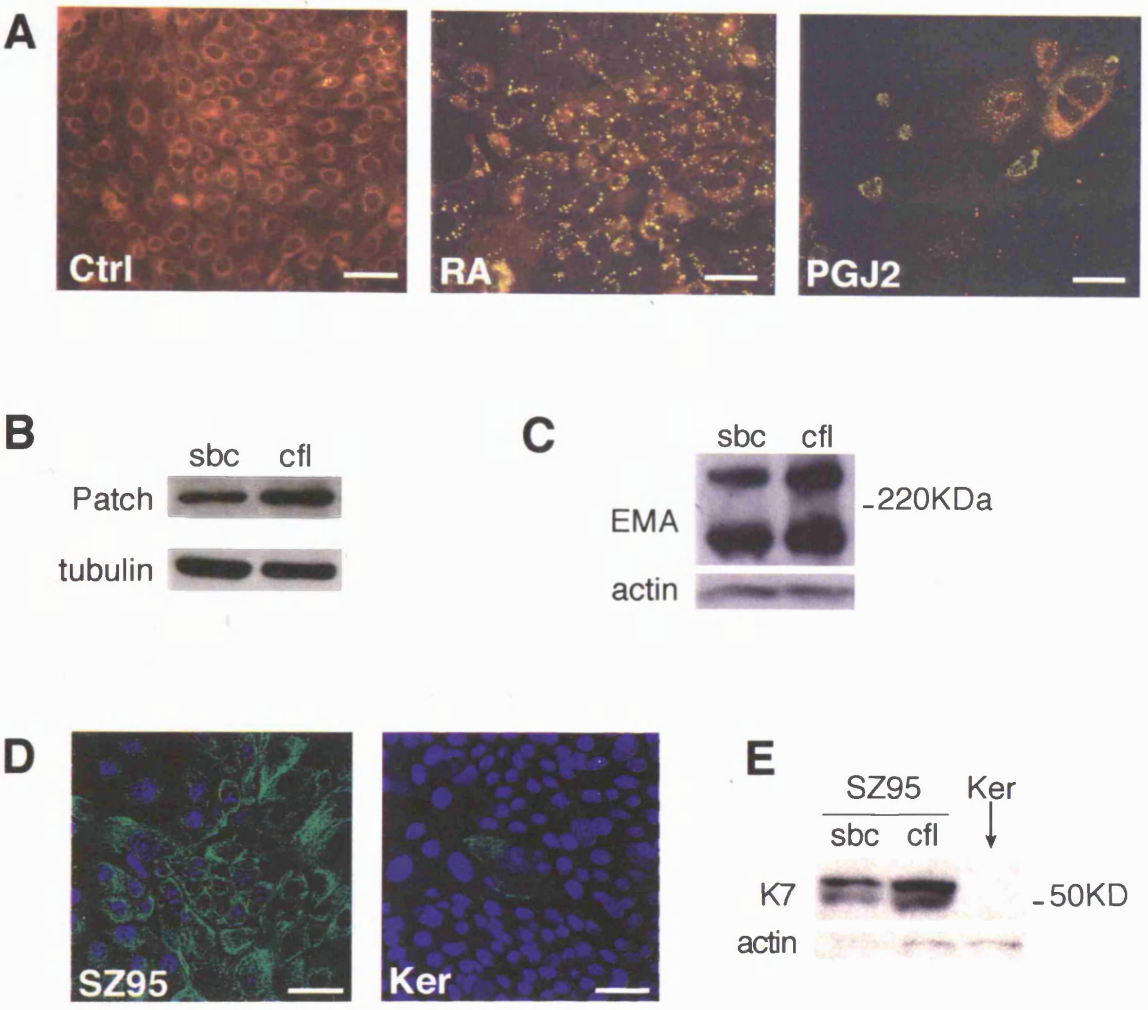

Figure 6.3. SZ95 cells are a model of sebaceous differentiation. (A) SZ95 cells untreated (Ctrl) or incubated with retinoic acid (RA) for 7 days or prostaglandin J2 (PGJ2) for 6 days and stained with nile red. (B,C) Western blot of total lysates from subconfluent (sbc) and confluent (cfl) SZ95 cells probed with anti-Patch (B) or anti-EMA (C) antibodies (top panels) and, as loading control, anti-tubulin (B) or anti-actin (C) antibodies (bottom panels). (D) SZ95 cells and primary keratinocytes immunostained with anti-keratin 7 antibody. (E) Western blot of total lysates of subconfluent (sbc) or confluent (cfl) SZ95 cells and primary keratinocytes (Ker) probed with anti-keratin 7 antibody (top panel) and, as loading control, anti-actin antibody (bottom panel). Scale bars: 50μm.

droplets of various sizes. In a different experiment, I incubated SZ95 cells for 6 days with prostaglandinJ2, a potent activator of PPARγ (Forman et al., 1995; Kliewer et al., 1995), a nuclear receptor involved in lipid production and terminal differentiation of both sebocytes and adipocytes (Rosenfield et al., 2000). This treatment took the differentiation process much further than RA. The cells not only filled up with lipid droplets, but eventually burst, recapitulating the final stage of sebaceous terminal differentiation *in vivo* (Fig. 6.3A, right hand panel).

Another way to induce SZ95 cell differentiation is to let the cells reach confluence (Niemann et al., 2003; Zouboulis et al., 1999). I confirmed that this was the case by western blotting total lysates of subconfluent and confluent SZ95 cells. I probed the lysates with anti Patch antibody (Fig. 6.3B) and showed that the protein was more abundant in confluent cells, as indicated by Niemann et al. (2003). Interestingly, EMA expression also appeared to increase at confluence (Fig.6.3C).

I next examined whether SZ95 cells expressed keratin 7, since this is a marker of sebaceous differentiation *in vivo* (Fig. 6.2). Every SZ95 cell was labelled with anti-keratin 7 antibody (Fig. 6.3D left hand panel), independently of whether the cells were pre or post confluent. I observed only occasional weak staining in suprabasal primary IFE keratinocytes (Fig. 6.3D, right hand panel). I confirmed the immunofluorescence data by using the same antibody to probe total lysates of SZ95 cells and primary IFE keratinocytes (Fig. 6.3E). The amount of keratin 7 expressed by SZ95 cells was similar in pre and post confluent cultures, and I did not detect any expression in IFE keratinocytes.

6.4 SZ95 cells can undergo IFE differentiation

When I stained SZ95 cells with an antibody to an IFE marker, cornifin, I obtained an unexpected result. I found that some SZ95 cells were positively stained for both cornifin and keratin 7 (Fig. 6.4A). The fraction of cornifin positive cells tended to vary according to the confluency of the culture. When cultured at low density, SZ95 cells

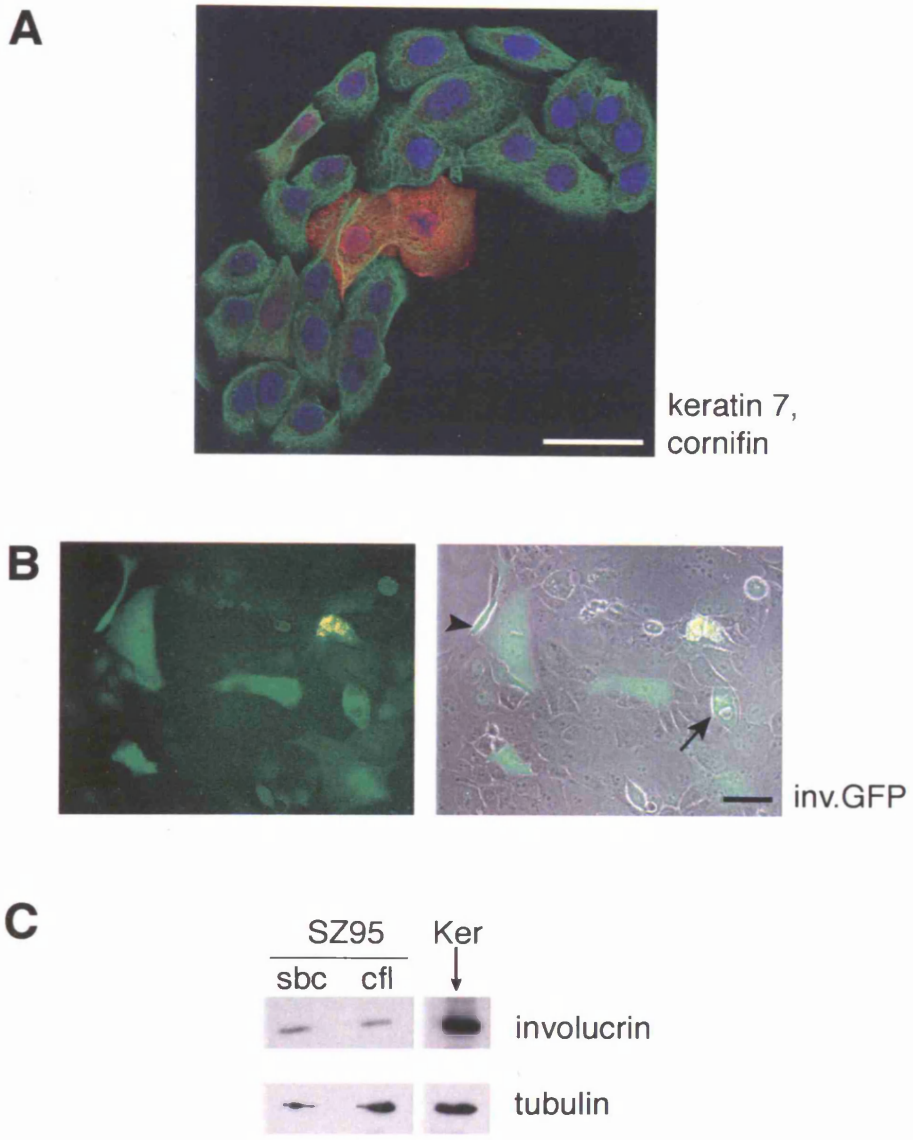

Figure 6.4. SZ95 cells are bipotential. (A) SZ95 cells immunostained with anti-keratin 7 (green) and anti-cornifin (red) antibodies. Blue fluorescence is DAPI nuclear counterstaining. (B) SZ95 cells transduced with inv.GFP retroviral vector. Left panel: endogenous fluorescence; right panel: fluorescence and phase contrast. Arrow indicates a suprabasal GFP positive cell, arrowhead a positive cell at the border of the colony. (H) Western blot of total lysates of subconfluent (sbc) or confluent (cfl) SZ95 cells and primary keratinocytes (Ker) probed with anti-involucrin antibody (top panels) and, as loading control, anti-tubulin antibody (bottom panel). Scale bars: 50μm.

aggregated in small colonies, each containing one or more cornifin positive cell. In proportion, there were fewer positive cells in more dense cultures, and cells expressing high levels of cornifin were very rare in confluent sheets. I never observed cornifin positive, keratin 7 negative SZ95 cells.

I obtained similar results when I used involucrin as a marker of interfollicular differentiation. In each coverslip examined I always noticed positively stained cells, and when I transduced SZ95 cells with a retroviral vector carrying part of the involucrin promoter driving expression of GFP (inv.GFP, (Ghazizadeh et al., 1997) I observed green fluorescent cells (Fig. 6.4B). Both cornifin and involucrin positive cells very often appeared flattened, and either suprabasal (arrow in Fig. 6.4B) or elongated along the edge of the colony (arrowhead in Fig. 6.4B), although the correlation was not absolute.

I confirmed the results of the immunostaining by performing Western blots on SZ95 cells. I compared involucrin expression levels in lysates of SZ95 cells and primary keratinocytes. As expected, keratinocytes expressed involucrin, and lower levels were present in SZ95 cells (Fig. 6.4C). As observed already in immunostaining, confluent SZ95 expressed lower levels of involucrin compared to subconfluent cultures. These observations suggested that SZ95 are bipotential and able to undergo both interfollicular and sebaceous differentiation.

6.5 Analysis of SZ95 differentiation at clonal density and on dermal substrates

To eliminate the possibility that the involucrin/cornifin positive SZ95 cells reflected a mixture of two cell types in the original cultures I set up clonogenicity assays similar to those used for primary keratinocytes and I assessed the resulting clones for involucrin expression (Fig. 6.5A). SZ95 presented colony formation efficiency similar to keratinocytes, even though the size of the clones obtained was smaller and overall more homogeneous. Like in the case of the keratinocytes, I observed in triplicate and

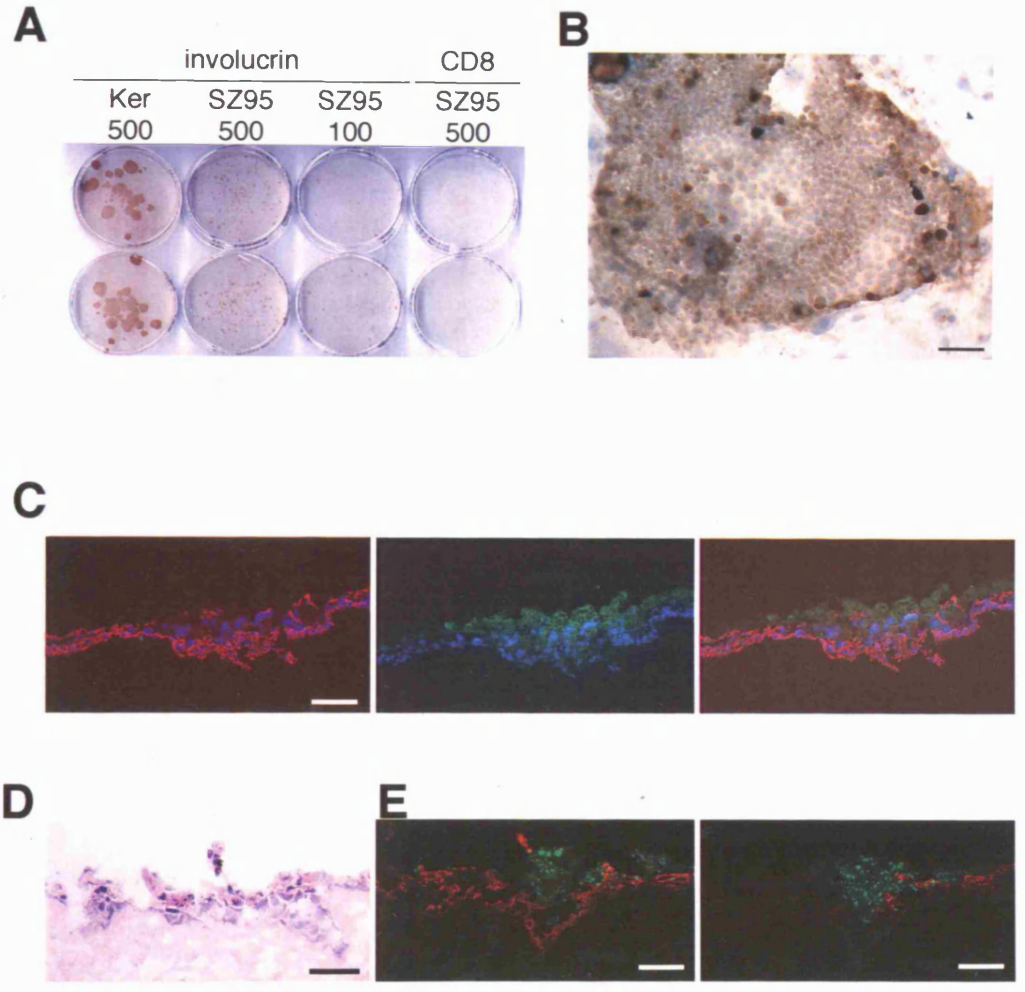

Figure 6.5. Every SZ95 clone is bipotential and IFE and SG differentiated cells segregate on DED. (A,B) The indicated number of primary keratinocytes or SZ95 cells was seeded on 6cm diameter dishes, cultured for three weeks and subsequently fixed and stained with anti-involucrin or, as negative control, anti-CD8 antibody. B is a high magnification picture of a clone of SZ95 cells immunostained with anti-involucrin antibody. Blue is hematoxylin nucelar counterstaining. (C-E) SZ95 cells were cultured on DED for two weeks and subsequently stained. (C) Red fluorescence is keratin 7, green fluorescence is cornifin. Right hand panel: merge. (D) Histological section. (E) Adjacent sections stained with (left panel) nile red and anti-keratin 7 antibody or (right panel) nile red and anti-involucrin antibody. Scale bars: 50μm.

independent experiments that every SZ95 clone stained positive for involucrin, and when I analyzed the dishes more closely I could observe some intensely positive cells, mainly at the periphery of each clone (Fig. 6.5B).

The culture of keratinocytes on de-epidermalized dermis (DED) at the aqueous/air interface is the best way to promote the full interfollicular epidermal differentiation programme (Prunieras et al., 1983). After two weeks on DED culture, SZ95 cells were clearly distinguishable on the top surface of the culture (Fig. 6.5D). Interestingly, when cultured in these conditions not all cells were brightly stained with the anti-keratin 7 antibody (Fig. 6.5C, left hand panel). Cornifin positive cells were only weakly stained with the keratin 7 antibody, and were not evenly distributed in the cultures, but rather appeared clusterd on top of keratin 7 bright cells (Fig. 6.5C). I obtained similar results when I stained the cultures with the anti-involucrin antibody or I examined the location of GFP positive cells in cultures of SZ95 cells transduced with inv.GFP. In this case I still observed clustered GFP positive cells, but they were not always located at the interface with the air, as indicated in Fig. 6.5C.

I stained serial sections of DED cultures with the anti-involucrin or anti-keratin 7 antibodies together with Nile Red to compare the location of terminally differentiated interfollicular and sebaceous cells (Fig. 6.5E). Neither Nile Red nor involucrin staining overlapped with intense keratin 7 staining, but some cells were stained positive by both Nile Red and anti-involucrin antibody. This staining suggested that keratin 7 bright cells could be bipotential progenitors.

6.7 Myc favours sebaceous and impairs interfollicular differentiation of SZ95 cells

Since Myc activation *in vivo* stimulates sebaceous differentiation (Arnold and Watt, 2001), I investigated whether there was a relationship between endogenous Myc and sebaceous differentiation in SZ95 cultures (Fig. 6.6). I observed Myc positive nuclear staining in all the samples I analyzed, irrespectively of the cell density, as expected for

an immortalized cell line. Interestingly, though, the intensity of the staining varied from cell to cell and was usually very low in bright involucrin positive cells (Fig. 6.6A). On the contrary, I found no correlation between the intensity of Myc staining and the number and size of cytoplasmic lipid droplets, as I observed Myc bright cells with

either numerous big or few small droplets (arrows in Fig. 6.6B), and the same was true for dim cells (arrowheads in Fig. 6.6B). Unfortunately I could not simultaneously label SZ95 cells with Nile Red and anti-involucrin antibody, because the permeabilization treatment required to visualize involucrin destroyed the lipid compartment. In conclusion, while it appeared that cells undergoing interfollicular differentiation expressed lower levels of Myc, Nile Red positive cells could have high or low levels of Myc.

In order to better investigate the role of Myc in sebaceous lineage commitment I transduced SZ95 cells with a retrovirus encoding for a fusion protein between Myc and the ligand binding domain of the oestrogen receptor (MycER, (Arnold and Watt, 2001; Frye et al., 2003). The ER domain was the same fused to stabilized β-catenin in the K14ΔNβ-cateninER transgenic mice. Insensitive to endogenous oestrogen, the fusion protein would be activated in the presence of 4OHT (Littlewood et al., 1995). Following two days of incubation with 4OHT SZ95 MycER cells showed an increase in the number and size of cytoplasmic lipid droplets (Fig. R6.7A).

I stained MycER and control empty vector (EV) transduced cells with the anti-involucrin and anti-cornifin antibodies following three days of incubation with 200nM 4OHT (Fig. 6.7B). In order to evaluate whether there was an effect on IFE differentiation of SZ95 cells, I took pictures of five different microscopic fields per condition analyzed using the same confocal detection settings for EV and MycER cells. I scored as positive the cells with staining of intensity higher than a set threshold. Following these criteria, I could obtain quantitative data, which demonstrated that the number of involucrin and cornifin expressing cells was reduced following MycER activation (Fig. 6.7C,D).

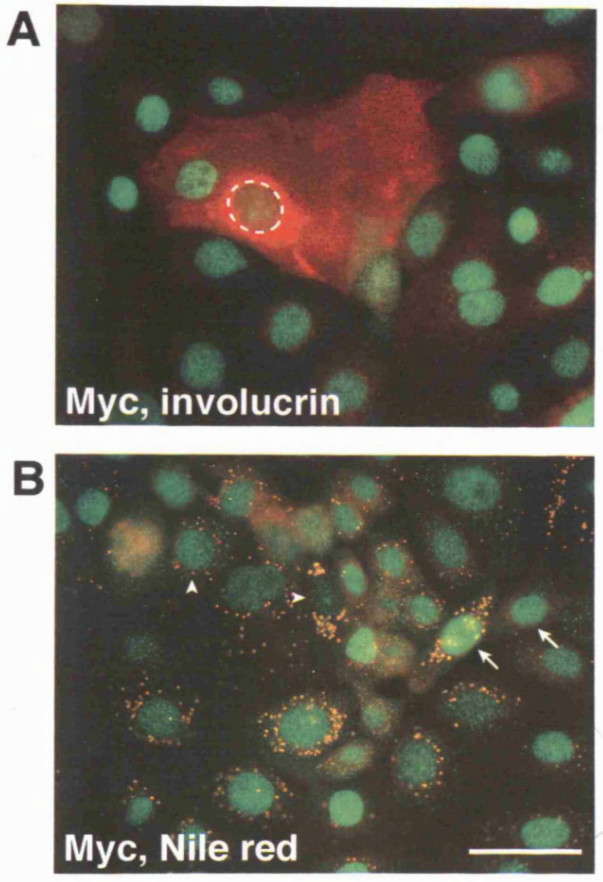

Figure 6.6. SZ95 cells express different levels of c-Myc. SZ95 cells immunostained with anti-myc antibody (green fluorescence) and anti-involucrin antibody (red fluorescence in A) or nile red (orange dots in B). Dashed line in A encircles the nucleus of an involucrin bright, myc dim cell. In B arrows indicate myc bright cells with (left) or without (right) cytoplasmic lipid droplets; arrowheads point at myc dim cells with many big (right) or few small (left) lipid droplets. Scale bars: 50μm.

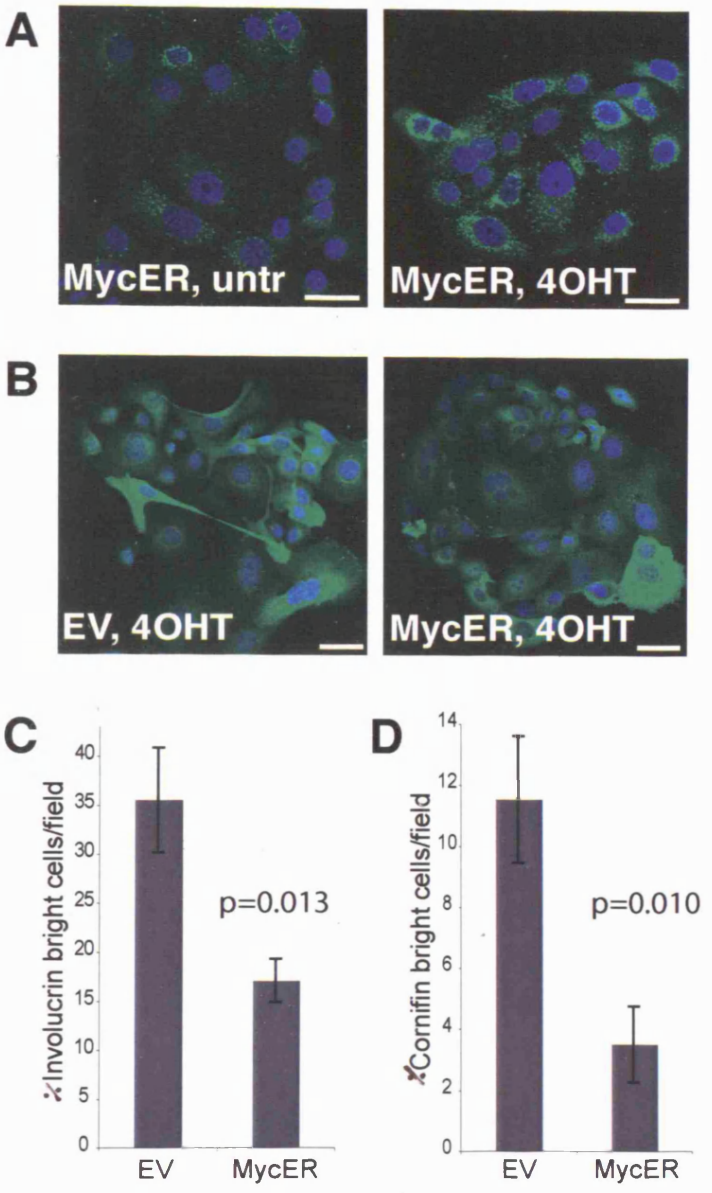

Figure 6.7. Myc enhances sebaceous differentiation and inhibits interfollicular differentiation of SZ95 cells. (A) MycER infected SZ95 cells were untreated (untr) or incubated with 200nM 4OHT for 2 days and subsequently stained with nile red. (B-D) Empty vector (EV) and MycER infected SZ95 were incubated with 200nM 4OHT for 3 days and subsequently stained with anti-involucrin (B, C) or anti-cornifin (D) antibodies. The number of involucrin (C) or cornifin (D) bright cells was counted. C and D are representative of triplicate experiments. Blue immunofluorescence in (A,B) is DAPI nuclear counterstain. Scale bars: 25μm.

The reduction in the number of involucrin/cornifin positive cells together with the increase in number and size of lipid droplets suggests that Myc activation impaired interfollicular and favoured sebaceous differentiation of SZ95 cells, in agreement with the observation of ectopic sebaceous differentiation in K14.MycER transgenic mice (Arnold and Watt, 2001; Braun et al., 2003).

6.8 β-catenin signalling enhances interfollicular differentiation of SZ95 cells.

Since in the K14ΔNβ-cateninER transgenic mice I observed loss of sebaceous glands I examined whether SZ95 cells would also be affected by β-catenin activation. I used retroviral vectors carrying either stabilized β-catenin (ΔNβ-catenin, T2 mutant, Zhu and Watt, 1999) or ΔNβ-cateninER to transduce SZ95 cells.

The expression of involucrin and cornifin increased in both 4OHT treated ΔNβ-cateninER and ΔNβ-catenin SZ95 cells compared to EV (Fig. 6.8), with no appreaciable differences between the constitutively active and 4OHT dependent mutants. I observed some bright involucrin positive EV cells but in all β-catenin transduced cultures bright cells were more numerous and showed the characteristic morphology of differentiating suprabasal interfollicular keratinocytes (Fig. 6.7A). Involucrin and cornifin positive cells were in many cases elongated and at the border of the colonies, sometimes organized in bundles embracing neighbouring negative or weakly positive cells. Isolated bright cells presented long cytoplasmic extensions while brightly stained cells in the middle of colonies were mainly suprabasal and had a complex tri-dimensional shape that extended over various basal cells.

I counted the number of EV and ΔNβ-catenin transduced cells showing bright staining using the same method described in paragraph 6.7. I observed a 2fold increase in involucrin positive cells and 3fold increase in cornifin positive cells. The anti-cornifin antibody always gave lower background signal, which probably accounted for the lower number of positive EV cells and the higher increase observed in ΔNβ-catenin

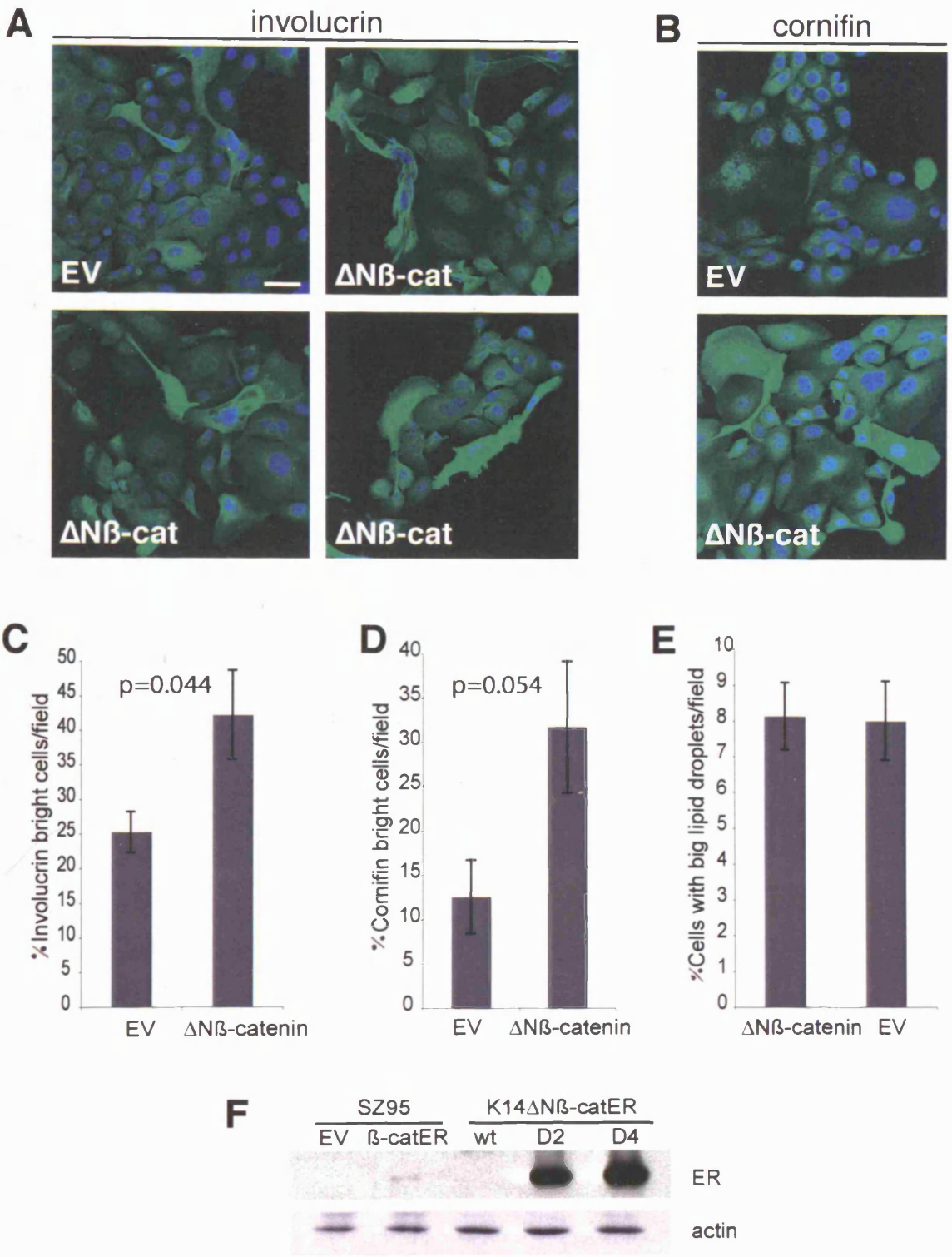

Figure 6.8. ß-catenin enhances interfollicular differentiation of SZ95 cells. (A-E) Empty vector (EV) and ΔNß-catenin infected SZ95 cells were stained with anti-involucrin (A,C) or anti-cornifin (B,D) antibodies or with nile red (E). A and B are representative pictures from two indipendent infections.The number of involucrin (C) or cornifin (D) bright cells was counted. Also the number of cells containing big cytoplasmic lipid droplets was scored (E). C,D and E represent single experiments. (F) Western blot of total lysates of SZ95 cells infected with empty vector (EV) or ΔNß-cateninER and K14Δ Nß-cateninER keratinocyte lines (wild type, D2 and D4) probed with anti-ER (top panel) or anti-actin (bottom panel) antibodies. Blue immunofluorescence in (A,B) is DAPI nuclear counterstain. Scale bars: 25μm.

transduced cells. These observations suggest that β-catenin signalling induces non-sebaceous differentiation of epidermal cells.

When I stained ΔNβ-catenin and EV cells with Nile Red I did not observe differences in the number of cells containing big and numerous lipid droplets (Fig. 6.8E). This observation should not be considered as evidence that β-catenin does not impair sebaceous differentiation of SZ95 cells, as also terminally differentiating IFE keratinocytes produce high amounts of lipids, distinguishable from the sebaceous only by performing thin layer chromatography (Zouboulis et al., 1991).

The strength of β-catenin signalling is a critical determinant of its effects in intact epidermis (see chapters 3 to 5). I therefore investigated the level of β-catenin in transduced SZ95 cells by Western blotting. ΔNβ-cateninER SZ95 lysates contained an amount of fusion protein much lower than D2 and D4 cell lines and similar to 3953 cells (Fig. 6.8F, compare with Fig. 3.2). This may explain why, even though I observed a change in involucrin and cornifin expression, not all cells were dramatically affected.

6.9 Time-lapse analysis of the effects of Myc and β-catenin activation in SZ95 cells

I noticed that SZ95 cells expressing active β-catenin or Myc had a different morphology from EV cells (Fig. 6.9A). EV cells tended to form compact colonies even when cultured at relatively low density. I normally observed few single cells and the colonies were round or in shapes that maximized the area to perimeter ratio (Fig. 6.9A, left hand panel). In contrast, ΔNβ-catenin transduced SZ95 cells appeared more motile and formed less compact colonies, typically surrounded by single cells (Fig. 6.9A, middle panel). The appearance of MycER cells incubated with 4OHT for as little as two days was different again (Fig. 6.9A, right hand panel). While 4OHT did not have any evident effect on EV cells, it caused MycER colonies to compact to the point that they looked almost perfectly round. In all the bigger MycER colonies there was debris

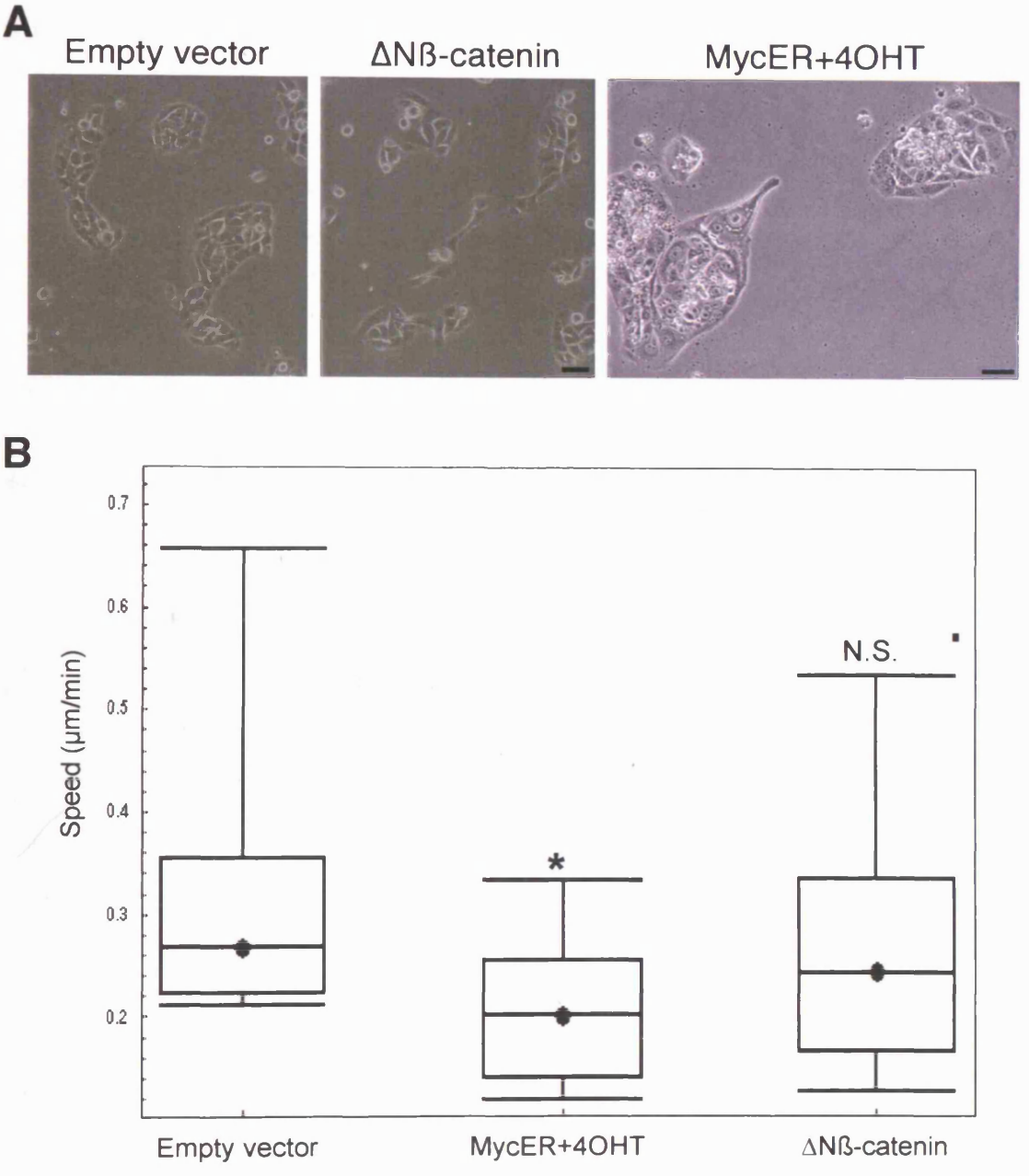

Figure 6.9. Time-lapse video microscopy of MycER and ΔNß-catenin infected SZ95 cells. (A) Morphology of SZ95 cells transduced with empty vector (left hand panel), Δ Nß-catenin (middle panel) or MycER (right hand panel). MycER cells were incubated with 200nM 4OHT for 48 hours. Scale bars: 50µm. (B) 'Box and wiskers' graph representing the speed of empty vector, MycER (incubated with 4OHT) and ΔNß-catenin SZ95 cells on plastic. Black spots represent the median, boxes include 50% and bars (wiskers) 80% of the values around the median. MycER cells were significantly slower than empty vector cells (asterisk), ΔNß-catenin cells speed was not significantly different from empty vector (N.S.). The graph represents the tracking of 12 cells in a single movie per cell type.

accumulation, mainly in the central region, so that each colony strikingly resembled a sebaceous gland, only in two dimensions.

I performed some preliminary analysis of the behaviour of EV, ΔNβ-catenin and MycER SZ95 cells (the last ones incubated with 4OHT) using time-lapse videomicroscopy for a period of 48 hours. I seeded the three types of cells at low density, about 50 cells/mm^2, making sure that they were mainly single cells or grouped in very small colonies. During the 48 hours of recording, MycER cells were the most efficient at forming sebaceous gland-like colonies, while ΔNβ-catenin cells were the least efficient and the EV cells were at an intermediate level. At the end of the recording period, while no or few single MycER and EV cells were left, there were still many single ΔNβ-catenin cells, despite the total cell numbers were similar (Table 6.1).

I tracked a randomized sample of cells in each movie and analysed the results with Mathematica software. MycER cells moved at a significantly lower speed than EV (Fig. 6.9B). This is in agreement with previous observations that Myc inhibits migration of keratinocytes on various extracellular matrix substrates (Frye et al., 2003). In contrast, even though ΔNβ-catenin cells had the typical morphology of migrating cells, their average speed was similar to EV (Fig. 6.9B).

While tracking single EV, ΔNβ-catenin and MycER cells I noticed that other parameters had opposite values in Myc and ΔNβ-catenin expressing cells (Table 6.1). Confirming previous observations that ΔNβ-catenin reduced cohesiveness of SZ95 cells, ΔNβ-catenin transduced cells separated more often than EV cells from their colony of origin. MycER cells were very different, as I extremely rarely observed the detachment of a cell from the originating colony, and single cells would join a colony extremely quickly as soon as they were in its proximity.

The analysis of the time lapse microscopy data gave me some information also on the degree of terminal differentiation reached by the three different types of cells, because I could observe cells bursting at the culmination of sebocyte deifferentiation. I observed the same number of bursts in EV and ΔNβ-catenin cells, while MycER cells bursted at higher frequency, in agreement with their more differentiated morphology.

TABLE 6.1
Analysis of SZ95 cells time-lapse video microscopy

	Empty vector	MycER+4OHT	ΔNß-catenin
% single cells beginning	21.9	15.5	26.2
% single cells end	5.9	1.8	13.8
cells detaching from colony/tracked cells	5/12	2/12	8/12
cells bursting/tracked cells	4/18	5/12	4/18

6.10 Discussion

Genetic manipulation of cultured epidermal cells allows us to investigate in more detail the mechanisms responsible for the alterations observed *in vivo* and to translate to humans the information acquired from mouse models. Reliable and specific differentiation markers and representative tissue culture models are crucial for the study of lineage commitment in vitro. Differentiation markers recognized by antibodies are preferable because they allow analysis at the single cell level. I have identified keratin 7 as the most selective sebaceous marker and I have used cornifin and involucrin as markers of IFE differentiation.

SZ95 cells expressed markers of both sebaceous and interfollicular differentiation. The observation that every SZ95 clone contained involucrin and cornifin positive cells indicates that SZ95 cells contain bipotential progenitors of sebocytes and IFE keratinocytes. When SZ95 cells reached confluence and sebaceous differentiation was induced (Niemann et al., 2003) and involucrin and cornifin expression decreased. On DED, a culture system optimized to favour IFE terminal differentiation, keratin 7 expression was mainly restricted to the basal cells and involucrin/cornifin positive cells were clustered, suprabasal and separated from Nile Red positive areas, suggesting that keratin 7 bright cells could be at least bipotential progenitors. This could reflect a physiological role of SG stem cells in the maintenance of both SG and SG duct, which is a continuum with the HF infundibulum and the IFE. Alternatively, it may indicate that, like IFE stem cells, also SG stem cells can give rise to all epidermal compartments when challenged with the appropriate stimuli (Ferraris et al., 1997).

The role of β-catenin and Myc in driving epidermal lineage commitment is clearly indicated by the phenotype of several transgenic mouse models (Chapters 3 and 4, and (Arnold and Watt, 2001; Braun et al., 2003; Gat et al., 1998; Niemann et al., 2002; Waikel et al., 2001). Retroviral transduction of SZ95 cells with Myc and β-catenin allowed me to investigate in more detail the role of these two genes in epidermal lineage commitment. Myc activation favoured sebaceous at the expense of

interfollicular differentiation as observed *in vivo* (Arnold and Watt, 2001; Braun et al., 2003). β-catenin activation, in the absence of culture conditions permissive for hair formation, increased the number of SZ95 cells undergoing IFE differentiation. Myc and β-catenin thus influence epidermal lineage commitment also in cultured epidermal cells.

Time-lapse video microscopy analysis of infected SZ95 cells suggested that Myc and β-catenin act at least in part by altering motility and cell adhesion. The reduction in cell motility resulting from Myc activation has been observed also in cultured keratinocytes and reflects direct repression of genes involved in cell adhesion and cytoskeleton remodelling (Dr Ela Frye, personal communication). In addition, Myc expressing SZ95 cells presented increased cell-cell adhesion, while β-catenin infected SZ95 were less efficient in forming cohesive colonies and maintained a higher proportion of single cells compared to EV. Many signalling pathways enhance cell motility by impairing the stability of cadherin complexes at cell borders and as a consequence increase the levels of cytoplasmic β-catenin. A link between β-catenin activation and loss of cadherin mediated adhesion has never been described (Nelson and Nusse, 2004). However, β-catenin plays an active role in regulating cell-cell adhesion and β-catenin activation can lead to a change in cadherin expression profile (Bienz and Hamada, 2004). β-catenin signalling is responsible for the switch from E to P-cadherin expression in HF bud formation, an event blocked by ectopic E-cadherin expression (Jamora et al., 2003).

The proportion of β-catenin transduced SZ95 undergoing terminal sebocyte differentiation was lower than the proportion of Myc transduced cells but similar to EV, when measured as the number of cells bursting during time-lapse microscopy. These observations, coupled with the fact that in K14ΔNβ-cateninER mice differentiating sebocytes appeared normal at times when sebaceous progenitors were already involved in ectopic hair follicle formation (cfr Chapter 3), suggest that activation of β-catenin signalling does not affect terminally differentiating sebocytes but rather reprograms SG stem cells to differentiate along the HF lineages.

In conclusion, the experiments described in this chapter indicate that cultured epidermal cells can be used to analyze the mechanisms regulating lineage commitment at the

single cell level. The results observed will be strengthened when repeated in primary sebocyte cultures. As SZ95 cells can be induced to undergo IFE differentiation, it is now reasonable to investigate whether Myc activation could stimulate sebocyte differentiation in cultured keratinocytes.

Chapter 7. Final discussion and future prospectives

I have investigated various aspects of the effect of β-catenin activation in adult epidermal cells both in vivo and in vitro. The data I presented in Chapter 3 and Chapter 4 and part of Chapter 5 are part of two publications with joint first authorship for myself and Dr David Prowse and Violeta Silva-Vargas:

Cristina Lo Celso, David M. Prowse, Fiona M. Watt (2004). Transient activation of β-catenin signalling in adult mouse epidermis is sufficient to induce new hair follicles but continuous activation is required to maintain hair follicle tumours. *Development* 131, 1787-1799.

Violeta Silva-Vargas, Cristina Lo Celso, Adam Giangreco, Tyler Ofstad, David M. Prose, Kristin M. Braun, Fiona M. Watt (2004). β-catenin and Hedgehog signal strength can specify number and location of hair follicles in adult epidermis without recruitment of bulge stem cells. *Developmental Cell* 9, 121-131.

In this chapter I discuss the major issues raised by my work and suggest directions for future research.

7.1. Lineage commitment and epidermal cells multipotency

I described the K14ΔNβ-cateninER transgenic mice, in which I could control the activation of β-catenin signalling at specific stages of the hair cycle and for different lengths of time by applying the drug 4-hydroxytamoxifen (4OHT) on the skin. My results have been confirmed in a different study comparing transgenic mice hemizygous

and homozygous for a stabilized form of β-catenin: while hemizygous mice only showed anagen induction, a double dose of β-catenin signalling determined also ectopic hair follicle formation (Lowry et al., 2005).

Although much emphasis is placed on the reservoir of stem cells in the hair follicle bulge, it is now generally accepted that epidermal stem cell populations reside in HF, IFE and SG and normally maintain the compartment in which they are located. Activation of β-catenin in the basal layer of IFE, SG and ORS led to ectopic HF formation, suggesting that adult epidermal stem cells are multipotent. Lineage marking analysis performed on the K14ΔNβ-cateninER mice indicated that more than one cell contributes to the formation of the ectopic HF (Silva-Vargas et al., 2005). According to the Epidermal Proliferative Unit model, single stem cells are surrounded by committed TA cells, and thus both stem and TA cells could contribute to ectopic HF formation.

The question remains whether already committed cells can be reversed to the level of multipotent progenitors. By driving expression of ΔNβ-cateninER with the keratin 10 (Bailleul et al., 1990) or the involucrin promoters (Carroll et al., 1993), which would target keratinocytes at earlier and later stages of interfollicular differentiation, it would be possible to assess whether IFE cells that have started the process of differentiation could be reverted to a different lineage.

In the last part of my thesis I have shown that it is possible to influence the choice between interfollicular and sebaceous differentiation in cultured cells, and the challenge is now to develop the appropriate culture system to allow also hair differentiation *in vitro*. Moreover, the possibility to examine single cultured cells in real time allows direct observation of the events leading to lineage choice, and it will be extremely informative to analyse lineage selection in stem or transit amplifying clones. The involucrin-GFP retroviral vector (Ghazizadeh et al., 1997) is an example of lineage marker that could be used in this kind of analysis.

I observed that in the epidermis there are cells with different sensitivity to β-catenin activation. No ectopic HF formation was observed from the bulge area at any 4OHT dose even though multipotent epidermal stem cells are concentrated there. Bulge cells

express β-catenin repressors like TCF3 (DasGupta and Fuchs, 1999) and their microenvironment is not permissive for differentiation (Tumbar et al., 2004). It is possible that these characteristics increase the bulge cells threshold required to allow HF morphogenesis and that their response is blocked by neighbouring cells already forming HF via lateral inhibition, a phenomenon observed also during placode formation (Millar, 2002). The keratin 15 promoter could be used to drive expression of ΔNβ-cateninER in the bulge area (Liu et al., 2003) and analyze the response of bulge cells within intact epidermis.

7.2 Epithelial-mesenchymal interaction

An aspect of epidermal, and particularly hair follicle biology, that is receiving growing attention is the crosstalk between the epithelial and mesenchymal components of the skin (Rendl et al., 2005). In K14ΔNβ-cateninER mice, β-catenin induced hair germs are able to recruit dermal papillae but it is possible that the number of responsive dermal cells limits the number of hair follicles that can develop. All epidermal stem and transit amplifying cells could be equally multipotent and responsive to β-catenin but only some of them would succeed in giving rise to ectopic hair follicles because they need the support of the correct dermal counterpart. This could explain for example why the number of follicles did not increase even after a second 4OHT treatment.

Wnt signalling is active in the dermal condensate and in the dermal papilla (DasGupta and Fuchs, 1999) and it has been shown to maintain the hair inductive characteristics of cultured dermal papilla cells (Kishimoto et al., 2000). Expression of ΔNβ-cateninER driven by a dermal promoter could be a way to increase the number of ectopic hair follicles. If a DP specific promoter was used, 4OHT treatment could regulate anagen onset and duration and override the matrix cell timer for catagen initiation (Paus and Cotsarelis, 1999).

Moreover, lineage marking strategies would be useful to identify the origin of the new dermal papilla cells in K14ΔNβ-cateninER mice and to understand whether with the

appropriate stimulus any dermal fibroblast can participate in dermal papilla formation of if β-catenin activation in the epidermis leads to the recruitment of specialized dermal cells.

7.3. β-catenin and stem cell self-renewal

Activation of β-catenin signalling is associated with stem cell self-renewal in several tissues (Megason and McMahon, 2002; Reya et al., 2003; Liu et al., 2004). In the K14ΔNβ-cateninER transgenic mice ectopic follicles developed independently of the existing bulge stem cell compartment and LRC were eventually lost due to proliferation following long 4OHT treatment. Lowry et al. (2005) indicated proliferation as the only effect of β-catenin signalling in bulge stem cells. My analysis of the effects of β-catenin activation was not focused on the bulge region. Nevertheless, microarray analysis pointed out the induction of several genes involved in proliferation and now associated with stem cell activation.

The overall number of epidermal stem cells increased in K14ΔNβ-cateninER transgenic mice because β-catenin induced hair follicles contained their own reservoir of putative epidermal stem cells. A further characterization of these ectopic CD34 positive cells is needed to confirm their stem cell nature. A bulge-specific, inducible marking system could be used to differentially label and isolate CD34 positive cells from the original HF bulge and the β-catenin induced follicles. It would be possible to compare the multipotentiality of these two populations by grafting them onto nude mice, and gene expression profiling would indicate whether wild type and β-catenin induced stem cells are identical or not.

7.4. Mechanisms of β-catenin action

Microarray analysis of β-catenin target genes allowed me to identify a large number of transcription factors and signalling pathways involved in anagen initiation and HF induction. I have described some examples of crosstalk between β-catenin and other signalling pathways indicating how β-catenin acts as a master regulator of very diverse signals, as schematized in Fig. 7.1 A much wider number of interactions could be analyzed by crossing the K14ΔNβ-cateninER with other knock out or transgenic mice, or by treating them with 4OHT and drugs interfering with other pathways. In addition, a broader understanding of hair follicle regulation and the mechanisms of β-catenin action in the epidermis will be achieved when the unknown genes on the arrays have been characterized. Finally, analysis of β-catenin target genes, titration of β-catenin signal and lineage tracing experiments will permit investigation of how individual cells integrate multiple signals received simultaneously.

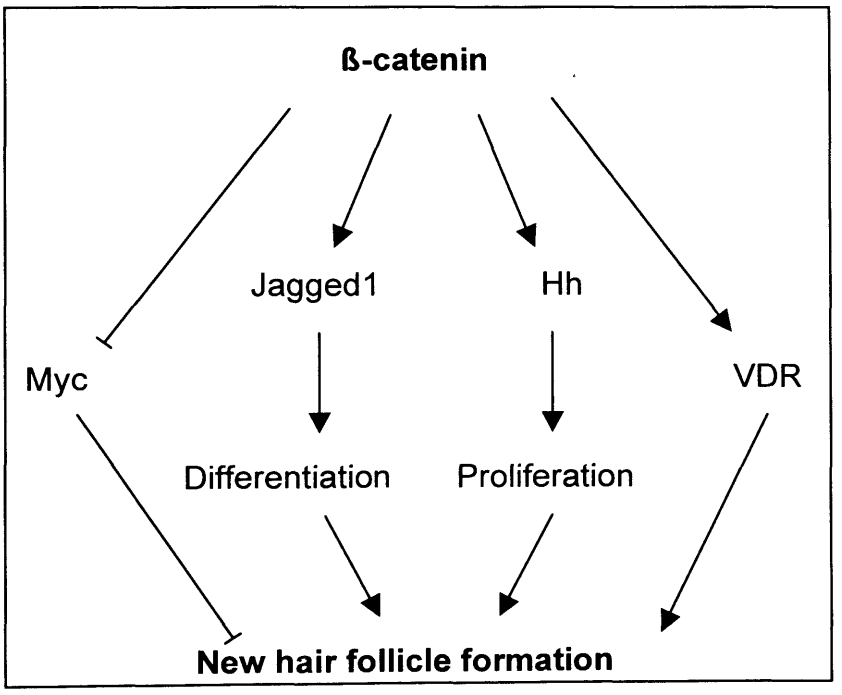

Figure 7. 1.

Interactions between ß-catenin and other transcription factors and signalling pathways described in this thesis. β-catenin activates Notch and Hedgehog signalling to regulate both defferentiation and proliferation. Vitamin D receptor is also induced and cooperates with β-catenin when not bound to vitamin D. Myc and β-catenin antagonize each other's effects.

7.8. Concluding remark

It is clear that β-catenin has a critical role in the regulation of several biological processes. I believe that the combination of the *in vivo* and *in vitro* approaches now available will allow a detailed understanding of the mechanisms of β-catenin action in epidermal cells and that the versatility of ΔNβ-cateninER fusion protein will help addressing many questions still unsolved in skin biology, such as the regulation of stem cell number and plasticity, and the mechanisms leading to tumour formation.

Until recently, most studies in skin biology focused on the activation or deletion of a single gene or pathway. This thesis demonstrates the advantage of regulating timing and dosage of β-catenin signalling to study the mechanisms regulating epidermal stem cell self-renewal and differentiation. The use of promoters active in specific epidermal/dermal compartments to control the expression of multiple transgenes is a way to further develop this approach that will no doubt contribute to improve our understanding of epidermal stem cell biology.

Bibliography

Aberle, H., Butz, S., Stappert, J., Weissig, H., Kemler, R., and Hoschuetzky, H. (1994). Assembly of the cadherin-catenin complex in vitro with recombinant proteins. J Cell Sci *107*, 3655-3663.

Adami, J. G. (1901). The causation of cancerous and other new growths. British Medical Journal *1*, 621-628.

Akhurst, R. J., Fee, F., and Balmain, A. (1988). Localized production of TGF-beta mRNA in tumour promoter-stimulated mouse epidermis. Nature *331*, 363-365.

Alberts, B., Bray, D., Lewis, J., Raff, M., Roberts, K., and Watson, J. D. (1989). Molecular biology of the cell, second edn (London: Garland).

Allen, M., Grachtchouk, M., Sheng, H., Grachtchouk, V., Wang, A., Wei, L., Liu, J., Ramirez, A., Metzger, D., Chambon, P., *et al.* (2003). Hedgehog signaling regulates sebaceous gland development. Am J Pathol *163*, 2173-2178.

Andl, T., Reddy, S. T., Gaddapara, T., and Millar, S. E. (2002). WNT signals are required for the initiation of hair follicle development. Dev Cell *2*, 643-653.

Arnold, I., and Watt, F. M. (2001). c-Myc activation in transgenic mouse epidermis results in mobilization of stem cells and differentiation of their progeny. Curr Biol *11*, 558-568.

Artavanis-Tsakonas, S., Rand, M. D., and Lake, R. J. (1999). Notch signaling: cell fate control and signal integration in development. Science *284*, 770-776.

Aulehla, A., Wehrle, C., Brand-Saberi, B., Kemler, R., Gossler, A., Kanzler, B., and Herrmann, B. G. (2003). Wnt3a plays a major role in the segmentation clock controlling somitogenesis. Dev Cell *4*, 395-406.

Bailey, A. M., and Posakony, J. W. (1995). Suppressor of hairless directly activates transcription of enhancer of split complex genes in response to Notch receptor activity. Genes Dev *9*, 2609-2622.

Bailleul, B., Surani, M. A., White, S., Barton, S. C., Brown, K., Blessing, M., Jorcano, J., and Balmain, A. (1990). Skin hyperkeratosis and papilloma formation in transgenic mice expressing a ras oncogene from a suprabasal keratin promoter. Cell *62*, 697-708.

Barrandon, Y., and Green, H. (1987). Three clonal types of keratinocyte with different capacities for multiplication. Proc Natl Acad Sci U S A *84*, 2302-2306.

Barrandon, Y., Morgan, J. R., Mulligan, R. C., and Green, H. (1989). Restoration of growth potential in paraclones of human keratinocytes by a viral oncogene. Proc Natl Acad Sci U S A *86*, 4102-4106.

Barth, A. I., Pollack, A. L., Altschuler, Y., Mostov, K. E., and Nelson, W. J. (1997). NH2-terminal deletion of beta-catenin results in stable colocalization of mutant beta-catenin with adenomatous polyposis coli protein and altered MDCK cell adhesion. J Cell Biol *136*, 693-706.

Benetti, R., Copetti, T., Dell'Orso, S., Melloni, E., Brancolini, C., Monte, M., and Schneider, C. (2005). The calpain system is involved in the constitutive regulation of beta-catenin signaling functions. J Biol Chem *280*, 22070-22080.

Bickenbach, J. R. (1981). Identification and behavior of label-retaining cells in oral mucosa and skin. J Dent Res *60 Spec No C*, 1611-1620.

Bienz, M., and Hamada, F. (2004). Adenomatous polyposis coli proteins and cell adhesion. Curr Opin Cell Biol *16*, 528-535.

Bikle, D. D. (2004). Vitamin D regulated keratinocyte differentiation. J Cell Biochem *92*, 436-444.

Billoni, N., Gautier, B., Mahe, Y. F., and Bernard, B. A. (1997). Expression of retinoid nuclear receptor superfamily members in human hair follicles and its implication in hair growth. Acta Derm Venereol *77*, 350-355.

Bitgood, M. J., Shen, L., and McMahon, A. P. (1996). Sertoli cell signaling by Desert hedgehog regulates the male germline. Curr Biol *6*, 298-304.

Blanpain, C., Lowry, W. E., Geoghegan, A., Polak, L., and Fuchs, E. (2004). Self-renewal, multipotency, and the existence of two cell populations within an epithelial stem cell niche. Cell *118*, 635-648.

Blessing, M., Ruther, U., and Franke, W. W. (1993). Ectopic synthesis of epidermal cytokeratins in pancreatic islet cells of transgenic mice interferes with cytoskeletal order and insulin production. J Cell Biol *120*, 743-755.

Bolognia, J. L., and Braverman, I. M. (1999). Manifestazioni cutanee di malattie sistemiche, In Principi di medicina interna, Harrison, ed. (Milano: McGraw Hill), pp. 360-392.

Bonifas, J. M., Pennypacker, S., Chuang, P. T., McMahon, A. P., Williams, M., Rosenthal, A., De Sauvage, F. J., and Epstein, E. H., Jr. (2001). Activation of expression of hedgehog target genes in basal cell carcinomas. J Invest Dermatol *116*, 739-742.

Botchkarev, V. A., Botchkareva, N. V., Nakamura, M., Huber, O., Funa, K., Lauster, R., Paus, R., and Gilchrest, B. A. (2001). Noggin is required for induction of the hair follicle growth phase in postnatal skin. Faseb J *15*, 2205-2214.

Botchkarev, V. A., Botchkareva, N. V., Roth, W., Nakamura, M., Chen, L. H., Herzog, W., Lindner, G., McMahon, J. A., Peters, C., Lauster, R., *et al.* (1999). Noggin is a mesenchymally derived stimulator of hair-follicle induction. Nat Cell Biol *1*, 158-164.

Botchkarev, V. A., and Sharov, A. A. (2004). BMP signaling in the control of skin development and hair follicle growth. Differentiation *72*, 512-526.

Brantjes, H., Barker, N., van Es, J., and Clevers, H. (2002). TCF: Lady Justice casting the final verdict on the outcome of Wnt signalling. Biol Chem *383*, 255-261.

Braun, K. M., Niemann, C., Jensen, U. B., Sundberg, J. P., Silva-Vargas, V., and Watt, F. M. (2003). Manipulation of stem cell proliferation and lineage commitment: visualisation of label-retaining cells in wholemounts of mouse epidermis. Development *130*, 5241-5255.

Braun, K. M., and Watt, F. M. (2004). Epidermal label-retaining cells: background and recent applications. J Investig Dermatol Symp Proc *9*, 196-201.

Bull, J. J., Muller-Rover, S., Patel, S. V., Chronnell, C. M., McKay, I. A., and Philpott, M. P. (2001). Contrasting localization of c-Myc with other Myc superfamily transcription factors in the human hair follicle and during the hair growth cycle. J Invest Dermatol *116*, 617-622.

Burke, R., Nellen, D., Bellotto, M., Hafen, E., Senti, K. A., Dickson, B. J., and Basler, K. (1999). Dispatched, a novel sterol-sensing domain protein dedicated to the release of cholesterol-modified hedgehog from signaling cells. Cell *99*, 803-815.

Byrne, C., Tainsky, M., and Fuchs, E. (1994). Programming gene expression in developing epidermis. Development *120*, 2369-2383.

Cadigan, K. M., and Nusse, R. (1997). Wnt signaling: a common theme in animal development. Genes Dev *11*, 3286-3305.

Callahan, C. A., and Oro, A. E. (2001). Monstrous attempts at adnexogenesis: regulating hair follicle progenitors through Sonic hedgehog signaling. Curr Opin Genet Dev *11*, 541-546.

Candi, E., Schmidt, R., and Melino, G. (2005). The cornified envelope: a model of cell death in the skin. Nat Rev Mol Cell Biol *6*, 328-340.

Carroll, J. M., Albers, K. M., Garlick, J. A., Harrington, R., and Taichman, L. B. (1993). Tissue- and stratum-specific expression of the human involucrin promoter in transgenic mice. Proc Natl Acad Sci U S A *90*, 10270-10274.

Carroll, J. M., Romero, M. R., and Watt, F. M. (1995). Suprabasal integrin expression in the epidermis of transgenic mice results in developmental defects and a phenotype resembling psoriasis. Cell *83*, 957-968.

Catalano, R. A., and Lillie, R. D. (1975). Elimination of precipitates in oil red O fat stain by adding dextrin. Stain Technol *50*, 297-299.

Chan, E. F., Gat, U., McNiff, J. M., and Fuchs, E. (1999). A common human skin tumour is caused by activating mutations in beta- catenin. Nat Genet *21*, 410-413.

Chen, C. H., Sakai, Y., and Demay, M. B. (2001). Targeting expression of the human vitamin D receptor to the keratinocytes of vitamin D receptor null mice prevents alopecia. Endocrinology *142*, 5386-5389.

Cheng, H. T., Miner, J. H., Lin, M., Tansey, M. G., Roth, K., and Kopan, R. (2003). Gamma-secretase activity is dispensable for mesenchyme-to-epithelium transition but required for podocyte and proximal tubule formation in developing mouse kidney. Development *130*, 5031-5042.

Chia, I. V., and Costantini, F. (2005). Mouse axin and axin2/conductin proteins are functionally equivalent in vivo. Mol Cell Biol *25*, 4371-4376.

Chiang, C., Swan, R. Z., Grachtchouk, M., Bolinger, M., Litingtung, Y., Robertson, E. K., Cooper, M. K., Gaffield, W., Westphal, H., Beachy, P. A., and Dlugosz, A. A. (1999). Essential role for Sonic hedgehog during hair follicle morphogenesis. Dev Biol *205*, 1-9.

Chida, K., Hashiba, H., Fukushima, M., Suda, T., and Kuroki, T. (1985). Inhibition of tumor promotion in mouse skin by 1 alpha,25-dihydroxyvitamin D3. Cancer Res *45*, 5426-5430.

Chuang, P. T., and McMahon, A. P. (1999). Vertebrate Hedgehog signalling modulated by induction of a Hedgehog-binding protein. Nature *397*, 617-621.

Ciani, L., and Salinas, P. C. (2005). WNTs in the vertebrate nervous system: from patterning to neuronal connectivity. Nat Rev Neurosci *6*, 351-362.

Clevers, H., and van de Wetering, M. (1997). TCF/LEF factor earn their wings. Trends Genet *13*, 485-489.

Compton, C. C., Gill, J. M., Bradford, D. A., Regauer, S., Gallico, G. G., and O'Connor, N. E. (1989). Skin regenerated from cultured epithelial autografts on full-thickness burn wounds from 6 days to 5 years after grafting. A light, electron microscopic and immunohistochemical study. Lab Invest *60*, 600-612.

Compton, C. C., Nadire, K. B., Regauer, S., Simon, M., Warland, G., O'Connor, N. E., Gallico, G. G., and Landry, D. B. (1998). Cultured human sole-derived keratinocyte grafts re-express site-specific differentiation after transplantation. Differentiation *64*, 45-53.

Cong, F., Schweizer, L., and Varmus, H. (2004). Wnt signals across the plasma membrane to activate the beta-catenin pathway by forming oligomers containing its receptors, Frizzled and LRP. Development *131*, 5103-5115.

Cotsarelis, G. (1997). The hair follicle: dying for attention. Am J Pathol *151*, 1505-1509.

Cotsarelis, G., Sun, T. T., and Lavker, R. M. (1990). Label-retaining cells reside in the bulge area of pilosebaceous unit: implications for follicular stem cells, hair cycle, and skin carcinogenesis. Cell *61*, 1329-1337.

Crowe, R., Henrique, D., Ish-Horowicz, D., and Niswander, L. (1998). A new role for Notch and Delta in cell fate decisions: patterning the feather array. Development *125*, 767-775.

Dahmane, N., Lee, J., Robins, P., Heller, P., and Ruiz i Altaba, A. (1997). Activation of the transcription factor Gli1 and the Sonic hedgehog signalling pathway in skin tumours. Nature *389*, 876-881.

Damalas, A., Kahan, S., Shtutman, M., Ben-Ze'ev, A., and Oren, M. (2001). Deregulated beta-catenin induces a p53- and ARF-dependent growth arrest and cooperates with Ras in transformation. Embo J *20*, 4912-4922.

DasGupta, R., and Fuchs, E. (1999). Multiple roles for activated LEF/TCF transcription complexes during hair follicle development and differentiation. Development *126*, 4557-4568.

De Langhe, S. P., Sala, F. G., Del Moral, P. M., Fairbanks, T. J., Yamada, K. M., Warburton, D., Burns, R. C., and Bellusci, S. (2005). Dickkopf-1 (DKK1) reveals that fibronectin is a major target of Wnt signaling in branching morphogenesis of the mouse embryonic lung. Dev Biol *277*, 316-331.

Devgan, V., Mammucari, C., Millar, S. E., Brisken, C., and Dotto, G. P. (2005). p21WAF1/Cip1 is a negative transcriptional regulator of Wnt4 expression downstream of Notch1 activation. Genes Dev *19*, 1485-1495.

Dominguez, I., Itoh, K., and Sokol, S. Y. (1995). Role of glycogen synthase kinase 3 beta as a negative regulator of dorsoventral axis formation in Xenopus embryos. Proc Natl Acad Sci U S A *92*, 8498-8502.

Dover, R. (1994). Cell Kinetics of keratinocytes, In The KEratinocyte Handbook, I. M. Leigh, E. B. Lanes, and F. M. Watt, eds. (Cambridge: Cambridge University Press), pp. 203-234.

Dover, R., and Wright, N. A. (1991). Structure of the skin, In Physiology, Biochemistry, and Molecular Biology of the Skin, L. A. Goldsmith, ed. (Oxford: Oxford University Press), pp. 239-265.

Duncan, A. W., Rattis, F. M., DiMascio, L. N., Congdon, K. L., Pazianos, G., Zhao, C., Yoon, K., Cook, J. M., Willert, K., Gaiano, N., and Reya, T. (2005). Integration of Notch and Wnt signaling in hematopoietic stem cell maintenance. Nat Immunol *6*, 314-322.

Elder, J. T., Fisher, G. J., Zhang, Q. Y., Eisen, D., Krust, A., Kastner, P., Chambon, P., and Voorhees, J. J. (1991). Retinoic acid receptor gene expression in human skin. J Invest Dermatol *96*, 425-433.

Ellis, T., Gambardella, L., Horcher, M., Tschanz, S., Capol, J., Bertram, P., Jochum, W., Barrandon, Y., and Busslinger, M. (2001). The transcriptional repressor CDP (Cutl1) is essential for epithelial cell differentiation of the lung and the hair follicle. Genes Dev *15*, 2307-2319.

Fernandes, K. J., McKenzie, I. A., Mill, P., Smith, K. M., Akhavan, M., Barnabe-Heider, F., Biernaskie, J., Junek, A., Kobayashi, N. R., Toma, J. G., *et al.* (2004). A dermal niche for multipotent adult skin-derived precursor cells. Nat Cell Biol *6*, 1082-1093.

Ferraris, C., Bernard, B. A., and Dhouailly, D. (1997). Adult epidermal keratinocytes are endowed with pilosebaceous forming abilities. Int J Dev Biol *41*, 491-498.

Filali, M., Cheng, N., Abbott, D., Leontiev, V., and Engelhardt, J. F. (2002). Wnt-3A/beta-catenin signaling induces transcription from the LEF-1 promoter. J Biol Chem *277*, 33398-33410.

Filipe, M. I., and Lake, B. D. (1990). Histochemistry in Pathology, Second Edition edn (London: Churchill Livingstone).

Fisher, G. J., and Voorhees, J. J. (1996). Molecular mechanisms of retinoid actions in skin. Faseb J *10*, 1002-1013.

Forman, B. M., Tontonoz, P., Chen, J., Brun, R. P., Spiegelman, B. M., and Evans, R. M. (1995). 15-Deoxy-delta 12, 14-prostaglandin J2 is a ligand for the adipocyte determination factor PPAR gamma. Cell *83*, 803-812.

Fre, S., Huyghe, M., Mourikis, P., Robine, S., Louvard, D., and Artavanis-Tsakonas, S. (2005). Notch signals control the fate of immature progenitor cells in the intestine. Nature *435*, 964-968.

Freeman, M. (2000). Feedback control of intercellular signalling in development. Nature *408*, 313-319.

Frye, M., Gardner, C., Li, E. R., Arnold, I., and Watt, F. M. (2003). Evidence that Myc activation depletes the epidermal stem cell compartment by modulating adhesive interactions with the local microenvironment. Development *130*, 2793-2808.

Fuchs, E., Merrill, B. J., Jamora, C., and DasGupta, R. (2001). At the roots of a never-ending cycle. Dev Cell *1*, 13-25.

Fuchs, E., Tumbar, T., and Guasch, G. (2004). Socializing with the neighbors: stem cells and their niche. Cell *116*, 769-778.

Funayama, N., Fagotto, F., McCrea, P., and Gumbiner, B. M. (1995). Embryonic axis induction by the armadillo repeat domain of beta-catenin: evidence for intracellular signaling. J Cell Biol *128*, 959-968.

Gailani, M. R., Ståhle-Bäckdahl, M., Leffell, D., Glynn, M., Zaphiropoulos, P. G., Pressman, C., Undén, A. B., Dean, M., Brash, D. E., Bale, A. E., and Toftgård, R.

(1996). The role of the human homologue of *Drosophila patched* in sporadic basal cell carcinomas. Nature Genetics *14*, 78-81.

Galceran, J., Sustmann, C., Hsu, S. C., Folberth, S., and Grosschedl, R. (2004). LEF1-mediated regulation of Delta-like1 links Wnt and Notch signaling in somitogenesis. Genes Dev *18*, 2718-2723.

Gallico, G. G., 3rd, O'Connor, N. E., Compton, C. C., Kehinde, O., and Green, H. (1984). Permanent coverage of large burn wounds with autologous cultured human epithelium. N Engl J Med *311*, 448-451.

Gandarillas, A., and Watt, F. M. (1997). c-Myc promotes differentiation of human epidermal stem cells. Genes Dev *11*, 2869-2882.

Gat, U., DasGupta, R., Degenstein, L., and Fuchs, E. (1998). De Novo hair follicle morphogenesis and hair tumors in mice expressing a truncated beta-catenin in skin. Cell *95*, 605-614.

Ghali, L., Wong, S. T., Green, J., Tidman, N., and Quinn, A. G. (1999). Gli1 protein is expressed in basal cell carcinomas, outer root sheath keratinocytes and a subpopulation of mesenchymal cells in normal human skin. J Invest Dermatol *113*, 595-599.

Ghazizadeh, S., Carroll, J. M., and Taichman, L. B. (1997). Repression of retrovirus-mediated transgene expression by interferons: implications for gene therapy. J Virol *71*, 9163-9169.

Ghazizadeh, S., and Taichman, L. B. (2001). Multiple classes of stem cells in cutaneous epithelium: a lineage analysis of adult mouse skin. Embo J *20*, 1215-1222.

Glise, B., Jones, D. L., and Ingham, P. W. (2002). Notch and Wingless modulate the response of cells to Hedgehog signalling in the Drosophila wing. Dev Biol *248*, 93-106.

Godwin, A. R., and Capecchi, M. R. (1998). Hoxc13 mutant mice lack external hair. Genes Dev *12*, 11-20.

Grachtchouk, M., Mo, R., Yu, S., Zhang, X., Sasaki, H., Hui, C. C., and Dlugosz, A. A. (2000). Basal cell carcinomas in mice overexpressing Gli2 in skin. Nat Genet *24*, 216-217.

Grachtchouk, V., Grachtchouk, M., Lowe, L., Johnson, T., Wei, L., Wang, A., de Sauvage, F., and Dlugosz, A. A. (2003). The magnitude of hedgehog signaling activity defines skin tumor phenotype. Embo J *22*, 2741-2751.

Gu, Y., Hukriede, N. A., and Fleming, R. J. (1995). Serrate expression can functionally replace Delta activity during neuroblast segregation in the Drosophila embryo. Development *121*, 855-865.

Guger, K. A., and Gumbiner, B. M. (1995). beta-Catenin has Wnt-like activity and mimics the Nieuwkoop signaling center in Xenopus dorsal-ventral patterning. Dev Biol *172*, 115-125.

Guilford, P., Hopkins, J., Harraway, J., McLeod, M., McLeod, N., Harawira, P., Taite, H., Scoular, R., Miller, A., and Reeve, A. E. (1998). E-cadherin germline mutations in familial gastric cancer. Nature *392*, 402-405.

Guyton, K. Z., Kensler, T. W., and Posner, G. H. (2001). Cancer chemoprevention using natural vitamin D and synthetic analogs. Annu Rev Pharmacol Toxicol *41*, 421-442.

Haass, C., and Baumeister, R. (1999). The biological and pathological function of presenilin proteins--simple cell systems and a worm in Alzheimer's disease research. Eur Arch Psychiatry Clin Neurosci *249 Suppl 3*, 23-27.

Hahn, H., Wicking, C., Zaphiropoulous, P. G., Gailani, M. R., Shanley, S., Chidambaram, A., Vorechovsky, I., Holmberg, E., Unden, A. B., Gillies, S., *et al.* (1996). Mutations of the human homolog of Drosophila *patched* in the nevoid basal cell carcinoma syndrome. Cell *85*, 841-851.

Hahn, W. C., and Weinberg, R. A. (2002). Rules for making human tumor cells. N Engl J Med *347*, 1593-1603.

Hamilton, E. (1974). Cell kinetics in the sebaceous glands of the mouse. I. The glands in resting skin. Cell Tissue Kinet *7*, 389-398.

Handjiski, B. K., Eichmuller, S., Hofmann, U., Czarnetzki, B. M., and Paus, R. (1994). Alkaline phosphatase activity and localization during the murine hair cycle. Br J Dermatol *131*, 303-310.

Hardy, M. H. (1992). The secret life of the hair follicle. TIG *8*, 55-61.

Harlow, E., and Lane, D. (1988). Antibodies. A Laboratory Manual (New York: Cold Spring Harbor Laboratory).

Hart, M., Concordet, J. P., Lassot, I., Albert, I., del los Santos, R., Durand, H., Perret, C., Rubinfeld, B., Margottin, F., Benarous, R., and Polakis, P. (1999). The F-box protein beta-TrCP associates with phosphorylated beta-catenin and regulates its activity in the cell. Curr Biol *9*, 207-210.

Hart, M. J., de los Santos, R., Albert, I. N., Rubinfeld, B., and Polakis, P. (1998). Downregulation of beta-catenin by human Axin and its association with the APC tumor suppressor, beta-catenin and GSK3 beta. Curr Biol *8*, 573-581.

Hashimoto, K. (1970). The ultrastructure of the skin of human embryos. VI. Formation of the intradermal hair canal. Dermatologica *141*, 49-53.

Hayward, P., Brennan, K., Sanders, P., Balayo, T., DasGupta, R., Perrimon, N., and Martinez Arias, A. (2005). Notch modulates Wnt signalling by associating with Armadillo/beta-catenin and regulating its transcriptional activity. Development *132*, 1819-1830.

He, B., Barg, R. N., You, L., Xu, Z., Reguart, N., Mikami, I., Batra, S., Rosell, R., and Jablons, D. M. (2005). Wnt signaling in stem cells and non-small-cell lung cancer. Clin Lung Cancer *7*, 54-60.

He, T. C., Sparks, A. B., Rago, C., Hermeking, H., Zawel, L., da Costa, L. T., Morin, P. J., Vogelstein, B., and Kinzler, K. W. (1998). Identification of c-MYC as a target of the APC pathway. Science *281*, 1509-1512.

He, X., Saint-Jeannet, J. P., Woodgett, J. R., Varmus, H. E., and Dawid, I. B. (1995). Glycogen synthase kinase-3 and dorsoventral patterning in Xenopus embryos. Nature *374*, 617-622.

Headon, D. J., and Overbeek, P. A. (1999). Involvement of a novel Tnf receptor homologue in hair follicle induction. Nat Genet *22*, 370-374.

Henderson, B. R., and Fagotto, F. (2002). The ins and outs of APC and beta-catenin nuclear transport. EMBO Rep *3*, 834-839.

Hinck, L., Nathke, I. S., Papkoff, J., and Nelson, W. J. (1994). Beta-catenin: a common target for the regulation of cell adhesion by Wnt-1 and Src signaling pathways. Trends Biochem Sci *19*, 538-542.

Hofmann, M., Schuster-Gossler, K., Watabe-Rudolph, M., Aulehla, A., Herrmann, B. G., and Gossler, A. (2004). WNT signaling, in synergy with T/TBX6, controls Notch signaling by regulating Dll1 expression in the presomitic mesoderm of mouse embryos. Genes Dev *18*, 2712-2717.

Holbrook, K. A., Smith, L. T., Kaplan, E. D., Minami, S. A., Hebert, G. P., and Underwood, R. A. (1993). Expression of morphogens during human follicle development in vivo and a model for studying follicle morphogenesis in vitro. J Invest Dermatol *101*, 39S-49S.

Holick, M. F. (2003). Vitamin D: A millenium perspective. J Cell Biochem *88*, 296-307.

Honeycutt, K. A., and Roop, D. R. (2004). c-Myc and epidermal stem cell fate determination. J Dermatol *31*, 368-375.

Hooper, J. E., and Scott, M. P. (2005). Communicating with Hedgehogs. Nat Rev Mol Cell Biol *6*, 306-317.

Huber, A. H., Nelson, W. J., and Weis, W. I. (1997). Three-dimensional structure of the armadillo repeat region of beta-catenin. Cell *90*, 871-882.

Huber, O., Korn, R., McLaughlin, J., Ohsugi, M., Herrmann, B. G., and Kemler, R. (1996). Nuclear localization of b-catenin by interaction with transcription factor LEF-1. Mech Dev *59*, 3-10.

Huelsken, J., Vogel, R., Erdmann, B., Cotsarelis, G., and Birchmeier, W. (2001). beta-Catenin controls hair follicle morphogenesis and stem cell differentiation in the skin. Cell *105*, 533-545.

Huerta, S., Irwin, R. W., Heber, D., Go, V. L., Koeffler, H. P., Uskokovic, M. R., and Harris, D. M. (2002). 1alpha,25-(OH)(2)-D(3) and its synthetic analogue decrease tumor load in the Apc(min) Mouse. Cancer Res *62*, 741-746.

Hutchin, M. E., Kariapper, M. S., Grachtchouk, M., Wang, A., Wei, L., Cummings, D., Liu, J., Michael, L. E., Glick, A., and Dlugosz, A. A. (2005). Sustained Hedgehog signaling is required for basal cell carcinoma proliferation and survival: conditional skin tumorigenesis recapitulates the hair growth cycle. Genes Dev *19*, 214-223.

Ikeda, S., Kishida, S., Yamamoto, H., Murai, H., Koyama, S., and Kikuchi, A. (1998). Axin, a negative regulator of the Wnt signaling pathway, forms a complex with GSK-3beta and beta-catenin and promotes GSK-3beta-dependent phosphorylation of beta-catenin. Embo J *17*, 1371-1384.

Ingham, P. W., and McMahon, A. P. (2001). Hedgehog signaling in animal development: paradigms and principles. Genes Dev *15*, 3059-3087.

Jahoda, C. A., and Reynolds, A. J. (1996). Dermal-epidermal interactions. Adult follicle-derived cell populations and hair growth. Dermatol Clin *14*, 573-583.

Jakic-Razumovic, J., Browne, M. D., and Sale, G. E. (1992). Proliferation rates in epidermis of patients with graft-versus-host disease, non-specific inflammation and normal skin. Bone Marrow Transplant *10*, 27-31.

Jamora, C., DasGupta, R., Kocieniewski, P., and Fuchs, E. (2003). Links between signal transduction, transcription and adhesion in epithelial bud development. Nature *422*, 317-322.

Janes, S. M., Ofstad, T. A., Campbell, D. H., Watt, F. M., and Prowse, D. M. (2004). Transient activation of FOXN1 in keratinocytes induces a transcriptional programme that promotes terminal differentiation: contrasting roles of FOXN1 and Akt. J Cell Sci *117*, 4157-4168.

Jensen, U. B., Lowell, S., and Watt, F. M. (1999). The spatial relationship between stem cells and their progeny in the basal layer of human epidermis: a new view based on whole-mount labelling and lineage analysis. Development *126*, 2409-2418.

Jiang, T. X., Liu, Y. H., Widelitz, R. B., Kundu, R. K., Maxson, R. E., and Chuong, C. M. (1999). Epidermal dysplasia and abnormal hair follicles in transgenic mice overexpressing homeobox gene MSX-2. J Invest Dermatol *113*, 230-237.

Joannides, A., Gaughwin, P., Schwiening, C., Majed, H., Sterling, J., Compston, A., and Chandran, S. (2004). Efficient generation of neural precursors from adult human skin: astrocytes promote neurogenesis from skin-derived stem cells. Lancet *364*, 172-178.

Jones, P. H., Harper, S., and Watt, F. M. (1995). Stem cell patterning and fate in human epidermis. Cell *80*, 83-93.

Jones, P. H., and Watt, F. M. (1993). Separation of human epidermal stem cells from transit amplifying cells on the basis of differences in integrin function and expression. Cell *73*, 713-724.

Kaplan, E. D., and Holbrook, K. A. (1994). Dynamic expression patterns of tenascin, proteoglycans, and cell adhesion molecules during human hair follicle morphogenesis. Dev Dyn *199*, 141-155.

Karlsson, L., Bondjers, C., and Betsholtz, C. (1999). Roles for PDGF-A and sonic hedgehog in development of mesenchymal components of the hair follicle. Development *126*, 2611-2621.

Kawano, Y., and Kypta, R. (2003). Secreted antagonists of the Wnt signalling pathway. J Cell Sci *116*, 2627-2634.

Kielman, M. F., Rindapaa, M., Gaspar, C., van Poppel, N., Breukel, C., van Leeuwen, S., Taketo, M. M., Roberts, S., Smits, R., and Fodde, R. (2002). Apc modulates embryonic stem-cell differentiation by controlling the dosage of beta-catenin signaling. Nat Genet *32*, 594-605.

Kishimoto, J., Burgeson, R. E., and Morgan, B. A. (2000). Wnt signaling maintains the hair-inducing activity of the dermal papilla. Genes Dev *14*, 1181-1185.

Kliewer, S. A., Lenhard, J. M., Willson, T. M., Patel, I., Morris, D. C., and Lehmann, J. M. (1995). A prostaglandin J2 metabolite binds peroxisome proliferator-activated receptor gamma and promotes adipocyte differentiation. Cell *83*, 813-819.

Klingensmith, J., Nusse, R., and Perrimon, N. (1994). The Drosophila segment polarity gene dishevelled encodes a novel protein required for response to the wingless signal. Genes Dev *8*, 118-130.

Knudsen, K. A., Soler, A. P., Johnson, K. R., and Wheelock, M. J. (1995). Interaction of alpha-actinin with the cadherin/catenin cell-cell adhesion complex via alpha-catenin. J Cell Biol *130*, 67-77.

Knutson, D. D. (1974). Ultrastructural observations in acne vulgaris: the normal sebaceous follicle and acne lesions. J Invest Dermatol *62*, 288-307.

Kobielak, K., Pasolli, H. A., Alonso, L., Polak, L., and Fuchs, E. (2003). Defining BMP functions in the hair follicle by conditional ablation of BMP receptor IA. J Cell Biol *163*, 609-623.

Kolligs, F. T., Bommer, G., and Goke, B. (2002). Wnt/beta-catenin/tcf signaling: a critical pathway in gastrointestinal tumorigenesis. Digestion *66*, 131-144.

Kopan, R., Lee, J., Lin, M. H., Syder, A. J., Kesterson, J., Crutchfield, N., Li, C. R., Wu, W., Books, J., and Gordon, J. I. (2002). Genetic mosaic analysis indicates that the bulb region of coat hair follicles contains a resident population of several active multipotent epithelial lineage progenitors. Dev Biol *242*, 44-57.

Kopan, R., and Weintraub, H. (1993). Mouse notch: expression in hair follicles correlates with cell fate determination. J Cell Biol *121*, 631-641.

Kratochwil, K., Dull, M., Farinas, I., Galceran, J., and Grosschedl, R. (1996). Lef1 expression is activated by BMP-4 and regulates inductive tissue interactions in tooth and hair development. Genes Dev *10*, 1382-1394.

Krishnan, A. V., Peehl, D. M., and Feldman, D. (2003). The role of vitamin D in prostate cancer. Recent Results Cancer Res *164*, 205-221.

Kuhl, M., Sheldahl, L. C., Park, M., Miller, J. R., and Moon, R. T. (2000). The Wnt/Ca2+ pathway: a new vertebrate Wnt signaling pathway takes shape. Trends Genet *16*, 279-283.

Kulessa, H., Turk, G., and Hogan, B. L. (2000). Inhibition of Bmp signaling affects growth and differentiation in the anagen hair follicle. Embo J *19*, 6664-6674.

Kusakabe, T., Maeda, M., Hoshi, N., Sugino, T., Watanabe, K., Fukuda, T., and Suzuki, T. (2000). Fatty acid synthase is expressed mainly in adult hormone-sensitive cells or cells with high lipid metabolism and in proliferating fetal cells. J Histochem Cytochem *48*, 613-622.

Laemmli, U. K. (1970). Cleavage of structural proteins during the assembly of the head of bacteriophage T4. Nature *227*, 680-685.

Lako, M., Armstrong, L., Cairns, P. M., Harris, S., Hole, N., and Jahoda, C. A. (2002). Hair follicle dermal cells repopulate the mouse haematopoietic system. J Cell Sci *115*, 3967-3974.

Langbein, L., and Schweizer, J. (2005). Keratins of the human hair follicle. Int Rev Cytol *243*, 1-78.

Latham, J. A., Redfern, C. P., Thody, A. J., and De Kretser, T. A. (1989). Immunohistochemical markers of human sebaceous gland differentiation. J Histochem Cytochem *37*, 729-734.

Lavker, R. M., and Sun, T. T. (2000). Epidermal stem cells: properties, markers, and location. Proc Natl Acad Sci U S A *97*, 13473-13475.

Lechler, T., and Fuchs, E. (2005). Asymmetric cell divisions promote stratification and differentiation of mammalian skin. Nature *437*, 275-280.

Lecourtois, M., and Schweisguth, F. (1995). The neurogenic suppressor of hairless DNA-binding protein mediates the transcriptional activation of the enhancer of split complex genes triggered by Notch signaling. Genes Dev *9*, 2598-2608.

Legue, E., and Nicolas, J. F. (2005). Hair follicle renewal: organization of stem cells in the matrix and the role of stereotyped lineages and behaviors. Development *132*, 4143-4154.

Lever, W. F., and Schaumberg-Lever, G. (1993). Histopatology of the skin, Sixth edn (Philadelphia: J.B. Lippincott Company).

Levy, L., Broad, S., Zhu, A. J., Carroll, J. M., Khazaal, I., Peault, B., and Watt, F. M. (1998). Optimised retroviral infection of human epidermal keratinocytes: long-term expression of transduced integrin gene following grafting on to SCID mice. Gene Ther *5*, 913-922.

Li, G., and Pleasure, S. J. (2005). Morphogenesis of the dentate gyrus: what we are learning from mouse mutants. Dev Neurosci *27*, 93-99.

Li, M., Chiba, H., Warot, X., Messaddeq, N., Gerard, C., Chambon, P., and Metzger, D. (2001). RXR-alpha ablation in skin keratinocytes results in alopecia and epidermal alterations. Development *128*, 675-688.

Li, M., Indra, A. K., Warot, X., Brocard, J., Messaddeq, N., Kato, S., Metzger, D., and Chambon, P. (2000). Skin abnormalities generated by temporally controlled RXRalpha mutations in mouse epidermis. Nature *407*, 633-636.

Li, Y. C., Amling, M., Pirro, A. E., Priemel, M., Meuse, J., Baron, R., Delling, G., and Demay, M. B. (1998). Normalization of mineral ion homeostasis by dietary means prevents hyperparathyroidism, rickets, and osteomalacia, but not alopecia in vitamin D receptor-ablated mice. Endocrinology *139*, 4391-4396.

Li, Y. C., Pirro, A. E., Amling, M., Delling, G., Baron, R., Bronson, R., and Demay, M. B. (1997). Targeted ablation of the vitamin D receptor: an animal model of vitamin D-dependent rickets type II with alopecia. Proc Natl Acad Sci U S A *94*, 9831-9835.

Lin, K. K., Chudova, D., Hatfield, G. W., Smyth, P., and Andersen, B. (2004). Identification of hair cycle-associated genes from time-course gene expression profile data by using replicate variance. Proc Natl Acad Sci U S A *101*, 15955-15960.

Lin, M. H., Leimeister, C., Gessler, M., and Kopan, R. (2000). Activation of the Notch pathway in the hair cortex leads to aberrant differentiation of the adjacent hair-shaft layers. Development *127*, 2421-2432.

Lin, Y., Liu, A., Zhang, S., Ruusunen, T., Kreidberg, J. A., Peltoketo, H., Drummond, I., and Vainio, S. (2001). Induction of ureter branching as a response to Wnt-2b signaling during early kidney organogenesis. Dev Dyn *222*, 26-39.

Littlewood, T. D., Hancock, D. C., Danielian, P. S., Parker, M. G., and Evan, G. I. (1995). A modified oestrogen receptor ligand-binding domain as an improved switch for the regulation of heterologous proteins. Nucleic Acids Res *23*, 1686-1690.

Liu, B. Y., McDermott, S. P., Khwaja, S. S., and Alexander, C. M. (2004). The transforming activity of Wnt effectors correlates with their ability to induce the accumulation of mammary progenitor cells. Proc Natl Acad Sci U S A *101*, 4158-4163.

Liu, C., Kato, Y., Zhang, Z., Do, V. M., Yankner, B. A., and He, X. (1999). beta-Trcp couples beta-catenin phosphorylation-degradation and regulates Xenopus axis formation. Proc Natl Acad Sci U S A *96*, 6273-6278.

Liu, J. Y., Nettesheim, P., and Randell, S. H. (1994). Growth and differentiation of tracheal epithelial progenitor cells. Am J Physiol *266*, L296-307.

Liu, Y., Lyle, S., Yang, Z., and Cotsarelis, G. (2003). Keratin 15 promoter targets putative epithelial stem cells in the hair follicle bulge. J Invest Dermatol *121*, 963-968.

Lo Celso, C., Prowse, D. M., and Watt, F. M. (2004). Transient activation of beta-catenin signalling in adult mouse epidermis is sufficient to induce new hair follicles but continuous activation is required to maintain hair follicle tumours. Development *131*, 1787-1799.

Lorens, J. B., Jang, Y., Rossi, A. B., Payan, D. G., and Bogenberger, J. M. (2000). Optimization of regulated LTR-mediated expression. Virology *272*, 7-15.

Lowell, S., Jones, P., Le Roux, I., Dunne, J., and Watt, F. M. (2000). Stimulation of human epidermal differentiation by delta-notch signalling at the boundaries of stem-cell clusters. Curr Biol *10*, 491-500.

Lowell, S., and Watt, F. M. (2001). Delta regulates keratinocyte spreading and motility independently of differentiation. Mech Dev *107*, 133-140.

Lowry, W. E., Blanpain, C., Nowak, J. A., Guasch, G., Lewis, L., and Fuchs, E. (2005). Defining the impact of beta-catenin/Tcf transactivation on epithelial stem cells. Genes Dev *19*, 1596-1611.

Mackenzie, I. C. (1970). Relationship between mitosis and the ordered structure of the stratum corneum in mouse epidermis. Nature *226*, 653-655.

Marinkovich, M. P., Keene, D. R., Rimberg, C. S., and Burgeson, R. E. (1993). Cellular origin of the dermal-epidermal basement membrane. Dev Dyn *197*, 255-267.

Markowitz, D., Goff, S., and Bank, A. (1988a). Construction and use of a safe and efficient amphotropic packaging cell line. Virology *167*, 400-406.

Markowitz, D., Goff, S., and Bank, A. (1988b). A safe packaging line for gene transfer: separating viral genes on teo different plasmids. J Virol *62*, 1120-1124.

Mazzalupo, S., Wong, P., Martin, P., and Coulombe, P. A. (2003). Role for keratins 6 and 17 during wound closure in embryonic mouse skin. Dev Dyn *226*, 356-365.

McCrea, P. D., Turck, C. W., and Gumbiner, B. (1991). A homolog of the armadillo protein in Drosophila (plakoglobin) associated with E-cadherin. Science *254*, 1359-1361.

McGowan, K. M., and Coulombe, P. A. (1998). Onset of keratin 17 expression coincides with the definition of major epithelial lineages during skin development. J Cell Biol *143*, 469-486.

McMahon, A. P., and Moon, R. T. (1989). Ectopic expression of the proto-oncogene int-1 in Xenopus embryos leads to duplication of the embryonic axis. Cell *58*, 1075-1084.

Megason, S. G., and McMahon, A. P. (2002). A mitogen gradient of dorsal midline Wnts organizes growth in the CNS. Development *129*, 2087-2098.

Merrill, B. J., Gat, U., DasGupta, R., and Fuchs, E. (2001). Tcf3 and Lef1 regulate lineage differentiation of multipotent stem cells in skin. Genes Dev *15*, 1688-1705.

Michl, P., Ramjaun, A. R., Pardo, O. E., Warne, P. H., Wagner, M., Poulsom, R., D'Arrigo, C., Ryder, K., Menke, A., Gress, T., and Downward, J. (2005). CUTL1 is a target of TGF(beta) signaling that enhances cancer cell motility and invasiveness. Cancer Cell *7*, 521-532.

Mikkers, H., and Frisen, J. (2005). Deconstructing stemness. Embo J *24*, 2715-2719.

Mill, P., Mo, R., Fu, H., Grachtchouk, M., Kim, P. C., Dlugosz, A. A., and Hui, C. C. (2003). Sonic hedgehog-dependent activation of Gli2 is essential for embryonic hair follicle development. Genes Dev *17*, 282-294.

Mill, P., Mo, R., Hu, M. C., Dagnino, L., Rosenblum, N. D., and Hui, C. C. (2005). Shh controls epithelial proliferation via independent pathways that converge on N-Myc. Dev Cell *9*, 293-303.

Millar, S. E. (2002). Molecular mechanisms regulating hair follicle development. J Invest Dermatol *118*, 216-225.

Millar, S. E., Willert, K., Salinas, P. C., Roelink, H., Nusse, R., Sussman, D. J., and Barsh, G. S. (1999). WNT signaling in the control of hair growth and structure. Dev Biol *207*, 133-149.

Miller, E. D., Tran, M. N., Wong, G. K., Oakley, D. M., and Wong, R. O. (1999). Morphological differentiation of bipolar cells in the ferret retina. Vis Neurosci *16*, 1133-1144.

Miller, J. R. (2002). The Wnts. Genome Biol *3*, REVIEWS3001.

Miller, S. J., Burke, E. M., Rader, M. D., Coulombe, P. A., and Lavker, R. M. (1998). Re-epithelialization of porcine skin by the sweat apparatus. J Invest Dermatol *110*, 13-19.

Milliken, E. L., Zhang, X., Flask, C., Duerk, J. L., Macdonald, P. N., and Keri, R. A. (2005). EB1089, a vitamin D receptor agonist, reduces proliferation and decreases tumor growth rate in a mouse model of hormone-induced mammary cancer. Cancer Lett.

Moldes, M., Zuo, Y., Morrison, R. F., Silva, D., Park, B. H., Liu, J., and Farmer, S. R. (2003). Peroxisome-proliferator-activated receptor gamma suppresses Wnt/beta-catenin signalling during adipogenesis. Biochem J *376*, 607-613.

Molenaar, M., van-de-Wetering, M., Oosterwegel, M., Peterson-Maduro, J., Godsave, S., Korinek, V., Roose, J., Destree, O., and Clevers, H. (1996). XTcf-3 transcription factor mediates beta-catenin-induced axis formation in Xenopus embryos. Cell *86*, 391-399.

Morgenstern, J. P., and Land, H. (1990). Advanced mammalian gene transfer: high titre retroviral vectors with multiple drug selection markers and a complementary helper-free packaging cell line. Nucleic Acids Res *18*, 3587-3596.

Morris, R. J., Liu, Y., Marles, L., Yang, Z., Trempus, C., Li, S., Lin, J. S., Sawicki, J. A., and Cotsarelis, G. (2004). Capturing and profiling adult hair follicle stem cells. Nat Biotechnol *22*, 411-417.

Morris, R. J., and Potten, C. S. (1994). Slowly cycling (label-retaining) epidermal cells behave like clonogenic stem cells in vitro. Cell Prolif *27*, 279-289.

Morris, R. J., Tryson, K. A., and Wu, K. Q. (2000). Evidence that the epidermal targets of carcinogen action are found in the interfollicular epidermis of infundibulum as well as in the hair follicles. Cancer Res *60*, 226-229.

Morrison, S. J., Perez, S. E., Qiao, Z., Verdi, J. M., Hicks, C., Weinmaster, G., and Anderson, D. J. (2000). Transient Notch activation initiates an irreversible switch from neurogenesis to gliogenesis by neural crest stem cells. Cell *101*, 499-510.

Mulholland, D. J., Dedhar, S., Coetzee, G. A., and Nelson, C. C. (2005). Interaction of Nuclear Receptors with Wnt/{beta}-catenin/Tcf Signalling: Wnt you like to know? Endocr Rev.

Mullor, J. L., Dahmane, N., Sun, T., and Ruiz i Altaba, A. (2001). Wnt signals are targets and mediators of Gli function. Curr Biol *11*, 769-773.

Munger, B. L. (1991). The biology of the Merkel cell, In Physiology, Biochemistry, and Molecular Biology of the Skin, L. A. Goldsmith, ed. (Oxford: Oxford University Press), pp. 836-856.

Murayama, M., Tanaka, S., Palacino, J., Murayama, O., Honda, T., Sun, X., Yasutake, K., Nihonmatsu, N., Wolozin, B., and Takashima, A. (1998). Direct association of presenilin-1 with beta-catenin. FEBS Lett *433*, 73-77.

Murphy, M. J., Wilson, A., and Trumpp, A. (2005). More than just proliferation: Myc function in stem cells. Trends Cell Biol *15*, 128-137.

Nasemann, T., Sauerbrey, W., and Burgdorf, W. H. C. (1983). Fundamentals of Dermatology, Fifth Edition edn (New York: Springer-Verlag).

Nathke, I. (2005). Relationship between the role of the adenomatous polyposis coli protein in colon cancer and its contribution to cytoskeletal regulation. Biochem Soc Trans *33*, 694-697.

Nelson, W. J., and Nusse, R. (2004). Convergence of Wnt, beta-catenin, and cadherin pathways. Science *303*, 1483-1487.

Nemes, Z., and Steinert, P. M. (1999). Bricks and mortar of the epidermal barrier. Exp Mol Med *31*, 5-19.

Nicolas, M., Wolfer, A., Raj, K., Kummer, J. A., Mill, P., van Noort, M., Hui, C. C., Clevers, H., Dotto, G. P., and Radtke, F. (2003). Notch1 functions as a tumor suppressor in mouse skin. Nat Genet *33*, 416-421.

Niemann, C., Owens, D. M., Hulsken, J., Birchmeier, W., and Watt, F. M. (2002). Expression of DeltaNLef1 in mouse epidermis results in differentiation of hair follicles into squamous epidermal cysts and formation of skin tumours. Development *129*, 95-109.

Niemann, C., Unden, A. B., Lyle, S., Zouboulis, C. C., Toftgard, R., and Watt, F. M. (2003). Indian hedgehog and {beta}-catenin signaling: Role in the sebaceous lineage of normal and neoplastic mammalian epidermis. Proc Natl Acad Sci U S A.

Niemann, C., and Watt, F. M. (2002). Designer skin: lineage commitment in postnatal epidermis. Trends Cell Biol *12*, 185-192.

Nilsson, M., Unden, A. B., Krause, D., Malmqwist, U., Raza, K., Zaphiropoulos, P. G., and Toftgard, R. (2000). Induction of basal cell carcinomas and trichoepitheliomas in mice overexpressing GLI-1. Proc Natl Acad Sci U S A *97*, 3438-3443.

Nishimura, E. K., Jordan, S. A., Oshima, H., Yoshida, H., Osawa, M., Moriyama, M., Jackson, I. J., Barrandon, Y., Miyachi, Y., and Nishikawa, S. (2002). Dominant role of the niche in melanocyte stem-cell fate determination. Nature *416*, 854-860.

Noramly, S., and Morgan, B. A. (1998). BMPs mediate lateral inhibition at successive stages in feather tract development. Development *125*, 3775-3787.

Nusse, R. (2005). Wnt signaling in disease and in development. Cell Res *15*, 28-32.

Nusslein-Volhard, C., and Wieschaus, E. (1980). Mutations affecting segment number and polarity in Drosophila. Nature *287*, 795-801.

Odland, G. F. (1991). Structure of the skin, In Physiology, Biochemistry, and Molecular Biology of the Skin, L. A. Goldsmith, ed. (Oxford: Oxford University Press), pp. 3-62.

Ohta, T., Elnemr, A., Yamamoto, M., Ninomiya, I., Fushida, S., Nishimura, G., Fujimura, T., Kitagawa, H., Kayahara, M., Shimizu, K., *et al.* (2002). Thiazolidinedione, a peroxisome proliferator-activated receptor-gamma ligand, modulates the E-cadherin/beta-catenin system in a human pancreatic cancer cell line, BxPC-3. Int J Oncol *21*, 37-42.

Oliver, R. F., and Jahoda, C. A. (1988). Dermal-epidermal interactions. Clin Dermatol *6*, 74-82.

Oliver, T. G., Grasfeder, L. L., Carroll, A. L., Kaiser, C., Gillingham, C. L., Lin, S. M., Wickramasinghe, R., Scott, M. P., and Wechsler-Reya, R. J. (2003). Transcriptional profiling of the Sonic hedgehog response: a critical role for N-myc in proliferation of neuronal precursors. Proc Natl Acad Sci U S A *100*, 7331-7336.

Olivera-Martinez, I., Thelu, J., Teillet, M. A., and Dhouailly, D. (2001). Dorsal dermis development depends on a signal from the dorsal neural tube, which can be substituted by Wnt-1. Mech Dev *100*, 233-244.

Oro, A. E., and Higgins, K. (2003). Hair cycle regulation of Hedgehog signal reception. Dev Biol *255*, 238-248.

Oro, A. E., and Scott, M. P. (1997). Basal cell carcinoma in mice overexpressing sonic hedgehog. Science *276*, 817-821.

Oshima, H., Rochat, A., Kedzia, C., Kobayashi, K., and Barrandon, Y. (2001). Morphogenesis and renewal of hair follicles from adult multipotent stem cells. Cell *104*, 233-245.

Owens, D. M., Romero, M. R., Gardner, C., and Watt, F. M. (2003). Suprabasal alpha6beta4 integrin expression in epidermis results in enhanced tumourigenesis and disruption of TGFbeta signalling. J Cell Sci *116*, 3783-3791.

Owens, D. M., and Watt, F. M. (2001). Influence of beta1 integrins on epidermal squamous cell carcinoma formation in a transgenic mouse model: alpha3beta1, but not alpha2beta1, suppresses malignant conversion. Cancer Res *61*, 5248-5254.

Owens, D. M., and Watt, F. M. (2003). Contribution of stem cells and differentiated cells to epidermal tumours. Nat Rev Cancer *3*, 444-451.

Palmer, H. G., Gonzalez-Sancho, J. M., Espada, J., Berciano, M. T., Puig, I., Baulida, J., Quintanilla, M., Cano, A., de Herreros, A. G., Lafarga, M., and Munoz, A. (2001). Vitamin D(3) promotes the differentiation of colon carcinoma cells by the induction of E-cadherin and the inhibition of beta-catenin signaling. J Cell Biol *154*, 369-387.

Pan, Y., Lin, M. H., Tian, X., Cheng, H. T., Gridley, T., Shen, J., and Kopan, R. (2004). gamma-secretase functions through Notch signaling to maintain skin appendages but is not required for their patterning or initial morphogenesis. Dev Cell *7*, 731-743.

Panteleyev, A. A., Jahoda, C. A., and Christiano, A. M. (2001). Hair follicle predetermination. J Cell Sci *114*, 3419-3431.

Papkoff, J., and Schryver, B. (1990). Secreted int-1 protein is associated with the cell surface. Mol Cell Biol *10*, 2723-2730.

Parakkal, P. F., and Matoltsy, A. G. (1964). A Study Of The Differentiation Products Of The Hair Follicle Cells With The Electron Microscope. J Invest Dermatol *42*, 23-34.

Park, Y., and Gerson, S. L. (2005). DNA repair defects in stem cell function and aging. Annu Rev Med *56*, 495-508.

Paus, R., and Cotsarelis, G. (1999). The biology of hair follicles. N Engl J Med *341*, 491-497.

Pearton, D. J., Ferraris, C., and Dhouailly, D. (2004). Transdifferentiation of corneal epithelium: evidence for a linkage between the segregation of epidermal stem cells and the induction of hair follicles during embryogenesis. Int J Dev Biol *48*, 197-201.

Peat, N., Gendler, S. J., Lalani, N., Duhig, T., and Taylor-Papadimitriou, J. (1992). Tissue-specific expression of a human polymorphic epithelial mucin (MUC1) in transgenic mice. Cancer Res *52*, 1954-1960.

Peifer, M., McCrea, P. D., Green, K. J., Wieschaus, E., and Gumbiner, B. M. (1992). The vertebrate adhesive junction proteins β-catenin and plakoglobin and the Drosophila segment polarity gene armadillo form a multigene family with similar properties. J Cell Biol *118*, 681-691.

Peifer, M., Orsulic, S., Pai, L. M., and Loureiro, J. (1993). A model system for cell adhesion and signal transduction in Drosophila. Dev Suppl, 163-176.

Peifer, M., and Polakis, P. (2000). Wnt signaling in oncogenesis and embryogenesis--a look outside the nucleus. Science *287*, 1606-1609.

Peleg, S., Khan, F., Navone, N. M., Cody, D. D., Johnson, E. M., Pelt, C. S., and Posner, G. H. (2005). Inhibition of prostate cancer-meditated osteoblastic bone lesions by the low-calcemic analog 1alpha-hydroxymethyl-16-ene-26,27-bishomo-25-hydroxy vitamin D(3). J Steroid Biochem Mol Biol.

Pelengaris, S., Littlewood, T., Khan, M., Elia, G., and Evan, G. (1999). Reversible activation of c-Myc in skin: induction of a complex neoplastic phenotype by a single oncogenic lesion. Mol Cell *3*, 565-577.

Perez-Losada, J., and Balmain, A. (2003). Stem-cell hierarchy in skin cancer. Nat Rev Cancer *3*, 434-443.

Pierard-Franchimont, C., and Pierard, G. E. (1989). Stereotyped distribution of proliferating keratinocytes in disorders affecting the epidermis. Am J Dermatopathol *11*, 233-237.

Pinson, K. I., Brennan, J., Monkley, S., Avery, B. J., and Skarnes, W. C. (2000). An LDL-receptor-related protein mediates Wnt signalling in mice. Nature *407*, 535-538.

Pinto, D., and Clevers, H. (2005). Wnt control of stem cells and differentiation in the intestinal epithelium. Exp Cell Res *306*, 357-363.

Polakis, P. (1999). The oncogenic activation of beta-catenin. Curr Opin Genet Dev *9*, 15-21.

Porter, J. A., Ekker, S. C., Park, W. J., von Kessler, D. P., Young, K. E., Chen, C. H., Ma, Y., Woods, A. S., Cotter, R. J., Koonin, E. V., and Beachy, P. A. (1996). Hedgehog patterning activity: role of a lipophilic modification mediated by the carboxy-terminal autoprocessing domain. Cell *86*, 21-34.

Potten, C. S. (1981). Cell replacement in epidermis (keratopoiesis) via discrete units of proliferation. Int Rev Cytol *69*, 271-318.

Potten, C. S., and Hendry, J. H. (1973). Letter: Clonogenic cells and stem cells in epidermis. Int J Radiat Biol Relat Stud Phys Chem Med *24*, 537-540.

Potten, C. S., and Morris, R. J. (1988). Epithelial stem cells in vivo. J Cell Sci Suppl *10*, 45-62.

Powell, B. C., Passmore, E. A., Nesci, A., and Dunn, S. M. (1998). The Notch signalling pathway in hair growth. Mech Dev *78*, 189-192.

Prunieras, M., Regnier, M., and Woodley, D. (1983). Methods for cultivation of keratinocytes with an air-liquid interface. J Invest Dermatol *81*, 28s-33s.

Rangarajan, A., Talora, C., Okuyama, R., Nicolas, M., Mammucari, C., Oh, H., Aster, J. C., Krishna, S., Metzger, D., Chambon, P., *et al.* (2001). Notch signaling is a direct determinant of keratinocyte growth arrest and entry into differentiation. Embo J *20*, 3427-3436.

Reddy, S., Andl, T., Bagasra, A., Lu, M. M., Epstein, D. J., Morrisey, E. E., and Millar, S. E. (2001). Characterization of Wnt gene expression in developing and postnatal hair follicles and identification of Wnt5a as a target of Sonic hedgehog in hair follicle morphogenesis. Mech Dev *107*, 69-82.

Reddy, S. T., Andl, T., Lu, M. M., Morrisey, E. E., and Millar, S. E. (2004). Expression of Frizzled genes in developing and postnatal hair follicles. J Invest Dermatol *123*, 275-282.

Rendl, M., Lewis, L., and Fuchs, E. (2005). Molecular Dissection of Mesenchymal-Epithelial Interactions in the Hair Follicle. PLoS Biol *3*, e331.

Revest, J. M., Spencer-Dene, B., Kerr, K., De Moerlooze, L., Rosewell, I., and Dickson, C. (2001). Fibroblast growth factor receptor 2-IIIb acts upstream of Shh and Fgf4 and is required for limb bud maintenance but not for the induction of Fgf8, Fgf10, Msx1, or Bmp4. Dev Biol *231*, 47-62.

Reya, T., and Clevers, H. (2005). Wnt signalling in stem cells and cancer. Nature *434*, 843-850.

Reya, T., Duncan, A. W., Ailles, L., Domen, J., Scherer, D. C., Willert, K., Hintz, L., Nusse, R., and Weissman, I. L. (2003). A role for Wnt signalling in self-renewal of haematopoietic stem cells. Nature *423*, 409-414.

Reya, T., Morrison, S. J., Clarke, M. F., and Weissman, I. L. (2001). Stem cells, cancer, and cancer stem cells. Nature *414*, 105-111.

Reynolds, A. J., and Jahoda, C. A. (1992). Cultured dermal papilla cells induce follicle formation and hair growth by transdifferentiation of an adult epidermis. Development *115*, 587-593.

Rheinwald, J. G., and Green, H. (1975). Formation of a keratinizing epithelium in culture by a cloned cell line derived from a teratoma. Cell *6*, 317-330.

Riggleman, B., Schedl, P., and Wieschaus, E. (1990). Spatial expression of the Drosophila segment polarity gene armadillo is posttranscriptionally regulated by wingless. Cell *63*, 549-560.

Rijsewijk, F., Schuermann, M., Wagenaar, E., Parren, P., Weigel, D., and Nusse, R. (1987). The Drosophila homolog of the mouse mammary oncogene int-1 is identical to the segment polarity gene wingless. Cell *50*, 649-657.

Roberts, D. L., Marshall, R., and Marks, R. (1980). Detection of the action of salicylic acid on the normal stratum corneum. Br J Dermatol *103*, 191-196.

Romani, N., Holzmann, S., Tripp, C. H., Koch, F., and Stoitzner, P. (2003). Langerhans cells - dendritic cells of the epidermis. Apmis *111*, 725-740.

Romero, M. R., Carroll, J. M., and Watt, F. M. (1999). Analysis of cultured keratinocytes from a transgenic mouse model of psoriasis: effects of suprabasal integrin expression on keratinocyte adhesion, proliferation and terminal differentiation. Exp Dermatol *8*, 53-67.

Roper, E., Weinberg, W., Watt, F. M., and Land, H. (2001). p19ARF-independent induction of p53 and cell cycle arrest by Raf in murine keratinocytes. EMBO Rep *2*, 145-150.

Rosen, E. D., Sarraf, P., Troy, A. E., Bradwin, G., Moore, K., Milstone, D. S., Spiegelman, B. M., and Mortensen, R. M. (1999). PPAR gamma is required for the differentiation of adipose tissue in vivo and in vitro. Mol Cell *4*, 611-617.

Rosenfield, R. L., Deplewski, D., and Greene, M. E. (2000). Peroxisome proliferator-activated receptors and skin development. Horm Res *54*, 269-274.

Rosenfield, R. L., Kentsis, A., Deplewski, D., and Ciletti, N. (1999). Rat preputial sebocyte differentiation involves peroxisome proliferator-activated receptors. J Invest Dermatol *112*, 226-232.

Ross, S. E., Hemati, N., Longo, K. A., Bennett, C. N., Lucas, P. C., Erickson, R. L., and MacDougald, O. A. (2000). Inhibition of adipogenesis by Wnt signaling. Science *289*, 950-953.

Rowden, G. (1968). Ultrastructural studies of keratinized epithelia of the mouse. II. Aryl sulfatase in lysosomes of mouse epidermis and esophageal epithelium. J Invest Dermatol *51*, 51-61.

Sakanaka, C., and Williams, L. T. (1999). Functional domains of axin. Importance of the C terminus as an oligomerization domain. J Biol Chem *274*, 14090-14093.

Sambrook, J., Fritsch, E. F., and Maniatis, T. (1989). Molecular cloning. A laboratory manual. (New York: Cold Spring Harbor Laboratory Press).

Sato, N., Leopold, P. L., and Crystal, R. G. (1999). Induction of the hair growth phase in postnatal mice by localized transient expression of Sonic hedgehog. J Clin Invest *104*, 855-864.

Satokata, I., Ma, L., Ohshima, H., Bei, M., Woo, I., Nishizawa, K., Maeda, T., Takano, Y., Uchiyama, M., Heaney, S., *et al.* (2000). Msx2 deficiency in mice causes pleiotropic defects in bone growth and ectodermal organ formation. Nat Genet *24*, 391-395.

Schmidt-Ullrich, R., and Paus, R. (2005). Molecular principles of hair follicle induction and morphogenesis. Bioessays *27*, 247-261.

Schofield, R. (1978). The relationship between the spleen colony-forming cell and the haemopoietic stem cell. Blood Cells *4*, 7-25.

Schroeder, T., and Just, U. (2000). Notch signalling via RBP-J promotes myeloid differentiation. Embo J *19*, 2558-2568.

Seery, J. P., and Watt, F. M. (2000). Asymmetric stem-cell divisions define the architecture of human oesophageal epithelium. Curr Biol *10*, 1447-1450.

Sekiya, T., Adachi, S., Kohu, K., Yamada, T., Higuchi, O., Furukawa, Y., Nakamura, Y., Nakamura, T., Tashiro, K., Kuhara, S., *et al.* (2004). Identification of BMP and activin membrane-bound inhibitor (BAMBI), an inhibitor of transforming growth factor-beta signaling, as a target of the beta-catenin pathway in colorectal tumor cells. J Biol Chem *279*, 6840-6846.

Sieber-Blum, M. (2003). Ontogeny and plasticity of adult hippocampal neural stem cells. Dev Neurosci *25*, 273-278.

Sieber-Blum, M., Grim, M., Hu, Y. F., and Szeder, V. (2004). Pluripotent neural crest stem cells in the adult hair follicle. Dev Dyn *231*, 258-269.

Silva-Vargas, V., Lo Celso, C., Giangreco, A., Ofstad, T., Prowse, D. M., Braun, K. M., and Watt, F. M. (2005). Beta-catenin and Hedgehog signal strength can specify number and location of hair follicles in adult epidermis without recruitment of bulge stem cells. Dev Cell *9*, 121-131.

Sober, A. J., Koh, H. K., Tran, N. T., and Washington, C. V. (1999). Melanoma e altre neoplasie cutanee, In Principi di medicina interna, Harrison, ed. (Milano: McGraw Hill), pp. 615-653.

Sokol, S. Y., Klingensmith, J., Perrimon, N., and Itoh, K. (1995). Dorsalizing and neuralizing properties of Xdsh, a maternally expressed Xenopus homolog of dishevelled. Development *121*, 1637-1647.

Soriano, S., Kang, D. E., Fu, M., Pestell, R., Chevallier, N., Zheng, H., and Koo, E. H. (2001). Presenilin 1 negatively regulates beta-catenin/T cell factor/lymphoid enhancer factor-1 signaling independently of beta-amyloid precursor protein and notch processing. J Cell Biol *152*, 785-794.

Spradling, A., Drummond-Barbosa, D., and Kai, T. (2001). Stem cells find their niche. Nature *414*, 98-104.

Srivastava, A. K., Pispa, J., Hartung, A. J., Du, Y., Ezer, S., Jenks, T., Shimada, T., Pekkanen, M., Mikkola, M. L., Ko, M. S., *et al.* (1997). The Tabby phenotype is caused

by mutation in a mouse homologue of the EDA gene that reveals novel mouse and human exons and encodes a protein (ectodysplasin-A) with collagenous domains. Proc Natl Acad Sci U S A *94*, 13069-13074.

St-Jacques, B., Dassule, H. R., Karavanova, I., Botchkarev, V. A., Li, J., Danielian, P. S., McMahon, J. A., Lewis, P. M., Paus, R., and McMahon, A. P. (1998). Sonic hedgehog signaling is essential for hair development. Curr Biol *8*, 1058-1068.

Staal, F. J., and Clevers, H. C. (2005). WNT signalling and haematopoiesis: a WNT-WNT situation. Nat Rev Immunol *5*, 21-30.

Staricco, R. G., and Miller-Milinska, A. (1962). Activation of the amelanotic melanocytes in the outer root sheath of the hair follicle following ultra violet rays exposure. J Invest Dermatol *39*, 163-164.

Stenn, K. S., and Paus, R. (2001). Controls of hair follicle cycling. Physiol Rev *81*, 449-494.

Steventon, B., Carmona-Fontaine, C., and Mayor, R. (2005). Genetic network during neural crest induction: From cell specification to cell survival. Semin Cell Dev Biol.

Strauss, J. S., Downing, D. T., Ebling, F. J., and Stewart, M. E. (1991). Sebaceous gland, In Physiology, Biochemistry, and Molecular Biology of the Skin, L. A. Goldsmith, ed. (Oxford: Oxford University Press), pp. 712*740.

Taipale, J., and Beachy, P. A. (2001). The Hedgehog and Wnt signalling pathways in cancer. Nature *411*, 349-354.

Taipale, J., Chen, J. K., Cooper, M. K., Wang, B., Mann, R. K., Milenkovic, L., Scott, M. P., and Beachy, P. A. (2000). Effects of oncogenic mutations in Smoothened and Patched can be reversed by cyclopamine. Nature *406*, 1005-1009.

Tamai, K., Semenov, M., Kato, Y., Spokony, R., Liu, C., Katsuyama, Y., Hess, F., Saint-Jeannet, J. P., and He, X. (2000). LDL-receptor-related proteins in Wnt signal transduction. Nature *407*, 530-535.

Tamura, K., Taniguchi, Y., Minoguchi, S., Sakai, T., Tun, T., Furukawa, T., and Honjo, T. (1995). Physical interaction between a novel domain of the receptor Notch and the transcription factor RBP-J kappa/Su(H). Curr Biol *5*, 1416-1423.

Tani, H., Morris, R. J., and Kaur, P. (2000). Enrichment for murine keratinocyte stem cells based on cell surface phenotype. Proc Natl Acad Sci U S A *97*, 10960-10965.

Taylor, G., Lehrer, M. S., Jensen, P. J., Sun, T. T., and Lavker, R. M. (2000). Involvement of follicular stem cells in forming not only the follicle but also the epidermis. Cell *102*, 451-461.

Tetsu, O., and McCormick, F. (1999). Beta-catenin regulates expression of cyclin D1 in colon carcinoma cells. Nature *398*, 422-426.

Tharp, M. D. (1991). The Mast Cell and Its Mediators, In Physiology, Biochemistry, and Molecular Biology of the Skin, L. A. Goldsmith, ed. (Oxford: Oxford University Press), pp. 1099-1120.

Theisen, H., Purcell, J., Bennett, M., Kansagara, D., Syed, A., and Marsh, J. L. (1994). dishevelled is required during wingless signaling to establish both cell polarity and cell identity. Development *120*, 347-360.

Toma, J. G., Akhavan, M., Fernandes, K. J., Barnabe-Heider, F., Sadikot, A., Kaplan, D. R., and Miller, F. D. (2001). Isolation of multipotent adult stem cells from the dermis of mammalian skin. Nat Cell Biol *3*, 778-784.

Tomasz, M., Lipman, R., Chowdary, D., Pawlak, J., Verdine, G. L., and Nakanishi, K. (1987). Isolation and structure of a covalent cross-link adduct between mitomycin C and DNA. Science *235*, 1204-1208.

Tournoy, J., Bossuyt, X., Snellinx, A., Regent, M., Garmyn, M., Serneels, L., Saftig, P., Craessaerts, K., De Strooper, B., and Hartmann, D. (2004). Partial loss of presenilins causes seborrheic keratosis and autoimmune disease in mice. Hum Mol Genet *13*, 1321-1331.

Tumbar, T., Guasch, G., Greco, V., Blanpain, C., Lowry, W. E., Rendl, M., and Fuchs, E. (2004). Defining the epithelial stem cell niche in skin. Science *303*, 359-363.

van de Wetering, M., Cavallo, R., Dooijes, D., van Beest, M., van Es, J., Loureiro, J., Ypma, A., Hursh, D., Jones, T., Bejsovec, A., *et al.* (1997). Armadillo coactivates transcription driven by the product of the Drosophila segment polarity gene dTCF. Cell *88*, 789-799.

van de Wetering, M., Oosterwegel, M., Holstege, F., Dooyes, D., Suijkerbuijk, R., Geurts van Kessel, A., and Clevers, H. (1992). The human T cell transcription factor-1 gene. Structure, localization, and promoter characterization. J Biol Chem *267*, 8530-8536.

van den Brink, G. R., Bleuming, S. A., Hardwick, J. C., Schepman, B. L., Offerhaus, G. J., Keller, J. J., Nielsen, C., Gaffield, W., van Deventer, S. J., Roberts, D. J., and Peppelenbosch, M. P. (2004). Indian Hedgehog is an antagonist of Wnt signaling in colonic epithelial cell differentiation. Nat Genet *36*, 277-282.

van Genderen, C., Okamura, R. M., Farinas, I., Quo, R. G., Parslow, T. G., Bruhn, L., and Grosschedl, R. (1994). Development of several organs that require inductive epithelial-mesenchymal interactions is impaired in LEF-1-deficient mice. Genes Dev *8*, 2691-2703.

van Leeuwen, F., Samos, C. H., and Nusse, R. (1994). Biological activity of soluble *wingless* protein in cultured *Drosophila* imaginal disc cells. Nature (Lond) *368*, 342-344.

Van Mater, D., Kolligs, F. T., Dlugosz, A. A., and Fearon, E. R. (2003). Transient activation of beta -catenin signaling in cutaneous keratinocytes is sufficient to trigger the active growth phase of the hair cycle in mice. Genes Dev *17*, 1219-1224.

Van Raay, T. J., Moore, K. B., Iordanova, I., Steele, M., Jamrich, M., Harris, W. A., and Vetter, M. L. (2005). Frizzled 5 signaling governs the neural potential of progenitors in the developing Xenopus retina. Neuron *46*, 23-36.

Vasioukhin, V., Degenstein, L., Wise, B., and Fuchs, E. (1999). The magical touch: genome targeting in epidermal stem cells induced by tamoxifen application to mouse skin. Proc Natl Acad Sci U S A *96*, 8551-8556.

Vassar, R., Rosenberg, M., Ross, S., Tyner, A., and Fuchs, E. (1989). Tissue-specific and differentiation-specific expression of a human K14 keratin gene in transgenic mice. Proc Natl Acad Sci U S A *86*, 1563-1567.

Vauclair, S., Nicolas, M., Barrandon, Y., and Radtke, F. (2005). Notch1 is essential for postnatal hair follicle development and homeostasis. Dev Biol *284*, 184-193.

Veeman, M. T., Axelrod, J. D., and Moon, R. T. (2003). A second canon. Functions and mechanisms of beta-catenin-independent Wnt signaling. Dev Cell *5*, 367-377.

Viallet, J. P., Prin, F., Olivera-Martinez, I., Hirsinger, E., Pourquie, O., and Dhouailly, D. (1998). Chick Delta-1 gene expression and the formation of the feather primordia. Mech Dev *72*, 159-168.

Voeller, H. J., Truica, C. I., and Gelmann, E. P. (1998). Beta-catenin mutations in human prostate cancer. Cancer Res *58*, 2520-2523.

Wagers, A. J., Sherwood, R. I., Christensen, J. L., and Weissman, I. L. (2002). Little evidence for developmental plasticity of adult hematopoietic stem cells. Science *297*, 2256-2259.

Wagers, A. J., and Weissman, I. L. (2004). Plasticity of adult stem cells. Cell *116*, 639-648.

Waikel, R. L., Kawachi, Y., Waikel, P. A., Wang, X. J., and Roop, D. R. (2001). Deregulated expression of c-Myc depletes epidermal stem cells. Nat Genet *28*, 165-168.

Waite, K. A., and Eng, C. (2003). From developmental disorder to heritable cancer: it's all in the BMP/TGF-beta family. Nat Rev Genet *4*, 763-773.

Wang, L. C., Liu, Z. Y., Gambardella, L., Delacour, A., Shapiro, R., Yang, J., Sizing, I., Rayhorn, P., Garber, E. A., Benjamin, C. D., *et al.* (2000). Regular articles: conditional disruption of hedgehog signaling pathway defines its critical role in hair development and regeneration. J Invest Dermatol *114*, 901-908.

Wang, X., Zinkel, S., Polonsky, K., and Fuchs, E. (1997). Transgenic studies with a keratin promoter-driven growth hormone transgene: prospects for gene therapy. Proc Natl Acad Sci U S A *94*, 219-226.

Watt, F. M. (2001). Stem cell fate and patterning in mammalian epidermis. Curr Opin Genet Dev *11*, 410-417.

Watt, F. M., and Hogan, B. L. (2000). Out of Eden: stem cells and their niches. Science *287*, 1427-1430.

Weedon, D., and Strutton, G. (1981). Apoptosis as the mechanism of the involution of hair follicles in catagen transformation. Acta Derm Venereol *61*, 335-339.

Weiss, E. E., Kroemker, M., Rudiger, A. H., Jockusch, B. M., and Rudiger, M. (1998). Vinculin is part of the cadherin-catenin junctional complex: complex formation between alpha-catenin and vinculin. J Cell Biol *141*, 755-764.

Weissman, I. L. (2000). Stem cells: units of development, units of regeneration, and units in evolution. Cell *100*, 157-168.

Wieschaus, E., and Riggleman, R. (1987). Autonomous requirements for the segment polarity gene armadillo during Drosophila embryogenesis. Cell *49*, 177-184.

Wilson, N., Hynd, P. I., and Powell, B. C. (1999). The role of BMP-2 and BMP-4 in follicle initiation and the murine hair cycle. Exp Dermatol *8*, 367-368.

Wodarz, A., and Nusse, R. (1998). Mechanisms of Wnt signaling in development. Annu Rev Cell Dev Biol *14*, 59-88.

Xie, J., Murone, M., Luoh, S. M., Ryan, A., Gu, Q., Zhang, C., Bonifas, J. M., Lam, C. W., Hynes, M., Goddard, A., *et al.* (1998). Activating Smoothened mutations in sporadic basal-cell carcinoma. Nature *391*, 90-92.

Yardy, G. W., and Brewster, S. F. (2005). Wnt signalling and prostate cancer. Prostate Cancer Prostatic Dis *8*, 119-126.

Yates, K. E., Shortkroff, S., and Reish, R. G. (2005). Wnt influence on chondrocyte differentiation and cartilage function. DNA Cell Biol *24*, 446-457.

Yen, A., and Braverman, I. M. (1976). Ultrastructure of the human dermal microcirculation: the horizontal plexus of the papillary dermis. J Invest Dermatol *66*, 131-142.

Zhang, J., Niu, C., Ye, L., Huang, H., He, X., Tong, W. G., Ross, J., Haug, J., Johnson, T., Feng, J. Q., *et al.* (2003). Identification of the haematopoietic stem cell niche and control of the niche size. Nature *425*, 836-841.

Zhu, A. J. (1998) Role of integrins and cadherins in regulating keratinocyte growth and differentiaiton, Imperial Cancer Research Fund, London.

Zhu, A. J., and Watt, F. M. (1996). Expression of a dominant negative cadherin mutant inhibits proliferation and stimulates terminal differentiation of human epidermal keratinocytes. J Cell Sci *109*, 3013-3023.

Zhu, A. J., and Watt, F. M. (1999). beta-catenin signalling modulates proliferative potential of human epidermal keratinocytes independently of intercellular adhesion. Development *126*, 2285-2298.

Zinser, G. M., Sundberg, J. P., and Welsh, J. (2002). Vitamin D(3) receptor ablation sensitizes skin to chemically induced tumorigenesis. Carcinogenesis *23*, 2103-2109.

Zouboulis, C. C., Seltmann, H., Neitzel, H., and Orfanos, C. E. (1999). Establishment and characterization of an immortalized human sebaceous gland cell line (SZ95). J Invest Dermatol *113*, 1011-1020.

Zouboulis, C. C., Xia, L. Q., Detmar, M., Bogdanoff, B., Giannakopoulos, G., Gollnick, H., and Orfanos, C. E. (1991). Culture of human sebocytes and markers of sebocytic differentiation in vitro. Skin Pharmacol *4*, 74-83.

Zurawel, R. H., Chiappa, S. A., Allen, C., and Raffel, C. (1998). Sporadic medulloblastomas contain oncogenic beta-catenin mutations. Cancer Res *58*, 896-899.